

Advances Towards Regioselective Synthesis of Secondary Alkylboranes and 1,2-*cis* Glycosides

by

Hilary Ann Kerchner

A dissertation submitted in partial fulfillment
of the requirements for the degree of
Doctor of Philosophy
(Chemistry)
in the University of Michigan
2018

Doctoral Committee:

Professor John Montgomery, Chair
Associate Professor Nathaniel Szymczak
Professor Levi Thompson
Professor John Wolfe

Hilary Ann Kerchner

hkerch@umich.edu

ORCID iD: [0000-0002-7743-6238](https://orcid.org/0000-0002-7743-6238)

© Hilary Ann Kerchner 2018

Dedication

For the teachers, mentors, and coaches in my life, thank you all.

Acknowledgements

I would like to thank my advisor Professor John Montgomery for his guidance over the past five years. His support and help organizing a short stay at ICIQ introduced me to connections all over the world that I hold near and dear. I appreciated his encouragement as I planned, organized and attended several outreach events over the course of my time here at Michigan. I would like to acknowledge the other professors at Michigan that have helped me get to the point I am today. A special thanks to Professor John Wolfe for letting me rotate in his lab during my second semester at Michigan. Professor Nathaniel Szymczak taught one of my favorite classes and helped me understand organometallics better. Along with Professor Levi Thompson, I would like to thank my committee for the insightful conversations and support at both my candidacy and data meetings. Lastly, I would like to thank Professor Anne McNeil for being very supportive as my original research proposal advisor.

My co-workers in the Montgomery lab have made everyday in lab an experience that included laughter and thought provoking conversations. I am appreciative of all of the help that Dr. Hengbin Wang gave me as I began my transition into graduate school. I would also like to thank Dr. Jessica Stachowski, Alex Nett, Eric Wiensch, Annabel Ansel and Amie Frank. It has meant a lot to be surrounded by people who entertained all of my crazy ideas and fostered an environment for creativity.

Without the support of my family I would not have made it this far in my education. My parents, John and Jill Kerchner, my sister, Heather Emerich and my brother-in-law, Ryan Emerich have always believed in me and supported me from day one. My nieces, Kendall and

Laurel, inspire me everyday to become a better role model for not only them but for the next generation of females. I would like to thank my grandparents John and Sandy Kerchner and John and Janet Welther who have not only provided love and support but have filled my freezer with home cooked meals every time they visited. Lastly, I want to thank my husband, Jordan Boothe, for his love, guidance and support over the past five years. I cannot wait to see what life journeys are in store for us!

Table of Contents

Dedication	ii
Acknowledgements	iii
List of Schemes	ix
List of Tables	xiii
List of Figures.....	xv
List of Abbreviations	xviii
Abstract.....	xxiii
Chapter 1 Introduction to Copper-Catalyzed Hydroboration	1
1.1 General Overview of Thesis	1
1.2 Regioselectivity Explanations for Hydrofunctionalization of Olefins.....	1
1.3 Influence of Herbert C. Brown on Organic Synthesis	3
1.4 Copper-Catalyzed Hydroboration.....	8
1.4.1 Initial Proof of Concept for Copper-Catalyzed Hydroboration	9
1.4.2 Initial Copper-Catalyzed Hydroboration	9
1.4.3 Copper-Catalyzed Hydroboration of Other Olefin Classes	10
1.5 Conclusion	14
Chapter 2 Advances in Regioselective Hydroboration of Olefins	16
2.1 Introduction to Alkylboranes	16
2.2 Previous Synthesis of Secondary Alkylboranes and Gap in the Literature	17

2.3 Optimization of the Formal Hydroboration of Terminal Olefins	19
2.3.1 Rationale for Initial Optimization Conditions	19
2.3.2 Optimization Using Pinacolborane	20
2.3.3 Optimization with Bis(pinacolato)diboron	22
2.4 Mechanistic Hypothesis	23
2.5 Reaction Scope.....	24
2.6 Cross-Coupling of Newly Synthesized Secondary Alkylborane	26
2.7 Enantioselective Hydroboration of Terminal Olefins.....	28
2.8 Progress Towards Regioselective Hydroboration of 1,2-Disubstituted Olefins.....	30
2.9 Progress Towards the Synthesis of Tertiary Alkylboranes.....	33
2.10 Conclusion and Future Directions for Hydroboration of Olefins	35
Chapter 3 Introduction to Intramolecular Aglycone Delivery and Glycoside Activation ...	37
3.1 Factors that Affect Glycosylation Reactions	37
3.2 Indirect Glycosylation Methods Via Intramolecular Aglycone Delivery.....	40
3.3 Anomeric Identity and Activation for the Synthesis of 1,2- <i>cis</i> Glycosides.....	46
3.3.1 Activation of Alkenyl Glycosides.....	47
3.3.2 Recent Advances on Activation of Thioglycosides	51
Chapter 4 Advances in Intramolecular Aglycone Delivery via Latent-Activation.....	57
4.1 Montgomery Group Contributions to Glycosciences via Synthesis of 1,2- <i>cis</i> - Glycosides	57
4.2 Motivation and Project Goals	61
4.3 Continued Progress Towards Bench Stable Sugar Silanes	63
4.3.1 Synthesis of Mannose Sugar Silanes	63
4.3.2 Synthesis of Glucose Sugar Silanes.....	65

4.3.3 Mannose Sugar Silane Tethering and Aglycone Delivery.....	68
4.3.4 Glucose Sugar Silane Tethering and Aglycone Delivery	73
4.4 Progress Towards Asymmetric Hydrosilylation of Ketones	75
4.5 Conclusion and Future Directions For Latent-Activation for Intramolecular Aglycone Delivery.....	78
Chapter 5 Conclusion	80
5.1 Conclusion	80
Chapter 6 Experimental.....	83
6.1 General Considerations.....	83
6.2 Chapter 2 Experimental	84
6.2.1 Substrates Synthesized by Literature Procedures	84
6.2.2 Synthesis of Starting Material.....	84
6.2.3 Synthesis of Branched Alkylboranes.....	86
6.2.4 Synthesis of Trifluoroborate Salts	96
6.2.5 Photocatalytic Cross-coupling	98
6.2.6 Enantioselectivity Investigation.....	104
6.2.7 Hydroboration of 1,2-Disubstituted Olefins	114
6.2.8 Synthesis of Tertiary Alkylboranes	121
6.3 Chapter 4 Experimental	122
6.3.1 Synthesis of 2-Hydroxy Mannose 4-28	122
6.3.2 Synthesis of 2-Hydroxy Glucose Sugar 4-36 and 4-38	128
6.3.3 Synthesis of Sugar Silane from 2-Hydroxy Sugars	137
6.3.4 Tethering Alcohols to Sugar Silanes.....	142

6.3.5 Aglycone Delivery	149
6.3.6 Asymmetric Hydrosilylation of Ketones	152
6.4 NMR Spectra	161
References.....	216

List of Schemes

Scheme 1-1: (A) Two Regioisomeric Product from H-X Addition to an Olefin (B) Carbocation Stability in Acid-Catalyzed Hydrofunctionalization (C) Radical Stability in Photoredox Hydrofunctionalization	3
Scheme 1-2 Brown's Hydroboration in Ethereal Solvents Discovery.....	4
Scheme 1-3: Mechanism for Brown's Hydroboration	4
Scheme 1-4: (A) Synthesis of Icp_2BH (B) Enantioselective Hydroboration with Icp_2BH	6
Scheme 1-5: (A) Weinreb's Total Synthesis of Agelastatin A (B) Corey's Total Synthesis of Gibberellic Acid (C) Sato and Chida's Total Synthesis of Madangamine C	8
Scheme 1-6: (A) First Report of Copper-Boron Complex (B) First Indication Copper Catalyzed Hydroboration Reactions of Olefins	9
Scheme 1-7: (A) Formal Deuteroboration of Styrene Derivatives with High Diastereoselectivity (B) Enantioselective Hydroboration of Styrene Derivatives	10
Scheme 1-8: Hydroboration of 1,1-Disubstituted Styrene Derivatives	11
Scheme 1-9: Hydroboration of Mono-Substituted, Terminal Olefins	12
Scheme 1-10: Hoveyda's Hydroboration of 1,2-Disubstituted Olefins	13
Scheme 1-11: Copper-Hydride Hydroboration of Internal Olefins with Select Examples	14
Scheme 1-12: Copper-Catalyzed Borylations of π -Systems.....	15
Scheme 2-1: Synthetic Transformation of Alkylboronic Esters	16
Scheme 2-2: Mechanism for Stereoretentive Oxidation.....	17

Scheme 2-3: Previous Approaches to Secondary Alkylboranes and the Gap in the Literature....	19
Scheme 2-4: Examples of Regiocontrol for Hydrosilylation of Allenes (A) Metal Identity (B) Ligand Size	20
Scheme 2-5: Proposed Mechanism for the Formation of Linear Alkylborane 2-20.....	22
Scheme 2-6: (A) Mechanism for the Hydroboration of Terminal Olefins (B) Coordination of Olefin to Copper Complex for the Regio-Determining Step	24
Scheme 2-7: Substrate Scope for the Copper-Catalyzed Formal Hydroboration Reaction.....	26
Scheme 2-8: (A) Conditions for Photocatalytic Cross-Coupling of Secondary Alkyl Trifluoroborate Salts and Aryl Halides (B) Mechanism for Photocatalytic Cross-Coupling	27
Scheme 2-9: Photocatalytic Cross-Coupling of Newly Synthesized Trifluoroborate Salts. Note: Reported Yields Correspond to the Cross-Coupling Step.	28
Scheme 2-10: Investigation into Enantioselective Hydroboration of Terminal Olefins.....	30
Scheme 2-11: Hartwig's Directing Group Regiocontrolled Hydroboration of Internal Olefins ..	31
Scheme 2-12: Project Goals for Hydroboration of 1,1-Disubstituted Olefins.....	34
Scheme 2-13: Hydroboration of 2-70	35
Scheme 3-1: Koenigs and Knorr Glycosylation Reaction with Mechanism	38
Scheme 3-2: Factors that Affect Glycosylation Reactions	40
Scheme 3-3: General Scheme for Intramolecular Aglycone Delivery	41
Scheme 3-4: Hindsgaul and Barresi Introduction of Intramolecular Aglycone Delivery	42
Scheme 3-5: Fairbanks Iodonium Tethering for Intramolecular Aglycone Delivery.....	43
Scheme 3-6: (A) General Scheme for Oxidative Tethering and Aglycone Delivery (B) Affect of Tethering on the Stereochemical Outcome of the Mixed Acetal.....	44
Scheme 3-7: Silicon Tethering for Intramolecular Aglycone Delivery.....	46

Scheme 3-8: Fraser-Reid Serendipitous Discovery	48
Scheme 3-9: Relative Rates of Glycosylation Reactions of <i>n</i> -Pentenyl Glycosides Affected by Alcohol Protecting Group	48
Scheme 3-10: Mechanism of Glycosylation with <i>n</i> -Pentenyl Glycosides.....	49
Scheme 3-11: Various Latent-Active Glycosylation Reactions	50
Scheme 3-12: Lee's Activation of Thioglycosides with NIS/AW-300 MS	52
Scheme 3-13: "Disarmed" Thioglycosyl Donor and "Armed" Acceptor Addition via Hypervalent Iodine	53
Scheme 3-14: Activation of Thioglycosides with DIDMH for Glycosylation.....	54
Scheme 3-15: (A) Intermolecular Glycosylation Reaction Using Propargyl Co ₂ (CO) ₆ as the Glycosyl Acceptor (B) Mechanism for Glycosylation Reaction using Propargyl Co ₂ (CO) ₆ as Thioglycoside Activator.....	55
Scheme 3-16: Selective Alkyl Thioglycosides Activation	56
Scheme 4-1: Synthesis of a Glucose Sugar Silane from a 2-Hydroxy Sugar	57
Scheme 4-2: Dehydrogenative Silylation of Alcohols and Hydrosilylation of Ketones with Sugar Silanes	58
Scheme 4-3: The Effect of the Thiol Leaving Group on Aglycone Delivery.....	60
Scheme 4-4: Potential Mechanistic Pathways for Aglycone Delivery	61
Scheme 4-5: A) Sun's Intermolecular Glycosylation B) Proposed Mechanism for Sun's Intermolecular Glycosylation.....	62
Scheme 4-6: Synthesis of 2-Hydroxy Mannose Sugar Silane Precursor	64
Scheme 4-7: Synthesis of Several Mannose Sugar Silanes	65
Scheme 4-8: First Three Steps of the Synthesis of Glucose Sugar Silanes	65

Scheme 4-9: Addition of 2-Iodophenol to Orthoformate 4-31	66
Scheme 4-10: (A) Synthesis of Glucose β -2-Hydroxy Sugar (B) Synthesis of Glucose α -2-Hydroxy Sugar	67
Scheme 4-11: Synthesis of α - and β -Glucose Sugar Silanes.....	68
Scheme 4-12: Aglycone Deliveries with Mannose Derived Sugar Silanes	70
Scheme 4-13: Tethering and Aglycone Deliveries of Hydroxy Sugars.....	71
Scheme 4-14: Tethering of (-)-Menthol with both Anomers of Glucose Sugar Silanes	74
Scheme 4-15: Glucose Aglycone Delivery of (-)-Menthol.....	75
Scheme 4-16: Goals for Asymmetric Tethering before Aglycone Delivery	76
Scheme 4-17: General Trends for Nickel-Catalyzed Asymmetric Hydrosilylation of Acetophenone	77
Scheme 4-18: Asymmetric Hydrosilylation with Glucose Thiosugar Silane	78
Scheme 5-1: Summation of Regioselective Hydroboration of Olefins	81
Scheme 5-2: Summation of the Synthesis of Mannose Sugar Silane and Aglycone Tethering/Delivery of Menthol.....	81

List of Tables

Table 1-1: Regioselectivity of Sterically Encumbered Alkenes with Various Boranes	5
Table 1-2: Regioselectivity Affects on the Electronic of Benzene Groups on the Hydroboration of Alkynes with Various Boranes	6
Table 2-1: Initial Investigation into Regioselective Hydroboration of 2-19.....	21
Table 2-2: Copper-NHC Optimization for Hydroboration of 2-19	23
Table 2-3: Copper-Catalyzed Hydroboration of 2-Octene	32
Table 2-4: Investigation into the Hydroboration of 1,2-Disubstituted Olefins.....	33
Table 2-5: Optimization of Hydroboration for 1,1-Disubstituted Olefins.....	35
Table 4-1: Optimization of Tethering (-)-Menthol to Mannose Sugar Silanes	69
Table 4-2: Attempted Aglycone Delivery with Other Electrophilic Halogen Sources and Solvents	72
Table 4-3: Lewis Acid Screen for Aglycone Delivery	73
Table 6-1: Racemic SFC Trace for 4-Phenyl-2-butanol 3 Minute Run.....	105
Table 6-2: SFC Trace for Reaction with Ligand 2-59	106
Table 6-3: Racemic SFC Trace for 4-Phenyl-2-butanol.....	107
Table 6-4: HPLC Trace for Reaction with Ligand 2-60 at Room Temperature.....	108
Table 6-5: HPLC Trace for Reaction with Ligand 2-60 at -35 °C	109
Table 6-6 SFC Trace for Reaction with Ligand 2-61	110
Table 6-7: Racemic SFC Trace for 4-Phenyl-2-butanol 10 Minute Run.....	111

Table 6-8: Reaction Using Catalyst 2-62 in Tetrahydrofuran	112
Table 6-9: Reaction Using Catalyst 2-62 in Toluene.....	113
Table 6-10: Reaction Using Catalyst 2-62 in Tetrahydrofuran	114
Table 6-11: Calibration Curve for 2-27	115
Table 6-12 Hydroboration of Internal Olefins with Nickel and Palladium	116
Table 6-13 Hydroboration of Internal Olefins with Iron	117
Table 6-14 Hydroboration of Internal Olefins with Cobalt and Additive	117
Table 6-15 Hydroboration of Internal Olefin with Cobalt and No Additive	118
Table 6-16 Hydroboration of Internal Olefins with Palladium and Phosphine Ligands	119
Table 6-17 Hydroboration of Internal Olefins with Copper	120
Table 6-18: Racemic SFC Trace for 4-53.....	153
Table 6-19: SFC Trace for Reaction with Ligand A.....	154
Table 6-20: SFC Trace for Reaction with Ligand B.....	155
Table 6-21: SFC Trace for Reaction with Ligand C.....	156
Table 6-22: SFC Trace for Reaction with Ligand D at 0 °C	157
Table 6-23: SFC Trace for Reaction with Ligand D and <i>t</i> BuMe ₂ Si.....	158
Table 6-24: SFC Trace for Reaction with Ligand D and PhMe ₂ Si.....	159
Table 6-25: SFC Trace for Reaction with Ligand E.....	160
Table 6-26: SFC Trace for Reaction with Ligand F	161

List of Figures

Figure 3-1: Common 1,2- <i>cis</i> and 1,2- <i>trans</i> glycosides.....	37
Figure 3-2: (A) Solid-Support for Oxidative Tethering/ Intramolecular Aglycone Delivery (B) Sulfolipid-I.....	45
Figure 3-3: Various Leaving Groups of Glycosyl Donors.....	47
Figure 3-4: Structures of DMTST and IDCP.....	51
Figure 4-1: Diisopropyl Thiosugar Silanes.....	59
Figure 4-2: New Sugar Silanes	63
Figure 4-3: Various Electronics and Sterics of the Alkyne for Latent-Activation	79
Figure 6-1: Spectra for 1-Allyl-2-methylenecyclohexane	162
Figure 6-2: Spectra for Hex-5-enyl Pivalate.....	163
Figure 6-3: Spectra for 1-(But-3-enyl)-1 <i>H</i> -indole	164
Figure 6-4: Spectra for Compound 2-1	165
Figure 6-5: Spectra for Compound 2-27.....	166
Figure 6-6: Spectra for Compound 2-28.....	167
Figure 6-7: Spectra for Compound 2--29.....	168
Figure 6-8: Spectra for Compound 2-30.....	169
Figure 6-9: Spectra for Compound 2-32.....	170
Figure 6-10: Spectra for Compound 2-32.....	171
Figure 6-11: Spectra for Compound 2-33.....	172

Figure 6-12: Spectra for Compound 2-34.....	173
Figure 6-13: Spectra for Compound 2-35.....	174
Figure 6-14: Spectra for Compound 2-36.....	175
Figure 6-15: Spectra for Compound 2-37.....	176
Figure 6-16: Spectra for Compound 2-38.....	177
Figure 6-17: Spectra for 1-(3-(4,4,5,5-Tetramethyl-1,3,2-dioxaborolan-2-yl)propyl)-1 <i>H</i> -indole	178
Figure 6-18: Spectra for Compound 2-39.....	179
Figure 6-19: Spectra for Potassium (4-Phenylbutan-2-yl)trifluoroborate	180
Figure 6-20: Spectra for Potassium (6-hydroxyhexan-2-yl)trifluoroborate.....	181
Figure 6-21: Spectra for Potassium (6-(pivaloyloxy)hexan-2-yl)trifluoroborate	182
Figure 6-22: Spectra for Potassium (4-(1 <i>H</i> -indol-1-yl)butan-2-yl)trifluoroborate.....	183
Figure 6-23: Spectra for 2-52.....	184
Figure 6-24: Spectra for 2-53.....	185
Figure 6-25: Spectra for 2-54.....	186
Figure 6-26: Spectra for 2-55.....	187
Figure 6-27: Spectra for 2-56.....	188
Figure 6-28: Spectra for 2-57.....	189
Figure 6-29: Spectra for 2-58.....	190
Figure 6-30: Spectra for 2-68.....	191
Figure 6-31: Spectra for 2-71.....	192
Figure 6-32: Spectra for 4-24.....	193
Figure 6-33: Spectra for 4-25.....	194

Figure 6-34: Spectra for 4-26.....	195
Figure 6-35: Spectra for 4-27.....	196
Figure 6-36: Spectra for 4-28.....	197
Figure 6-37: Spectra for 4-31.....	198
Figure 6-38: Spectra for 4-32.....	199
Figure 6-39: Spectra for 4-33.....	200
Figure 6-40: Spectra for 4-35.....	201
Figure 6-41: Spectra for 4-36.....	202
Figure 6-42: Spectra for 4-37.....	203
Figure 6-43: Spectra for 4-38.....	204
Figure 6-44: Spectra for 4-21.....	205
Figure 6-45: Spectra for 4-29.....	206
Figure 6-46: Spectra for 4-30.....	207
Figure 6-47: Spectra for 4-22.....	208
Figure 6-48: Spectra for 4-39.....	209
Figure 6-49: Spectra for 4-40.....	210
Figure 6-50: Spectra for 4-41.....	211
Figure 6-51: Spectra for 4-42.....	212
Figure 6-52: Spectra for 4-44.....	213
Figure 6-53: Spectra for 4-46.....	214
Figure 6-54: Spectra for 4-48.....	215

List of Abbreviations

9-BBN: 9-borabicyclo(3.3.1)nonane

α : alpha

Å: angstrom

Ac: acetate

Ar: aryl

AW: acid washed

β : beta

Bn: benzyl

bpy: 2,2'-bipyridine

Bpin: pinacolboron

Boc: *tert*-butyloxycarbonyl protecting group

Bu: butyl

Bz: benzoyl

dba: dibenzylideneacetone

c: cyclo

C: Celsius

CFL: compact fluorescent light

cm: centimeters

cod: cyclcooctadiene

d: doublet

DDQ: 2,3-dichloro-5,6-dicyano-1,4-benzoquinone

DG: directing group

DIDMH: 1,3-diiodo-5,5-dimethylhydantoin

DMAP: 4-(dimethylamino)pyridine

dFCF₃ppy: 2-(2,4-difluorophenyl)-5-(trifluoromethyl)pyridine

DFT: density functional theory

dme: dimethoxyethane

DMF: dimethylformamide

dmpd: dimethylpentanediol

DMSO: dimethyl sulfoxide

DMTST: dimethyl(methylthio)sulfonium triflate

dr: diastereomeric ratio

dtbbpy: 4,4'-di-*tert*-butyl-2,2'-bipyridine

DTBMP: di-*tert*-butyl methyl pyridine

ee: enantiomeric excess

EI: electrospray ionization

er: enantiomeric ratio

Et: ethyl

EtOAc: ethyl acetate

equiv: equivalent

γ: gamma

GC-FID: gas chromatography-flame ionization detector

h: hour

HRMS: high resolution mass spectroscopy

i: iso, equal

i. e.: that is

IDCP: iodonium dicollidine perchlorate

icp: monoisopinocampheyl

IMes: 1,3-Bis(2,4,6-trimethylphenyl)-1,3-dihydro-2*H*-imidazol-2-ylidene

IPr: 1,3-Bis(2,6-diisopropylphenyl)-1,3-dihydro-2*H*-imidazol-2-ylidene

IPr*OMe: N,N'-Bis(2,6-bis(diphenylmethyl)-4-methoxyphenyl)imidazole-2-ylidene

IR: infrared spectroscopy

J: coupling constant

L: ligand

L_n: ligands

LG: leaving group

μ: micro

M: molarity, transition metal

m: multiplet

Me: methyl

mg: milligram

MHz: mega hertz

mL: milliliter

mmol: millimole

mol: mole

MOM: methoxymethyl

MS: molecular sieves, mass spectroscopy

Ms: mesyl

MSH: *O*-mesitylenesulfonylhydroxylamine

***n*:** normal

NBS: *N*-bromosuccinimide

NCS: *N*-chlorosuccinimide

NHC: *N*-heterocyclic carbene

NIS: *N*-iodosuccinimide

NMR: nuclear magnetic resonance

PG: protecting group

Ph: phenyl

PIFA: phenyliodine(III) bis(trifluoroacetate)

ppm: parts per million

Pr: propyl

R: generic group

rs: regioselectivity

rt: room temperature

s: singlet

(S)-DTBM-SEGPPOS: (*S*)-(+)-5,5'-Bis[di(3,5-di-*tert*-butyl-4-methoxyphenyl)phosphine]-4,4'-

bi-1,3-benzodioxole

Sia: *sec*-isoamyl, 1,2-dimethylpropyl

SET: single electron transfer

SFC: supercritical fluid chromatography

SIPr: 1,3-Bis-(2,6-diisopropylphenyl)imidazolium

t: tertiary

t: triplet

TBS: *tert*-butyldimethyl silyl

Temp: temperature

Teoc: 2-trimethylsilylethoxycarbonyl

Tf: trifluoromethanesulfonyl, triflate

THF: tetrahydrofuran

TIPS: *triisopropylsilyl*

TMS: trimethylsilyl

Tol: 4-methylbenzene

Ts: tosyl, *para*-toluenesulfonyl

W: watt

X: halogen, leaving group, generic group

Y: generic group

Abstract

The development of regioselective and diastereoselective processes provides chemists with versatile synthetic tools to access new synthetic pathways. This thesis focuses on two specific areas of regio- and diastereocontrol: hydroboration of olefins and intramolecular aglycone deliveries. The first chapter provides background literature containing existing reported strategies for regiocontrol using copper catalysts in hydroboration of olefins. This chapter lays the groundwork and motivation for investigation into the hydroboration of olefins. Subsequently, the second chapter discusses the development of a versatile procedure for the copper-catalyzed hydroboration of terminal olefins leading to the synthesis of secondary alkylboranes. This procedure provides the reversed regioselectivity compared with widely used hydroboration procedures. The newly synthesized secondary alkylboranes can be transformed to the corresponding trifluoroborate salts and used in photocatalytic cross-couplings to synthesize new carbon-carbon bonds. Furthermore, advances in the regioselective hydroboration of 1,1-disubstituted and 1,2-disubstituted alkenes are described, with efforts in the former of these areas providing the most promising outcomes for future applications.

The third chapter begins with a discussion of literature methods for intramolecular aglycone delivery in the synthesis of 1,2-*cis* glycosides. Within this context, an overview of activating thioglycosides and latent-activation of glycosides for intermolecular glycosylation reactions is provided. The fourth chapter describes the preparation of sugar silanes containing an *o*-(*p*-methoxyphenylethynyl)phenyl group and their utilization in intramolecular aglycone

delivery strategies. Beginning with the new silanes prepared, dehydrogenative silylation with menthol was accomplished with tris(pentafluorophenyl) borane catalyst, effectively tethering the aglycone. The tethered assemblies were then examined in intramolecular aglycone delivery strategies. High levels of diastereocontrol were observed, and future work will focus on optimization of the glycosylation yields.

Chapter 1 Introduction to Copper-Catalyzed Hydroboration

1.1 General Overview of Thesis

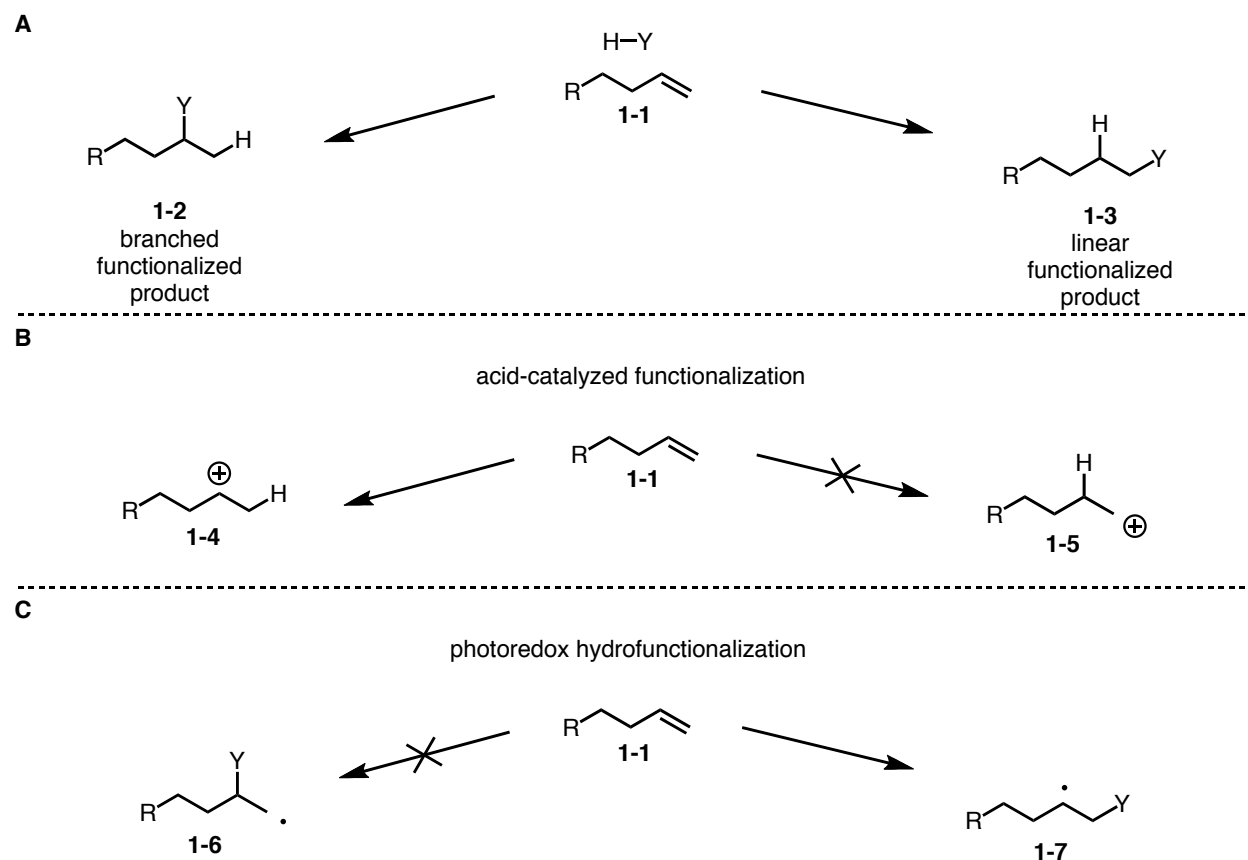
Of the multitude of topics taught in sophomore organic chemistry, regioselectivity and stereoselectivity are key pillars upon which notions of targeted synthesis provide a key foundation for strategies in targeted synthesis. From the difunctionalization of olefins to electrophilic aromatic substitution and Diels-Alder cycloadditions, notions of regioselectivity play a key role in how both students and researchers understand synthetic routes to drug targets, complex monomers, and beyond. Within these systems, regioselective outcomes are either rationalized via an electronic argument, a steric argument, or a combination of both sterics and electronics. These simplistic arguments often lead students to one straightforward result; however, in reality there are many other compounding factors contributing to regiocontrol. In the chapters that follow, this thesis discusses two projects that provide new methods for regio- and diastereocontrol: the synthesis of secondary alkylboranes from alkenes via copper-NHC catalysis, and the synthesis of 1,2-*cis* glycosides selectively via sugar silane intermediates

1.2 Regioselectivity Explanations for Hydrofunctionalization of Olefins

Hydrofunctionalization reactions of olefins are a sweeping set of reactions that comprise a large portion of topics in organic chemistry. The formal addition of “H-Y” to a terminal olefin results in two isomeric products, the branched functionalized product, in which functional group Y is added to the internal position of the olefin (**1-2**) and the linear functionalized product where functional group Y is added to the terminal position of the olefin (**1-3**) (Scheme 1-1 A).

One of the first reactions often taught in sophomore organic chemistry is the acid catalyzed electrophilic addition of “H-X” to an olefin. The first step of the mechanism proceeds with protonation of the olefin to give a carbocation, which is then attacked by the nucleophilic “X” species. The initial carbocation formation is what dictates the regioselectivity of the reaction. Two potential carbocations can be formed: secondary carbocation **1-4**, and a primary carbocation **1-5** (Scheme 1-1 B). The increased stability from hyperconjugation of neighboring carbons causes the secondary carbocation to be more stable, resulting in the predominant observation of the secondary branched product.

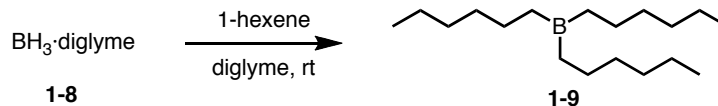
The analogous linear product can be synthesized but the regioselectivity is governed not by carbocation stability but rather radical stability. The Nicewicz group has demonstrated that an acridinium photooxidant can undergo a single electron transfer first adding the “X” group while simultaneously forming a secondary radical. The resulting radical undergoes a hydrogen abstraction from a hydrogen donor also present in solution (Scheme 1-1 C).¹ Similar arguments to carbocation stability apply to radical stability, but this method offers a switch in order of addition of the “H” and “X” atoms, thus favoring the formation of the linear functionalized product.



Scheme 1-1: (A) Two Regioisomeric Product from H-X Addition to an Olefin (B) Carbocation Stability in Acid-Catalyzed Hydrofunctionalization (C) Radical Stability in Photoredox Hydrofunctionalization

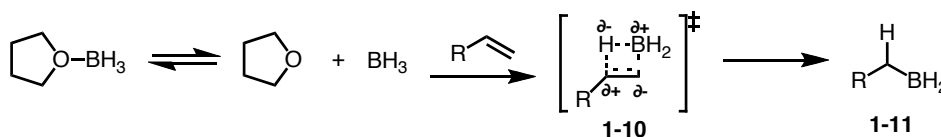
1.3 Influence of Herbert C. Brown on Organic Synthesis

Another reaction that is typically taught alongside the electrophilic addition of “H-X” unit is the hydroboration of olefins. It was first reported in 1948 that heating diborane and ethylene together at 100 °C resulted in the synthesis of triethylborane.² Several years later, it was discovered that diborane in ethereal solvents was able to undergo hydroboration with 1-hexene at room temperature (Scheme 1-2),^{3,4} a discovery made by Herbert C. Brown who would later go on to win the Nobel Prize in Chemistry for his work to incorporate boron into organic synthesis. In addition to research into a fundamental topic of organic chemistry, his work with borane in ethereal solvents led to the development and utility of the $\text{BH}_3 \cdot \text{THF}$ complex that is commercially available today.⁴



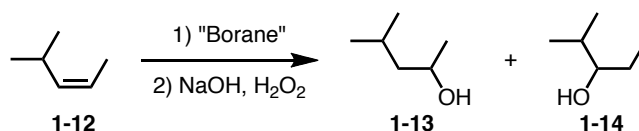
Scheme 1-2 Brown's Hydroboration in Ethereal Solvents Discovery

Brown has been credited with the widely accepted reaction mechanism for the hydroboration of alkenes.⁵ Rather than a two-step mechanism wherein regioselectivity of the reaction is dictated via stabilization of an intermediate (Scheme 1-3), this process is proposed to proceed through a concerted, one-step mechanism. Initially, the $\text{BH}_3 \cdot \text{THF}$ complex exists in equilibrium with the non-complexed BH_3 and THF molecule. Free BH_3 then reacts with an olefin via 4-membered transition state **1-10** due to the hydridic nature of the B-H bond, wherein partial charges align leading to a one-step formation of both C-H and C-B bonds. This mechanism leads to compound **1-11** as the major product.



Scheme 1-3: Mechanism for Brown's Hydroboration

This proposed mechanism explains the regioselectivity when the carbons of the olefin have different substitution patterns; however, sterics become a factor when substitution the olefin are of the same degree (Table 1-1).⁶ When *cis*-4-methyl-2-pentene (**1-12**) was subjected to hydroboration conditions with $\text{BH}_3 \cdot \text{THF}$, regioisomeric products **1-13** and **1-14** were observed in almost equal ratios after subsequent oxidation of the alkylboranes. When more sterically hindered disiamylborane (Sia_2BH) was used, selectivity shifted towards greater formation of the less sterically hindered alcohol **1-13**. Lastly, when the bulky 9-borabicyclo(3.3.1)nonane (9-BBN) was employed almost exclusive formation of **1-13** was observed. These results support the notion that there is a steric component to the hydroboration reaction between two electronically indistinguishable carbons.



Borane	1-13:1-14
BH ₃ ·THF	57:43
Sia ₂ BH	97:3
9-BBN	99.8:0.2

Table 1-1: Regioselectivity of Sterically Encumbered Alkenes with Various Boranes

In addition to hydroborations of alkenes, Brown was able to apply this hydroboration methodology to a different π -system: alkynes.⁷ Overall, monohydroboration was observed as the major product, as the monocarbonyl was isolated after oxidation. Terminal alkynes behaved in a similar manner as terminal alkenes, where boron incorporation occurred predominantly at the terminal carbon. Once again, regioselectivity of internal alkynes was dictated by the sterics of the alkyne substituents. Brown discovered that an additional electronic effect was seen when one of the substituents on the alkyne was a phenyl group, such as observed with phenylacetylene substrate **1-15** (Table 1-2). Subjecting this substrate to BH₃·THF was resulted in benzylic ketone **1-16** formation in approximately a 3:1 ratio with homobenzylic aldehyde **1-17**. As expected, use of the larger borane Sia₂BH favored the formation of aldehyde **1-17**. However, unlike the trend observed with sterics and selectivity in Table 1-1, the electronic contribution of the phenyl group resulted in 9-BBN favoring the benzylic ketone **1-16** in approximately a 2:1 ratio.

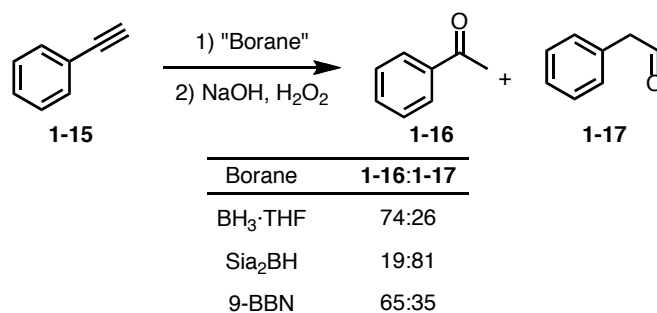
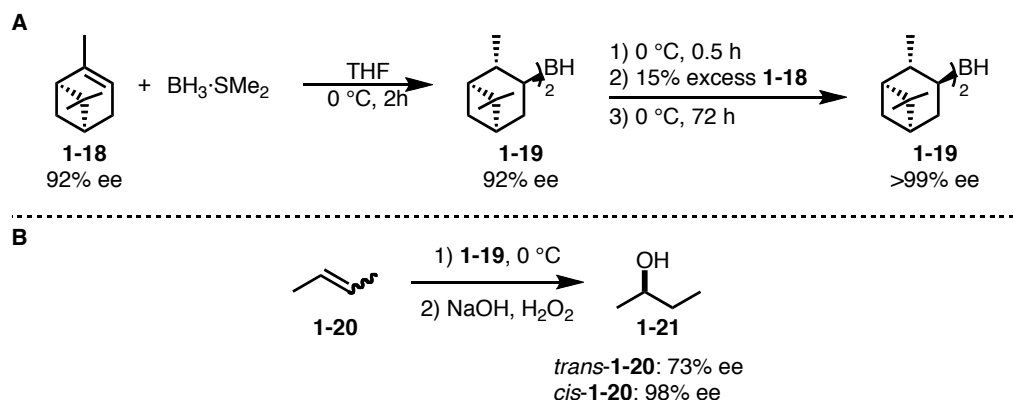


Table 1-2: Regioselectivity Affects on the Electronic of Benzene Groups on the Hydroboration of Alkynes with Various Boranes

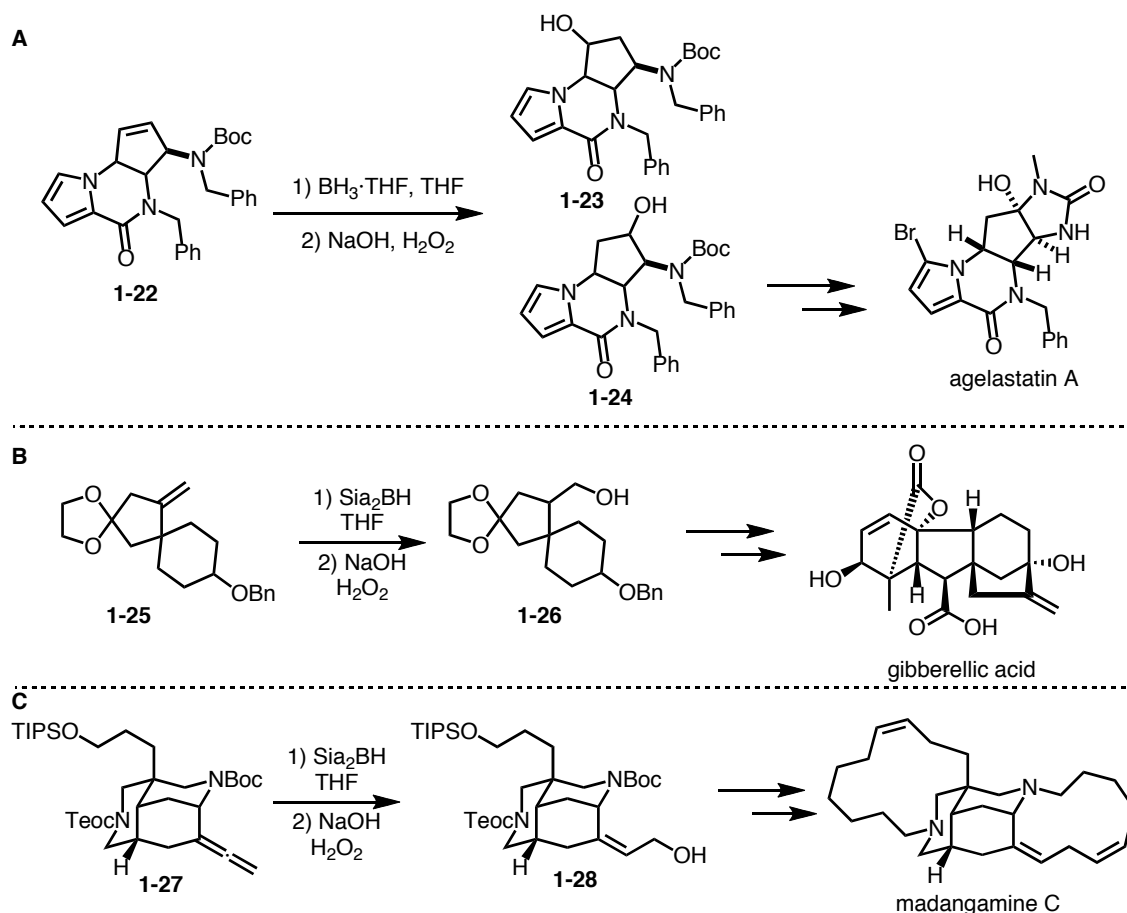
Moreover, Brown went on to report the first enantioselective hydroboration reactions using monoisopinocampheylborane (ipcBH₂, **1-19**) as a chiral boron source (Scheme 1-4).^{8,9} Brown was then able to improve the synthesis of **1-19** by truncating the mixing time of α -pinene (**1-18**) and BH₃·SMe₂ to synthesize desired **1-19**; however, the ee was not optimal, as it resembled the original enantioselectivity of **1-18** (Scheme 1-4 A). A series of cooling and mixing **1-19** with excess **1-18** increased the enantioselectivity of **1-19** to >99% ee, which was then used in subsequent hydroboration reactions (Scheme 1-4 B). Both *trans*- and *cis*-alkene **1-20** successfully were hydroborated but the enantioselectivities differed. The *trans*-isomer resulted in the formation of chiral alcohol **1-21** in 73% ee while the *cis*-isomer had higher enantioselectivity of 98% ee – indicating that *trans*-isomers are more difficult to react in an enantioselective fashion.



Scheme 1-4: (A) Synthesis of Icp₂BH (B) Enantioselective Hydroboration with Icp₂BH

Brown's investigation into the hydroboration of olefins and alkynes has provided a useful synthetic tool in total synthesis (Scheme 1-5). For example, Weinreb's total synthesis of the

antitumor agent agelastatin A, originally isolated from a marine sponge, utilized Brown's hydroboration conditions on internal olefin **1-22**, which resulted in the formation of two isomeric products, **1-23** and **1-24** (Scheme 1-5 A).¹⁰ Optimization efforts to bias selectivity towards the formation of desired product **1-24** proved unsuccessful, but selective oxidation allowed for separation of the isomers before proceeding forward. Corey also used a hydroboration reaction in his second generation total synthesis of gibberellic acid, a hormone found in plants and fungi (Scheme 1-5 B).¹¹ The hydroboration of **1-25** to **1-26** installs the functional handle needed to synthesize the bridged bicycle. More recently, Sato and Chida demonstrated how the hydroboration of **1-27** to **1-28** establishes the core structure of not only madangamine C, but, also madangamine E and madangamine A – three additional alkaloids isolated from marine sponges (Scheme 1-5 C).¹²



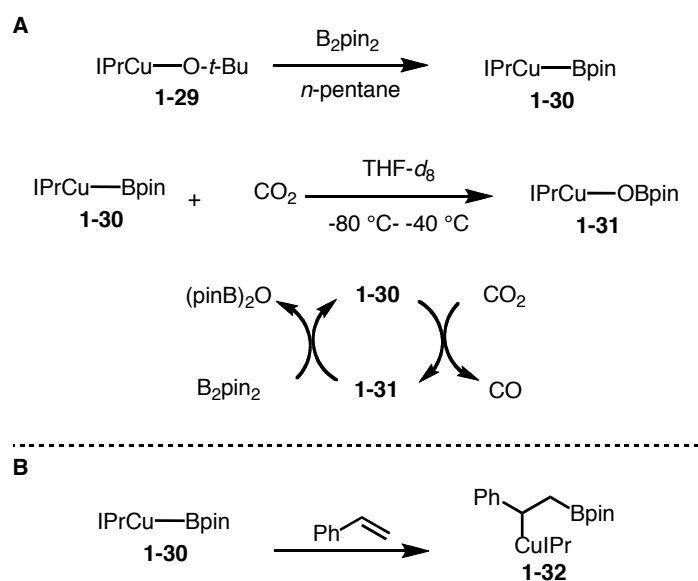
Scheme 1-5: (A) Weinreb's Total Synthesis of Agelastatin A (B) Corey's Total Synthesis of Gibberellic Acid (C) Sato and Chida's Total Synthesis of Madangamine C

1.4 Copper-Catalyzed Hydroboration

In 1985, the first report of metal-catalyzed hydroboration of olefins was described by Noth.¹³ He demonstrated that Wilkinson's rhodium catalysts $[\text{RhCl}(\text{PPh}_3)_3]$ preferred to undergo hydroboration of olefins rather than undergo reduction of ketones in the presence of catecholborane. Since this initial introduction of metal-catalyzed hydroboration of olefins, the field has taken off, and expanded the metal identity to include iridium,¹⁴ ruthenium,¹⁵ titanium,¹⁶ early transition metals,¹⁷ palladium,¹⁸ iron,¹⁹ cobalt,²⁰ manganese,²¹ nickel,²² and platinum²³ to name just a few. Copper not mentioned above, will be covered in greater depth later to be able to foster the experimental data discussed in Chapter 2.

1.4.1 Initial Proof of Concept for Copper-Boron Complex

The first introduction of a copper-boron complex was by Sadighi in 2005 (Scheme 1-6).²⁴ Discrete *N*-heterocyclic carbene (NHC)-copper(I) *tert*-butoxide complex **1-29** was subjected to ligand exchange conditions with bis(pinacolato)diboron (B_2pin_2) to form NHCCu-Bpin complex **1-30** where complex **1-30** successfully reduced CO_2 to CO (Scheme 1-6 A). Although this reaction is not a hydroboration, discussing it serves to demonstrate the chemical compatibility of boron and copper. Follow up investigation revealed the same **1-30** complex could readily react with an alkene, and upon alkene insertion between the copper and boron bond form stoichiometric isolable copper-boron species **1-32** (Scheme 1-6 B).²⁵

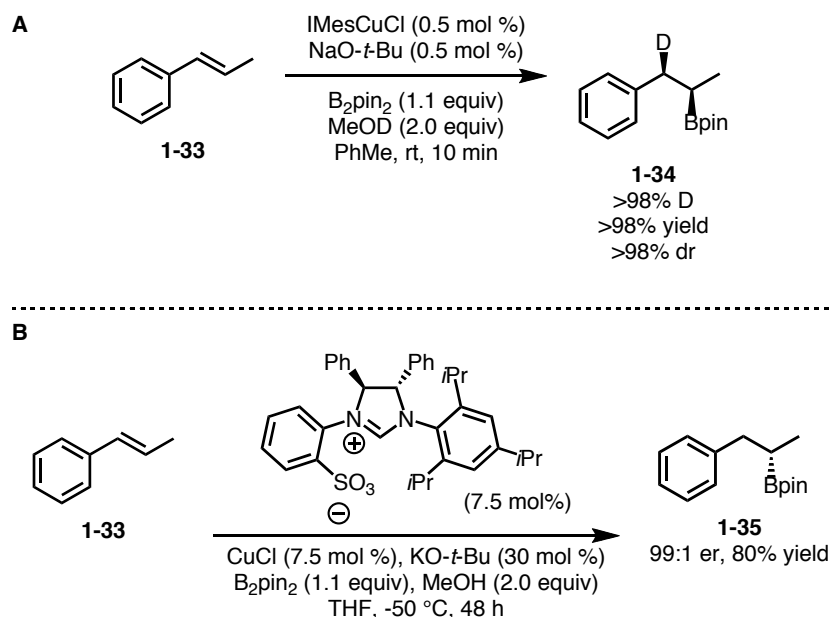


Scheme 1-6: (A) First Report of Copper-Boron Complex (B) First Indication Copper Catalyzed Hydroboration Reactions of Olefins

1.4.2 Initial Copper-Catalyzed Hydroboration

Three years later drawing inspiration from Sadighi, Hoveyda developed a catalytic method for copper-catalyzed hydroboration of olefins (Scheme 1-7).²⁶ The key to successful catalyst turnover was the addition of stoichiometric methanol to protonate the copper-carbon species, thereby preparing the catalyst for turnover. In this seminal work, it was also determined that the formal hydroboration occurs on the same face of the olefin, resulting in diastereoselectivity

analogous to the hydroboration methods previously established by Brown (Scheme 1-7 A). Lastly, the report demonstrated that by using a chelating chiral NHC ligand, enantioselective hydroboration could be achieved (Scheme 1-7 B).

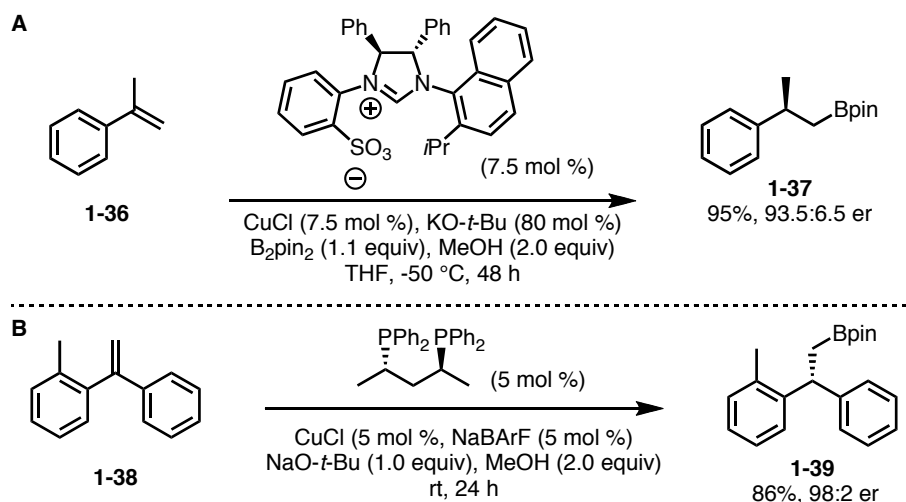


Scheme 1-7: (A) Formal Deuteroboration of Styrene Derivatives with High Diastereoselectivity (B) Enantioselective Hydroboration of Styrene Derivatives

1.4.3 Copper-Catalyzed Hydroboration of Other Olefin Classes

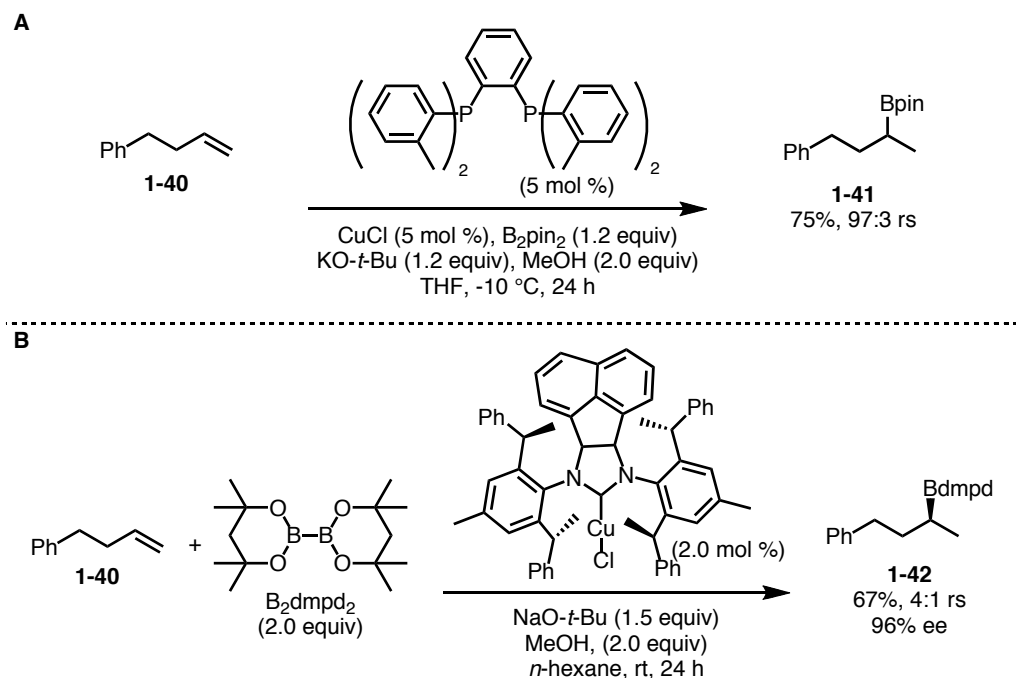
Expansion of the copper-catalyzed hydroboration reaction methodology to other olefin classes besides mono-substituted styrene derivatives followed shortly thereafter. One complicated substrate class chosen was 1,1-disubstituted styrene derivatives, which due to the increased substitution of the olefin would require the formation of a tertiary-copper complex. Two years after his publication, Hoveyda demonstrated that α -methyl styrene **1-36** and its derivatives readily undergo enantioselective hydroboration to chiral borylated product **1-37** via a copper-NHC complex formed *in situ* (Scheme 1-8 A).²⁷ Zhang was able to expand the substrate scope from simple alkyl and aryl substitution to diaryl-substitution and arrive at analogous enantioenriched alkylboranes using a chiral phosphine-copper complex (Scheme 1-8 B).²⁸ Shortly after this publication, mechanistic considerations by DFT studies indicated that the

hydroboration reaction of 1,1-disubstituted styrene derivatives does indeed involve a tertiary copper intermediate.²⁹



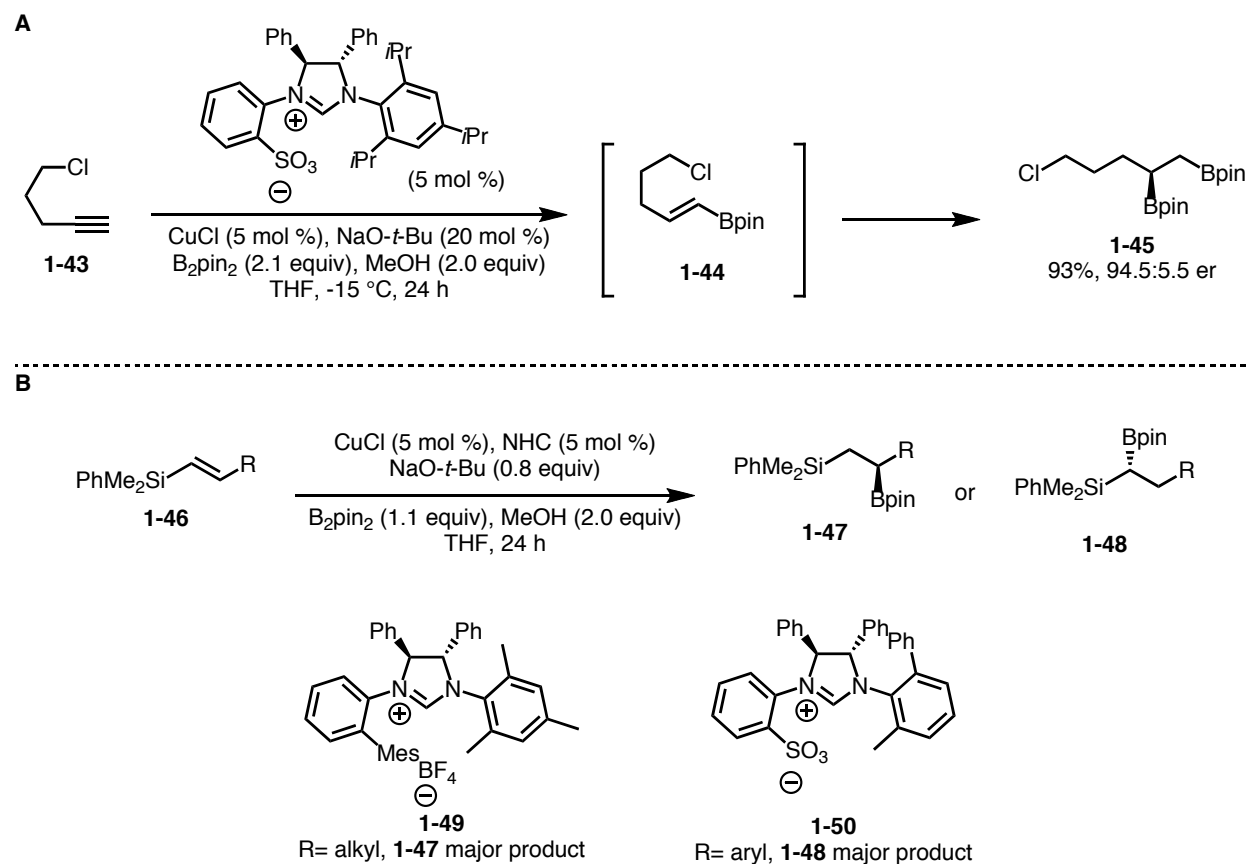
Scheme 1-8: Hydroboration of 1,1-Disubstituted Styrene Derivatives

Another class of terminal olefin that has been explored in copper-catalyzed hydroboration are non-conjugated, mono-substituted olefins. While our contributions in this field will be discussed further in Chapter 2, there are other notable reports that will be discussed in the pages that follow (Scheme 1-9). Ito developed a phosphine-copper catalyzed hydroboration of terminal olefins that leads to the formation of the secondary alkylborane over the linear alkylborane (Scheme 1-9 A).³⁰ Although regioselectivities for the branched alkylborane were high across multiple functionalized olefins, reaction yields were modest. Both the Hong and Shi groups recently reported NHC-copper systems that catalyze enantioselective hydroboration reactions for the synthesis of enantioenriched secondary alkylboranes (Scheme 1-9 B).³¹ Using NHCs that were designed and synthesized by the late Robert Gawley,³² chirality about the aromatic ring system is used to induce enantioselectivity but use of the larger boron source, bis(dimethylpentanediol)diboron (B_2dmpd_2), was necessary to increase enantioselectivity.



Scheme 1-9: Hydroboration of Mono-Substituted, Terminal Olefins

A significantly more difficult substrate class for hydroboration reactions is 1,2-disubstituted olefins. As mentioned previously, although Brown was able to successfully perform hydroboration reactions, he faced regioselectivity issues when electronics or sterics were not bias enough to significantly differentiate between the two carbon centers. Leveraging differences in olefin electronics, Hoveyda demonstrated that diborylation of alkyne **1-43** most likely proceeds through a vinylborane species **1-44**, indicating vinylboranes successfully undergo hydroboration reactions in high regioselectivity and enantioselectivity, as well as synthesizing vicinal diborane **1-45** using a chelating NHC-copper catalyst (Scheme 1-10 A).³³ Hoveyda was then able to expand this methodology to the hydroboration of vinylsilanes, thereby synthesizing enantioenriched vicinal and geminal borosilanes (Scheme 1-10 B).³⁴ The driving force for vicinal versus geminal borosilanes is tuned by based on the properties of the carbon substituent. An alkyl substituent with copper and ligand **1-49** leads to the vicinal borosilane **1-47**, while an aryl substituent with copper and ligand **1-50** leads to the geminal borosilane **1-48** due to the difference in the electronics of the olefin.

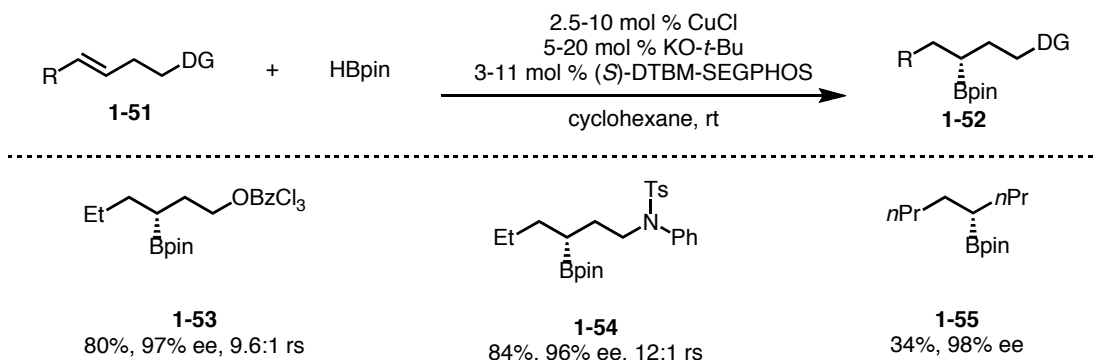


Scheme 1-10: Hoveyda's Hydroboration of 1,2-Disubstituted Olefins

As Hoveyda exploited the NHC-copper boron catalyst as the active catalyst for hydroboration of olefins with methanol as the proton source, Hartwig pioneered a complementary route for the synthesis of alkylboranes. Concurrent with these developments, Buchwald group demonstrated that a copper-hydride formed *in situ* could insert into a symmetric internal alkene³⁵ as Hartwig reported a regioselective insertion of an olefin into a copper-hydride via a directing group³⁶ to synthesize hydroaminated products.

With the knowledge that a copper-hydride could insert into an olefin, the concept of regioselective hydroboration of internal olefins using a directing group was further explored by Hartwig (Scheme 1-11).³⁷ Use of a homoallyl-directing group – such as protected nitrogens, ethers, or silyl ethers – achieved successful regioselective hydroboration. The use of chiral phosphine ligand, (*S*)-DTBMP-SEGPHOS, enabled high enantioselectivity in the reaction. After

performing DTF calculations, it was determined that hydride insertion is both the regiodetermining and enantiodetermining step of the reaction. This demonstrated that a directing group was not necessary for the reaction to proceed, although without one the overall reaction yield was low. This methodology was only applied to symmetric olefins (**1-55**) indicating the need for a directing group in order to achieve regioselectivity and enhance reactivity.

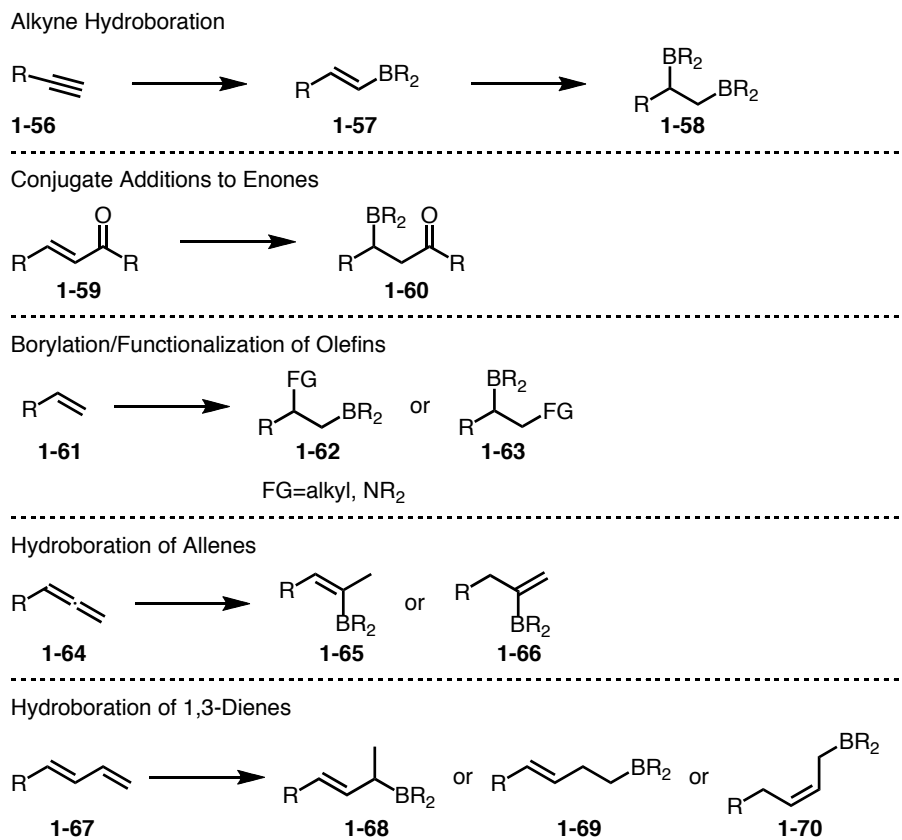


Scheme 1-11: Copper-Hydride Hydroboration of Internal Olefins with Select Examples

1.5 Conclusion

Even before the isolation of a copper-boron species in 2005, copper catalysis for the borylation of π -systems had been widely explored. As discussed in this chapter, the two main copper-catalyzed methods for the hydroboration of olefins use either (1) a copper-boron species to do alkene insertion followed by protonation by methanol, or (2) a copper-hydride species for insertion, followed by borylation by pinacolborane. These main strategies represent only a small subset of the copper catalyzed reactions in the presence of boronic starting materials (Scheme 1-12). With reagent control, alkynes are hydroborated to vinylborane species **1-57** or diborane species **1-58**.³³ Catalyzed by copper, conjugate addition to enone **1-59** leads to β -borylated product **1-60**.³⁸ Instead of protonating the copper-carbon species with methanol, the copper-carbon bond also can be alkylated³⁹ or aminated⁴⁰ forming **1-62** or **1-63**, depending on the ligand used. Similarly, regioselective hydroboration of allenes for the synthesis of **1-65** or **1-66** are divergent outcomes based on small differences in the reaction conditions.^{41,42} Furthermore,

regiocontrol in the hydroboration of 1,3-dienes can be achieved by copper catalysts.⁴² Overall, the use of the first row metal copper has catalyzed a wide variety of borylation reactions of many carbon-carbon π -systems.

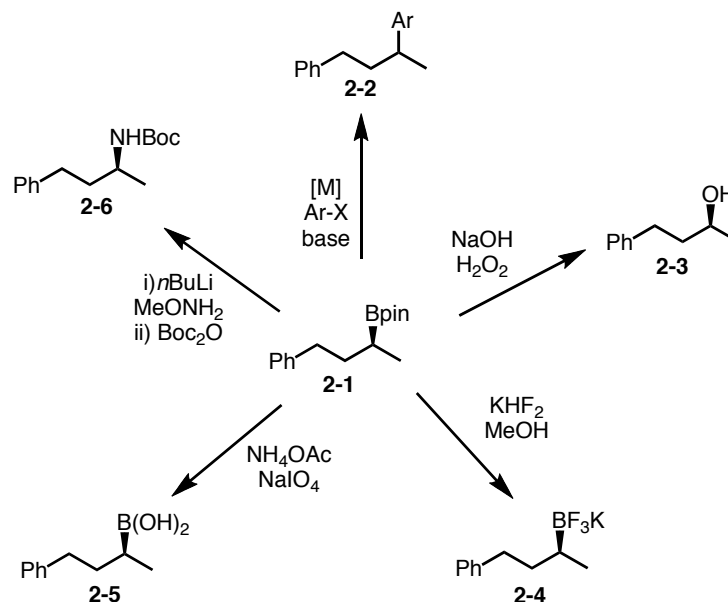


Scheme 1-12: Copper-Catalyzed Borylations of π -Systems

Chapter 2 Advances in Regioselective Hydroboration of Olefins

2.1 Introduction to Alkylboranes

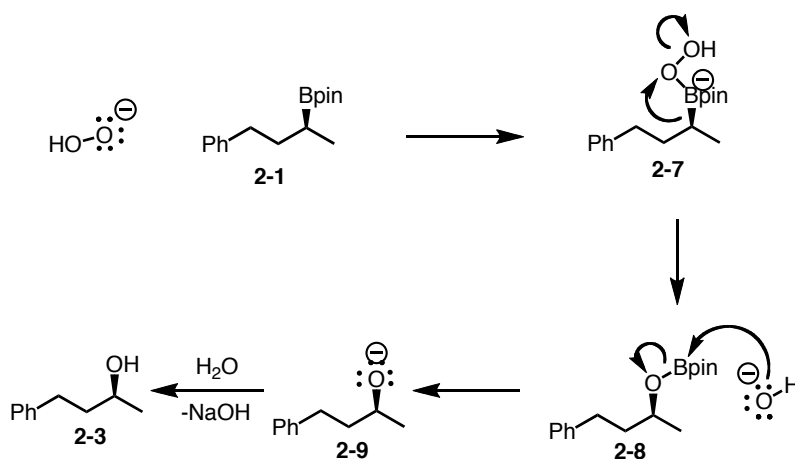
The versatility of organoboranes in synthesis has been of great interest to chemists for many years. Suzuki and Miyaura initially discovered the importance of carbon-boron bonds in cross-coupling reactions⁴³ while Morken,⁴⁴ Molander,⁴⁵⁻⁴⁹ and others⁵⁰⁻⁵³ have expanded upon this valuable functional moiety. Other useful transformations of carbon-boron esters such as oxidations,⁵⁴ aminations,⁵⁵ cleavage,⁵⁶ etc.¹⁵ as well as inter-conversion among boron identity⁵⁸⁻⁶⁰ have increased the attractiveness of synthesizing new organoboranes demanding the synthetic community to provide facile routes to alkylboranes (Scheme 2-1).



Scheme 2-1: Synthetic Transformation of Alkylboronic Esters

With the exception of some metal catalyzed cross-coupling, all of the previously mentioned boronic ester transformations are stereoretentive, maintaining the original

stereochemical identity of the carbon-boron bond. The mechanism of oxidation for the transformation of **2-1** to **2-3** demonstrates a generalizable pathway for the stereoretentive transformations (Scheme 2-2). First, a nucleophile is formed (deprotonation of hydrogen peroxide) followed by nucleophilic attack on the empty p orbital of the boron atom forming boronate species **2-7**. Boronate species **2-7** undergoes a 1,2-metallate shift at the boron center forming intermediate **2-8**. After an S_N2 attack at the boron center of **2-8**, alkoxy species **2-9** undergoes protonation, forming the desired oxidized product **2-3** with retention of the original stereocenter.

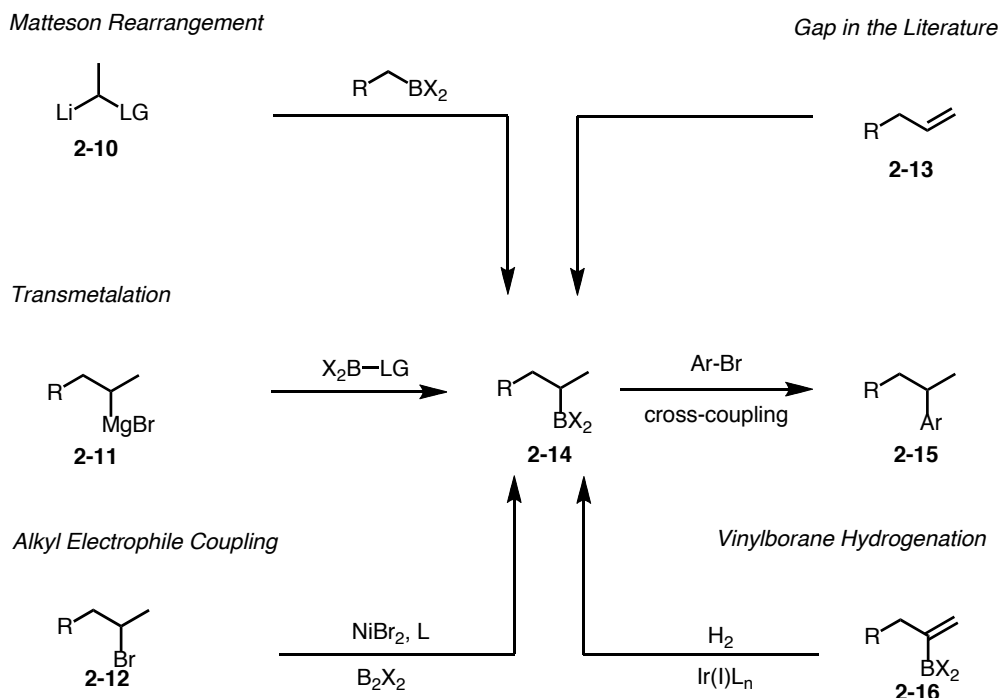


Scheme 2-2: Mechanism for Stereoretentive Oxidation

2.2 Previous Synthesis of Secondary Alkylboranes and Gap in the Literature

Due to their synthetic utility, syntheses of secondary alkylboranes have remained of interest in methodology development (Scheme 2-3). Variations of the Matteson rearrangement, which entails formation of a boronate species from an organolithium reagent that undergoes a 1,2-metallate shift, have been demonstrated to be desirable methods for the synthesis of secondary alkylboranes.⁶¹⁻⁶⁶ The transmetalation of organolithium or organomagnesium reagents to electrophilic boron species has been shown to be effective for synthesizing secondary alkylboranes.⁶⁷ Although both of these methods have shown to be useful, there is a limitation of

functional group compatibility as the strongly basic character of the organometallic reagents promotes undesirable side reactions. Metal-catalyzed cross-couplings efficiently convert secondary alkyl halides to organoboranes without observation of chain walking.^{68,69} While overcoming the challenge of cross-coupling sp^3 centers is no small feat, using halides as starting materials has its own synthetic drawbacks. Lastly, hydrogenation of vinylboranes has also been utilized for the synthesis of alkylboranes.⁷⁰⁻⁷² The synthesis of the vinylborane starting material involves hydroboration of alkynes. Although the aforementioned methods have their own niche in synthetic chemistry, at the onset of this investigation there were no reports of commercially available terminal olefins being directly converted to secondary alkylboranes. This would provide a facile method for transforming commodity chemicals and rapidly building up their complexity. Furthermore, accessing conditions that tolerate a wide variety of functional groups allows for the synthesis of new alkylboranes that can be transformed to other functional groups as well as new carbon-carbon bond via a variety of cross-coupling reactions. Additionally, it is important to note that the Ito group demonstrated a formal hydroboration of monosubstituted, terminal olefins via a copper-phosphine system; however, preparation of phosphine ligands provides additional synthetic challenges that may be circumvented using an alternative approach.³⁰

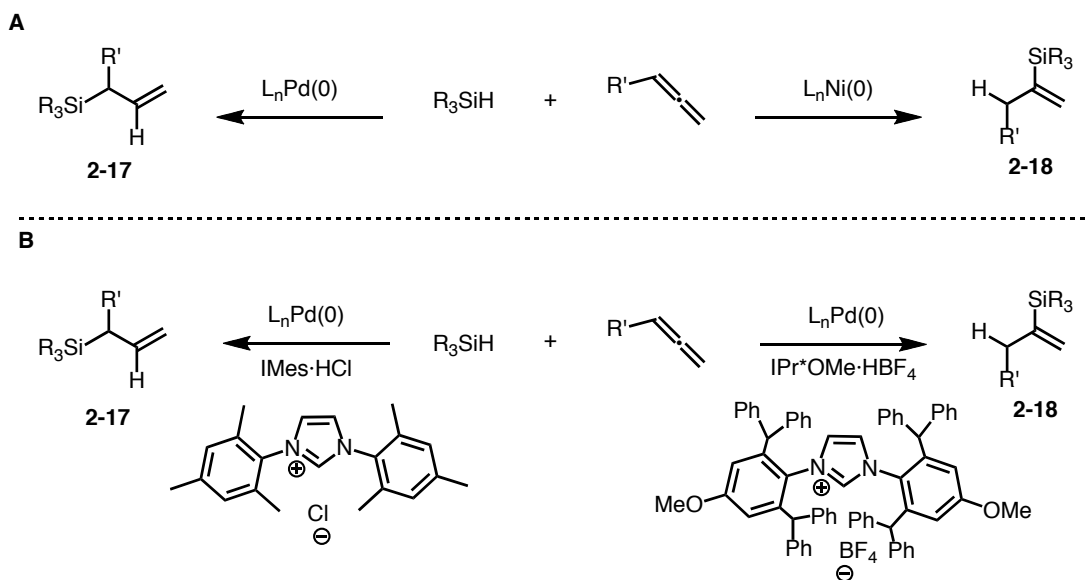


Scheme 2-3: Previous Approaches to Secondary Alkylboranes and the Gap in the Literature

2.3 Optimization of the Formal Hydroboration of Terminal Olefins

2.3.1 Rationale for Initial Optimization Conditions

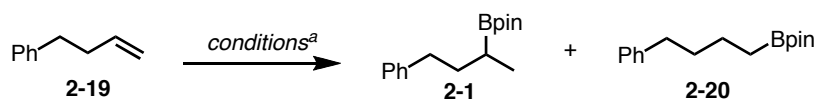
Regioreversal additions of H-X to π -systems has long been an interest of the Montgomery group.⁷³⁻⁷⁷ In 2013, it was reported that metal identity controls the regioselectivity for the hydrosilylation of allenes (Scheme 2-4 A).⁷⁶ Palladium favors the formation of allylsilanes (2-17), while nickel favors vinylsilanes (2-18). A followup investigation indicated that the size of the *N*-heterocyclic carbene (NHC) ligand employed affects the regioselectivity of the same addition, with a small ligand favoring 2-17 and a large ligand favoring 2-18 (Scheme 2-4 B).



Scheme 2-4: Examples of Regiocontrol for Hydrosilylation of Allenes (A) Metal Identity (B) Ligand Size

2.3.2 Optimization Using Pinacolborane

Drawing inspiration from the hydrosilylation of allenes, initial attempts for the hydroboration of terminal olefin **2-19** to the desired branched alkylborane **2-1** examined metal identity and ligand size (Table 2-1). When $\text{Pd}_2(\text{dba})_3$ was paired with what is typically classified as a small ligand, $\text{IMes}\cdot\text{HCl}$, and a large ligand, $\text{SIPr}\cdot\text{HCl}$, in tetrahydrofuran, decent reactivity was observed, 62% and 47%, respectively; unfortunately ~20:80 regioselectivity favoring undesirable alkylborane **2-20** was observed (entries 1-2). Similar regioselectivity results were observed when using $\text{Ni}(\text{cod})_2$ as a pre-catalyst (entries 3-4). Expanding the scope of the metal identity to platinum, cobalt, and rhodium did not increase the selectivity, rather exclusive or almost exclusive formation of undesired **2-20** was observed (entries 5-7).



Entry	Catalyst	Ligand ^b	Reagent	Solvent	2-1:2-20 ^c (yield)
1	Pd ₂ dba ₃	IMes	HBpin	THF	17:83 (62)
2	Pd ₂ dba ₃	SIPr	HBpin	THF	21:79 (47)
3	Ni(cod) ₂	IMes	HBpin	THF	21:79 (14)
4	Ni(cod) ₂	SIPr	HBpin	THF	13:87 (<5)
5	PtCl ₂	SIPr	HBpin	THF	7:93 (74)
6	CoBr ₂	SIPr	HBpin	THF	<2:98 (62)
7	Rh(PPh ₃) ₃ Cl	SIPr	HBpin	THF	<2:98 (33)

^aAll experiments were conducted at rt for 2 h at 0.2 M under nitrogen atmosphere. ^bLigand HCl salts were used with KO-*t*-Bu. ^cNMR yields are shown using 1,3,5-trimethoxybenzene as internal standard. Regioselectivity ratios were determined on crude reaction mixtures.

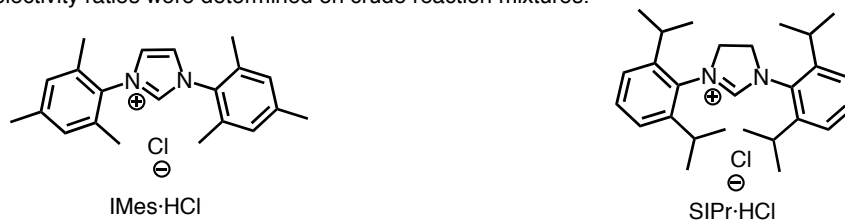
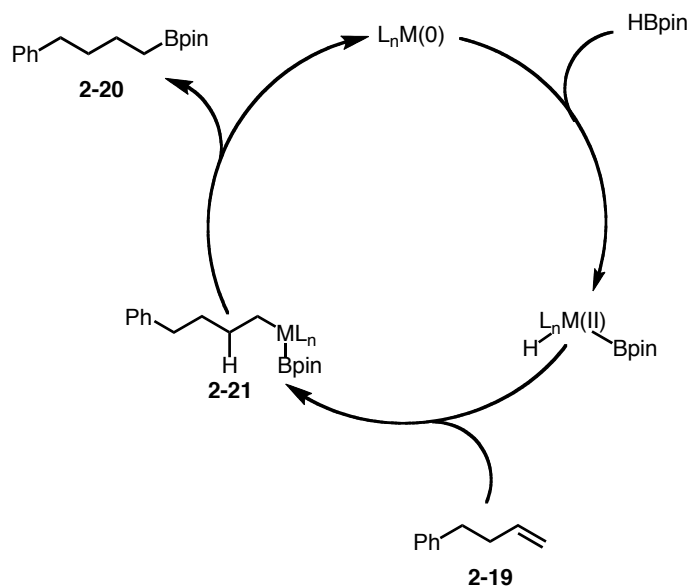


Table 2-1: Initial Investigation into Regioselective Hydroboration of 2-19

Without observing regioselectivity favoring the branched alkylborane **2-1**, the mechanism of the reaction was evaluated (Scheme 2-5). Initially, it was hypothesized that oxidative addition into the boron-hydrogen bond leads to the regiodetermining alkene insertion step. The alkene insertion between the metal-hydride bond occurs, leading to the linear alkylborane **2-20**. Unlike the hydrosilylation of allenes (in which pi-insertion into the metal-hydride bond could be switched to the metal-silyl bond depending on the metal identity), the insertion between the metal-boron bond was not able to be favored – leading to the desired branched alkylborane **2-1**.



Scheme 2-5: Proposed Mechanism for the Formation of Linear Alkylborane 2-20

2.3.3 Optimization with Bis(pinacolato)diboron

Taking into consideration the proposed mechanism outlined in Scheme 2-5, a new approach was devised drawing motivation from previous reports for hydroboration of terminal alkynes with a copper-NHC catalyst, which affords the branched vinylborane.⁷⁸ Copper precursors were screened alongside the IMes·HCl and SIPr·HCl ligands, with bis(pinacolato)diboron as the boron source and methanol as the proton source (Table 2-2). CuCl with IMes·HCl in tetrahydrofuran resulted in the initial observation for regio reversal to the branched alkylborane **2-1** (entry 1). Although reactivity was low (3% conversion to desired product) and regioselectivity limited (2:1), this was the first indication that regio reversal was possible in a metal-NHC system. Increasing the steric bulk of the ligand to SIPr·HCl resulted in increased regioselectivity and yield (entry 2). After screening several solvents, it was determined that acetonitrile was the optimal solvent for regioselectivity, providing 95:5 in favor of the desired product **2-1** (entry 3). After optimization of regioselectivity, attention turned to increasing the yield of the reaction. It was predicted that use of a copper pre-catalyst would increase the yield of the reaction as formation of the reactive copper species might vary by pre-

catalyst. This prediction was verified as copper(II) bromide and copper(II) acetate both increased the overall yield of the reaction (entries 4-5). The discrete IPrCuCl catalyst showed the highest isolable yield while maintaining high regioselectivity (entry 6). Although, the trade off between yield and regioselectivity could be argued between entry 4 and entry 6, a discrete NHC-copper(I) catalyst was chosen as it is commercially available and able to be conveniently synthesized on a multi-gram scale with relative ease.

Entry	Catalyst	Ligand ^b	Reagent	Solvent	2-1:2-20(% yield) ^c
1	CuCl	IMes	B ₂ pin ₂	THF	67:33 (3)
2	CuCl	SIPr	B ₂ pin ₂	THF	79:21 (48)
3	CuCl	SIPr	B ₂ pin ₂	CH ₃ CN	95:5 (52)
4	CuBr ₂	SIPr	B ₂ pin ₂	CH ₃ CN	96:4 (78)
5	Cu(OAc) ₂	SIPr	B ₂ pin ₂	CH ₃ CN	93:7 (62)
6	Cu(Cl)IPr	---	B ₂ pin ₂	CH ₃ CN	92:8 (81 ^d)

^aAll experiments were conducted at rt for 2 h at 0.2M under nitrogen atmosphere. Experiments used CH₃OH (2 equiv). ^bLigand HCl salts were used with KO-*t*-Bu. ^cNMR yields are shown using 1,3,5-trimethoxybenzene as internal standard. Regioselectivity ratios were determined on crude reaction mixtures. ^dIsolated.

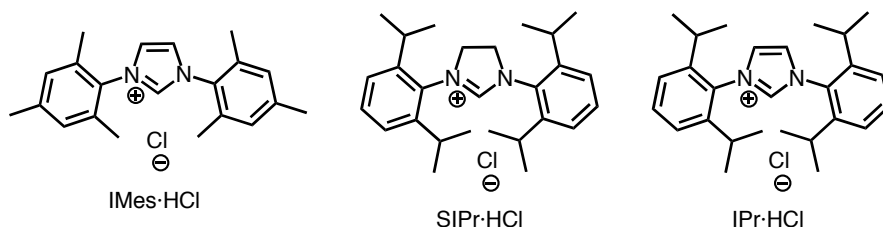
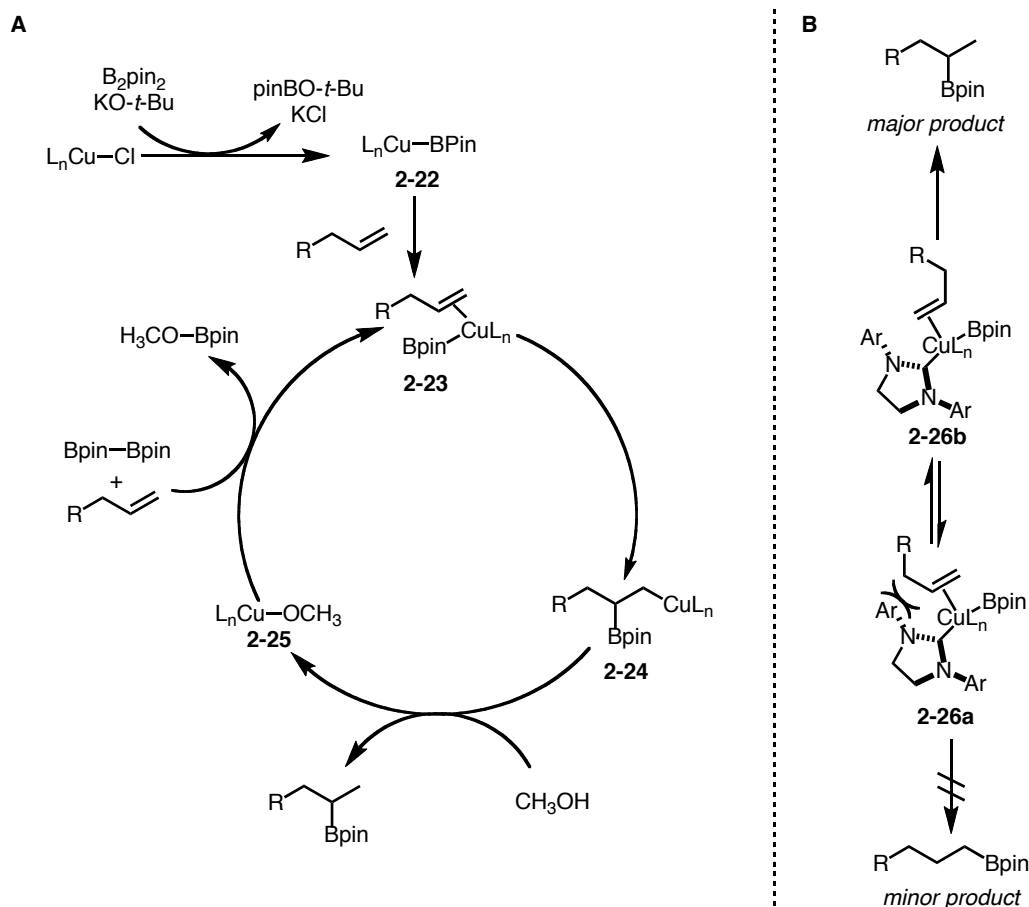


Table 2-2: Copper-NHC Optimization for Hydroboration of 2-19

2.4 Mechanistic Hypothesis

The proposed mechanism for the hydroboration reaction is analogous to other copper-catalyzed addition reactions conducted with bis(pinacolato)diboron (Scheme 2-6 A).^{27,39,40,78-81} The active copper-boron species **2-22** coordinates to the olefin forming complex **2-23**. Orientation of the olefin to the copper center leads to the regiodetermining step (**2-23** to **2-24**). Increasing the steric bulk of the NHC ligand disfavors the formation of the linear alkylborane

due to the increased steric clash between the ligand and substrate **2-26a** (Scheme 2-6 B). Complex **2-26b** avoids the steric interaction between the ligand and the substrate leading to the desired secondary alkylborane. Rapid protonation of the copper-carbon bond of **2-24** results in the desired branched alkylborane and copper alkoxy species **2-25**. To close the catalytic cycle, **2-23** is generated when **2-24** reacts with another equivalent of olefin and bis(pinacolato)diboron.

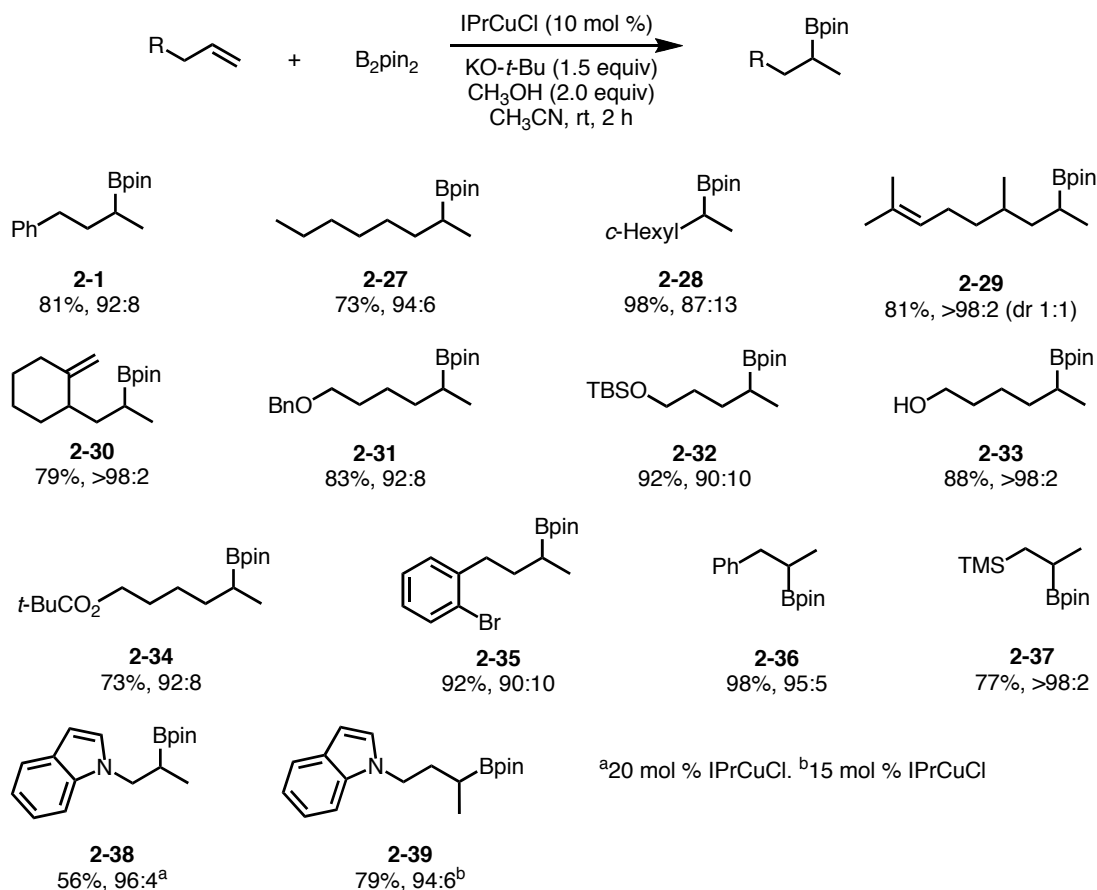


Scheme 2-6: (A) Mechanism for the Hydroboration of Terminal Olefins (B) Coordination of Olefin to Copper Complex for the Regio-Determining Step

2.5 Reaction Scope

Investigation into the scope of the copper-catalyzed hydroboration included a wide variety of functional groups (Scheme 2-7). A remote phenyl group is not needed to achieve high selectivity as 1-octene readily underwent hydroboration to **2-27** with 94:6 regioselectivity in 73% yield. Allylic branching of the olefin was tolerated (**2-28**), although regioselectivity was slightly

deteriorated to 87:13. Tri-substituted (**2-29**) and 1,1-disubstituted (**2-30**) olefins were tolerated with good yields and high regioselectivity, indicating that these olefins were inert to these reaction conditions. Benzyl- and silyl-ethers (**2-31** and **2-32**, respectively) performed well; however, synthesis of **2-33** demonstrated alcohols are also tolerated in these reaction conditions. Although this was not a surprising result, other previously mentioned methods for the synthesis of branched alkylboranes do not tolerate free alcohols – therefore, by tolerating free alcohols these reaction conditions expand the types of secondary alkylboranes that can be synthesized. Pivalates (**2-34**) were not observed to undergo transesterification, and the inclusion of aryl bromides into substrate **2-35** provides two different sites that may undergo further functionalization selectively depending upon the choice of cross-coupling reaction conditions. Allyl derived substrates **2-36** and **2-37** gave high selectivity for the branched secondary alkylborane without observation of racemization of the double bond to give the 3-borylated product. Higher catalyst loadings were required to provide adequate transformation of substrates bearing indole heterocycles **2-38** and **2-39**.

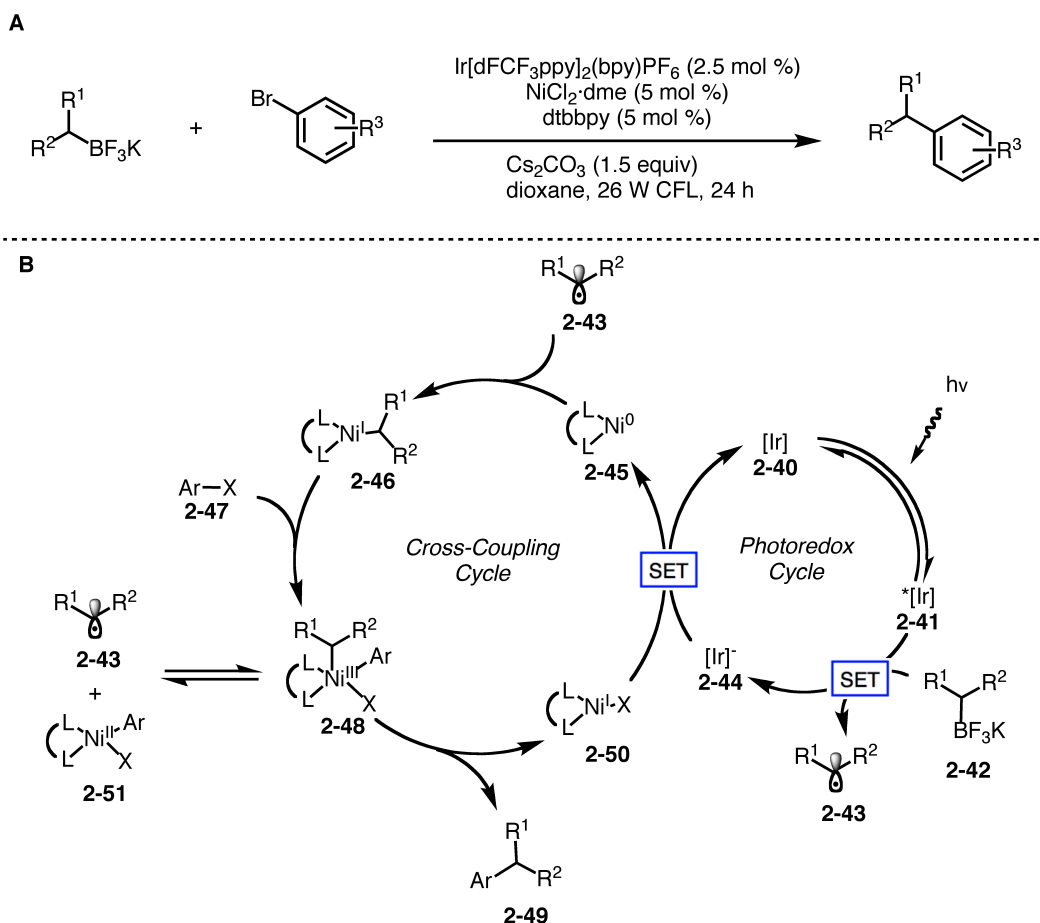


Scheme 2-7: Substrate Scope for the Copper-Catalyzed Formal Hydroboration Reaction

2.6 Cross-Coupling of Newly Synthesized Secondary Alkylborane

The development of a streamlined approach for the synthesis of secondary alkylboranes supports the advancement for Suzuki-type cross-coupling reactions. In particular, Molander's dual catalyst photocatalytic cross-coupling demonstrates the utility of secondary alkyl trifluoroborate salts (Scheme 2-8 A),⁴⁸ which themselves may be readily converted from pinacol boronic esters such as those described in the methodology outlined above. The mechanism for the cross-coupling reaction involves two catalytic cycles working in tandem (Scheme 2-8 B). Excitation of iridium catalyst **2-40**, allows **2-41** to undergo a single electron transfer with the secondary trifluoroborate species **2-42** resulting in radical **2-43** and reduced iridium **2-44**. Radical **2-43** combines with nickel(0) species **2-45** forming nickel(I) complex **2-46**. Oxidative addition into the aryl halide results in nickel(III) complex **2-48**. It is possible for the oxidative

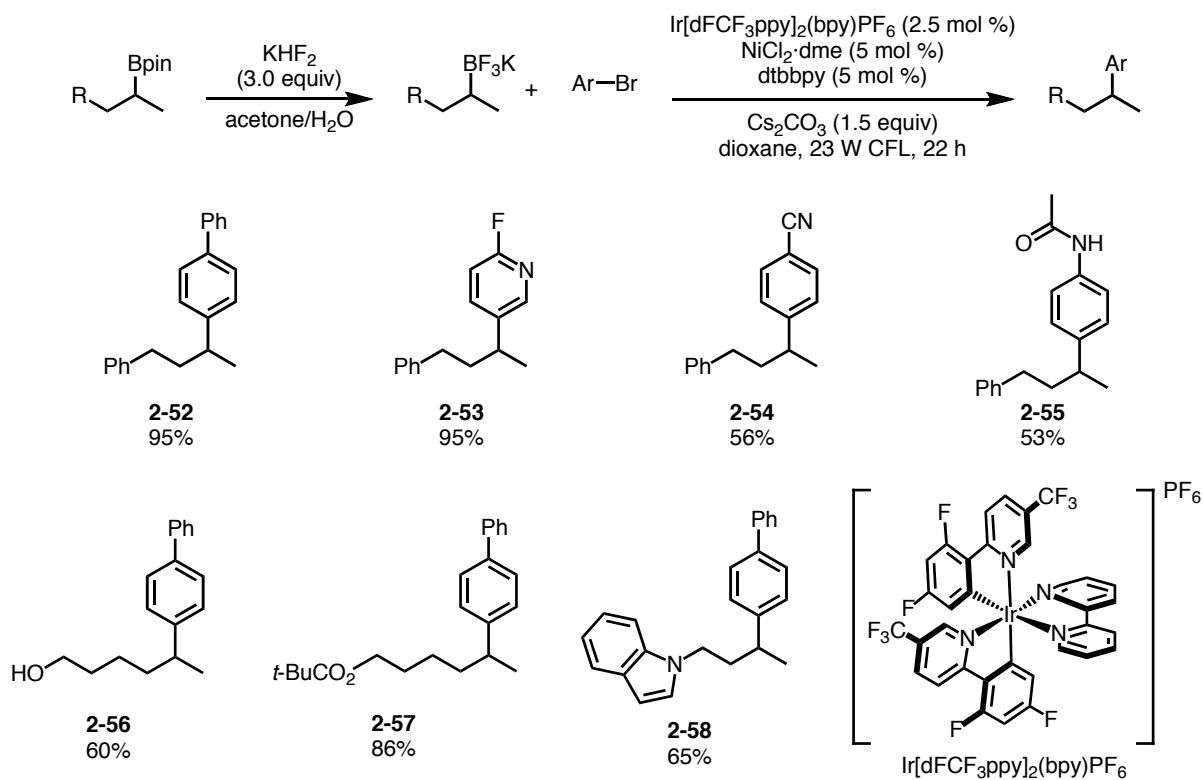
addition to the nickel center to occur before addition of the radical; however, both are plausible pathways.⁸² Rapid reductive elimination releases desired coupled product **2-49** and nickel(I) species **2-50**. Another single electron transfer between **2-50** and **2-44** closes both catalytic cycles.



Scheme 2-8: (A) Conditions for Photocatalytic Cross-Coupling of Secondary Alkyl Trifluoroborate Salts and Aryl Halides (B) Mechanism for Photocatalytic Cross-Coupling

Pinacol boronic esters **2-1**, **2-33**, **2-34** and **2-39** were readily converted to their respective trifluoroborate salts using potassium hydrogen difluoride in a mixture of acetone and water. These salts were subsequently subjected to the photocatalytic cross-coupling reaction conditions proposed by Molander (Scheme 2-9). Gratifyingly, the trifluoroborate salt derived from **2-1** underwent cross-coupling to **2-52** without observation of isomerization to the benzylic position. Heterocycles, as well as both electron-withdrawing and electron-donating aryl halides were proficient in the formation of new carbon-carbon bond forming products, **2-53** through **2-55**.

More interestingly, products that contained free alcohols, **2-56**, and esters, **2-57**, were isolated, displaying the utility of the formal hydroarylation of the starting olefin. Lastly, heterocycles incorporated in the trifluoroborate salts coupling partner were tolerated, **2-58**.



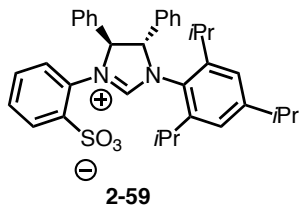
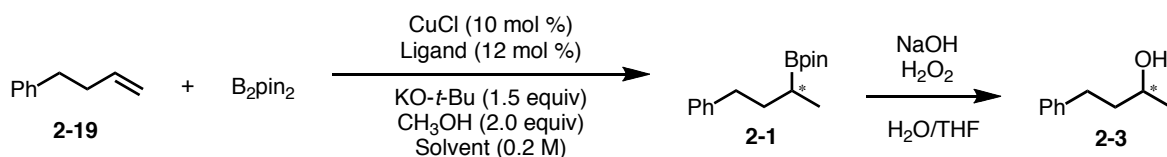
Scheme 2-9: Photocatalytic Cross-Coupling of Newly Synthesized Trifluoroborate Salts. Note: Reported Yields Correspond to the Cross-Coupling Step.

2.7 Enantioselective Hydroboration of Terminal Olefins

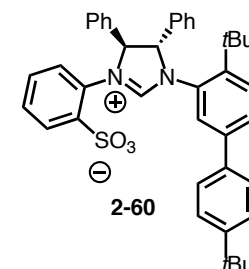
As mentioned previously (Scheme 2-1), most transformations of alkylboronic pinacol esters are stereoretentive, maintaining the original identity of the carbon-boron bond. Installing enantioenriched carbon-boron bonds using chiral boron reagents has been demonstrated as a powerful method to build up molecular complexity.^{54,56,83} Hartwig has demonstrated that chiral copper-phosphine catalysts are proficient in installing boranes with high enantioselectivity, through the use of a directing group on the olefin.³⁷ However, one of the most powerful advances was introduced by Hoveyda and coworkers when they demonstrated that a chelating chiral

copper-NHC complex readily performs asymmetric hydroboration on styrene derivatives^{26,27} and other activated olefins.^{84,85}

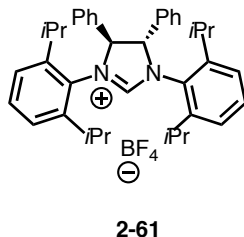
Using these examples as motivation, investigation into enantioselective hydroboration began with chiral copper-NHC catalysts (Scheme 2-10). In order to analyze the results of these chiral reactions via SFC (supercritical fluid chromatography) or HPLC (high-performance liquid chromatography), oxidation of the chiral alkylborane to a chiral alcohol was required (see Chapter 6 for more details). Chelating ligands **2-59** and **2-60** were synthesized and used in the aforementioned hydroboration method. Ligand **2-59** showed promise as 24% enantioselectivity was obtained; however, regioselectivity eroded to 86:14. Changing the non-chelating aryl group of the NHC to a biphenyl derivative decreased both enantioselectivity and regioselectivity to 13% and 79:13, respectively. Decreasing reaction temperature to -35 °C improved neither the enantioselectivity nor the regioselectivity. Previously, the Montgomery group has demonstrated that large NHCs with chiral backbones control regioselectivity and induce enantioselectivity for reductive couplings of alkynes and aldehydes.⁸⁶ Using the analogous chiral IPr ligand, **2-61**, low enantioselectivity was observed (8%) but high regiocontrol and reactivity were restored. Incorporating another *iso*-propyl group to the *para*-position of the aryl groups on the NHC, discrete copper complex **2-62** was synthesized to examine the enantioselectivity in varying solvents. In tetrahydrofuran, toluene, and acetonitrile the enantioselectivity was poor but the regioselectivity nevertheless remained high.



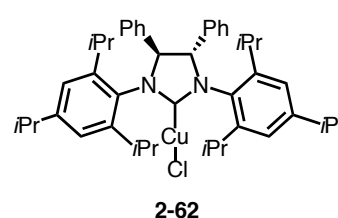
CH₃CN: 56%, 86:14, 24% ee



THF: 96%, 70:30, 15% ee
 THF (-35 °C): 33%, 79:21, 13% ee



CH₃CN: 85%, >98:2, 8% ee



5 mol % catalyst used
 THF: 41%, >98:2, 5% ee
 PhMe: 51%, >98:2, 7% ee
 CH₃CN: 33%, 95:5, 2% ee
 yields over 2 steps

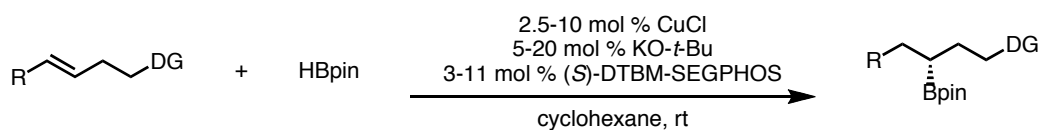
Scheme 2-10: Investigation into Enantioselective Hydroboration of Terminal Olefins

Further investigation into the enantioselective hydroboration of terminal olefins ceased as two attractive methods were published for this exact transformation. The first, by Aggarwal, detailed the development of a rhodium-catalyzed method using Nishiyama's catalyst.⁸⁷ The other methodology was reported using a chiral copper-NHC complex; however, the chirality was not on the backbone of the ligand and rather on the aryl groups derived from aniline.³¹

2.8 Progress Towards Regioselective Hydroboration of 1,2-Disubstituted Olefins

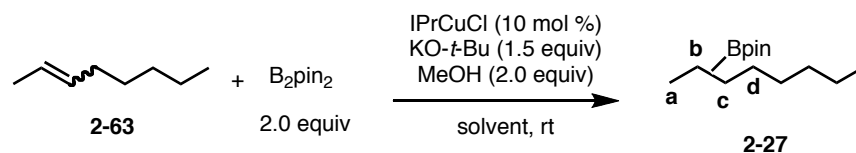
Recent advances in metal-catalyzed hydroboration of 1,2-disubstituted olefins often involve isomerization of the olefin to the terminal position before hydroboration occurs, resulting in the synthesis of linear alkylboranes.⁸⁸⁻⁹² Despite the prevalence of such transformations,

Hartwig demonstrated a copper-catalyzed hydroboration of internal olefins that do not undergo olefin isomerization (Scheme 2-11).³⁷ In this methodology, a remote directing group in unsymmetrical olefins was used to control the regioselectivity of the reactions; notably, a few examples were provided in which symmetrical olefins in the absence directing groups performed well under the non-regioselective hydroboration reaction conditions. While this methodology addresses both olefin isomerization and the hydroboration of unactivated symmetrical olefins, there is still a gap in the literature for the regioselective hydroboration of unactivated, asymmetrical olefins.



Scheme 2-11: Hartwig's Directing Group Regiocontrolled Hydroboration of Internal Olefins

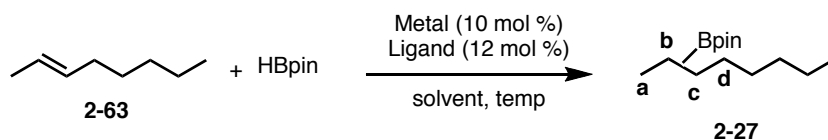
For this study, 2-octene (**2-63**) was chosen as the model substrate because the olefin was not activated, and distinguishing between a methyl group and a longer, linear alkyl chain makes analysis of products significantly easier. Both the *trans*- and *cis*-isomers are commercially available, and standards of **2-27a-d** for rapid analysis via GCFID are synthesized in a facile manner (see Chapter 6 for more information).^{37,93} Initially, the previously established copper-catalyzed hydroboration conditions for terminal olefins were examined (Table 2-3). *Trans*-**2-63** in both acetonitrile and dichloromethane did not result in any hydroboration products (entries 1-2). Similarly, *cis*-**2-63** also did not result in hydroboration products (entries 3-4).



Entry	<i>trans/cis</i>	solvent	yield
1	<i>trans</i>	CH ₃ CN	0%
2	<i>trans</i>	CH ₂ Cl ₂	0%
3	<i>cis</i>	CH ₃ CN	0%
4	<i>cis</i>	CH ₂ Cl ₂	0%

Table 2-3: Copper-Catalyzed Hydroboration of 2-Octene

Using pinacol borane as the boron and proton source, vast investigation into other metal and ligand sources were examined and are summarized in Table 2-4 (see Chapter 6 for more extensive data). Hartwig's hydroboration conditions resulted in incorporation to the **a**, **b**, and **c** positions without showing regioselectivity between the **b** and **c** positions (entry 1). Olefin isomerization was observed using both a cobalt and iron catalyst with ligand **2-64** as **2-27a** was the exclusive product formed (entries 2-3). Pd(OAc)₂ with ligand **2-65** in toluene at 100 °C resulted in the best regioselectivity for the **b/c** position; however, there was no selectivity between the two positions (entry 4). Decreasing the temperature to 80 °C to try and minimize olefin isomerization decreased overall reactivity (entry 5). Changing solvents to tetrahydrofuran also resulted in decreased reactivity and higher olefin isomerization, as more **2-27a** was observed (entry 6). Moving to a palladium(0) source, Pd₂(dba)₃ with ligand **2-66** showed comparable reactivity but higher olefin isomerization (entry 7). NiCl₂·dme resulted in the highest reactivity and highest selectivity for branched isomers **2-27b-d**; however, control over the regioselectivity was minimal (entry 8).



Entry	Metal	Ligand	Solvent	Temp	a:b:c:d	GCFID yield
1	CuCl ^a	(S)-DTBM-SEGPHOS	cyclohexane	rt	13:47:41:0	<1%:2%:2%:0%
2	CoI ₂ ^b	2-64	PhMe	60 °C	100:0:0:0	55% (isolated)
3	Fe(OAc) ₂ ^b	2-64	PhMe	60 °C	100:0:0:0	trace
4	Pd(OAc) ₂ ^a	2-65	PhMe	100 °C	19:39:40:3	11%:23%:24%:2%
5	Pd(OAc) ₂ ^a	2-65	PhMe	80 °C	31:17:20:32	3%:2%:2%:3%
6	Pd(OAc) ₂ ^a	2-65	THF	80 °C	70:13:6:10	2%:<1%:<1%:<1%
7	Pd ₂ (dba) ₃ ^{a,c}	2-66	PhMe	100 °C	60:22:14:4	34%:12%:8%:2%
8	NiCl ₂ ·dme ^a	2-66	PhMe	100 °C	12:27:34:27	11%:25%:31%:25%

^a12 mol % NaO-*t*-Bu added ^b30 mol % LiBHET₃ added ^c5 mol % catalyst loading

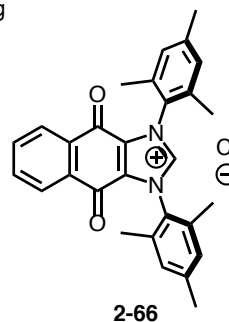
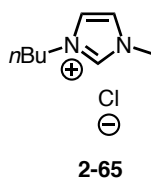
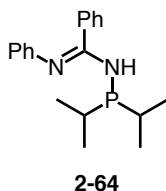
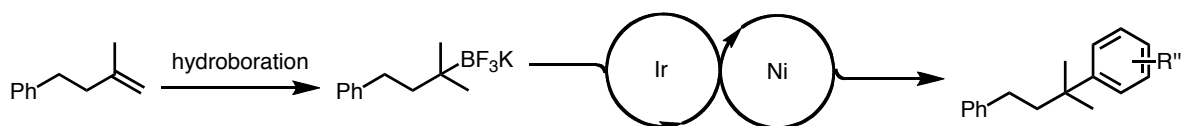


Table 2-4: Investigation into the Hydroboration of 1,2-Disubstituted Olefins

2.9 Progress Towards the Synthesis of Tertiary Alkylboranes

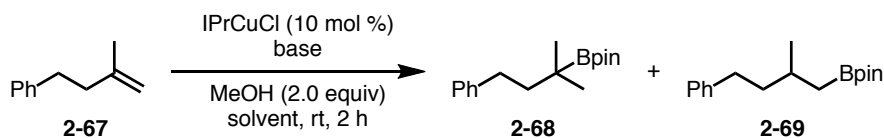
As mentioned previously, secondary alkylboranes can be synthesized via nickel or iron cross-coupling between an alkyl halide and a boron reagent; additionally, tertiary alkylboranes have been synthesized in an analogous manner.⁶⁸ While this method has been powerful, regioselective hydroboration of 1,1-disubstituted olefins would provide a complementary method. Furthermore, Molander developed a photocatalytic cross-coupling reaction using tertiary alkyl trifluoroborate salts, but again scope is limited due to narrow methodology for the synthesis of tertiary alkylboranes.⁹⁴ The goal of this project is to develop a hydroboration

methodology that utilizes 1,1-disubstituted olefins that provides precursors for photocatalytic cross-coupling (Scheme 2-12).



Scheme 2-12: Project Goals for Hydroboration of 1,1-Disubstituted Olefins

Investigation for regioselective hydroboration of **2-67** (Table 2-5) began with reaction conditions previously optimized for terminal olefins. Unfortunately, no desired product was observed using these reaction conditions (entry 1). Use of dichloromethane in lieu of acetonitrile resulted in 12% product formation and a 94:6 regioselectivity (entry 2). Changing the counter ion of the base from potassium to sodium increased the yield of the reaction drastically to 77%, although regioselectivity slightly deteriorated to 87:13 (entry 3). Increasing the equivalents of sodium *tert*-butoxide from 1.5 to 2.0 began to shut down the reaction (entry 4), but decreasing to 1.0 equivalent increased both reactivity and regioselectivity (entry 5). Again, these optimized conditions resulted in no observation of desired product when run with acetonitrile as the solvent (entry 6).



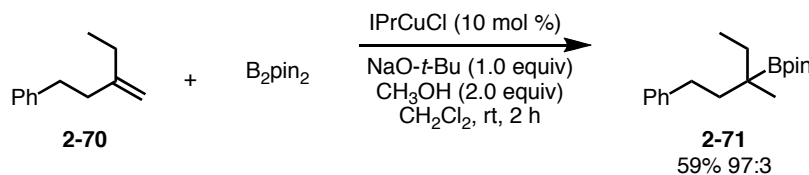
Entry	Solvent	Base	Equiv. Base	Yield ^b	2-68:2-69 ^c
1	CH ₃ CN	KO- <i>t</i> -Bu	1.5	0%	-
2	CH ₂ Cl ₂	KO- <i>t</i> -Bu	1.5	12%	94:6
3	CH ₂ Cl ₂	NaO- <i>t</i> -Bu	1.5	77%	87:13
4	CH ₂ Cl ₂	NaO- <i>t</i> -Bu	2.0	46%	80:20
5	CH ₂ Cl ₂	NaO- <i>t</i> -Bu	1.0	87%	91:9
6	CH ₃ CN	NaO- <i>t</i> -Bu	1.0	0%	-

^aAll experiments were conducted at rt for 2 h at 0.2 M under nitrogen atmosphere. ^bIsolated.

^cRegioselectivity ratios were determined on crude reaction mixtures.

Table 2-5: Optimization of Hydroboration for 1,1-Disubstituted Olefins

Examining the effects of the substituents on the olefin, when the methyl group was extended to the ethyl group (**2-70**) a decrease in yield was observed (Scheme 2-13). This decrease in yield suggests the steric bulk of the olefin may play a role in the ability of the active catalyst to coordinate. At present, the nature of the solvent, the base (and equivalence), and the steric attributes of the olefin all significantly impact the desired hydroboration transformation.



Scheme 2-13: Hydroboration of 2-70

2.10 Conclusion and Future Directions for Hydroboration of Olefins

Overall, conditions were established for efficient synthesis of branched, secondary, alkylboranes from terminal olefins. This method has shown how rapid complexity of simple commodity feedstocks is established as new carbon-carbon bonds are formed in a three-step process. Moving to other olefin classes continues to provide a difficult challenge. The lack of directing groups or electronic bias in the hydroboration of 1,2-disubstituted olefins remains difficult, as not only regioselectivity but also olefin isomerization is difficult to control.

Hydroboration of 1,1-disubstituted olefins provides its own challenges as well. Seemingly small differences (such as the base counter ion) result in large differences in reactivity. Furthermore, the steric character of the substituents of the olefin drastically impacts the efficiency of the reaction.

The most direct path for future hydroboration work will be investigating the differences in the 1,1-disubstituted reaction conditions from the monosubstituted reaction conditions. Expansion of the substrate scope to include a variety of functional groups highlighting chemoselectivity would increase the attractiveness of the reaction. Furthermore, transforming the newly synthesized tertiary pinacol esters to the corresponding trifluoroborate salts would provide access to cross-coupling partners for photocatalysis similar to that demonstrated with secondary alkylboranes. It is unclear the direct path to take for regioselective hydroboration of 1,2-disubstituted olefins as olefin isomerization is a large barrier to overcome, not to mention the subtle variation in substituents that need to be differentiated.

Chapter 3 Introduction to Intramolecular Aglycone Delivery and Glycoside Activation

3.1 Factors that Affect Glycosylation Reactions

O-Glycosides are present in a number of natural products, which possess antibiotic properties.⁹⁵ Two of the most common monosaccharides are glucose and mannose, a C-2 epimer of glucose. The positioning of the anomeric oxygen relative to the C-2 substituent partially defines the name of the glycoside, resulting in four different combinations α -1,2-*cis* glucose, β -1,2-*trans* glucose, β -1,2-*cis* mannose and α -1,2-*trans* mannose (Figure 3-1). The difference in orientation between 1,2-*cis* glycosides and 1,2-*trans* glycosides is significant, and results in very different properties. One example of the major effects of these properties is in comparing polymers of glucose in nature. Polymeric 1,2-*cis* glycosides take the form of amylose (starch), which is the sweet taste in potatoes; on the other hand, polymeric 1,2-*trans* glycoside bears the structure of cellulose, which gives wood its structure.⁹⁶

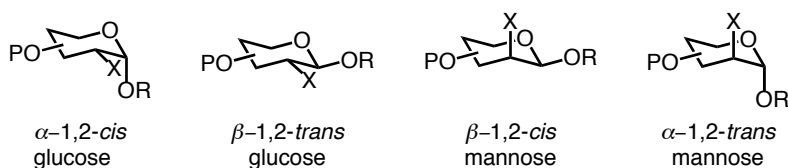
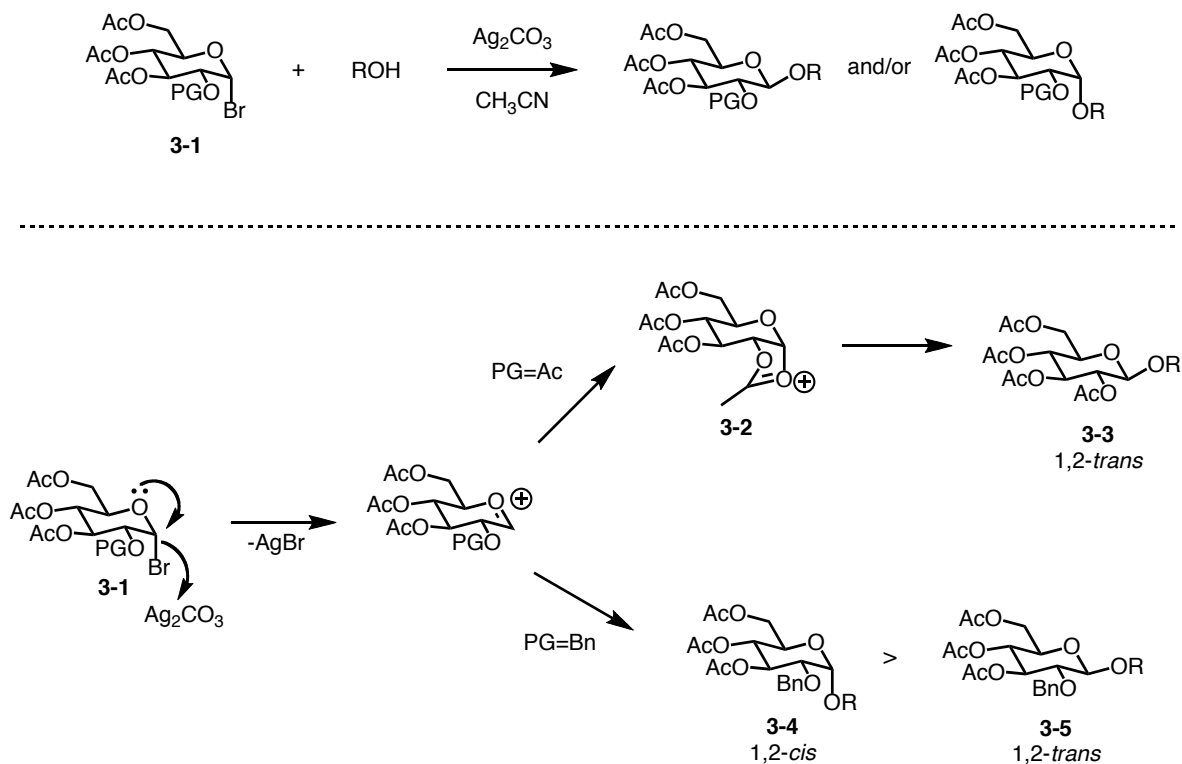


Figure 3-1: Common 1,2-*cis* and 1,2-*trans* glycosides

Due to the importance of the stereochemical layout at the anomeric carbon, methods to synthesize both the *trans* and *cis* glucoside have been of interest. One of the first insights into controlled glycosylation is credited to Koenigs and Knorr.⁹⁷ In this reaction, the anomeric bromide in bromosugar **3-1** was replaced with an alcohol through the use of a silver carbonate promoter (Scheme 3-1). The protecting group on the C-2 alcohol plays a major role in the

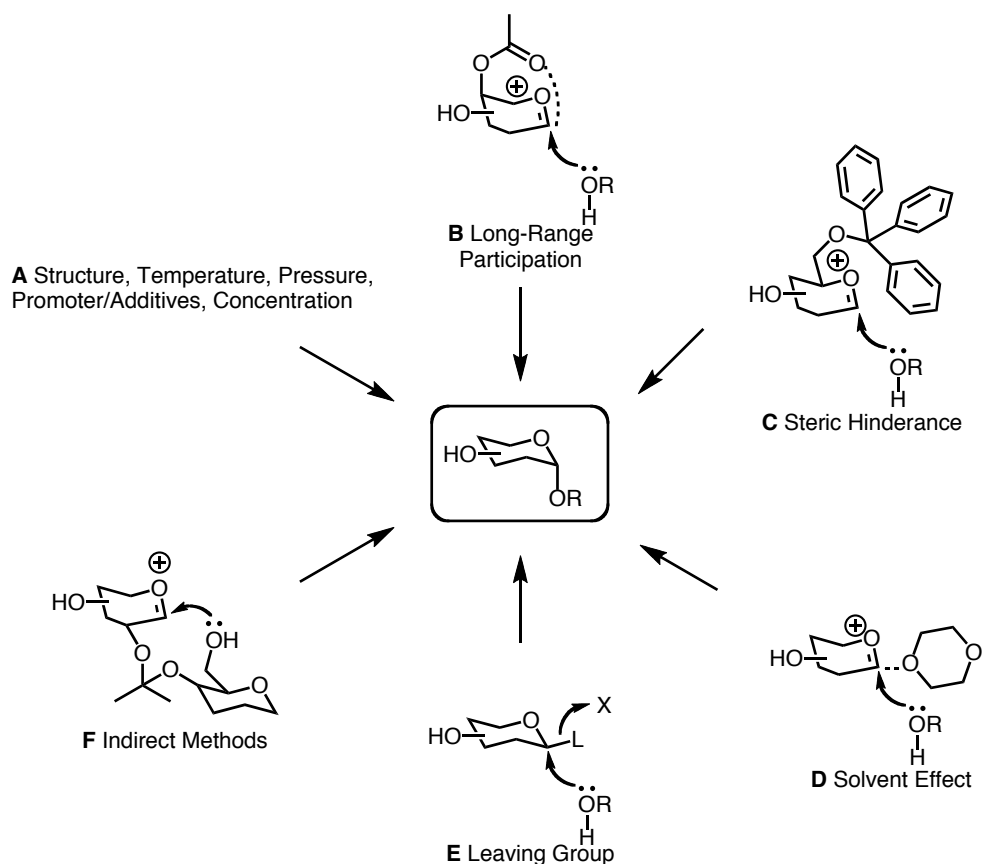
stereochemical outcome. If the protecting group employed was acetate, neighboring group participation through a cyclic intermediate **3-2** results in exclusive addition of the alcohol trans to the C-2 position, **3-3**. However, if the neighboring group could not participate in the reaction such as a benzyl group, a mixture of anomers were observed favoring the 1,2-*cis* product **3-4**.



Scheme 3-1: Koenigs and Knorr Glycosylation Reaction with Mechanism

Neighboring group participation is one of the most common methods to synthesize 1,2-*trans* glycosides. However, 1,2-*cis* glycosides provide a different challenge, as there are many factors involved that affect the stereochemical outcome at the anomeric position (Scheme 3-2).⁹⁸ The anomeric effect itself plays a major role in glycosylation reactions, as thermodynamic conditions lead to the more stable anomer. Temperature, pressure, additives and concentration of the reaction are just a few of the myriad alterations to reaction conditions that affect the glycosylation reaction. In addition to changing conditions, the structure of the starting carbohydrate also plays a role in reactivity. Long-range group participation (Scheme 3-2 B),

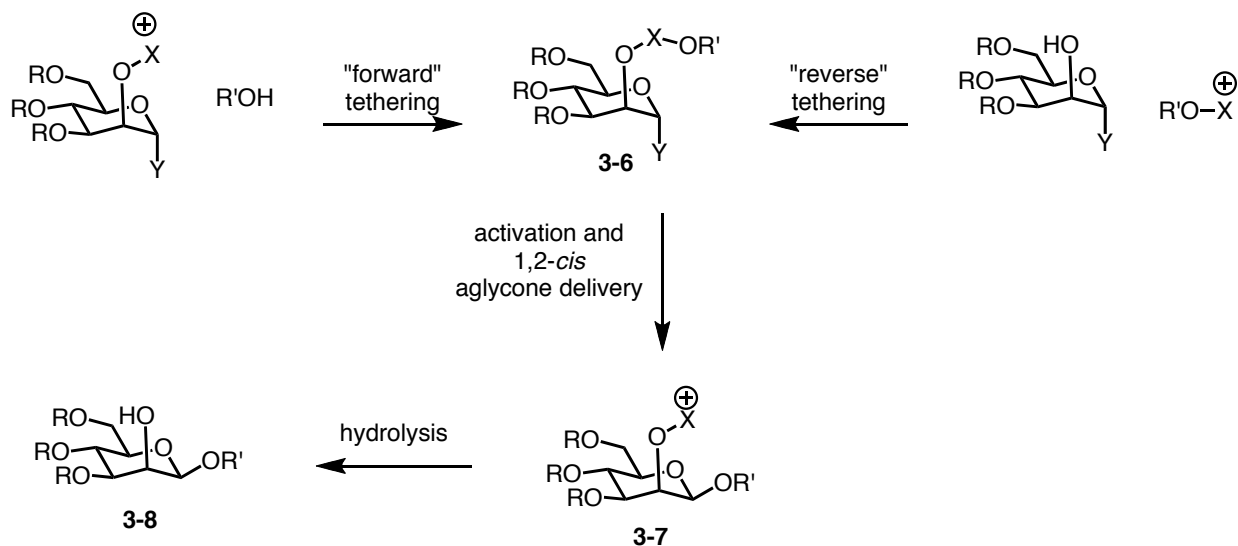
similar to neighboring group participation but from another protected alcohol, and steric hindrance (Scheme 3-2 C) from the alcohol protecting groups – more specifically, the C-6 substituent – have potential to inhibit the attack of the incoming alcohol. Coordination of solvent to the intermediate oxocarbenium ion additionally affects the stereochemical outcome of the glycosylation reaction (Scheme 3-2 D). The identity of the leaving group affects the mode of glycosylation (Scheme 3-2 E). Furthermore, indirect aglycone deliveries (Scheme 3-2 F) such as intramolecular aglycone delivery, ‘molecular clamp’ methods, and leaving group-based methods are powerful techniques to control glycosylation reactions. Most relevant to the work presented in the following chapter, intramolecular aglycone delivery and leaving group identity will be discussed further.



Scheme 3-2: Factors that Affect Glycosylation Reactions

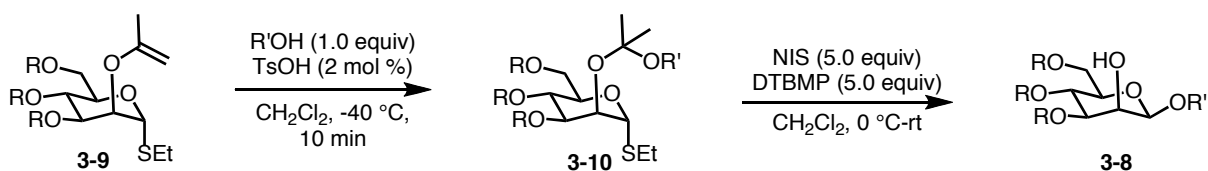
3.2 Indirect Glycosylation Methods Via Intramolecular Aglycone Delivery

Intramolecular aglycone delivery is a very straightforward and powerful method for synthesizing 1,2-*cis* glycosides with high stereochemical control (Scheme 3-3). This process begins with tethering of the aglycone to the starting substrate. This either occurs in a ‘forward’ tethering manner – where the sugar molecule acts as the electrophile and the external alcohol is the nucleophile – or in a ‘reverse’ tethering manner – where the aglycone is the electrophile and the sugar is the nucleophilic alcohol. Regardless of the method chosen, both methods arrive at the tethering aglycone-sugar species **3-6**. Activation of intermediate **3-6** and delivery of the aglycone from the same side of the tether forms the 1,2-*cis*-glycosidic bond (**3-7**). Hydrolysis to the free C-2 hydroxyl group **3-8** completes the intramolecular aglycone delivery process.



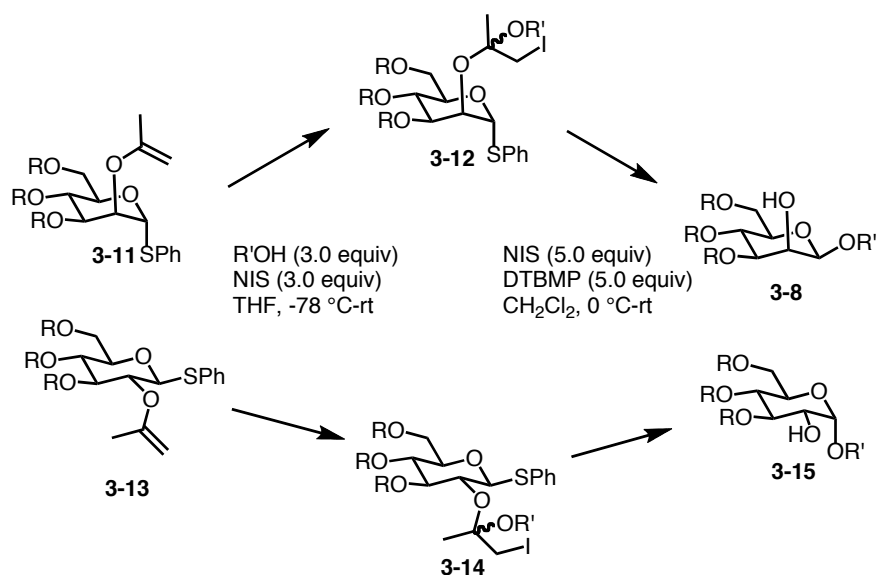
Scheme 3-3: General Scheme for Intramolecular Aglycone Delivery

Intramolecular aglycone delivery was first introduced by Hindsgaul and Barresi in the early 1990s (Scheme 3-4).⁹⁹ Using an acid-catalyzed 'forward' tethering, mixed acetal **3-10** was synthesized. Subsequently, use of *N*-iodosuccinimide (NIS) as an activator promotes exclusive formation of **3-8**. Addition of di-*tert*-butyl methyl pyridine (DTBMP) increased glycosylation yields by inhibiting the breakdown of the mixed acetal. Mechanistic studies revealed that more sterically hindered mixed acetals were converted *in situ* to less sterically hindered alcohols under aglycone delivery conditions, but the observed product was always a 1-2-*cis* glycoside – suggestive of an intramolecular S_N2 type mechanism.¹⁰⁰ Although this was the first introduction to intramolecular aglycone delivery, the scope was very limited, as increased steric bulk of the aglycone decreased the efficiency of the reaction and the reaction was limited to the mannose derived sugars.^{99–101}



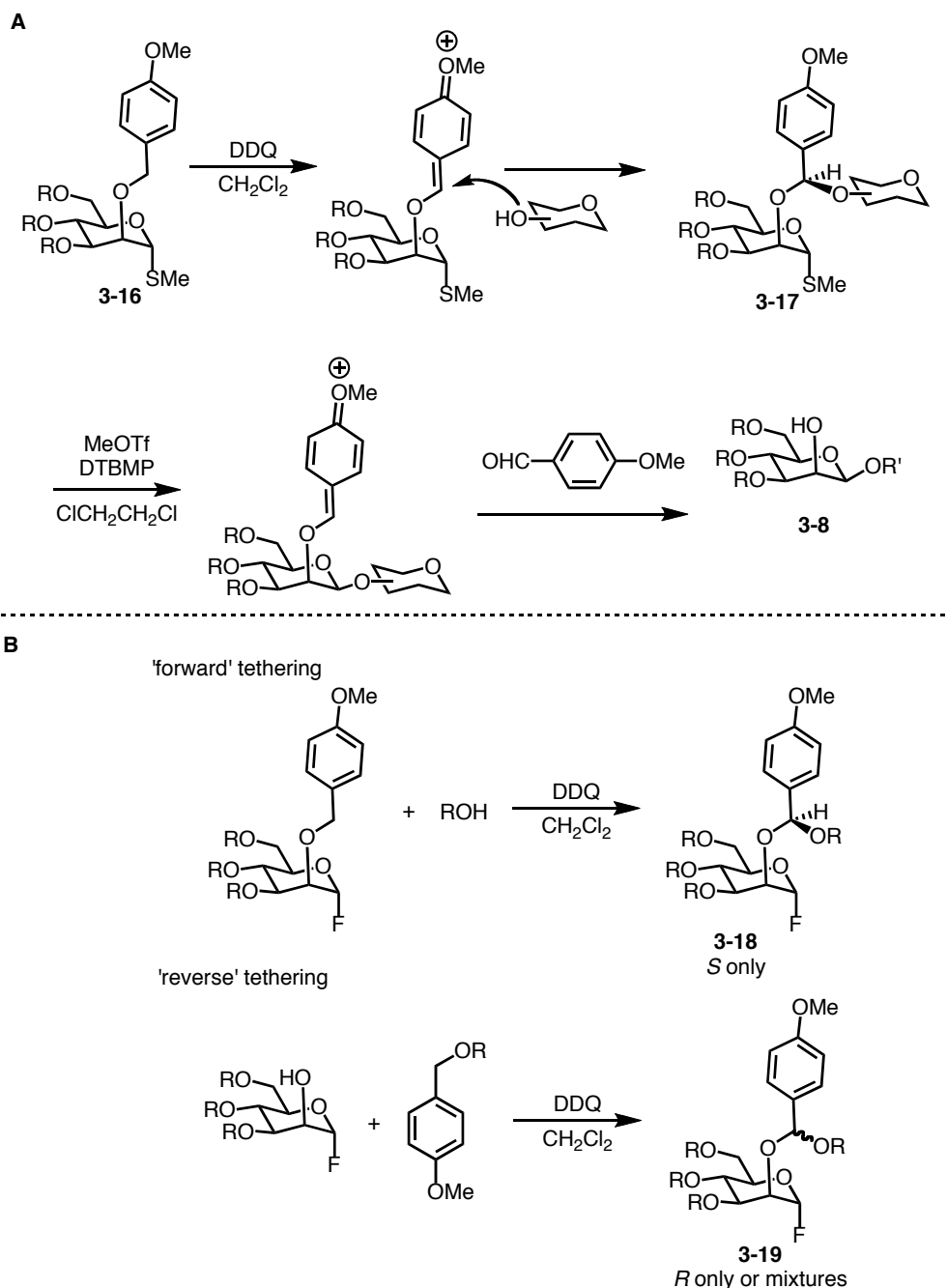
Scheme 3-4: Hindsgaul and Barresi Introduction of Intramolecular Aglycone Delivery

Fairbanks expanded upon Barresi and Hindsgaul's work by using an iodonium tethering method to synthesize mixed acetals to be used in intramolecular aglycone deliveries (Scheme 3-5).¹⁰² Using NIS and sugars similar to those used by Hindsgaul, tethering of primary and simple secondary alcohols was achieved in both the mannose and glucose sugar series. As both the tethering conditions and the aglycone delivery conditions were similar, a one-pot tethering/delivery approach was developed.¹⁰³ Subsequently, a second generation method was developed using 1,2-disubstituted allyl groups to expand the scope to be able to tether more complex secondary alcohols.^{104,105} Although the use of 1,2-disubstituted allyl groups improved the original Fairbanks method, tethering of the alcohol was truncated before full conversion in order to preserve the aglycone delivery as the tethered compound decomposed – this resulted in lower conversions, which means the overall process was not as efficient.



Scheme 3-5: Fairbanks Iodonium Tethering for Intramolecular Aglycone Delivery

Ogawa and Ito have done extensive work using oxidative tethering methods for aglycone delivery.^{106–117} Uniformly, these methods make use of a *para*-methoxyphenyl group installed on the C-2 hydroxy position (**3-16**), which was oxidatively tethered using 2,3-dichloro-5,6-dicyano-*p*-benzoquinone (DDQ) to form mixed acetal **3-17** that subsequently undergoes aglycone delivery (Scheme 3-6 A). Interestingly, the ‘forward’ tethering reaction arrives at the *S*-only diastereomer **3-18** while the ‘reverse’ tethering produced either the *R*-only diastereomer or a mixture of *R* and *S* **3-19** (Scheme 3-6 B).¹¹¹ Although it is currently accepted that the tethering operates under kinetic conditions, it remains unclear what caused the stereoselectivity of the tethering. In certain cases, the identity of the tethered species does not affect the aglycone delivery, while in others it plays a significant role,^{111,114} indicating that the effectiveness of aglycone delivery is substrate dependent.



Scheme 3-6: (A) General Scheme for Oxidative Tethering and Aglycone Delivery (B) Affect of Tethering on the Stereochemical Outcome of the Mixed Acetal

Inspired by the initial groundwork laid by Ito and Ogawa, several advancements and applications have been developed using the oxidative tethering method for aglycone delivery. Ito and Ogawa have applied their method to a system involving a polymer support. The *p*-alkoxybenzyl group was attached to both the C-2 position and polymer support **3-20** acts as a

“gatekeeper” – only releasing desired product from the aglycone delivery (Figure 3-2 A).¹¹⁸ Bertozzi applied the oxidative tethering/intramolecular aglycone delivery method to the synthesis of the α,α -trehalose core of Sulfolipid-I (**3-21**) and its derivatives (Figure 3-2 B).^{119,120} Establishing a synthetic pathway to Sulfolipid-I and its derivatives allowed for more extensive exploration into the biological activity since it is known that these compounds affect the human immune system.

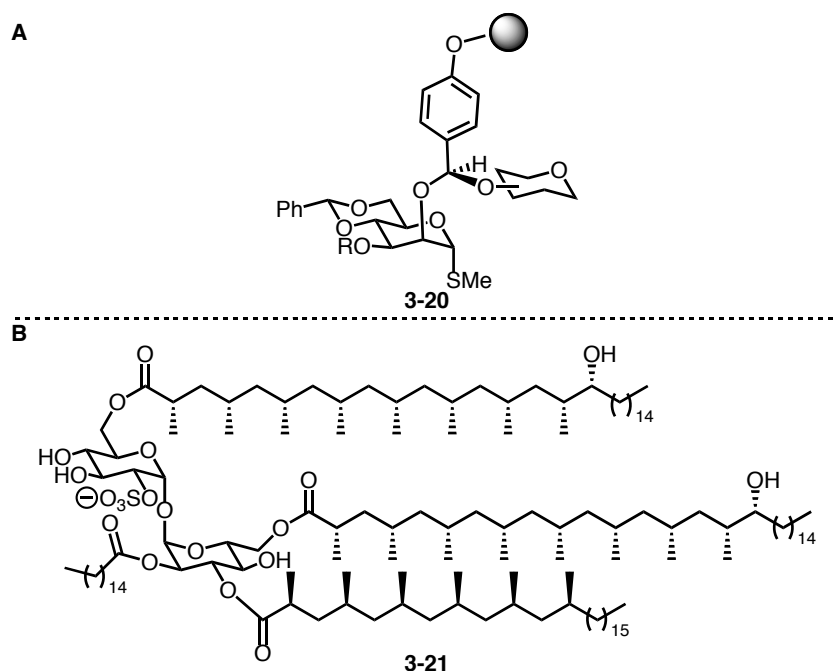
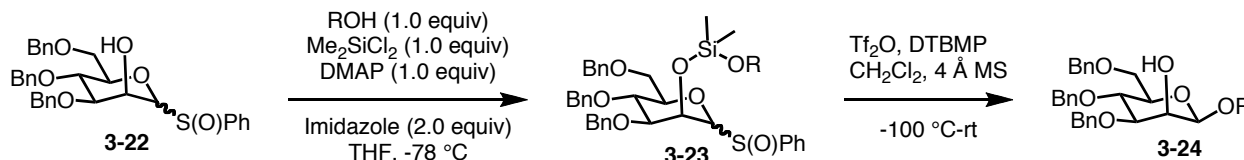


Figure 3-2: (A) Solid-Support for Oxidative Tethering/ Intramolecular Aglycone Delivery (B) Sulfolipid-I

Stork advanced the field by revealing that silicon tethers perform intramolecular aglycone deliveries after an *in situ* tethering of both alcohol components using dichlorodimethylsilane and mannose-derived donor **3-22** (Scheme 3-7).¹²¹ He later demonstrated that the order of tethering and oxidation of the thioglycoside could be reversed.¹²² Simultaneously, Bols revealed that a similar silicon tethering intramolecular aglycone delivery technique was possible using glucose and galactose sugar donors.^{123,124} Furthermore, Bols extended the silicon tethering from the C-2 alcohol to the C-3, and C-4 alcohols all of which successfully underwent intramolecular

aglycone delivery but not as cleanly.¹²⁵ Aglycone delivery after C-3 tethering resulted in a mixture of α/β selectivity (1:4), while delivery from C-4 tethering gave modest yields (45%), and delivery from C-6 tethering had high conversion but low desired product as the 1,6-anhydrosugar was the major product. Advancement of silicon tethering for intramolecular aglycone delivery by the Montgomery group will be discussed in Chapter 4.



Scheme 3-7: Silicon Tethering for Intramolecular Aglycone Delivery

3.3 Anomeric Identity and Activation for the Synthesis of 1,2-*cis* Glycosides

The identity of the anomeric leaving group of the glycosyl donor is widely varied (Figure 3-3).¹²⁶ The earliest examples by Michael,¹²⁷ Fischer,¹²⁸ Koenigs and Knorr⁹⁷ used bromides, chlorides, hemiacetals, and acetates as leaving groups for glycosylation reactions. For many years, these anomeric leaving groups were used to synthesize a variety of glycosylations spanning from simple bond formation to complex oligosaccharide synthesis. It was not until the 1970's that a deeper understanding of glycosylation caused exploration into new anomeric leaving groups on glycosyl donors, including the first examples of thioglycosides,¹²⁹⁻¹³¹ *O*-imidates¹³² and thioimidates.¹³³ Consequently, glycoscience boomed and led to the development of many new anomeric leaving groups, as well as non-traditional glycosylation groups such as glycols¹³⁴ and epoxides.¹³⁵ While all of these glycosyl donors have their own niche in glycosylation reactions, focus herein will be on the activation of thioglycosides and alkenyl glycosides, as these anomeric groups are the most relevant to further discussion in Chapter 4.

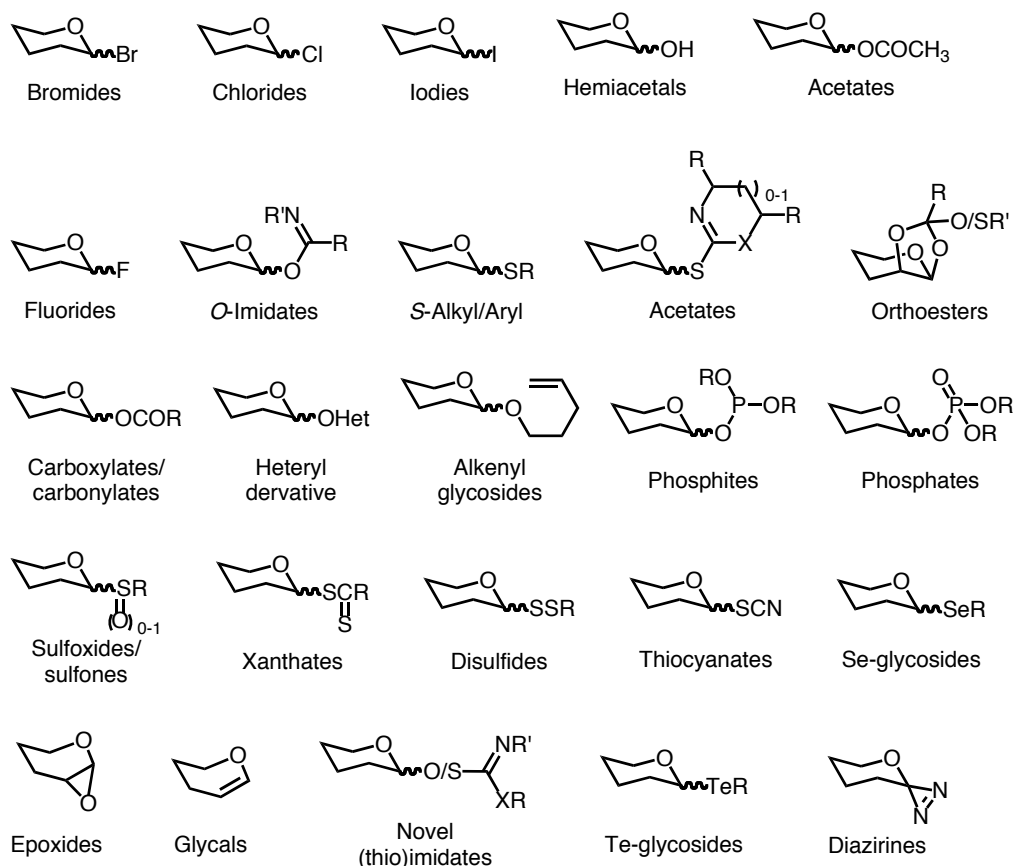
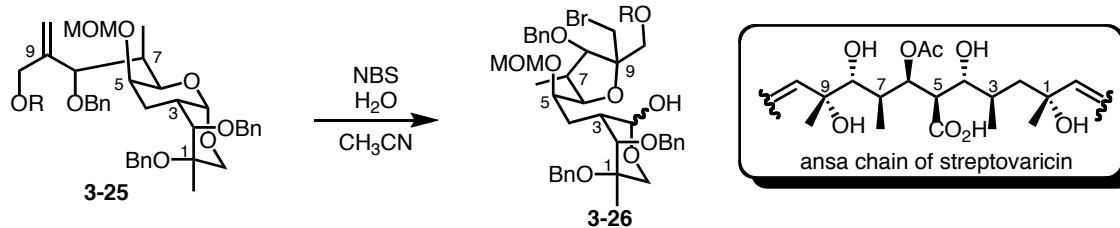


Figure 3-3: Various Leaving Groups of Glycosyl Donors

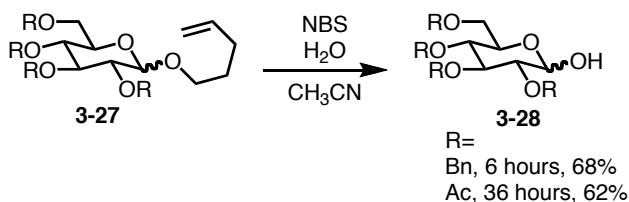
3.3.1 Activation of Alkenyl Glycosides

A serendipitous reaction by Fraser-Reid led to the discovery of *n*-pentenyl glycosides as efficient glycosylation partners. During the synthesis of the ansa chain of streptovaricin, compound **3-25** was subjected to a mixture of *N*-bromosuccinimide (NBS) in water in attempts to form the bromohydrin – but rather than the expected product, **3-26** was isolated (Scheme 3-8).^{136,137}



Scheme 3-8: Fraser-Reid Serendipitous Discovery

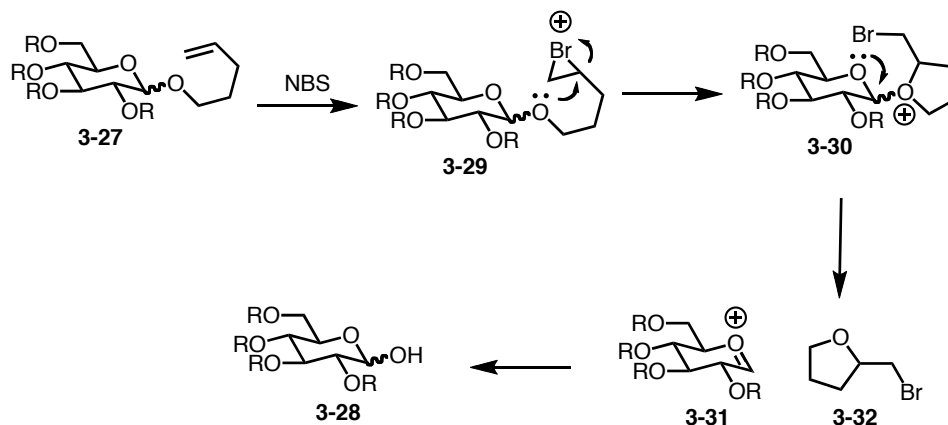
This unforeseen reactivity was further explored using formal carbohydrates with a pent-4-enyl group (also known as *n*-pentenyl glycosides) and different alcohol protecting groups. Observations led to the hypothesis that the *n*-pentenyl glycosides can undergo glycosylation to the hemi-acetal; however, the protecting group of the alcohols has a major effect on the relative rates of the reaction (Scheme 3-9). Each reaction was stopped at approximately 50% conversion to determine relative rates of the reaction. Benzyl protected **3-27** only took 6 hours to reach 50% conversion while acetate protected **3-27** took 36 hours to reach the same point.¹³⁸



Scheme 3-9: Relative Rates of Glycosylation Reactions of *n*-Pentenyl Glycosides Affected by Alcohol Protecting Group

The differences in rates supported the formation of an oxocarbenium ion, which was stabilized by the alcohol protecting groups protecting and the concept of armed/disarmed was introduced. An armed glycosyl donor refers to the oxocarbenium ion being stabilized by the electron donating capabilities of the protecting groups, whereas disarmed refers to the instability of the oxocarbenium ion due to the electron withdrawing effects of the protecting group.¹³⁹ Typically, an armed glycosyl donor and a disarmed glycosyl acceptor favor facile glycosylation formation. The accepted mechanism for the glycosylation reaction with *n*-pentenyl glycosides is shown below in Scheme 3-10. The alkene of *n*-pentenyl glycoside **3-27** forms bromonium ion **3-29** in the presence of NBS. The bromonium ion is then opened with the anomeric oxygen

forming furanylium **3-30**. Here, the alcohol protecting groups affect the rate of formation of oxocarbenium ion **3-31**, which undergoes glycosylation. By-product **3-32** is volatile and does not interfere with the desired reaction.

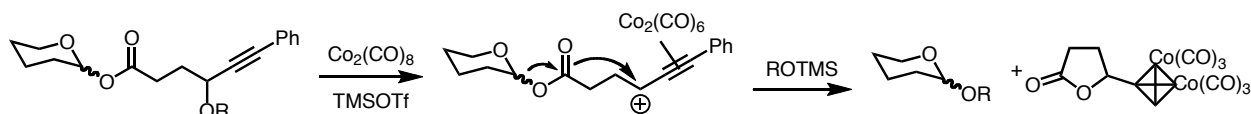


Scheme 3-10: Mechanism of Glycosylation with *n*-Pentenyl Glycosides

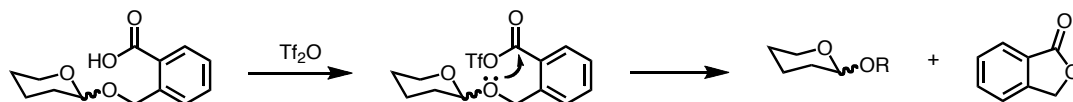
Fraser-Reid's work with *n*-pentenyl glycosides inspired many others to advance latent-active glycosylation methods (Scheme 3-11). In 1997, Mukai, Hanaoka and coworkers published a glycosylation method wherein a dicobalthexacarbonyl-complexed propynyl ether derivative – once activated with a Lewis acid – produced the desired glycosylation product and a cobalt-complexed γ -lactone (Scheme 3-11 A).¹⁴⁰ Yields of glycosylation were modest, but α/β selectivity was variable. A few years later in 2001, Kim reported a latent-active glycosylation via activation of 2-(hydroxycarbonyl)benzyl glycosides (Scheme 3-11 B).¹⁴¹ Kim's glycosylation reaction has good stereoselectivity, as β -mannosides and α -glucosides were at times exclusively formed, successfully synthesizing 1,2-*cis* glycosides via an intermolecular glycosylation reaction. Subsequent investigations by Hotha demonstrated that gold affinity for alkynes could be used for activation of propargyl glycosides (Scheme 3-11 C).¹⁴² Heating this reaction to 60 °C increases the rate of production of the desired glycoside and methyleneoxirane which can further rearrange to the unreactive cyclopropanone. Follow up studies demonstrated how activation of propargyl alkynes with AuBr₃ was orthogonal to activation of *n*-pentenyl glycosides with

NIS/TMSOTf.¹⁴³ In 2015, Yu furthered the activation of alkynes for glycosylation when *ortho*-(methyltosylaminoethynyl)benzyl glycosides were activated with trimethylsilyl trifluoromethanesulfonate (TMSOTf) (Scheme 3-11 D).¹⁴⁴ The reaction is believed to go through a keteniminium cation that is intramolecularly attacked with the anomeric oxygen forming a 1*H*-isochromene. This method has been used for the synthesis of oligosaccharides. That same year, another latent-active glycosylation involving an interrupted Pummerer reaction was published by Wang (Scheme 3-11 E).^{145–147} The byproduct in the glycosylation reaction is 2-(2-propylsulfinyl)benzyl alcohol which is one of the starting materials for synthesizing the original glycoside making the reaction very atom economical.

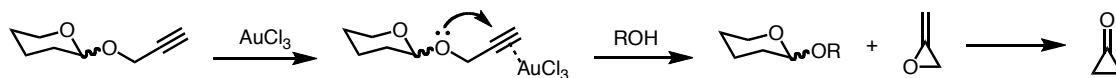
A: $\text{Co}_2(\text{CO})_6$ -propargyl cation glycosylation (Mukai/Hanaoka, 1997)



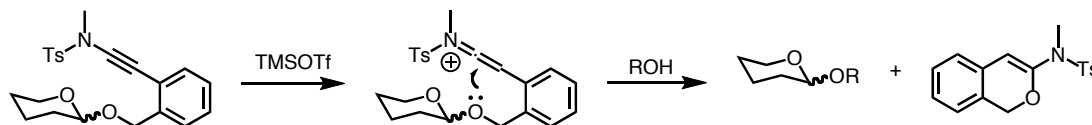
B: 2-(Hydroxycarbonyl)benzyl glycosylation (Kim, 2001)



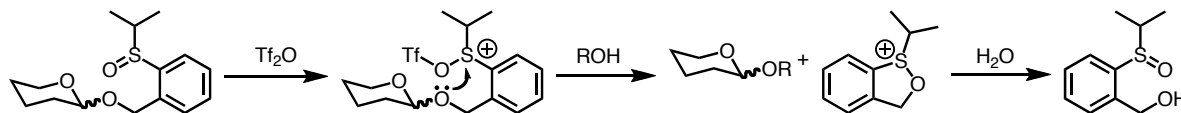
C: Propargyl glycosylation (Hotha, 2006)



D: Keteniminium glycosylation (Yu, 2015)



E: Interrupted Pummerer glycosylation (Wang, 2015)



Scheme 3-11: Various Latent-Active Glycosylation Reactions

As mentioned above, Fraser-Reid's work inspired numerous latent-active glycosylations with his serendipitous discovery that *n*-pentenyl glycosides underwent glycosylation when

exposed to NBS. Thus far, there are no reports of intramolecular glycosylations using latent-activation methods.

3.3.2 Recent Advances on Activation of Thioglycosides

Seminal work by Ferrier¹²⁹ and Garegg¹³¹ activated thioglycosides for glycosylation through the use of mercury (II) salts, which have high affinity for sulfur group complexation. Concurrently, Nicolaou reported activation of thioglycosides with *N*-bromosuccinimide and 4 Å MS.¹³⁰ While these methods served as groundbreaking development in thioglycoside methodology, the toxicity of mercury salts means they tend to be avoided in chemical syntheses. Additionally, the α/β selectivity using these methods tends to be low. Over the years, other methods to activate thioglycosides have been developed and include the use of MeOTf,^{148,149} dimethyl(methylthio)sulfonium triflate (DMTST),¹⁵⁰ and iodonium dicollidine perchlorate (IDCP)^{151,152} (Figure 3-1) which are only a subset of the extensive list of thioglycoside activators¹⁵³ where NIS and triflic acid (TfOH) are the most commonly used activators.¹⁵⁴ Even though there is an extensive repertoire of thioglycoside activators, there is still a push to find new methods of activation that eliminate toxic chemicals, expand the scope of glycosylations, and avoid sub-ambient temperatures.

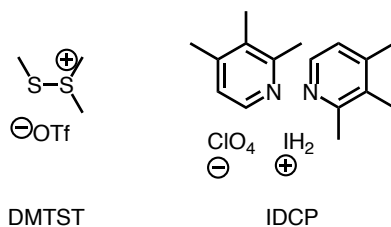
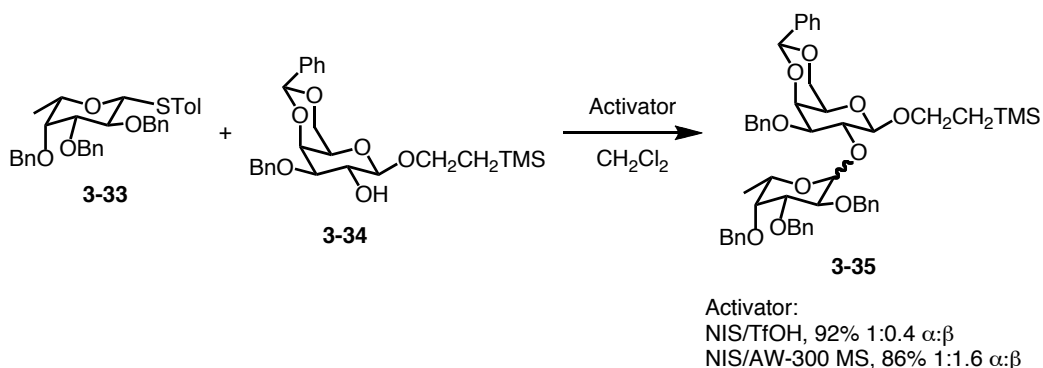


Figure 3-4: Structures of DMTST and IDCP

In glycosylation reactions, rigorously anhydrous conditions are needed due to water competing as the glycosyl acceptor, which inhibits desired glycosylation reactions. Often, molecular sieves are used to ensure dry reaction conditions. Lee showed how acid washed

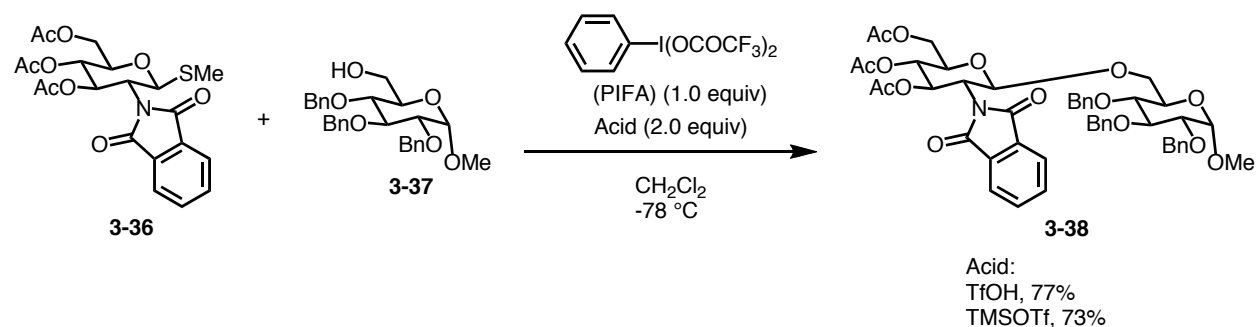
molecular sieves could play a dual role in addition to drying the reaction (Scheme 3-12).¹⁵⁴ When paired with NIS, acid washed (AW)-300 molecular sieves (MS) activate thioglycosyl donor **3-33** and glycosyl acceptor **3-34** forming **3-35** in 86% yield with 1:1.6 α : β selectivity. When compared to standard activation conditions of NIS/TfOH, comparable yields were obtained, although a switch in α : β selectivity was observed – indicating TfOH and AW-300 MS play a role in the α / β selectivity of the reaction. Furthermore, the NIS/AW300-MS methodology could be applied to a one-pot synthesis of a branched trisaccharide starting with three distinct sugar moieties.



Scheme 3-12: Lee's Activation of Thioglycosides with NIS/AW-300 MS

In the mid 1990's, Fukase demonstrated that hypervalent iodine PhIO – when paired with various inorganic Lewis acids (i.e. $\text{Sn}(\text{OTf})_2$, $\text{SnCl}_4\text{-AgClO}_4$, $\text{SbCl}_3\text{-AgClO}_4$) – activate thioglycosides forming new *O*-glycosides.¹⁵⁵ Product α / β selectivity was affected by the identity of the Lewis acid(s) added to the reaction conditions. More recently, Kajimoto, Kita and coworkers eliminated the need for inorganic Lewis acids when phenyliodine(III) bis(trifluoroacetate) (PIFA) and an organic Lewis acid (i.e. TfOH, TMSOTf) perform similar glycosylation reactions by activating thioglycosides.¹⁵⁶ Typically, glycosylation reactions are performed with aforementioned “armed” donors (sugars with protected alcohols that stabilize the oxocarbenium ion) and “disarmed” acceptors (sugars with electron withdrawing groups that

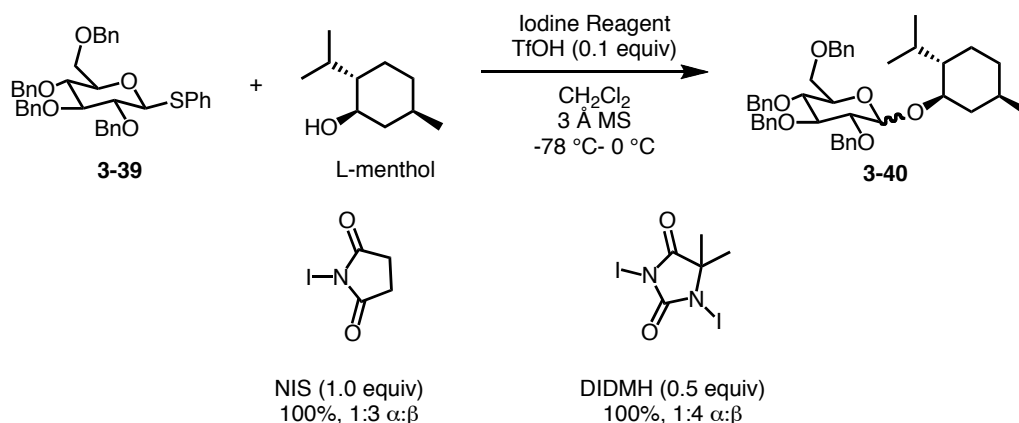
destabilize the oxocarbenium ion); however, using PIFA “disarmed” thioglycoside donor **3-36** and “armed” acceptor **3-37** proceeded in the glycosylation reaction in high yields (Scheme 3-13).



Scheme 3-13: "Disarmed" Thioglycosyl Donor and "Armed" Acceptor Addition via Hypervalent Iodine

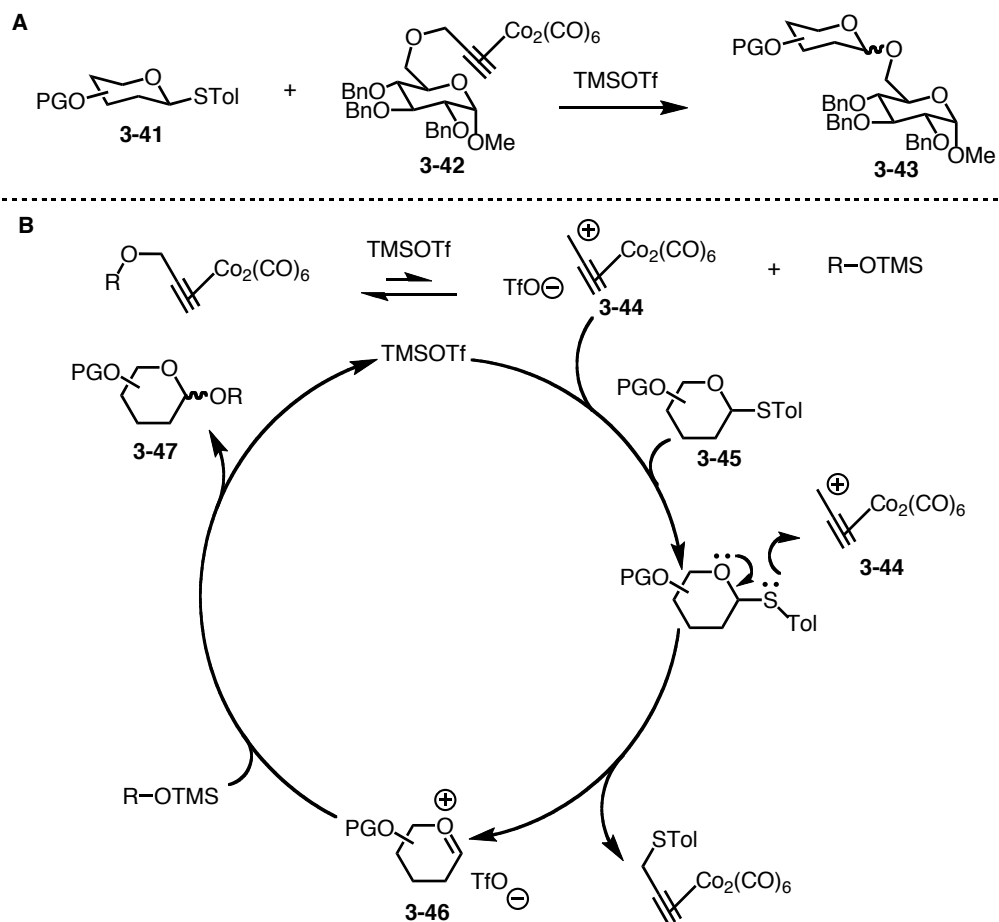
Applicability of hypervalent iodine as a thioglycoside activator for glycosylation helps attain the overarching goal of synthetic glycosciences: reproducibility of methodology. An iterative glycosylation-deprotection automatic flow system utilizing a water- and air-stable hypervalent iodine species was used to synthesize a β -1,6-glucan tetramer in 16% yield over 6 steps.¹⁵⁷ The reaction was optimized to maximize yield while minimizing undesirable by-products by using strained olefins as acid scavengers instead of the typical amine bases seen in glycosylation reactions.

Distinct from NIS or hypervalent iodine compound use, another iodine activation method for thioglycosides is 1,3-diiodo-5,5-dimethylhydantoin (DIDMH).¹⁵⁸ When paired with TfOH or AgOTf, glycosylation with thioglycoside **3-39** and L-menthol resulted in quantitative yields and increased α/β selectivity of **3-40** compared to typical NIS/TfOH methodology (Scheme 3-14). Furthermore, the authors note that using DIDMH is more atom economical, as one molecule of DIDMH can activate two thioglycosides as opposed to the single molecule activation of one molecule of NIS.



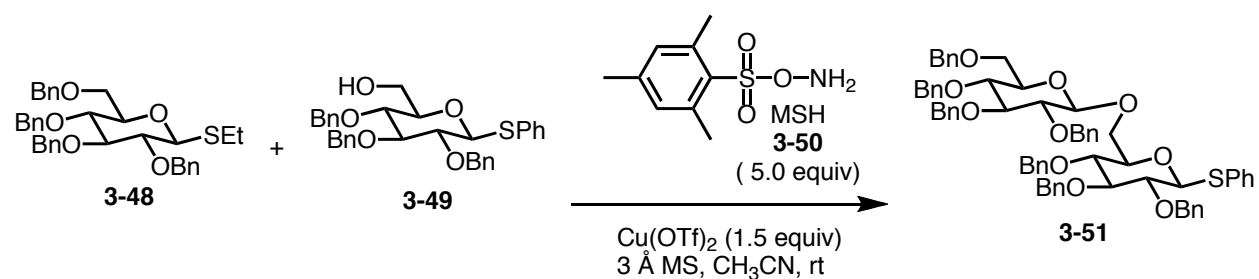
Scheme 3-14: Activation of Thioglycosides with DIDMH for Glycosylation

Although the use of iodine-based reagents (i.e., NIS, hypervalent iodine, or DIDMH) provides good yield and selectivity, halogenated starting materials require special waste disposal. Consequently, a push for methods of thioglycoside activation that do not use iodine reagents are of interest. Drawing inspiration from Mukai and Hanaoka's latent-active glycosylation reaction,¹⁴⁰ an intermolecular glycosylation using $\text{Co}_2(\text{CO})_6$ propargyl cation as an activator was reported (Scheme 3-15 A).¹⁵⁹ A propargyl $\text{Co}_2(\text{CO})_6$ appended to glycosyl donor **3-42** was activated with TMSOTf, thereby initiating the glycosylation reaction with thioglycoside donor **3-41** to form **3-43**. The mechanism of this reaction involves cationic cobalt species **3-44**, which undergoes nucleophilic attack by the sulfur forming oxocarbenium species **3-45**, which forms the desired product with the depropargylated glycosyl donor (Scheme 3-15 B). This methodology provides efficient glycosylation reactions, as yields range from moderate to excellent; however, the α/β selectivity ranges from one anomer, to a mixture, to the other anomer. The shift in α/β selectivity indicates that the stereoselectivity of the reaction was dictated by the identity of the donor/acceptor, and not by the activation method.



Scheme 3-15: (A) Inter-molecular Glycosylation Reaction Using Propargyl $\text{Co}_2(\text{CO})_6$ as the Glycosyl Acceptor (B) Mechanism for Glycosylation Reaction using Propargyl $\text{Co}_2(\text{CO})_6$ as Thioglycoside Activator

Intriguingly, several thioglycoside activations do not fully discriminate between ethyl thioglycosides and phenyl thioglycosides. An orthogonal approach to those outlined above which is able to discriminate between alkyl thioglycosides and phenyl thioglycosides provided the inspiration for developing an electropositive nitrogen promoter (Scheme 3-16).¹⁶⁰ In combination with $\text{Cu}(\text{OTf})_2$, the soft Lewis acidity of *O*-mesitylenesulfonylhydroxylamine (MSH) **3-50** was able to activate the soft alkyl thioglycoside **3-48** – even in the presence of the phenyl thioglycoside **3-49** – forming **3-51** albeit in 50% yield.



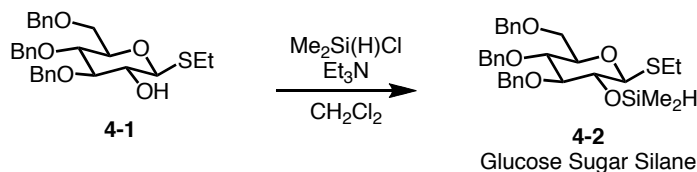
Scheme 3-16: Selective Alkyl Thioglycosides Activation

In conclusion, there are a countless number of thioglycoside activation promoters for glycosylation reactions. Each method provides its own advantages or disadvantages; however, further investigation into thioglycosides activations would provide more atom economical or orthogonal alternatives to those currently in literature.

Chapter 4 Advances in Intramolecular Aglycone Delivery via Latent-Activation

4.1 Montgomery Group Contributions to Glycosciences via Synthesis of 1,2-*cis*- Glycosides

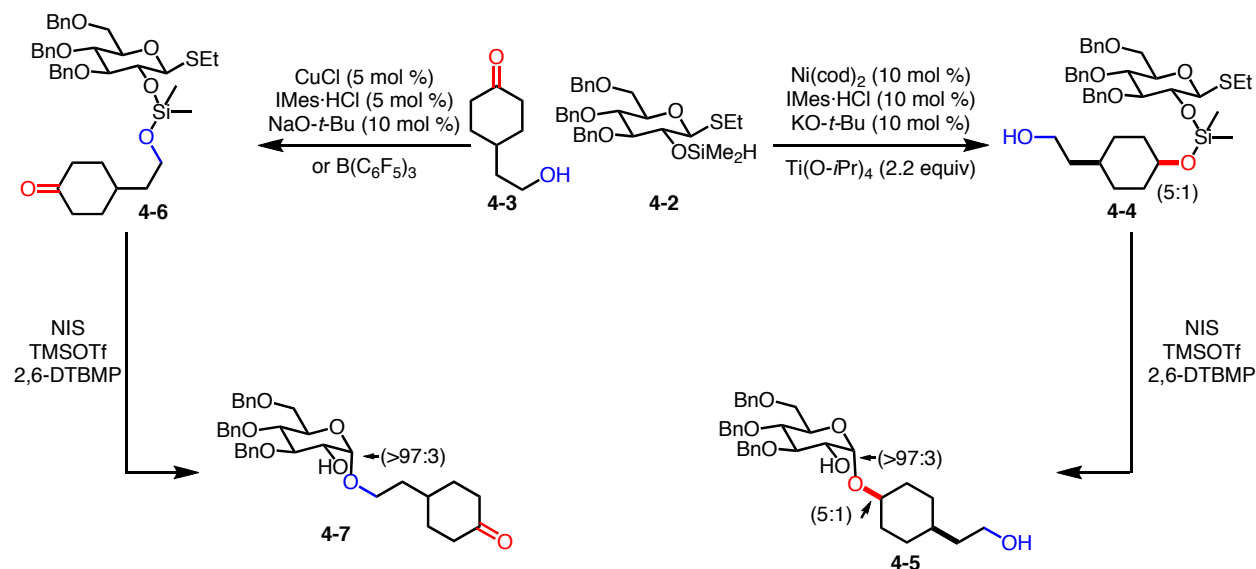
As mentioned previously in Chapter 3, Stork laid the groundwork for the synthesis of 1,2-*cis* glycosides by using a silicon group to tether a sugar and aglycone to enable glycosylations by intramolecular aglycone delivery.¹²¹ The Montgomery group has expanded upon this work with the synthesis of sugar silanes.^{161–163} Instead of a three-component synthesis with two alcohols and a silicon group to synthesize the precursor for aglycone delivery, the silane was attached to the sugar itself using dimethylchlorosilane (Scheme 4-1). Not only did this synthesis eliminate unproductive homocoupling of alcohols, this process additionally installed a silicon-hydride functionality that could be further exploited through its use in hydrosilylation,¹⁶¹ dehydrogenative silylation,^{161,163} and reductive coupling¹⁶² reactions. The remainder of this introduction will focus on the application of hydrosilylation and dehydrogenative silylation pathways developed by the Montgomery group with sugar silane systems.



Scheme 4-1: Synthesis of a Glucose Sugar Silane from a 2-Hydroxy Sugar

The Montgomery group demonstrated that *in situ* generation of a nickel-IMes complex catalyzes the hydrosilylation of ketones with the dimethyl sugar silane, tethering the aglycone to the sugar with 5:1 diastereoselectivity (Scheme 4-2).¹⁶¹ Using conditions similar to Stork's glycosylation to activate the thioglycoside tethered substrate **4-4**, the 1,2-*cis* glycoside was

achieved in high regioselectivity at the anomeric position.¹⁶¹ Moreover, dehydrogenative silylation using a copper-IMes complex tethered the sugar silane with a free alcohol, which may then undergo aglycone delivery under analogous glycosylation conditions (Scheme 4-2).¹⁶¹ These methods are orthogonal to one another in that the selected catalyst system will chemoselectively react in divergent pathways from one another. Substrate **4-3** contains both a ketone and alcohol functionality, but exclusively undergoes either hydrosilylation or dehydrogenative silylation based on choice of reaction conditions. Complementary to the copper-IMes complex, which tethers primary and other simple alcohols well, dehydrogenative silylation of secondary and more complex alcohols was achieved using tris(pentafluorophenyl)borane as the catalyst.¹⁶³ Lastly, delivery of the aglycone is not limited to the C-2 position of the sugar; C-6 sugar silanes will also undergo tethering and aglycone delivery upon subjection to similar conditions, although specialized trans diol protecting groups are required.¹⁶³



Scheme 4-2: Dehydrogenative Silylation of Alcohols and Hydrosilylation of Ketones with Sugar Silanes

While the synthesis of sugar silanes introduced facile new ways to catalytically tether the aglycone species and expand the scope of the aglycone, there remains space to improve upon this methodology. Dimethyl sugar silanes are non-chromatographable, and deprotect on contact with

silica gel chromatography to the corresponding C2-alcohol. Additionally, dimethyl sugar silanes are not bench stable and require storage under vacuum or freezing in benzene to slow decomposition – neither option being ideal for the synthetic community. As a graduate student in the Montgomery group, Dr. Allison Knauff discovered that upon exchanging the dimethyl groups on the silane for diisopropyl groups, the sugar became chromatographable due to the increase of sterics around the silicon center – which is hypothesized to disrupt the hydrogen bonding-and acidity-based degradation effects of silica gel chromatography (Figure 4-1).¹⁶⁴ Bench stability of diisopropyl sugar silanes is substantially greater than the related dimethyl sugar silanes, as they can be stored in a desiccator for several months without noticeable deterioration in reactivity.

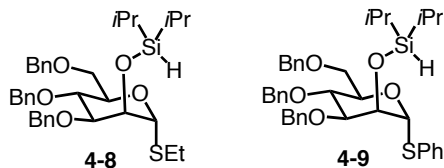
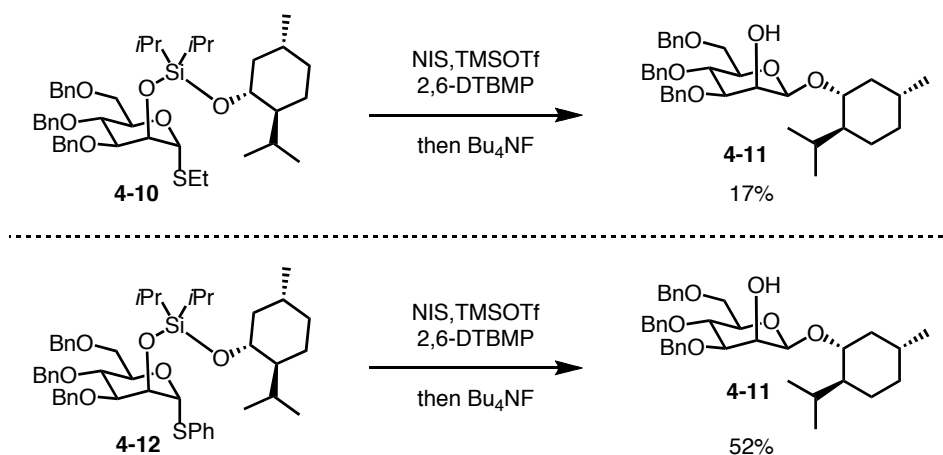


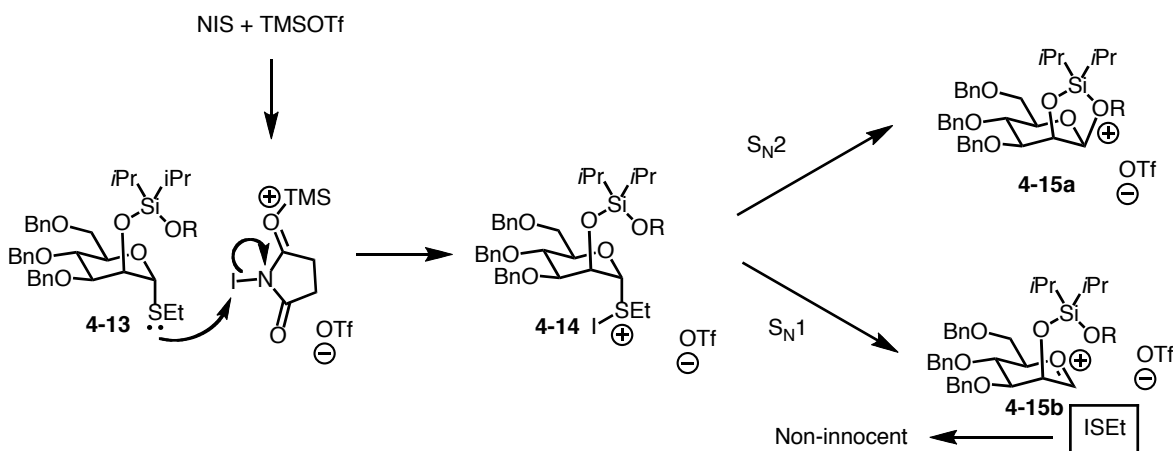
Figure 4-1: Diisopropyl Thiosugar Silanes

While increased bench stability was one of the goals to improving existing sugar silane methodology, this increase in bench stability carried with it an inherent increase in stability of the silicon-hydride bond – thereby decreasing the reactivity of the sugar silanes. Simple alcohols could be tethered readily; however, more complex secondary alcohols – such as menthol – required more forceful conditions. Upon generation of the menthol-tethered sugar silane, it was observed that the identity of the thiol-leaving group played a role in the efficiency of subsequent aglycone delivery (Scheme 4-3). The thiophenyl-tethered silane **4-12** was superior to the thioethyl-tethered silane **4-10**, increasing the yield of aglycone delivery from 17% to 52%.



Scheme 4-3: The Effect of the Thiol Leaving Group on Aglycone Delivery

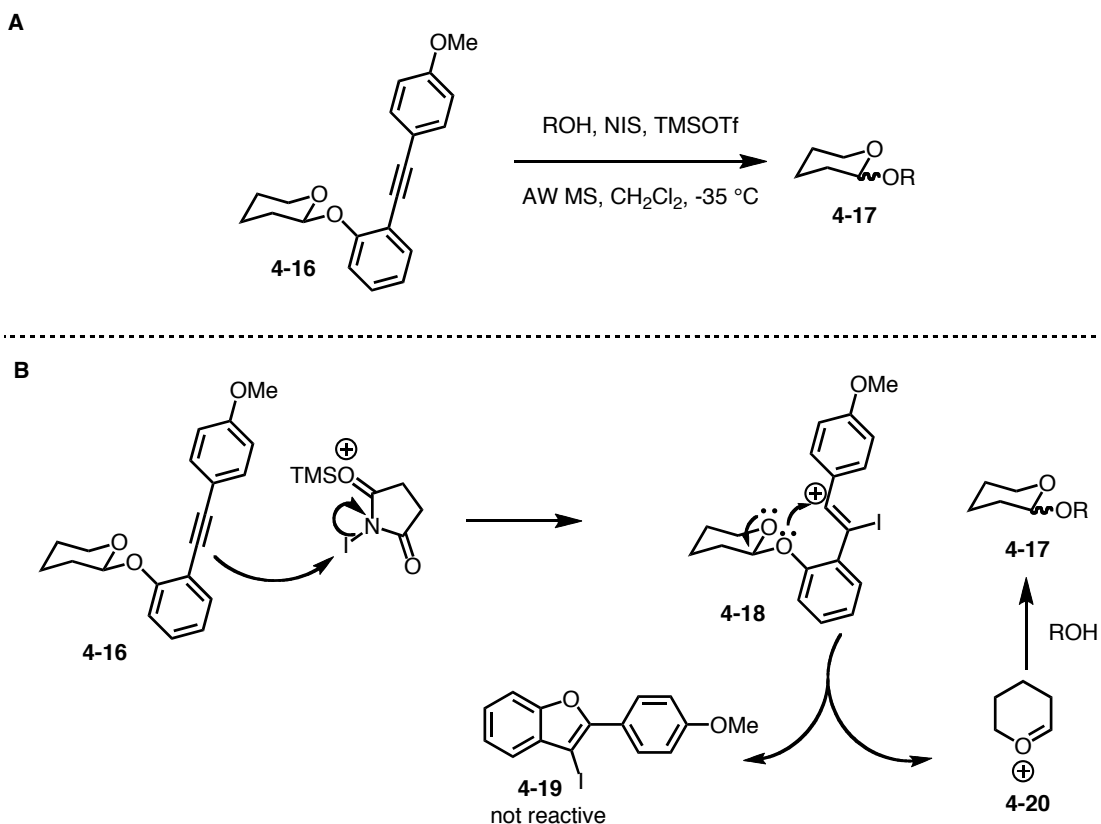
At this point, the mechanism of aglycone delivery is still not fully understood (Scheme 4-4). What has been accepted is that TMSOTf activates *N*-iodosuccinimide, increasing reactivity and generating a much more electrophilic iodine species, which can be attacked by the nucleophilic sulfur atom from thioglycoside **4-13**. From activated thioglycoside **4-14**, there are two potential possibilities: (a) An S_N2 -like attack of the aglycone results in the formation of cationic silicon species **4-15a**, which upon addition of Bu_4NF results in the desired 1,2-*cis* glycoside product, or (b) an S_N1 -like pathway thought to proceed via oxocarbenium ion structure **4-15b**, which would be susceptible to nucleophilic attack from the aglycone resulting in the same cationic silicon species as described above (**4-15a**). It is important to note that both pathways liberate an activated thiol species, which is non-innocent at times and can result in non-productive pathways that are harmful to the aglycone delivery process.¹⁶⁵ It is hypothesized that the true mechanistic pathway contains characteristics of both of the aforementioned possible pathways, potentially incorporating a tight ion pair interaction, which would help explain why the identity of the thio-leaving group is significant. Further computations and mechanistic studies need to be performed in order to probe these mechanistic hypotheses.



Scheme 4-4: Potential Mechanistic Pathways for Aglycone Delivery

4.2 Motivation and Project Goals

As developments outlined in Section 4.1 have highlighted, alkyl groups on the silicon dictate stability of the sugar silane. As efficient aglycone delivery relies on the nature of the leaving group at the anomeric position, other classes of leaving groups is one option to explore to increase the efficiency of the intramolecular aglycone delivery. Recently, the Sun group reported an intermolecular *O*-glycosylation reaction using an *o*-(*p*-methoxyphenylethynyl)phenyl group as the leaving group (Scheme 4-5 A).¹⁶⁶ Using the same TMSOTf/NIS activated electrophilic iodine source as previously published by Montgomery, the nucleophilic alkyne from **4-16** attacks the iodine forming vinyl cation **4-18**. Cyclization from the anomeric oxygen to the vinyl cation results in oxocarbenium ion **4-20** and benzofuran byproduct **4-19** (Scheme 4-5 B). Compound **4-20** then proceeds to intermolecular glycosylation. Isolation and characterization of **4-19** indicates that the benzofuran byproduct remains inert under glycosylation reaction conditions.



Scheme 4-5: A) Sun's Intermolecular Glycosylation B) Proposed Mechanism for Sun's Intermolecular Glycosylation

Based on Sun's and Montgomery's prior results, it was hypothesized that by combining the use of diisopropyl groups to increase stability and the *o*-(*p*-methoxyphenylethynyl)phenyl group as the leaving group to eliminate by-product interference, more efficient intramolecular glycosylation could be achieved. The goal of this project is to explore the reactivity and stability of sugar silanes that contain the *o*-(*p*-methoxyphenylethynyl)phenyl leaving group (**4-21**, **4-22**) in efforts to increase the scope and user-friendliness of sugar silane chemistry for aglycone delivery (Figure 4-2).

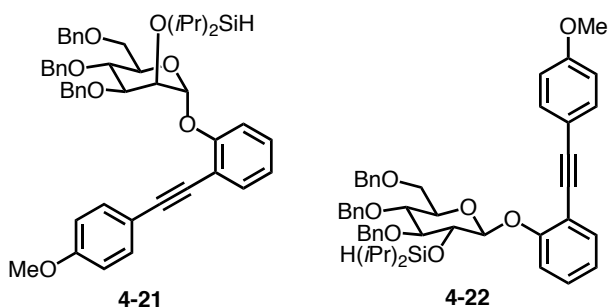
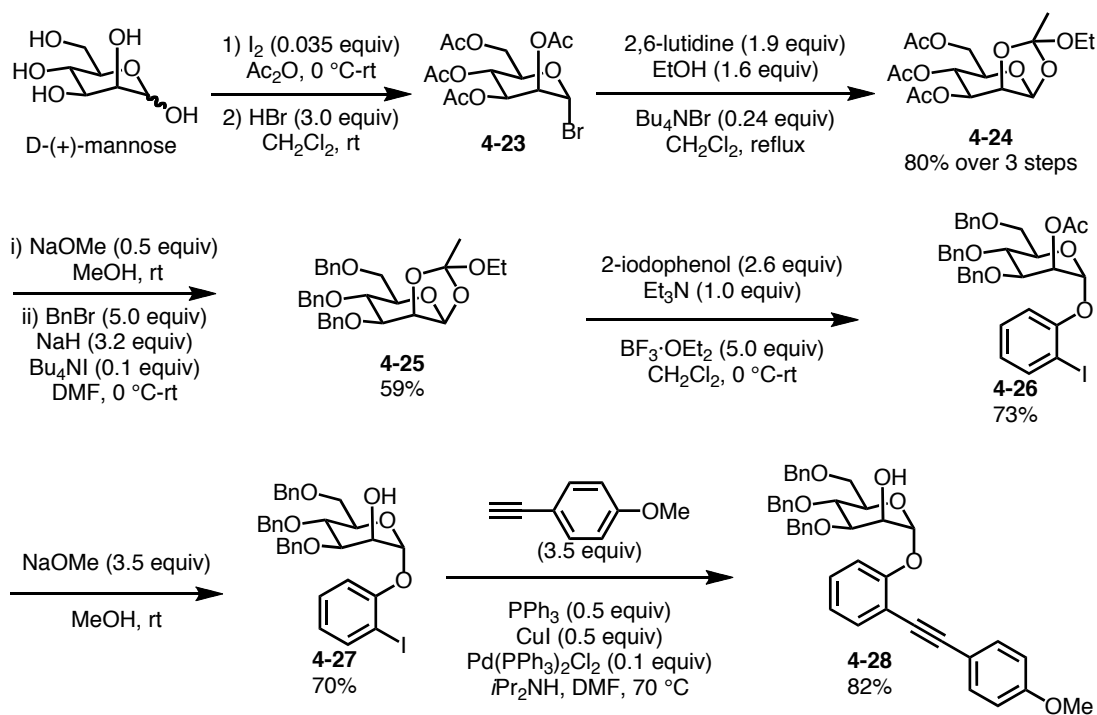


Figure 4-2: New Sugar Silanes

4.3 Continued Progress Towards Bench Stable Sugar Silanes

4.3.1 Synthesis of Mannose Sugar Silanes

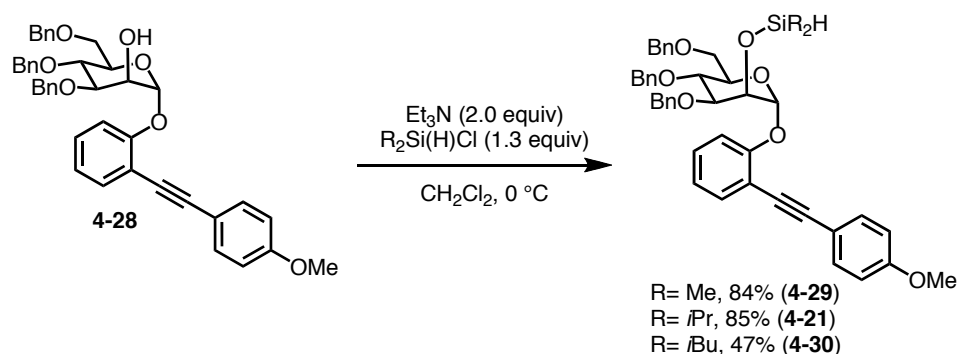
The synthesis of C-2 hydroxy mannose with the *o*-(*p*-methoxyphenylethynyl)phenyl leaving group was achieved in seven steps with five discrete isolations (Scheme 4-6). Commercially available D-(+)-mannose was globally protected and α -brominated to generate polyacetylated bromosugar **4-23**. Subsequently, **4-23** was transformed to orthoformate **4-24** before protecting group manipulation generated benzyl protected **4-25**. Opening of orthoformate **4-25** with 2-iodophenol led to the α -anomer **4-26**. Upon deprotection of the C-2 alcohol, **4-27** was used as a cross-coupling partner with *para*-methoxyphenyl acetylene in a Sonogashira cross-coupling reaction affording **4-28**. Although the synthesis was straightforward, future optimization of a more convergent synthesis would eliminate one step and address some of the purification issues. For instance, performing the Sonogashira cross-coupling on 2-iodophenol before addition to **4-25** may help reduce the palladium byproducts that tend to be difficult to remove.



Scheme 4-6: Synthesis of 2-Hydroxy Mannose Sugar Silane Precursor

Using reaction conditions previously established by the Montgomery lab,¹⁶¹ **4-28** was then transformed to the desired sugar silane substrates (Scheme 4-7). After a liquid-liquid extraction, dimethyl sugar silane **4-29** was isolated as viscous yellow oil that was used without further purification. The yellow discoloration was attributed to NMR-silent impurities from the Sonogashira cross-coupling reaction, as diisopropyl sugar silane **4-21** was chromatographable (silica gel) and isolated as a white crystalline solid. Diisopropyl sugar silane **4-21** was found to be bench stable, as decomposition was not observed after being left open to air at room temperature for several months. While the yields of **4-29** and **4-21** were above 80%, diisobutyl sugar silane **4-30** was isolated after silica gel chromatography in 47% yield. Low yields are attributed to semi-stability upon exposure to silica gel. Diisobutyl sugar silane **4-30** could be isolated from silica gel chromatography if a small amount was exposed for a short period of time. However, prolonged exposure to silica gel resulted in decomposition of **4-30** to the diisobutyl silyloxane and **4-28**. Despite this drawback, there is no further observed effect on the

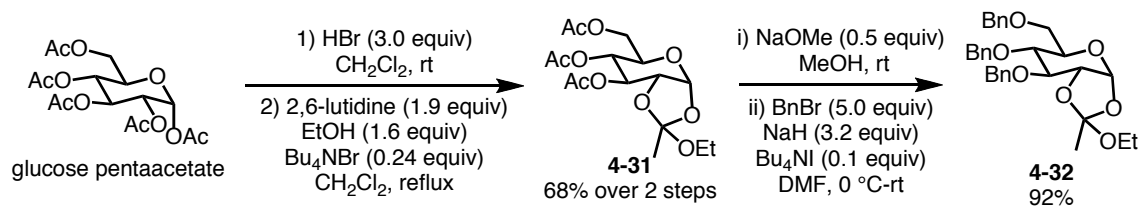
bench stability of **4-30**, as several months storage in the freezer did not result in decomposition or decreased reactivity.



Scheme 4-7: Synthesis of Several Mannose Sugar Silanes

4.3.2 Synthesis of Glucose Sugar Silanes

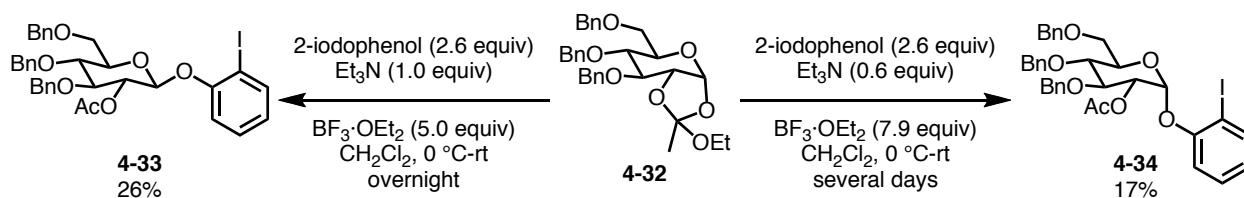
The synthesis of glucose-derived sugar silanes was initially analogous to the synthesis of mannose sugar silanes described above (Scheme 4-8). Glucose pentaacetate is not only commercially available but is inexpensive to begin the synthesis here rather than performing the global protection on glucose. Glucose pentaacetate was α -brominated then transformed to the orthoformate **4-31** in 68% yield over two steps. Protecting group manipulation to the benzyl-protected sugar **4-32** was achieved in high yield (92%).



Scheme 4-8: First Three Steps of the Synthesis of Glucose Sugar Silanes

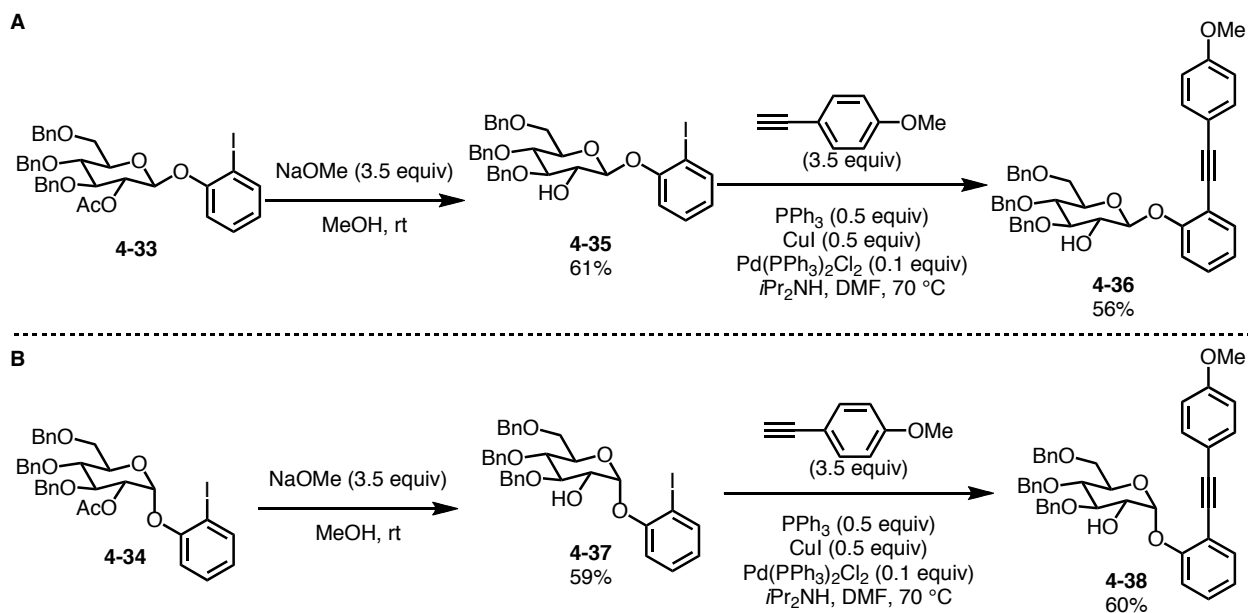
Unlike the aforementioned mannose-based synthesis, addition of 2-iodophenol to **4-32** provided a greater challenge, requiring an adjustment in reaction conditions (Scheme 4-9). Performing the addition while gradually warming from 0 °C to room temperature overnight resulted in formation of the expected β -anomer **4-33**, albeit in low (26%) yield. In an attempt to improve the yield, more equivalents of $\text{BF}_3 \cdot \text{OEt}_2$ were added over an extended period of time.

However, instead of the anticipated increase in yield of the β -anomer, α -anomer **4-34** was isolated. The results of this reaction likely indicates that the addition of 2-iodophenol is reversible and that the thermodynamic product is the α -anomer **4-34**, which has increased stability due to the anomeric effect. Increasing the yield of the reaction and controlling the equilibrium of this reversible step remains an outstanding optimization problem, but this serendipitous discovery allowed for derivatization of the glucose sugar silane to allow for comparison of both the α - and β -anomers.



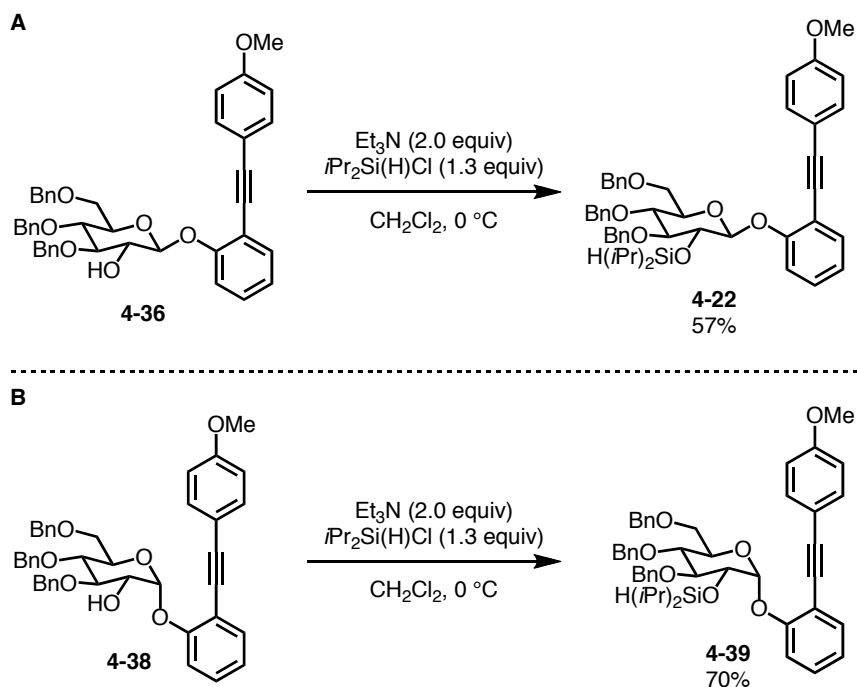
Scheme 4-9: Addition of 2-Iodophenol to Orthoformate **4-31**

It is important to note that previously the Montgomery lab had not been able to study both anomers as prior sugar silane substrates in the glucose series were produced as solely the β -anomer. Being able to study the behavior of both anomers in not only the synthesis but also the tethering and aglycone delivery steps would provide insight into reactivity and selectivity of the silane. For the remainder of the synthesis, both α - and β -anomers followed the same synthetic route to the 2-hydroxy glucose sugar as utilized previously for the mannose series (Scheme 4-10). Deprotection of **4-33** and **4-34** to the free alcohol **4-35** and **4-37** using sodium methoxide and methanol gave modest yields of 61% and 59%, respectively. Both anomers performed similarly in the Sonogashira cross-coupling reaction resulting in the formation of β -anomer **4-36** and α -anomer **4-38**.



Scheme 4-10: (A) Synthesis of Glucose β -2-Hydroxy Sugar (B) Synthesis of Glucose α -2-Hydroxy Sugar

The final step of the synthesis of glucose sugar silanes **4-22** and **4-39** followed reaction protocols established by the Montgomery lab (Scheme 4-11).¹⁶¹ Although the β -anomer **4-22** was isolated in only 57% yield compared to the α -anomer **4-39** which was isolated in 70% yield, this was not significant enough of a disparity to indicate a difference in reactivity between the two anomers.

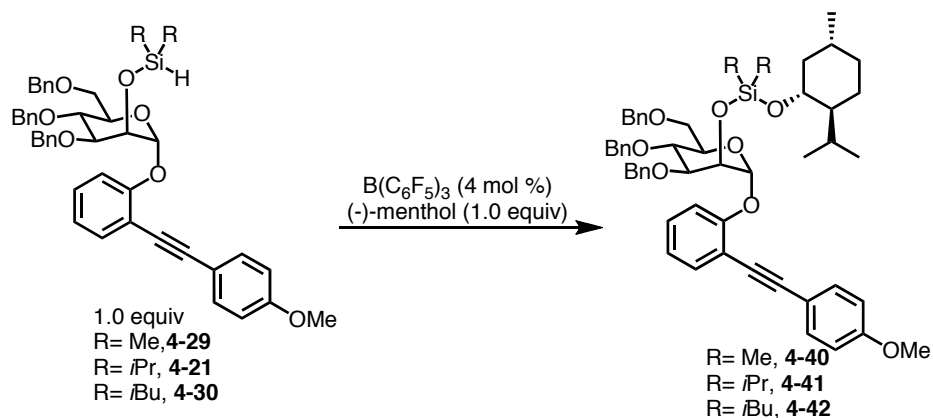


Scheme 4-11: Synthesis of α - and β -Glucose Sugar Silanes

4.3.3 Mannose Sugar Silane Tethering and Aglycone Delivery

To explore the scope of silane tethering and subsequent aglycone delivery, (-)-menthol was chosen as the model alcohol. As mentioned earlier, diisopropyl thiosugar silane was able to tether to menthol, but aglycone delivery was not as efficient when compared to dimethyl thiosugars (72-74%) (Scheme 4-3). Both copper and borane-catalyzed dehydrogenative silylation methods were investigated with substrate **4-29** to see the compatibility of the alkyne under these conditions. Desired product formation was only observed with the borane catalyst and further optimization of the tethering was required (Table 4-1). Initial results showed **4-29** was able to be tethered in a 49% isolated yield; however, the incomplete conversion of starting material resulted in inseparable mixture of **4-40** and (-)-methanol, which artificially lowered the isolated yield (entry 1). Adding 4 Å molecular sieves (entry 2) and extending the time (entry 3) were detrimental and decreased the yield of the reaction. However, when silane **4-21** was used instead of **4-29** the product and remaining (-)-menthol cleanly separated and **4-41** was isolated in a 55%

yield (entry 4). By increasing the equivalence of silane to 1.1 equivalents and adding a second 4 mol % catalyst after 5 hours of reaction time, **4-40** was cleanly isolated in 60% yield (entry 5), **4-41** in 85% yield (entry 6) and **4-42** in 65% yield (entry 7). Even though silane **4-21** has more sterics than **4-30**, the higher yield was credited to the user-friendliness of the crystalline solid over the viscous liquid of **4-30** that tends to be more difficult to handle.



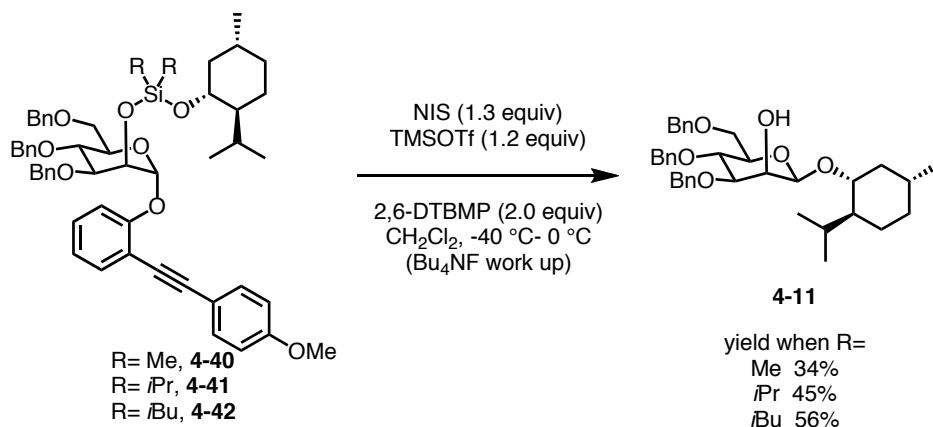
Entry	Silane	Modification	Time	Result
1	4-29	-	2 h	49% +mixed fractions ^a
2	4-29	4 Å MS (200 mg/mmol)	4 h	40% + mixed fractions ^a
3	4-29	4 Å MS (400 mg/mmol)	overnight	27% + mixed fractions ^a
4	4-21	4 Å MS (400 mg/mmol)	overnight	55%
5	4-29	8 mol % catalyst ^b 1.1 equiv silane	overnight	85%
6	4-21	8 mol % catalyst ^b 1.1 equiv silane	overnight	60%
7	4-30	8 mol % catalyst ^b 1.1 equiv silane	overnight	65%

^ainseparable mixture of **4-39** and (-)-menthol ^b4 mol % of catalyst added at time=0 h, 4 mol % catalyst added at time=5 h

Table 4-1: Optimization of Tethering (-)-Menthol to Mannose Sugar Silanes

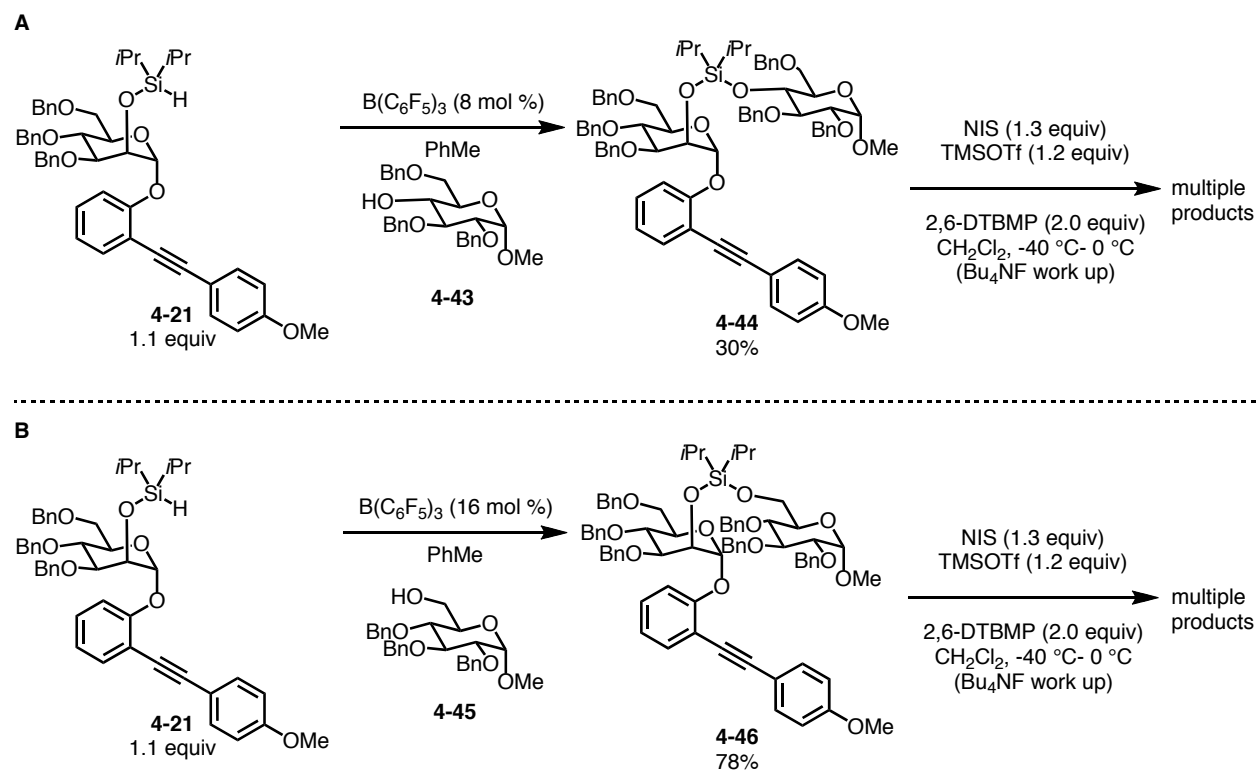
4-40, **4-41**, and **4-42** were subjected to aglycone delivery conditions employing the use of NIS, TMSOTf, and 2,6-DTBMP (Scheme 4-12). After letting the reactions run for several hours, full conversion of starting material was not observed; in fact, extending reaction time to 16 hours did not drive the reaction to completion, leading to the recovery of 2-hydroxy sugar **4-28** and untethered (-)-menthol. Of the substrates explored, **4-40** was the least efficient for aglycone

delivery, while **4-42** was the most efficient with a 56% isolated yield of **4-11**. Surprisingly, the yields among the three silanes do not follow any steric trend, as **4-40** was the least efficient in terms of conversion, despite the initial hypothesis that it would be the most efficient.



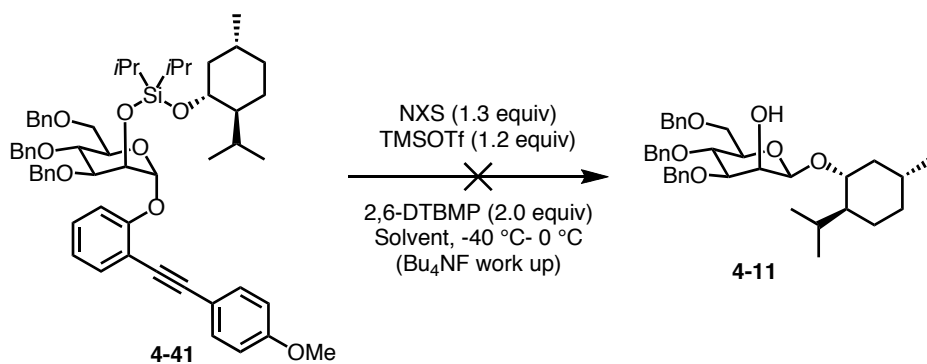
Scheme 4-12: Aglycone Deliveries with Mannose Derived Sugar Silanes

With preliminary results for aglycone delivery with (-)-menthol in hand, more complex aglycones were examined (Scheme 4-13). Sugar silane **4-21** was used in these experiments, as the solid silane could be prepared on a multigram scale. As described in the literature, tethered 4-hydroxy sugars are the Achilles heel of silicon tethered intramolecular aglycone deliveries where de-benzylation and delivery of the C-6 hydroxy group is often observed.¹²² Substrate **4-43** was not only more difficult to tether, but the aglycone delivery resulted in the formation of a several identifiable products, likely indicating the decomposition of **4-44** under these reaction conditions (Scheme 4-13 A). Less sterically hindered C-6 hydroxy sugar **4-45** underwent tethering with greater ease, yet still resulted in several unidentifiable products during the aglycone delivery step (Scheme 4-13 B). At present, it is hypothesized that changing the sterics around the silane would not significantly impact the tethering or aglycone delivery of the saccharides. Rather, these results suggest aglycone delivery using the *o*-(*p*-methoxyphenylethynyl)phenyl leaving group requires further optimization.



Scheme 4-13: Tethering and Aglycone Deliveries of Hydroxy Sugars

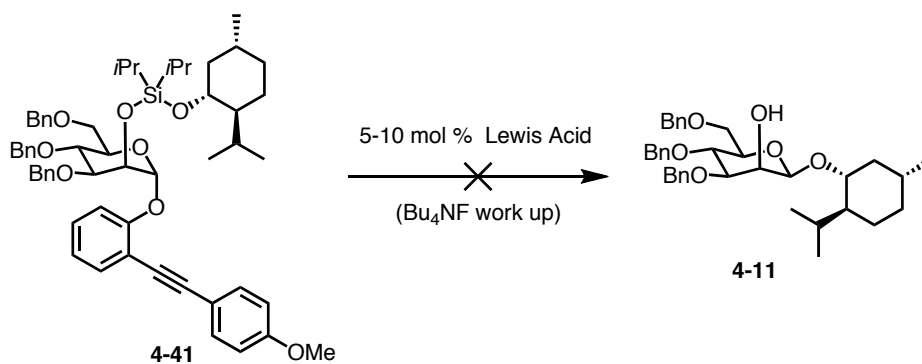
Investigation into optimizing the efficiency of the aglycone delivery involved changing the electrophilic halogen source or solvent of the reaction (Table 4-2). Neither *N*-chlorosuccinimide, NCS, (entry 1), nor *N*-bromosuccinimide, NBS, (entry 2) resulted in the desired product, demonstrating that the more electrophilic iodine species was needed. Furthermore, using NIS but changing the solvent from dichloromethane to dichloroethane (entry 3), toluene (entry 4) or tetrahydrofuran (entry 5) negatively impacted the reaction, as formation of the desired product was not observed.



Entry	NXS	Solvent
1	NCS	CH ₂ Cl ₂
2	NBS	CH ₂ Cl ₂
3	NIS	C ₂ H ₄ Cl ₂
4	NIS	PhMe
5	NIS	THF

Table 4-2: Attempted Aglycone Delivery with Other Electrophilic Halogen Sources and Solvents

Expanding optimization experiments to include other Lewis acids that could activate the alkyne to the benzofuran by-product were investigated (Table 4-3). *In situ* generated cationic gold did not result in desired product formation (entry 1). AlCl₃ (entry 2), PtCl₃ (entry 3) and AuCl₃ (entry 4) did not show any reactivity, as the C2-hydroxy sugar **4-28** and untethered (-)-menthol were observed after the tetrabutyl ammonium fluoride work up. Increasing the temperature of the reaction with AuCl₃ (entry 5) and Cu(OTf)₂ also gave the untethered starting materials, **4-28** and (-)-menthol. The results of Table 4-2 and Table 4-3 show that the NIS/TMSOTf combination is, to our knowledge, the best for activating the *o*-(*p*-methoxyphenylethynyl)phenyl leaving group. Further optimization could focus on further improving these established reaction conditions by examining the equivalents, solvent, and temperature effects of the reaction.



Entry	Lewis Acid	Solvent	Temp
1 ^a	PPh ₃ AuCl/AgOTf	CH ₂ Cl ₂	rt
2	AlCl ₃	CH ₂ Cl ₂	rt
3	PtCl ₂	CH ₂ Cl ₂	rt
4	AuCl ₃	CH ₂ Cl ₂	rt
5	AuCl ₃	C ₂ H ₄ Cl ₂	80 °C
6 ^a	Cu(OTf) ₂	C ₂ H ₄ Cl ₂	80 °C

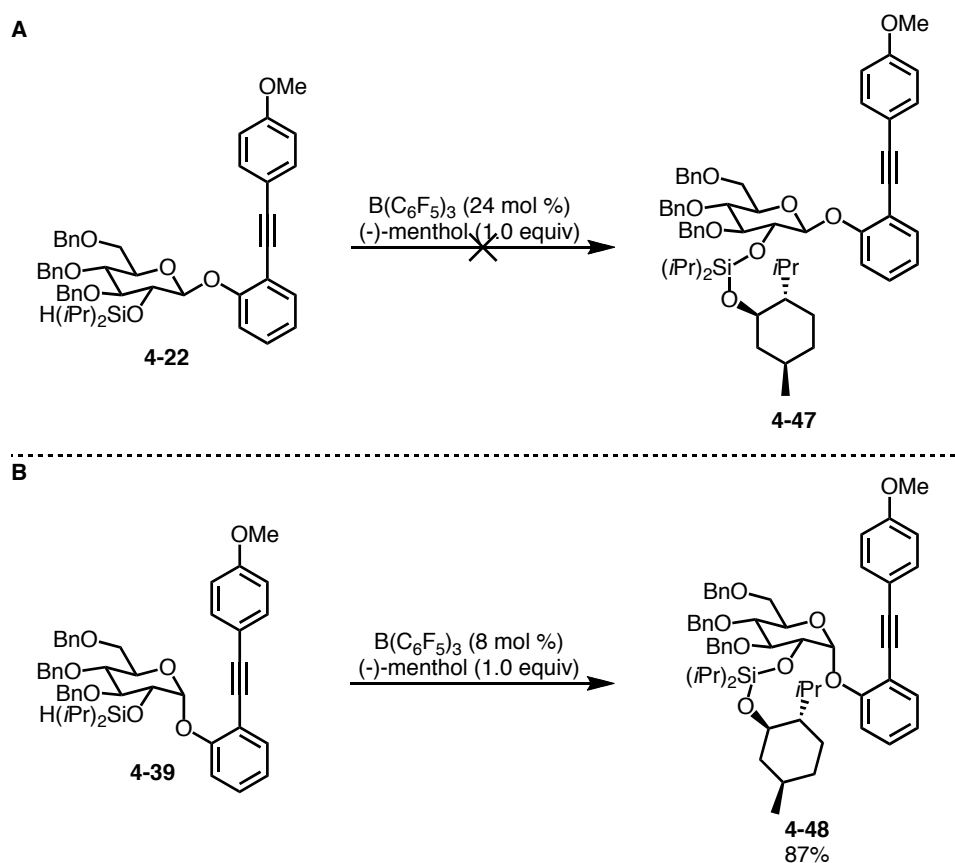
^a2.0 equiv MeOH added to the reaction

Table 4-3: Lewis Acid Screen for Aglycone Delivery

4.3.4 Glucose Sugar Silane Tethering and Aglycone Delivery

With both the β -anomer **4-22** and the α -anomer **4-39** in hand, the goal of exploring differences in reactivity could be further pursued. Upon submission to the optimized tethering conditions there was a stark contrast in reactivity between both anomers (Scheme 4-14). The β -anomer **4-22** proved difficult to tether, even when catalyst loading was increased. Possible product formation occurred when the reaction unintentionally dried up; however, the resulting material was isolated along with several inseparable impurities, making it difficult to state with certainty that **4-47** was formed. Heating the reaction to 50 °C with increased catalyst loading was detrimental to the reaction, as multiple unwanted by-products were observed. Conversely, α -anomer **4-39** tethered very well, resulting in the synthesis of **4-48** in an 87% yield. These results were unexpected, given the 1-2-*trans* orientation of **4-22** was the same relative configuration as the thiosugar silane **4-2** that was previously used in both the tethering and aglycone delivery

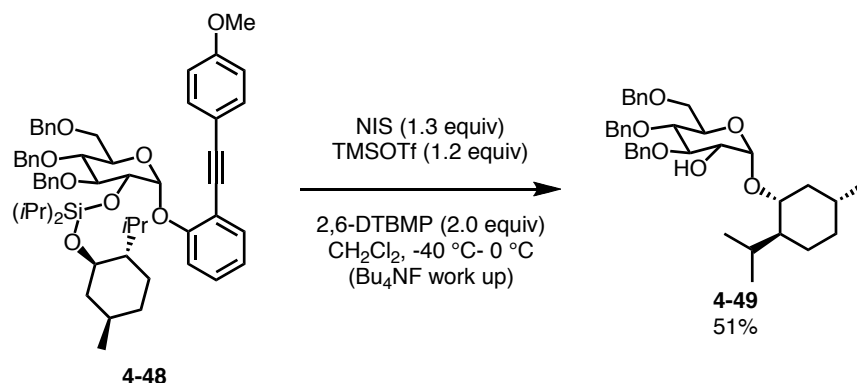
steps. Examining the size of the anomeric group has led to some hypotheses regarding the preferred conformation of the *o*-(*p*-methoxyphenylethynyl)phenyl leaving group. If the alkyne orientation points back towards the C-6 position, steric interaction with the benzyl-protected alcohol would force the alkyne to rotate toward the opposite side of the sugar – oriented towards the silane. This orientation would make the silicon-hydride bond inaccessible, thus inhibiting the formation of the cationic silicon species derived from the borane catalyst and rendering the silane unreactive. Upon subsection of **4-22** to catalyst and (-)-menthol, unreacted silane was isolated, which supports this hypothesis.



Scheme 4-14: Tethering of (-)-Menthol with both Anomers of Glucose Sugar Silanes

When **4-48** was subjected to the aglycone delivery conditions, the desired 1,2-*cis* glycoside **4-49** was obtained in 51% yield without observation of the 1,2-*trans* glycoside (Scheme 4-15). These results provide valuable insight into the mechanism of the reaction. For

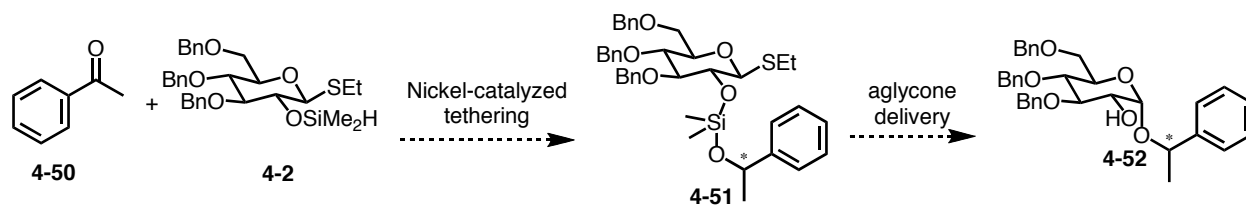
the 1,2-*cis* tethered sugar **4-48** to undergo intramolecular aglycone delivery, either an S_N1 type mechanism or a double inversion pathway must be involved. The direct displacement of the anomeric leaving group by the aglycone is very unlikely in the *cis* orientation when compared to the delivery of the aglycone to an oxocarbenium ion intermediate.



Scheme 4-15: Glucose Aglycone Delivery of (-)-Menthol

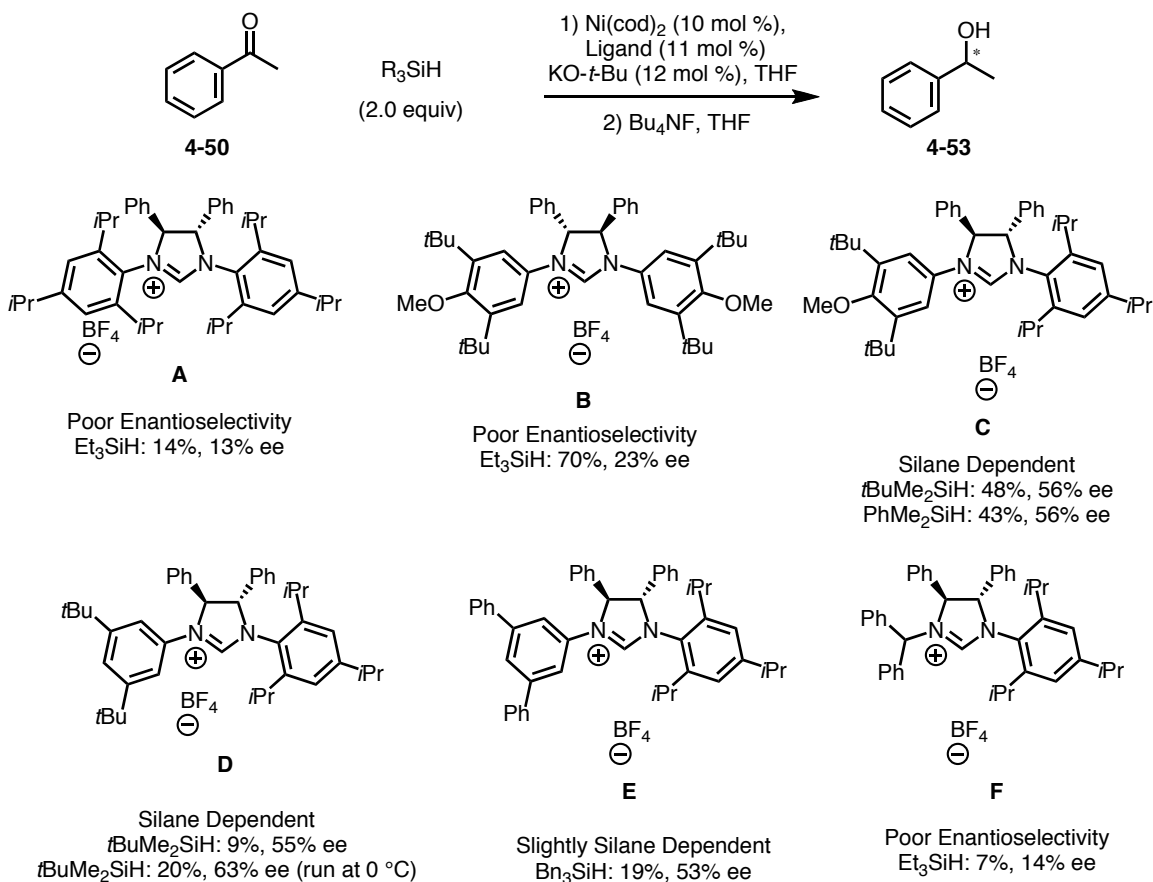
4.4 Progress Towards Asymmetric Hydrosilylation of Ketones

Additional work that has been conducted in this area includes the asymmetric hydrosilylation of pro-chiral ketones. The motivation for this work was to expand the utility of previously established methodology by setting an additional stereocenter in the tethering step. This chirality would be maintained throughout aglycone delivery, thereby setting two stereocenters over the course of the reaction sequence (Scheme 4-16). Based on the racemic hydrosilylation of ketones previously performed with nickel,¹⁶¹ it was hypothesized that the asymmetric hydrosilylation could also be accomplished via use of a nickel catalyst system. The only prior report of asymmetric nickel-catalyzed hydrosilylation of ketones up to this point employed the use of a nickel(II) precatalyst and phosphine ligands system open to air.¹⁶⁷ Although this method lends itself well to setting up reactions without a glove box, this methodology may not translate well to sugar silane substrates, as the air stability of sugar silanes is variable. Therefore, a nickel-*N*-heterocyclic carbene (NHC) approach was taken that mimics reaction conditions previously established by the Montgomery group.¹⁶¹



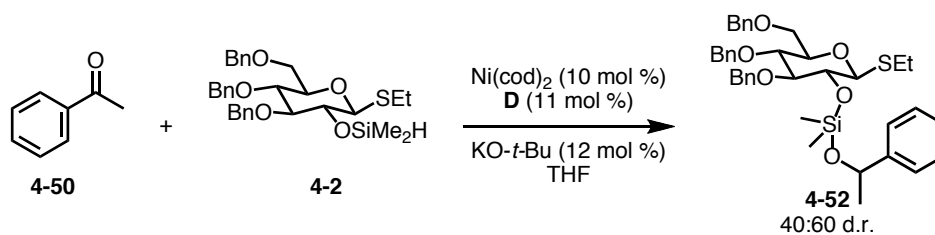
Scheme 4-16: Goals for Asymmetric Tethering before Aglycone Delivery

Initial investigations employed the use of commercially available silanes instead of the synthetically precious sugar silanes, as this allowed for deeper investigation due to a rapid screening approach (Scheme 4-17). The Montgomery group has previously demonstrated that C2-symmetric NHC **A** provides high enantioselectivity when employed in analogous reductive coupling reactions.⁸⁶ When applied to the hydrosilylation of acetophenone to form product **4-53**, poor enantioselectivity was achieved (13% ee). Shifting ligands from an *ortho/para*-substituted ligand to a *meta/para*-substituted ligand, **B** provided an increase in yield, yet poor enantioselectivity (23% ee) remained. Use of ligand **C** – a non-C2 symmetric hybrid of ligand **A** and **B** – provided decent enantioselectivity (56% ee), but was very dependent on the identity of the silane. Removal of the *para*-methoxy group (ligand **D**) showed a similar silane dependency. while cooling reactions to 0 °C slightly increased the enantioselectivity to 63% ee. Further alteration of the *meta*-substituents from *tert*-butyl groups to phenyl groups (ligand **E**) narrowed the range of silane dependence, but still maintained moderate enantioselectivity (53% ee). Moving away from an aniline derived NHC to mixed aniline/amine NHC **F** drastically decreased the enantioselectivity indicating the free rotation around the nitrogen-carbon bond was detrimental to the enantioselectivity of the reaction.



Scheme 4-17: General Trends for Nickel-Catalyzed Asymmetric Hydrosilylation of Acetophenone

After gaining insight into the nickel-catalyzed hydrosilylation of ketones with various simple silanes, focus shifted to using sugar silanes as the silane source (Scheme 4-18). When sugar silane **4-2** was employed in the hydrosilylation reaction with ligand **D** (which showed the most promise in previous screens) low diastereoselectivity (40:60) was observed. The silane dependence that was observed in initial screenings appears to play a large role in sugar silane optimizations as well. To improve the asymmetric hydrosilylation of ketones with sugar silanes, further optimization reactions must be conducted using the desired sugar silane.



Scheme 4-18: Asymmetric Hydrosilylation with Glucose Thiosugar Silane

4.5 Conclusion and Future Directions For Latent-Activation for Intramolecular Aglycone Delivery

In summary, further insights into the tethering and intramolecular aglycone delivery of sugar silanes were developed. Five new sugar silanes were synthesized – three in the mannose series with the 1,2-*trans* orientation and two in the glucose series in both the 1,2-*cis* and 1,2-*trans* orientation – all bearing an *o*-(*p*-methoxyphenylethynyl)phenyl leaving group. Dehydrogenative silylation was performed with optimized conditions using tris(pentafluorophenyl)borane. All three mannose-derived silanes were successful in both tethering and aglycone delivery reactions, albeit with moderate aglycone delivery yields. Additionally, the α -glucose anomer successfully was tethered and performed modestly in subsequent aglycone delivery. The inability for the β -glucose anomer to undergo dehydrogenative silylation with (-)-menthol may be attributed to the steric hindrance of the *o*-(*p*-methoxyphenylethynyl)phenyl leaving group.

Optimization of the activation of the *o*-(*p*-methoxyphenylethynyl)phenyl leaving group in the intramolecular aglycone delivery should be further explored. Varying the equivalents of the electrophilic iodine species is predicted to have a large effect on the efficiency of the aglycone delivery. Other modes of activation, such as the use of hypervalent iodine species, could provide insight as to whether other activation pathways are accessible that may confer higher yields or greater selectivity. Lastly, other alkynes can be installed to vary the electronics and the sterics for

the latent-activation (Figure 4-3). Cyclopropane (**4-53**) and tosyl-protected amines (**4-54**) would provide a difference in electronics for the initial nucleophilic attack of the electrophilic iodine species. Adding an extra methylene spacer (**4-55**) would result in a benzopyran by-product rather than the observed benzofuran, potentially changing the efficiency of the reaction.

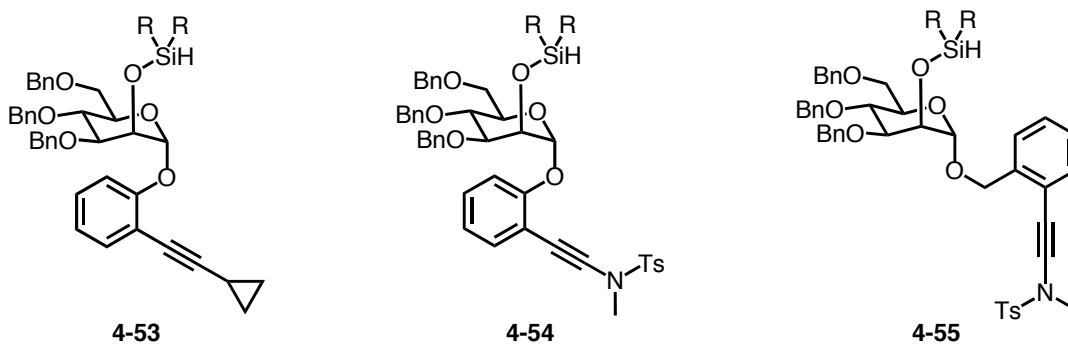


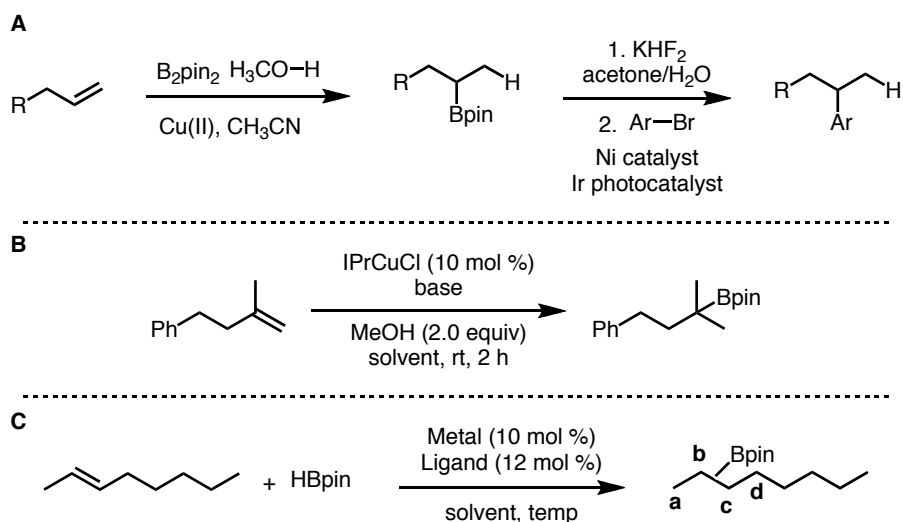
Figure 4-3: Various Electronics and Sterics of the Alkyne for Latent-Activation

Additionally, exploration into the asymmetric hydrosilylation of ketones with sugar silanes resulted in the conclusion that optimization must be performed using the synthetically precious sugar silane.

Chapter 5 Conclusion

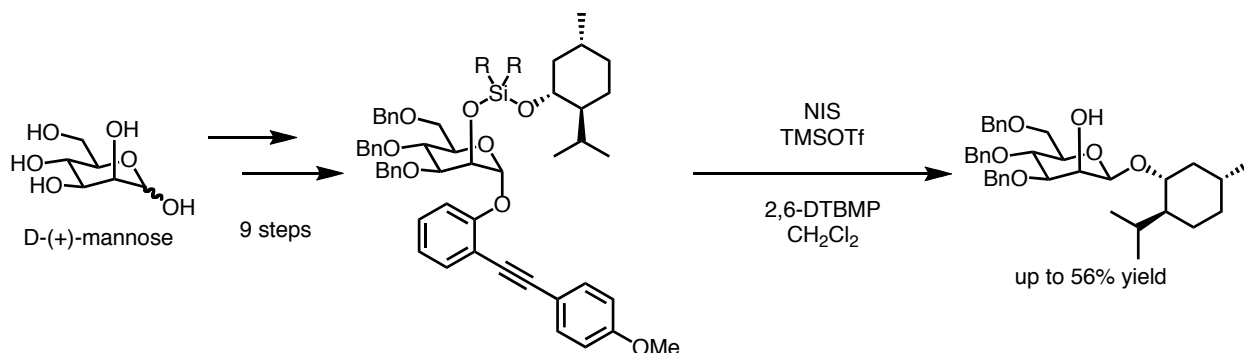
5.1 Conclusion

In summary, two areas of research have been explored for regioselective additions to small molecules. The first area explored was the regioselective synthesis of secondary alkylboranes from additions to olefins (Scheme 5-1). A copper-*N*-heterocyclic carbene catalyst was shown to control the regioselectivity of hydroboration of terminal olefins, selectively synthesizing secondary alkylboranes. These products were later converted into cross-coupling partners for a subsequent dual catalyst/photocatalytic reaction (Scheme 5-1 A). When this hydroboration methodology was applied to 1,1-disubstituted olefins, a few modifications to the reaction conditions were necessary for high yields and regioselectivity; however, it remains unclear as to how these changes in conditions impact observed differences in reactivity (Scheme 5-1 B). Furthermore, regioselective hydroboration of 1,2-disubstituted olefins without directing groups remains an unsolved challenge in the field (Scheme 5-1 C). Finding a catalyst system that is not prone to chain walking and can differentiate minute steric differences in alkyl substituents was probed, but proved unsuccessful.



Scheme 5-1: Summation of Regioselective Hydroboration of Olefins

The second synthetic method pursued was the synthesis of 1,2-*cis* glycosides from a latent-active intramolecular aglycone delivery (Scheme 5-2). After successful synthesis of five new sugar silanes, tethering and aglycones delivery methods were explored. (-)-Menthol was tethered to four silanes; albeit with modest aglycone delivery. Further attempts at optimizing the aglycone delivery with different Lewis Acids concluded that the use of an *N*-iodosuccinimide/trimethylsilyltriflate system provided optimal activity thus far; however, further investigation is necessary.



Scheme 5-2: Summation of the Synthesis of Mannose Sugar Silane and Aglycone Tethering/Delivery of Menthol

In conclusion, progress has been made towards an ultimate goal of complete regio- and diastereocontrol in chemical synthesis. Further catalyst design is necessary to facilitate

regioselective hydroboration of unactivated internal olefins, as well as optimization of latent-active intramolecular aglycone delivery.

Chapter 6 Experimental

6.1 General Considerations

All reactions were conducted in a flame-dried or oven dried (120 °C) glassware with magnetic stirring under an atmosphere of dry nitrogen. Solvents were purified under nitrogen using a solvent purification system (Innovative Technology, Inc. Model # Sps-400-3 and PS-400-3). Unless otherwise noted all reagents were used as received. Allyltrimethylsilane, TMSOTf, 2,6-lutidine, diisopropylamine and allylbenzene were distilled. Copper salts (Sigma Aldrich, Strem Chemicals, Inc), *N*-heterocyclic carbene salts (Sigma Aldrich, Strem), KO-*t*-Bu (Strem), NaO-*t*-Bu (Strem) B₂pin₂ (Combi Blocks, recrystallized from pentane) were stored and weighed in an inert atmosphere. NIS (recrystallized from dioxane/ether) and 2,6-DTBMP (recrystallized from pentane) were stored away from light and at -20 °C. IPrCuCl was synthesized¹⁶⁸, stored, and weighed in an inert atmosphere. MeOH was distilled from CaH₂ and stored under nitrogen.

¹H and ¹³C were obtained in CDCl₃ at rt in a Varian Mercury 400 MHz instrument, a Varian Unity 500 MHz, or a Varian Unity 700 MHz instrument. Chemical shifts of ¹H NMR spectra were recorded in parts per million (ppm) on the δ scale from an internal standard of residual chloroform (7.24 ppm). Chemical shifts of ¹³C NMR spectra were recorded in ppm from the central peak of CDCl₃ (77.1 ppm) on the δ scale. High-resolution mass spectra (HRMS) were obtained at the University of Michigan Mass Spectrometry Laboratory on a VG-70-250-s spectrometer manufactured by Micromass Corp. (Manchester UK). When noted, Biotage purification was performed on an Isolera One purification system with SNAP silica columns.

Regioisomeric ratios were determined on crude reaction mixtures using GC. GCMS analysis was carried out on a HP 6980 Series GC System with HP-5MS column (30 m x 0.250 mm x 0.25 μ m). GCFID analysis was carried out on a HP 6980N Series GC system with a HP-5 column (30 m x 0.32 mm x 0.25 μ m).

6.2 Chapter 2 Experimental

6.2.1 Substrates Synthesized by Literature Procedures

The following substrates were prepared according to literature procedures:

tert-Butyldimethyl(pent-4-enyloxy)silane,¹⁶⁹

(*R*)-4,8-Dimethylnona-1,7-diene,¹⁷⁰

((Hex-5-enyloxy)methyl)benzene,^{171,172}

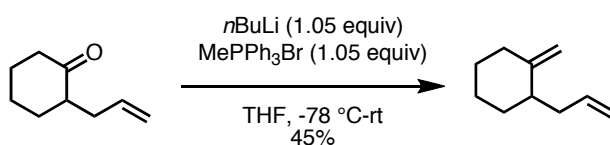
1-Allyl-1*H*-indole,^{173,174}

(3-methylbut-3-enyl)benzene^{170,175}

(3-methylenepentyl)benzene^{170,176}

6.2.2 Synthesis of Starting Material

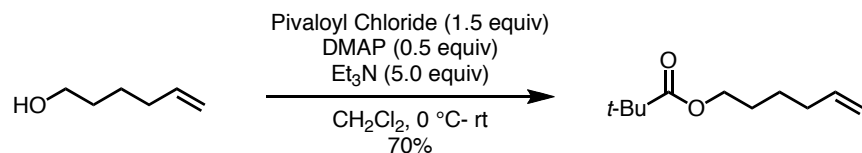
1-Allyl-2-methylenecyclohexane



Methyltriphenylphosphonium bromide (2.7 g, 7.6 mmol) was added to a flask and backfilled with N_2 . THF (18 mL, 0.4M) was added and the reaction was cooled to 0 °C. *n*-butyllithium solution (3.0 mL, 2.5M, 7.6 mmol) was added dropwise. The mixture was allowed to stir at 0 °C for 30 minutes before being cooled to -78 °C. 2-allyl-cyclohexanone (0.68 mL, 7.2 mmol) was added dropwise. The reaction was allowed to stir overnight; gradually warming to rt. 75 mL

saturated NH_4Cl was added. The aqueous layer was washed with Et_2O (3x75 mL). The organic layers were combined, washed with brine dried over MgSO_4 , filtered, and concentrated. The reaction mixture was purified via column chromatography (100% hexanes) (442 mg, 3.2 mmol, 45 % yield). $^1\text{H NMR}$ (500 MHz, CDCl_3): δ 5.87 – 5.72 (m, 1H), 5.08 – 4.93 (m, 2H), 4.67 (s, 1H), 4.58 (s, 1H), 2.43 – 2.33 (m, 1H), 2.30 – 2.21 (m, 1H), 2.12 – 1.97 (m, 3H), 1.84 – 1.74 (m, 1H), 1.72 – 1.61 (m, 2H), 1.51 – 1.40 (m, 2H), 1.25 – 1.12 (m, 1H). $^{13}\text{C NMR}$ (126 MHz, CDCl_3): δ 152.64, 137.80, 115.38, 105.38, 42.83, 36.89, 35.36, 33.49, 28.75, 24.72. **IR (thin film):** ν 2926, 2854, 1642, 1446, 992, 909, 889, 495, 416 cm^{-1} . **HRMS (EI) (m/z):** $[\text{M}^+]$ calculated for $\text{C}_{10}\text{H}_{16}$, 136.1252 found, 136.1253.

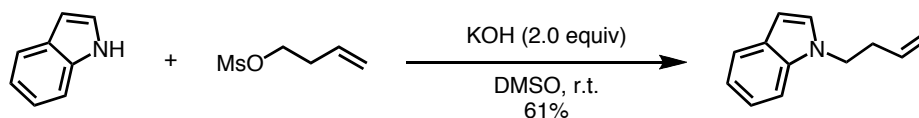
Hex-5-enyl pivalate



DMAP (611 mg, 5.0 mmol) was added to a flask and backfilled with N_2 . CH_2Cl_2 (44 mL 0.2 M) was added and the reaction was cooled to 0 °C. 5-hexen-1-ol (1.2 mL, 10 mmol) and freshly distilled Et_3N (7.0 mL, 50.0 mmol) were added. Pivaloyl chloride (2.0 mL, 15.0 mmol) was added dropwise. The reaction was allowed to stir overnight; gradually warming to rt. 30 mL saturated NaHCO_3 was added. The aqueous layer was washed with EtOAc (3x50 mL). The organic layers were combined, washed with brine, dried over MgSO_4 , filtered, and concentrated. The reaction mixture was purified via column chromatography (5% EtOAc in hexanes) (1.29 g, 7.01 mmol, 70% yield). $^1\text{H NMR}$ (500 MHz, CDCl_3): δ 5.80 (ddt, $J = 16.9, 10.2, 6.6$ Hz, 1H), 5.09 – 4.89 (m, 2H), 4.06 (t, $J = 6.6$ Hz, 2H), 2.13 – 2.04 (m, 2H), 1.69 – 1.59 (m, 2H), 1.51 – 1.39 (m, 2H), 1.19 (s, 9H). $^{13}\text{C NMR}$ (126 MHz, CDCl_3): δ 178.63, 138.40, 114.75, 64.21, 38.73, 33.27, 28.05, 27.20, 25.20. **IR (thin film):** ν 2975, 2938, 2871, 1728, 1480, 1459, 1283,

1036, 994, 910 cm^{-1} . **HRMS (EI) (m/z):** $[\text{M}^+]$ calculated for $\text{C}_{11}\text{H}_{20}\text{O}_2$, 184.1463 found, 184.1467.

1-(But-3-enyl)-1H-indole



Indole (562 mg, 4.8 mmol) and crushed KOH pellets (539 mg, 9.6 mmol) were added to a flask and backfilled with N_2 . DMSO (20 mL, 0.25 M) and then but-3-enyl methanesulfonate (1.44 g, 9.6 mmol) were added. The reaction mixture was allowed to stir at rt overnight. 100 mL H_2O was added. The reaction mixture was extracted with EtOAc (3x100 mL). The organic layers were combined, washed with brine, dried over MgSO_4 , filtered, and concentrated. The reaction was purified via column chromatography (100% hexanes) (505 mg, 2.95 mmol, 61%). **^1H NMR (500 MHz, CDCl_3):** δ 7.65 (d, $J = 7.9$ Hz, 1H), 7.37 (d, $J = 8.2$ Hz, 1H), 7.26 – 7.20 (m, 1H), 7.16 – 7.06 (m, 2H), 6.50 (s, 1H), 5.80 (ddt, $J = 17.1, 10.3, 6.8$ Hz, 1H), 5.09 (d, $J = 17.0$ Hz, 1H), 5.07 (d, $J = 10.0$ Hz, 1H), 4.20 (t, $J = 7.2$ Hz, 2H), 2.60 (q, $J = 7.1, 6.7$ Hz, 2H). **^{13}C NMR (126 MHz, CDCl_3):** δ 135.84, 134.65, 128.60, 127.70, 121.36, 120.95, 119.24, 117.36, 109.30, 101.03, 45.98, 34.54. **IR (thin film):** ν 2927, 1641, 1612, 1510, 1463, 1313, 913, 735, 714 cm^{-1} . **HRMS (EI) (m/z):** $[\text{M}^+]$ calculated for $\text{C}_{12}\text{H}_{13}\text{N}$, 171.1048 found, 171.1049.

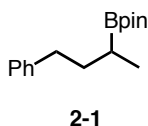
6.2.3 Synthesis of Branched Alkylboranes

General procedures for copper-catalyzed hydroboration of alkenes:

1.5 mL of acetonitrile was added to a solid mixture of IPrCuCl (0.03 mmol) and $\text{KO-}t\text{-Bu}$ (0.45 mmol) under N_2 . The reaction was allowed to stir at rt for 10 minutes. B_2pin_2 (0.6 mmol) was added under N_2 and the reaction was allowed to stir for an additional 30 minutes at rt. The alkene (0.3 mmol) and MeOH (0.6 mmol) were added to the mixture by syringe. The reaction mixture

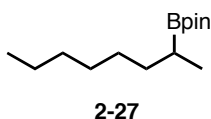
was allowed to stir at rt for 2 h and was then filtered through silica gel, eluting with 50% v/v EtOAc/hexanes. The solvent was removed *in vacuo*, and the crude residue was purified via flash chromatography on silica gel to afford the desired product.

4,4,5,5-Tetramethyl-2-(4-phenylbutan-2-yl)-1,3,2-dioxaborolane (2-1)



The title compound was prepared from IPrCuCl (14.6 mg, 0.03 mmol), KO-*t*-Bu (50 mg, 0.45 mmol), B₂pin₂ (152 mg, 0.6 mmol), 4-phenyl-1-butene (40 mg, 0.3 mmol) and MeOH (19 mg, 0.6 mmol) by following the general procedure. The crude residue was purified via flash chromatography (100% hexanes to 4% EtOAc in hexanes) to afford the desired product as a 92:8 mixture of regioisomers (63 mg, 0.24 mmol, 81% yield). ¹H NMR (500 MHz, CDCl₃): δ 7.30 – 7.23 (m, 2H), 7.23 – 7.13 (m, 3H), 2.69 – 2.57 (m, 2H), 1.85 – 1.74 (m, 1H), 1.64 – 1.54 (m, 1H), 1.27 (s, 12H), 1.14 – 0.99 (m, 4H). ¹³C NMR (126 MHz, CDCl₃): δ 143.08, 128.42, 128.18, 125.48, 82.87, 35.31, 35.29, 24.79, 24.74, 15.41. The spectral data matched the literature.⁶⁸

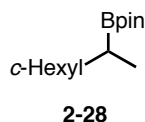
4,4,5,5-Tetramethyl-2-(octan-2-yl)-1,3,2-dioxaborolane (2-27)



The title compound was prepared from IPrCuCl (14.6 mg, 0.03 mmol), KO-*t*-Bu (50 mg, 0.45 mmol), B₂pin₂ (152 mg, 0.6 mmol), 1-octene (34 mg, 0.3 mmol) and MeOH (19 mg, 0.6 mmol) by following the general procedure. The crude residue was purified via flash chromatography (100% hexanes to 4% EtOAc in hexanes) to afford the desired product as a 95:5 mixture of regioisomers (56 mg, 0.23 mmol, 77% yield). ¹H NMR (500 MHz, CDCl₃): δ 1.47 – 1.39 (m,

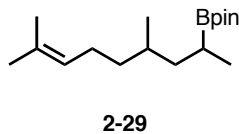
1H), 1.33 – 1.18 (m, 21H), 1.03 – 0.92 (m, 4H), 0.92 – 0.82 (m, 3H). ¹³C NMR (126 MHz, CDCl₃): δ 82.73, 33.25, 31.87, 29.54, 28.94, 24.74, 24.71, 22.65, 15.52, 14.11. The spectral data matched the literature.⁷¹

2-(1-Cyclohexylethyl)-4,4,5,5-tetramethyl-1,3,2-dioxaborolane (2-28)



The title compound was prepared from IPrCuCl (14.6 mg, 0.03 mmol), KO-*t*-Bu (50 mg, 0.45 mmol), B₂pin₂ (152 mg, 0.6 mmol), vinylcyclohexane (33 mg, 0.3 mmol) and MeOH (19 mg, 0.6 mmol) by following the general procedure. The crude residue was purified via flash chromatography (100% hexanes to 4% EtOAc in hexanes) to afford the desired product as an 87:13 mixture of regioisomers (70 mg, 0.29 mmol, 98% yield). ¹H NMR (500 MHz, CDCl₃): δ 1.83 – 1.57 (m, 5H), 1.40 – 1.19 (m, 15H), 1.19 – 1.08 (m, 1H), 1.08 – 0.83 (m, 6H). ¹³C NMR (126 MHz, CDCl₃): δ 82.68, 40.46, 32.68, 31.81, 26.75, 26.70, 24.80, 24.72, 12.50. ¹¹B NMR (128 MHz, CDCl₃): δ 34.29. IR (thin film): ν 2978, 2921, 2851, 1378, 1370, 1357, 1308, 1143, 863, 845 cm⁻¹. HRMS (EI) (m/z): [M⁺] calculated for C₁₄H₂₇BO₂, 238.2104 found, 238.2113. The spectral data matched the literature.⁷¹

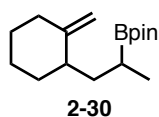
2-(4,8-dimethylnon-7-en-2-yl)-4,4,5,5-tetramethyl-1,3,2-dioxaborolane (2-29)



The title was prepared from IPrCuCl (14.6 mg, 0.03 mmol), KO-*t*-Bu (50 mg, 0.45 mmol), B₂pin₂ (152 mg, 0.6 mmol), ((*R*)-4,8-dimethylnona-1,7-diene (46 mg, 0.3 mmol) and MeOH (19 mg, 0.6 mmol) by following the general procedure. The crude residue was purified via flash chromatography (100% hexanes to 4% EtOAc in hexanes) to afford the desired product observed

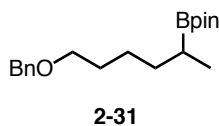
as a single isomer (1:1 diastereomeric ratio) (69 mg, 0.24 mmol, 81% yield). **¹H NMR (500 MHz, CDCl₃):** δ 5.07 (m, 1H), 2.04 – 1.82 (m, 2H), 1.65 (s, 3H), 1.57 (s, 3H), 1.49 – 1.35 (m, 1H), 1.35 – 1.16 (m, 14H), 1.13 – 0.98 (m, 2H), 0.91 (m, 3H), 0.83 (m, 3H). **¹³C NMR (126 MHz, CDCl₃):** δ 130.84, 130.82, 125.12, 125.11, 82.73, 82.70, 41.04, 40.27, 37.29, 37.26, 31.62, 31.02, 25.71, 25.58, 25.54, 24.74, 24.71, 24.70, 24.66, 19.75, 19.33, 17.64, 17.62, 16.11, 15.39. **¹¹B NMR (128 MHz, CDCl₃):** δ 34.28. **IR (thin film):** ν 2957, 2914, 1460, 1370, 1314, 1144, 861, 688 cm⁻¹. **HRMS (EI) (m/z):** [M⁺] calculated for C₁₇H₃₃BO₂, 280.2574 found, 280.2579.

4,4,5,5-tetramethyl-2-(1-(2-methylenecyclohexyl)propan-2-yl)-1,3,2-dioxaborolane (2-30)



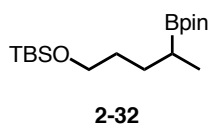
The title compound was prepared from IPrCuCl (14.6 mg, 0.03 mmol), KO-*t*-Bu (50 mg, 0.45 mmol), B₂pin₂ (152 mg, 0.6 mmol), 1-allyl-2-methylenecyclohexane (41 mg, 0.3 mmol) and MeOH (19 mg, 0.6 mmol) by following the general procedure. The crude residue was purified via flash chromatography (100% hexanes to 4% EtOAc in hexanes) to afford the desired product observed as a single isomer (66 mg, 0.25 mmol, 83% yield). **¹H NMR (500 MHz, CDCl₃):** δ 4.63 (s, 1H), 4.58 (d, *J* = 7.6, 1.5 Hz, 1H), 2.22 (m, 1H), 2.17 – 2.08 (m, 1H), 2.04 – 1.95 (m, 1H), 1.80 (dt, *J* = 13.4, 7.9 Hz, 1H), 1.76 – 1.62 (m, 2H), 1.58 – 1.34 (m, 5H), 1.31 – 1.18 (m, 14H), 1.11 – 1.00 (m, 1H), 0.99 – 0.93 (m, 3H). **¹³C NMR (126 MHz, CDCl₃):** δ 105.96, 105.74, 82.73, 42.08, 41.99, 35.59, 35.38, 34.44, 34.41, 33.78, 33.52, 28.85, 28.84, 24.75, 24.75, 24.71, 24.68, 23.87, 15.96, 15.78. **¹¹B NMR (128 MHz, CDCl₃):** δ 34.48. **IR (thin film):** ν 2976, 2926, 2854, 1462, 1370, 1312, 1144, 859, 688 cm⁻¹. **HRMS (EI) (m/z):** [M⁺] calculated for C₁₆H₂₉BO₂, 264.2261 found, 264.2274.

2-(6-(Benzyloxy)hexan-2-yl)-4,4,5,5-tetramethyl-1,3,2-dioxaborolane (2-31)



The title compound was prepared from IPrCuCl (14.6 mg, 0.03 mmol), KO-*t*-Bu (50 mg, 0.45 mmol), B₂pin₂ (152 mg, 0.6 mmol), ((hex-5-enyloxy)methyl)benzene (57 mg, 0.3 mmol) and MeOH (19 mg, 0.6 mmol) by following the general procedure. The crude residue was purified via flash chromatography (100% hexanes to 4% EtOAc in hexanes) to afford the desired product as a 92:8 mixture of regioisomers (79 mg, 0.25 mmol, 83% yield). **¹H NMR (500 MHz, CDCl₃):** δ 7.39 – 7.33 (m, 4H), 7.33 – 7.25 (m, 1H), 4.51 (s, 2H), 3.48 (t, *J* = 6.7 Hz, 2H), 1.64 (m, 2H), 1.55 – 1.44 (m, 1H), 1.44 – 1.35 (m, 2H), 1.35 – 1.20 (m, 14H), 1.07 – 0.94 (m, 4H). **¹³C NMR (126 MHz, CDCl₃):** δ 138.75, 128.27, 127.54, 127.37, 82.77, 72.76, 70.50, 32.99, 29.95, 25.49, 24.73, 24.70, 15.44. **¹¹B NMR (128 MHz, CDCl₃):** δ 34.34. **IR (thin film):** ν 2930, 2856, 1455, 1370, 1213, 1143, 1103, 732 cm⁻¹. **HRMS (EI) (m/z):** [M⁺] calculated for C₁₉H₃₁BO₃, 318.2366, found, 318.2370.

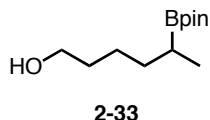
tert-Butyldimethyl(4-(4,4,5,5-tetramethyl-1,3,2-dioxaborolan-2-yl)pentyloxy)silane (2-32)



The title compound was prepared from IPrCuCl (14.6 mg, 0.03 mmol), KO-*t*-Bu (50 mg, 0.45 mmol), B₂pin₂ (152 mg, 0.6 mmol), *tert*-butyldimethyl(pent-4-enyloxy)silane (60 mg, 0.3 mmol) and MeOH (19 mg, 0.6 mmol) by following the general procedure. The crude residue was purified via flash chromatography (100% hexanes to 5% EtOAc in hexanes) to afford the desired product as a 90:10 mixture of regioisomers (91 mg, 0.28 mmol, 92% yield). **¹H NMR (500 MHz, CDCl₃):** δ 3.61 – 3.51 (m, 2H), 1.55 – 1.46 (m, 2H), 1.46 – 1.37 (m, 1H), 1.31 – 1.24 (m,

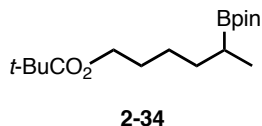
1H), 1.20 (m, 12H), 1.01 – 0.91 (m, 4H), 0.86 (m, 9H), 0.01 (m, 6H). ¹³C NMR (126 MHz, CDCl₃): δ 82.78, 63.60, 32.27, 29.26, 25.99, 24.75, 24.71, 18.38, 15.53, -5.24. ¹¹B NMR (128 MHz, CDCl₃): δ 33.95. IR (thin film): ν 2929, 2858, 1462, 1386, 1314, 1251, 1145, 1096, 833, 773 cm⁻¹. HRMS (EI) (m/z): [M+H⁺] calculated for C₁₇H₃₈BO₃Si, 329.2678 found, 329.2680.

5-(4,4,5,5-Tetramethyl-1,3,2-dioxaborolan-2-yl)hexan-1-ol (2-33)



The title compound was prepared from IPrCuCl (14.6 mg, 0.03 mmol), KO-*t*-Bu (50 mg, 0.45 mmol), B₂pin₂ (152 mg, 0.6 mmol), 5-hexen-1-ol (30 mg, 0.3 mmol) and MeOH (19 mg, 0.6 mmol) by following the general procedure. The crude residue was purified via flash chromatography (100% hexanes to 20% EtOAc in hexanes) to afford the desired product observed as a single isomer (64 mg, 0.28 mmol, 93% yield). ¹H NMR (500 MHz, CDCl₃): δ 3.63 (t, *J* = 6.5 Hz, 2H), 1.56 (quint, *J* = 6.9 Hz, 2H), 1.49 – 1.26 (m, 6H), 1.23 (s, 12H), 1.06 – 0.88 (m, 4H). ¹³C NMR (126 MHz, CDCl₃): δ 82.86, 62.83, 32.77, 32.61, 24.91, 24.74, 24.69, 15.46. ¹¹B NMR (128 MHz, CDCl₃): δ 34.11. IR (thin film): ν 3362, 2977, 2928, 2872, 1462, 1370, 1313, 1143, 858 cm⁻¹. HRMS (EI) (m/z): [M+H⁺] calculated for C₁₂H₂₅BO₃, 229.1970 found, 229.1970.

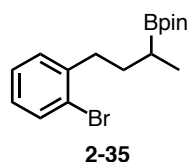
5-(4,4,5,5-Tetramethyl-1,3,2-dioxaborolan-2-yl)hexyl pivalate (2-34)



The title compound was prepared from IPrCuCl (14.6 mg, 0.03 mmol), KO-*t*-Bu (50 mg, 0.45 mmol), B₂pin₂ (152 mg, 0.6 mmol), hex-5-enyl pivalate (55 mg, 0.3 mmol) and MeOH (19 mg, 0.6 mmol) by following the general procedure. The crude residue was purified via flash

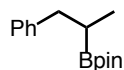
chromatography (100% hexanes to 4% EtOAc in hexanes) to afford the desired product as a 96:4 mixture of regioisomers (73 mg, 0.23 mmol, 78% yield). **¹H NMR (500 MHz, CDCl₃):** δ 4.09 – 3.97 (m, 2H), 1.66 – 1.55 (m, 2H), 1.51 – 1.41 (m, 1H), 1.39 – 1.27 (m, 3H), 1.23 (s, 12H), 1.18 (s, 9H), 1.03 – 0.93 (m, 4H). **¹³C NMR (126 MHz, CDCl₃):** δ 178.62, 82.82, 64.50, 38.70, 32.81, 28.86, 27.20, 25.27, 24.74, 24.70, 15.43. **¹¹B NMR (128 MHz, CDCl₃):** δ 34.35. **IR (thin film):** ν 2975, 2932, 2871, 1727, 1370, 1315, 1284, 1144, 859 cm⁻¹. **HRMS (EI) (m/z):** [M+H⁺] calculated for C₁₇H₃₄BO₄, 313.2545 found, 313.2546.

2-(4-(2-Bromophenyl)butan-2-yl)-4,4,5,5-tetramethyl-1,3,2-dioxaborolane (2-35)



The title compound was prepared from IPrCuCl (14.6 mg, 0.03 mmol), KO-*t*-Bu (50 mg, 0.45 mmol), B₂pin₂ (152 mg, 0.6 mmol), 4-(2-bromophenyl)-1-butene (63 mg, 0.3 mmol) and MeOH (19 mg, 0.6 mmol) by following the general procedure. The crude residue was purified via flash chromatography (100% hexanes to 4% EtOAc in hexanes) to afford the desired product as a 90:10 mixture of regioisomers (94 mg, 0.28 mmol, 92% yield). **¹H NMR (500 MHz, CDCl₃):** δ 7.48 (d, *J* = 7.8 Hz, 1H), 7.24 – 7.15 (m, 2H), 7.00 (dt, *J* = 8.3, 4.1 Hz, 1H), 2.79 – 2.67 (m, 2H), 1.79 – 1.67 (m, 1H), 1.62 – 1.52 (m, 1H), 1.24 (s, 12H), 1.13 – 0.99 (m, 4H). **¹³C NMR (126 MHz, CDCl₃):** δ 142.29, 132.64, 130.31, 127.28, 127.24, 124.37, 82.94, 35.54, 33.55, 24.83, 24.78, 15.41. **¹¹B NMR (128 MHz, CDCl₃):** δ 34.29. **IR (thin film):** ν 2976, 1469, 1369, 1315, 1142, 747, 411 cm⁻¹. **HRMS (EI) (m/z):** [M⁺] calculated for C₁₆H₂₄BBrO₂, 338.1053 found, 338.1051.

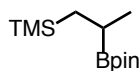
4,4,5,5-Tetramethyl-2-(1-phenylpropan-2-yl)-1,3,2-dioxaborolane (2-36)



2-36

Following a modified procedure 1.5 mL of acetonitrile was added to a solid mixture of IPrCuCl (14.6 mg, 0.03 mmol), KO-*t*-Bu (50 mg 0.45 mmol), and B₂pin₂ (152 mg, 0.6 mmol). Allylbenzene (35 mg, 0.3 mmol) and MeOH (19 mg 0.6 mmol) were immediately added to the mixture by syringe. The reaction mixture was allowed to stir at rt for 2 h and was then filtered through silica gel, eluting with 50% v/v EtOAc/hexanes. The solvent was removed *in vacuo*, and the crude residue was purified via flash chromatography on silica gel to afford the desired product. The crude residue was purified via flash chromatography (100% hexanes to 4% EtOAc in hexanes) to afford the desired product as a 95:5 mixture of regioisomers (72 mg, 0.29 mmol, 98% yield). ¹H NMR (500 MHz, CDCl₃): δ 7.28 – 7.13 (m, 5H), 2.82 (dd, *J* = 13.6, 7.5 Hz, 1H), 2.55 (dd, *J* = 13.6, 8.4 Hz, 1H), 1.38 (m, 1H), 1.19 (m, 12H), 0.98 (d, *J* = 7.4 Hz, 3H). ¹³C NMR (126 MHz CDCl₃): δ 142.28, 128.86, 127.96, 125.51, 82.94, 38.94, 24.69, 24.67, 15.17. The spectral data matched the literature.²⁶

Trimethyl(2-(4,4,5,5-tetramethyl-1,3,2-dioxaborolan-2-yl)propyl)silane (2-37)

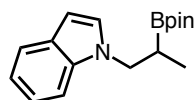


2-37

Following a modified procedure 1.5 mL of acetonitrile was added to a solid mixture of IPrCuCl (14.6 mg, 0.03 mmol), KO-*t*-Bu (50 mg 0.45 mmol), and B₂pin₂ (152 mg, 0.6 mmol). Allyltrimethylsilane (34 mg, 0.3 mmol) and MeOH (19 mg 0.6 mmol) were immediately added to the mixture by syringe. The reaction mixture was allowed to stir at rt for 2 h and was then filtered through silica gel, eluting with 50% v/v EtOAc/hexanes. The solvent was removed *in*

vacuo, and the crude residue was purified via flash chromatography on silica gel to afford the desired product. The crude residue was purified via flash chromatography (100% hexanes to 4% EtOAc in hexanes) to afford the desired product as a single regioisomers (52 mg, 0.23 mmol, 77% yield). **¹H NMR (500 MHz, CDCl₃):** δ 1.21 (s, 12H), 1.10 – 1.04 (m, 1H), 0.99 (d, *J* = 7.2 Hz, 3H), 0.77 (dd, *J* = 14.6, 7.4 Hz, 1H), 0.40 (dd, *J* = 14.6, 6.9 Hz, 1H), -0.04 (s, 9H). **¹³C NMR (126 MHz, CDCl₃):** δ 82.78, 24.78, 24.76, 19.88, 19.35, -0.86. **¹¹B NMR (128 MHz, CDCl₃):** δ 34.36. **IR (thin film):** ν 2952, 1459, 1378, 1315, 1246, 1226, 1144, 834, 689 cm⁻¹. **HRMS (EI) (m/z):** [M-CH₃⁺] calculated for C₁₁H₂₃BO₂Si, 227.1639 found, 227.1637.

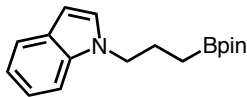
1-(2-(4,4,5,5-Tetramethyl-1,3,2-dioxaborolan-2-yl)propyl)-1*H*-indole (2-38)



2-38

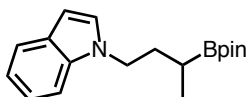
The title compound was prepared from IPrCuCl (29.2 mg, 0.06 mmol), KO-*t*-Bu (50 mg, 0.45 mmol), B₂pin₂ (152 mg, 0.6 mmol), 1-allyl-1*H*-indole (47 mg, 0.3 mmol) and MeOH (19 mg, 0.6 mmol) by following the general procedure. The crude residue was purified via flash chromatography (100% hexanes to 4% EtOAc in hexanes) to afford the desired product as a 94:6 mixture of regioisomers (48 mg, 0.17 mmol, 56% yield). **¹H NMR (500 MHz, CDCl₃):** δ 7.61 (d, *J* = 7.9, 1.1 Hz, 1H), 7.39 (d, *J* = 8.3 Hz, 1H), 7.22 – 7.12 (m, 2H), 7.07 (td, *J* = 7.5, 7.0, 1.0 Hz, 1H), 6.46 (d, *J* = 3.0 Hz, 1H), 4.31 (dd, *J* = 14.1, 6.7 Hz, 1H), 4.00 (dd, *J* = 14.1, 9.1 Hz, 1H), 1.77 – 1.63 (m, 1H), 1.23 – 1.17 (m, 14H), 0.94 (d, *J* = 7.4 Hz, 3H). **¹³C NMR (126 MHz, CDCl₃):** δ 136.13, 128.46, 128.24, 121.03, 120.69, 118.96, 109.75, 100.53, 83.40, 48.98, 24.72, 24.68, 13.30. **¹¹B NMR (128 MHz, CDCl₃):** δ 33.35. **IR (thin film):** ν 2975, 2931, 2873, 1512, 1462, 1371, 1317, 1216, 1142, 966, 853, 714 cm⁻¹. **HRMS (EI) (m/z):** [M+H⁺] calculated for C₁₇H₂₅BNO₂, 286.1973 found, 286.1975.

1-(3-(4,4,5,5-Tetramethyl-1,3,2-dioxaborolan-2-yl)propyl)-1H-indole



The title compound was synthesized according to a literature procedure for use as an authentic standard for the analysis of **2-38**.⁷¹ **¹H NMR (500 MHz, CDCl₃):** δ 7.62 (d, *J* = 7.8 Hz, 1H), 7.39 (d, *J* = 8.0 Hz, 1H), 7.23 – 7.16 (m, 1H), 7.14 – 7.04 (m, 2H), 4.12 (t, *J* = 7.3, 5.5 Hz, 2H), 2.00 – 1.88 (m, 2H), 1.25 (s, 13H), 0.80 (t, *J* = 7.7 Hz, 2H). **¹³C NMR (126 MHz, CDCl₃):** δ 135.95, 128.52, 127.94, 121.16, 120.81, 119.05, 109.51, 100.70, 83.17, 48.28, 24.90, 24.84. **IR (thin film):** ν 2976, 1463, 1370, 1314, 1219, 1142, 967, 845, 737 cm⁻¹. **HRMS (EI) (m/z):** [M+H⁺] calculated for C₁₇H₂₅BNO₂, 286.1973 found, 286.1976.

1-(3-(4,4,5,5-Tetramethyl-1,3,2-dioxaborolan-2-yl)butyl)-1H-indole (2-39)



2-39

The title compound was prepared from IPrCuCl (21.9 mg, 0.045 mmol), KO-*t*-Bu (50 mg, 0.45 mmol), B₂pin₂ (152 mg, 0.6 mmol), 1-(but-3-enyl)-1H-indole (51 mg, 0.3 mmol) and MeOH (19 mg, 0.6 mmol) by following the general procedure. The crude residue was purified via flash chromatography (100% hexanes to 4% EtOAc in hexanes) to afford the desired product as a 94:6 mixture of regioisomers (71 mg, 0.24 mmol, 79% yield). **¹H NMR (500 MHz, CDCl₃):** δ 7.63 (d, *J* = 7.8 Hz, 1H), 7.42 (d, *J* = 8.2 Hz, 1H), 7.24 – 7.18 (m, 1H), 7.14 – 7.06 (m, 2H), 6.50 – 6.47 (m, 1H), 4.22 – 4.09 (m, 2H), 2.05 – 1.95 (m, 1H), 1.87 – 1.77 (m, 1H), 1.28 (s, 12H), 1.12 – 1.00 (m, 4H). **¹³C NMR (126 MHz, CDCl₃):** δ 135.94, 128.52, 127.80, 121.14, 120.81, 119.03, 109.50, 100.72, 83.15, 45.78, 33.67, 24.83, 24.77, 15.46. **¹¹B NMR (128 MHz, CDCl₃):**

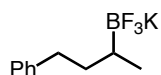
δ 34.37. **IR (thin film):** ν 2975, 2871, 1463, 1387, 1369, 1315, 1142, 737 cm^{-1} . **HRMS (EI)** (m/z): $[\text{M}+\text{H}^+]$ calculated for $\text{C}_{18}\text{H}_{27}\text{BNO}_2$, 300.2129 found, 300.2131.

6.2.4 Synthesis of Trifluoroborate Salts

General Procedure for Synthesis of Trifluoroborate Salts^{46,177}

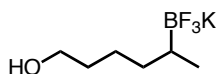
Acetone (0.5 M) was added to the boronic ester (1.0 equiv) and cooled in an ice bath. KHF_2 (3.0 equiv) and deionized water (1.5 M) were added. The reaction was capped with a septum, and a nitrogen line was inserted. The ice bath was removed, and the reaction was allowed to stir at rt. After 30 min the reaction mixture was concentrated. The pinacol and water were azeotroped with toluene, and the residual solvent was removed on high vacuum. The crude material was extracted with hot acetone (4x20 mL) and filtered. The mixture was concentrated to < 1 mL and copious amounts of hexanes were added. The mixture was sonicated for ~2 min, and the suspension was placed in the freezer (-20 °C) overnight. The resulting white crystalline solid was collected via vacuum filtration washing with hexanes.

Potassium (4-phenylbutan-2-yl)trifluoroborate



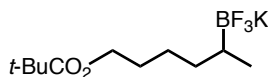
Following the general procedure, KHF_2 (618 mg, 8.70 mmol) and deionized H_2O (1.9 mL) were added to acetone (5.8 mL) and 4,4,5,5-tetramethyl-2-(4-phenylbutan-2-yl)-1,3,2-dioxaborolane (780 mg, 2.90 mmol). The white solid was precipitated from 200 mL of hexanes affording the desired product (495 mg, 2.06 mmol, 71 % yield). **^1H NMR (500 MHz, Acetone- d_6):** δ 7.22 – 7.12 (m, 4H), 7.09 – 7.03 (m, 1H), 2.71 – 2.62 (m, 1H), 2.58 – 2.47 (m, 1H), 1.77 – 1.66 (m, 1H), 1.36 – 1.23 (m, 1H), 0.82 (d, J = 7.2 Hz, 3H), 0.32 (s, 1H). **^{13}C NMR (126 MHz, Acetone- d_6):** δ 145.79, 128.92, 128.42, 125.31, 36.93, 36.16, 16.16. The spectral data matched the literature.⁵⁰

Potassium trifluoro(6-hydroxyhexan-2-yl)borate



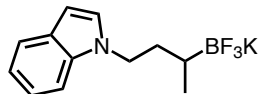
Following the general procedure, KHF_2 (351 mg, 4.5 mmol) and deionized H_2O (1.0 mL) were added to acetone (3.0 mL) and 5-(4,4,5,5-tetramethyl-1,3,2-dioxaborolan-2-yl)hexan-1-ol (342 mg, 1.5 mmol). The white solid was precipitated from 150 mL of hexanes affording the desired product (217 mg, 1.04 mmol, 70 % yield). $^1\text{H NMR}$ (500 MHz, Acetone- d_6): δ 3.50 (q, $J = 6.2$ Hz, 2H), 3.23 (t, $J = 5.4$ Hz, 1H), 1.50 – 1.38 (m, 4H), 1.31 – 1.20 (m, 1H), 1.06 – 0.94 (m, 1H), 0.74 (d, $J = 7.6$ Hz, 3H), 0.26 (s, 1H). $^{13}\text{C NMR}$ (126 MHz, Acetone- d_6): δ 62.98, 34.74, 34.37, 26.01, 16.39. $^{11}\text{B NMR}$ (128 MHz, Acetone- d_6): δ 5.50. $^{19}\text{F NMR}$ (377 MHz, Acetone- d_6): δ -147.33. IR (KBr pellet): ν 3594, 3430, 2934, 2853, 1459, 1276, 1087, 1067, 1003, 904 cm^{-1} . HRMS (EI) (m/z): [M-K $^-$] calculated for $\text{C}_6\text{H}_{13}\text{BF}_3\text{O}$, 169.1017 found, 169.1016.

Potassium trifluoro(6-(pivaloyloxy)hexan-2-yl)borate



Following the general procedure, KHF_2 (169 mg, 2.16 mmol) and deionized H_2O (0.5 mL) were added to acetone (1.4 mL) and 5-(4,4,5,5-tetramethyl-1,3,2-dioxaborolan-2-yl)hexyl pivalate (225 mg, 0.72 mmol). The white solid was precipitated from 150 mL of hexanes affording the desired product (144 mg, 0.49 mmol, 69 % yield). $^1\text{H NMR}$ (500 MHz, Acetone- d_6): δ 4.01 (t, $J = 6.8$ Hz, 2H), 1.64 – 1.48 (m, 2H), 1.48 – 1.41 (m, 2H), 1.32 – 1.25 (m, 1H), 1.16 (s, 9H), 1.07 – 0.99 (m, 1H), 0.75 (d, $J = 7.2$ Hz, 3H), 0.26 (s, 1H). $^{13}\text{C NMR}$ (126 MHz, Acetone- d_6): δ 178.28, 65.23, 39.14, 33.95, 27.45, 25.85, 25.21, 16.19. $^{11}\text{B NMR}$ (128 MHz, Acetone- d_6): δ 5.52. $^{19}\text{F NMR}$ (377 MHz, Acetone- d_6): δ -147.39. IR (KBr pellet): ν 3432, 2970, 2938, 2868, 1720, 1480, 1463, 1290, 1179 cm^{-1} . HRMS (EI) (m/z): [M-K $^-$] calculated for $\text{C}_{11}\text{H}_{21}\text{BF}_3\text{O}_2$ 253.1592 found, 253.1595.

Potassium (4-(1*H*-indol-1-yl)butan-2-yl)trifluoroborate



Following the general procedure, KHF_2 (234 mg, 3.0 mmol) and deionized H_2O (0.67 mL) were added to acetone (2.0 mL) and **17** (300 mg, 1.0 mmol). The white solid was precipitated from 150 mL of hexanes affording the desired product (182 mg, 0.65 mmol, 65 % yield). $^1\text{H NMR}$ (500 MHz, Acetone- d_6): δ 7.55 – 7.47 (m, 1H), 7.43 (d, $J = 8.3$ Hz, 1H), 7.24 (d, $J = 3.2, 1.1$ Hz, 1H), 7.08 (ddt, $J = 8.3, 6.9, 1.2$ Hz, 1H), 6.95 (ddt, $J = 9.1, 7.8, 1.6$ Hz, 1H), 6.36 – 6.33 (m, 1H), 4.28 – 4.13 (m, 2H), 1.95 – 1.81 (m, 1H), 1.61 – 1.51 (m, 1H), 0.85 (d, $J = 7.2$ Hz, 3H), 0.37 (s, 1H). $^{13}\text{C NMR}$ (126 MHz, Acetone- d_6): δ 137.30, 129.89, 129.31, 121.73, 121.47, 119.60, 110.84, 100.92, 47.30, 35.80, 16.89. $^{11}\text{B NMR}$ (128 MHz, Acetone- d_6): δ 5.09. $^{19}\text{F NMR}$ (377 MHz, Acetone- d_6): δ -146.71. IR (KBr plate): ν 3621, 3052, 2933, 2868, 1890, 1612, 1464, 751 cm^{-1} . HRMS (EI) (m/z): $[\text{M}-\text{K}^-]$ calculated for $\text{C}_{12}\text{H}_{14}\text{BF}_3\text{N}$, 240.1177 found, 2410.1179.

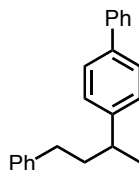
6.2.5 Photocatalytic Cross-coupling

General Procedure for Photocatalytic Cross-Couplings⁴⁶

Following the Molander procedure, to a thin threaded culture tube, $\text{NiCl}_2 \cdot \text{dme}$ (2.2 mg, 0.01 mmol) and 4,4'-di-*tert*-2,2'-bipyridine (2.7 mg, 0.01 mmol) were added under N_2 . THF (0.4 mL, 0.5 M) was added and vial was heated with a heat gun until the solids were fully dissolved. The reaction mixture was concentrated *in vacuo* leaving behind a blue/green solid. The aryl bromide (0.2 mmol), potassium trifluoroborate salt (0.3 mmol), $\text{Ir}[\text{dFCF}_3\text{ppy}]_2(\text{bpy})\text{PF}_6^{48}$ (5.0 mg, 0.005 mmol) and Cs_2CO_3 (98 mg, 0.3 mmol) were added. The reaction vial was sealed with a septum and purged with N_2 four times. 4.0 mL (0.05 M) 1,4-dioxane (freeze, pumped, thawed three times) were added. The reaction was stirred ~4 cm away from two 23 W compact fluorescent

(CFL) light bulbs while a fan was blown across to keep constant temperature. After ~22 h the reaction was filtered through a Celite plug with 20 mL EtOAc. The solvent was removed *in vacuo*, and the crude residue was purified via flash chromatography on silica gel to afford the desired product.

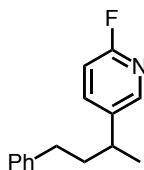
4-(4-Phenylbutan-2-yl)biphenyl (2-52)



2-52

The general procedure was followed using NiCl₂·dme (2.2 mg, 0.01 mmol), 4,4'-di-*tert*-2,2'-bipyridine (2.7 mg, 0.01 mmol), 4-bromobiphenyl (47 mg, 0.2 mmol), potassium (4-phenylbutan-2-yl)trifluoroborate (72 mg, 0.3 mmol), Ir[dFCF₃ppy]₂(bpy)PF₆ (5.0 mg, 0.005 mmol), and Cs₂CO₃ (98 mg, 0.3 mmol) in 4 mL 1,4-dioxane. The crude residue was purified via column chromatography (5% EtOAc in hexanes) to afford the desired product (54 mg, 0.190 mmol, 95% yield). **¹H NMR (500 MHz, CDCl₃):** δ 7.66 – 7.60 (m, 2H), 7.60 – 7.53 (m, 2H), 7.50 – 7.42 (m, 2H), 7.37 – 7.32 (m, 1H), 7.32 – 7.25 (m, 4H), 7.22 – 7.15 (m, 3H), 2.84 – 2.75 (m, 1H), 2.61 – 2.55 (m, 2H), 2.05 – 1.89 (m, 2H), 1.34 (d, *J* = 7.4 Hz, 3H), 1.29 – 1.25 (m, 1H). **¹³C NMR (126 MHz, CDCl₃):** δ 146.41, 142.48, 141.10, 138.87, 128.69, 128.37, 128.26, 127.47, 127.11, 126.98, 126.97, 125.65, 39.94, 39.15, 33.93, 22.48. **IR (thin film):** ν 3025, 29.21, 1601, 1485, 1452, 836, 763, 731, 695 cm⁻¹. **HRMS (EI) (m/z):** [M⁺] calculated for C₂₂H₂₂, 286.1722 found, 286.1727.

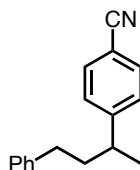
2-Fluoro-5-(4-phenylbutan-2-yl)pyridine (2-53)



2-53

The general procedure was followed using NiCl₂·dme (2.2 mg, 0.01 mmol), 4,4'-di-*tert*-2,2'-bipyridine (2.7 mg, 0.01 mmol), 5-bromo-2-fluoropyridine (35 mg, 0.2 mmol), potassium (4-phenylbutan-2-yl)trifluoroborate (72 mg, 0.3 mmol), Ir[dFCF₃ppy]₂(bpy)PF₆ (5.0 mg, 0.005 mmol), and Cs₂CO₃ (98 mg, 0.3 mmol) in 4 mL 1,4-dioxane. The crude residue was purified via column chromatography (5% EtOAc in hexanes) to afford the desired product (43 mg, 0.189 mmol, 95% yield). ¹H NMR (500 MHz, CDCl₃): δ 8.03 (s, 1H), 7.61 (td, *J* = 8.1, 2.5 Hz, 1H), 7.31 – 7.23 (m, 2H), 7.23 – 7.15 (m, 1H), 7.15 – 7.08 (m, 2H), 6.88 (dd, *J* = 8.4, 2.9 Hz, 1H), 2.82 – 2.71 (m, 1H), 2.57 – 2.47 (m, 2H), 2.01 – 1.84 (m, 2H), 1.29 (d, *J* = 7.0 Hz, 3H). ¹³C NMR (126 MHz, CDCl₃): δ 162.32 (d, *J* = 236.8 Hz), 146.29 (d, *J* = 14.2 Hz), 141.65, 139.84 (d, *J* = 4.9 Hz), 139.33 (d, *J* = 7.6 Hz), 128.38, 128.26, 125.89, 109.23 (d, *J* = 37.2 Hz), 39.61, 36.06, 33.64, 22.23. IR (thin film): ν 3026, 2921, 1594, 1481, 1454, 1400, 1249, 831, 731, 698 cm⁻¹. HRMS (EI) (*m/z*): [M+H⁺] calculated for C₁₅H₁₆FN, 230.1340 found, 230.1337.

4-(4-Phenylbutan-2-yl)benzonitrile (2-54)

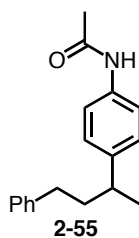


2-54

The general procedure was followed using NiCl₂·dme (2.2 mg, 0.01 mmol), 4,4'-di-*tert*-2,2'-bipyridine (2.7 mg, 0.01 mmol), 4-bromobenzonitrile (36 mg, 0.2 mmol), potassium (4-phenylbutan-2-yl)trifluoroborate (72 mg, 0.3 mmol), Ir[dFCF₃ppy]₂(bpy)PF₆ (5.0 mg, 0.005

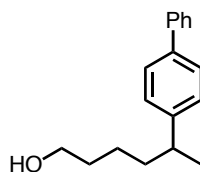
mmol), and Cs₂CO₃ (98 mg, 0.3 mmol) in 4 mL 1,4-dioxane. The crude residue was purified via column chromatography (5% EtOAc in hexanes) to afford the desired product (26 mg, 0.112 mmol, 56% yield). **¹H NMR (500 MHz, CDCl₃):** δ 7.64 – 7.58 (m, 2H), 7.35 – 7.25 (m, 4H), 7.21 – 7.15 (m, 1H), 7.14 – 7.07 (m, 2H), 2.83 – 2.73 (m, 1H), 2.57 – 2.42 (m, 2H), 1.97 – 1.87 (m, 2H), 1.28 (d, *J* = 6.9 Hz, 3H). **¹³C NMR (126 MHz, CDCl₃):** δ 152.91, 141.73, 132.31, 128.37, 128.26, 127.90, 125.88, 119.08, 109.86, 39.65, 39.46, 33.69, 21.99. **IR (thin film):** ν 3027, 2924, 2226, 1606, 1495, 1454, 1032, 1018, 836, 748, 698 cm⁻¹. **HRMS (EI) (m/z):** [M⁺] calculated for C₁₇H₁₇N, 235.1361 found, 235.1361.

***N*-(4-(4-phenylbutane-2-yl)phenyl)acetamide (2-55)**



The general procedure was followed using NiCl₂·dme (2.2 mg, 0.01 mmol), 4,4'-di-*tert*-2,2'-bipyridine (2.7 mg, 0.01 mmol), *N*-(4-bromophenyl)acetamide (43 mg, 0.2 mmol), potassium (4-phenylbutan-2-yl)trifluoroborate (72 mg, 0.3 mmol), Ir[dFCF₃ppy]₂(bpy)PF₆ (5.0 mg, 0.005 mmol), and Cs₂CO₃ (98 mg, 0.3 mmol) in 4 mL 1,4-dioxane. The crude residue was purified via column chromatography (5% EtOAc in hexanes) to afford the desired product (28 mg, 0.106 mmol, 53% yield). **¹H NMR (500 MHz, CDCl₃):** δ 7.45 – 7.40 (m, 2H), 7.28 – 7.23 (m, 2H), 7.19 – 7.09 (m, 5H), 2.76 – 2.63 (m, 1H), 2.58 – 2.42 (m, 2H), 2.17 (s, 3H), 1.92 – 1.83 (m, 2H), 1.31 – 1.20 (m, 4H). **¹³C NMR (126 MHz, CDCl₃):** δ 168.12, 143.38, 142.45, 135.69, 128.33, 128.25, 127.54, 125.62, 120.06, 39.93, 38.94, 33.85, 24.57, 22.54. **IR (thin film):** ν 3296, 2922, 1660, 1602, 1537, 1514, 1412, 1370, 1318, 1264, 836 cm⁻¹. **HRMS (EI) (m/z):** [M⁺] calculated for C₁₈H₂₂NO, 268.1696 found, 268.1694.

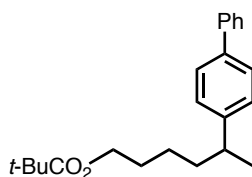
5-(Biphenyl-4-yl)hexan-1-ol (2-56)



2-56

The general procedure was followed using NiCl₂·dme (2.2 mg, 0.01 mmol), 4,4'-di-*tert*-2,2'-bipyridine (2.7 mg, 0.01 mmol), 4-bromobiphenyl (35 mg, 0.2 mmol), potassium trifluoro(6-hydroxyhexan-2-yl)borate (62 mg, 0.3 mmol), Ir[dFCF₃ppy]₂(bpy)PF₆ (5.0 mg, 0.005 mmol), and Cs₂CO₃ (98 mg, 0.3 mmol) in 4 mL 1,4-dioxane. The crude residue was purified via column chromatography (10% EtOAc in hexanes) to afford the desired product (31 mg, 0.122 mmol, 60% yield). **¹H NMR (500 MHz, CDCl₃):** δ 7.60 (d, *J* = 10.0 Hz, 2H), 7.53 (d, *J* = 7.9 Hz, 2H), 7.43 (t, *J* = 7.6 Hz, 2H), 7.36 – 7.30 (m, 1H), 7.27 – 7.24 (m, 2H), 3.61 (t, *J* = 6.7 Hz, 2H), 2.75 (sextet, *J* = 7.0 Hz, 1H), 1.68 – 1.60 (m, 2H), 1.60 – 1.53 (m, 2H), 1.41 – 1.31 (m, 1H), 1.29 (d, *J* = 6.9 Hz, 4H), 1.27 – 1.18 (m, 1H). **¹³C NMR (126 MHz, CDCl₃):** δ 146.70, 141.09, 138.77, 128.66, 127.36, 127.04, 126.96, 126.94, 62.93, 39.61, 38.17, 32.85, 23.91, 22.29. **IR (thin film):** ν 3341, 2925, 1485, 1452, 1408, 1312, 1073, 1039, 1007, 836 cm⁻¹. **HRMS (EI) (m/z):** [M⁺] calculated for C₁₈H₂₂O, 254.1671 found, 254.1666.

5-(Biphenyl-4-yl)hexyl pivalate (2-57)

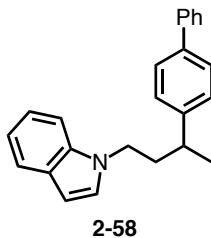


2-57

The general procedure was followed using NiCl₂·dme (2.2 mg, 0.01 mmol), 4,4'-di-*tert*-2,2'-bipyridine (2.7 mg, 0.01 mmol), 4-bromobiphenyl (35 mg, 0.2 mmol), potassium trifluoro(6-

(pivaloyloxy)hexan-2-yl)borate (88 mg, 0.3 mmol), Ir[dFCF₃ppy]₂(bpy)PF₆ (5.0 mg, 0.005 mmol), and Cs₂CO₃ (98 mg, 0.3 mmol) in 4 mL 1,4-dioxane. The crude residue was purified via column chromatography (5% EtOAc in hexanes) to afford the desired product (58 mg, 0.173 mmol, 86% yield). **¹H NMR (500 MHz, CDCl₃):** δ 7.62 – 7.56 (m, 2H), 7.55 – 7.50 (m, 2H), 7.47 – 7.40 (m, 2H), 7.35 – 7.30 (m, 1H), 7.28 – 7.23 (m, 2H), 4.03 (t, *J* = 6.6 Hz, 2H), 2.78 – 2.68 (m, 1H), 1.71 – 1.54 (m, 4H), 1.39 – 1.26 (m, 5H), 1.16 (s, 9H). **¹³C NMR (126 MHz, CDCl₃):** δ 178.54, 146.54, 141.13, 138.83, 128.66, 127.34, 127.05, 126.97, 126.94, 64.14, 39.48, 38.69, 37.87, 28.64, 27.15, 23.96, 22.29. **IR (thin film):** ν 2958, 1725, 1485, 1283, 1152, 837, 765, 732, 696 cm⁻¹. **HRMS (EI) (m/z):** [M+H⁺] calculated for C₂₃H₃₁O₂, 339.2319 found, 339.2316.

1-(3-(Biphenyl-4-yl)butyl)-1*H*-indole (2-58)



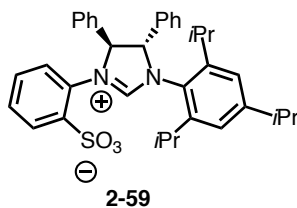
The general procedure was followed using NiCl₂·dme (2.2 mg, 0.01 mmol), 4,4'-di-*tert*-2,2'-bipyridine (2.7 mg, 0.01 mmol), 4-bromobiphenyl (35 mg, 0.2 mmol), potassium (4-(1*H*-indol-1-yl)butan-2-yl)trifluoroborate (88 mg, 0.3 mmol), Ir[dFCF₃ppy]₂(bpy)PF₆ (5.0 mg, 0.005 mmol), and Cs₂CO₃ (98 mg, 0.3 mmol) in 4 mL 1,4-dioxane. The crude residue was purified via column chromatography (1% EtOAc in hexanes) to afford the desired product (43 mg, 0.131 mmol, 65% yield). **¹H NMR (500 MHz, CDCl₃):** δ 7.66 – 7.56 (m, 5H), 7.46 (td, *J* = 7.8, 2.0 Hz, 2H), 7.36 (dd, *J* = 8.3, 6.3 Hz, 1H), 7.29 (dd, *J* = 8.2, 1.9 Hz, 2H), 7.24 (d, *J* = 8.5 Hz, 1H), 7.21 – 7.16 (m, 1H), 7.13 – 7.09 (m, 1H), 7.06 – 7.03 (m, 1H), 6.51 – 6.46 (m, 1H), 4.11 – 3.97 (m, 2H), 2.82 – 2.72 (m, 1H), 2.27 – 2.12 (m, 2H), 1.32 (d, *J* = 7.0 Hz, 3H). **¹³C NMR (126 MHz, CDCl₃):** δ

145.09, 140.91, 139.35, 135.82, 128.75, 128.60, 127.68, 127.46, 127.37, 127.13, 127.00, 121.30, 120.93, 119.20, 109.36, 100.97, 44.57, 38.04, 37.11, 22.87. **IR (thin film):** ν 2956, 2157, 1510, 1485, 1462, 1315, 1262, 1007, 763, 731 cm^{-1} . **HRMS (EI) (m/z):** $[\text{M}+\text{H}^+]$ calculated for $\text{C}_{24}\text{H}_{23}\text{N}$, 326.1903 found, 326.1900.

6.2.6 Enantioselectivity Investigation

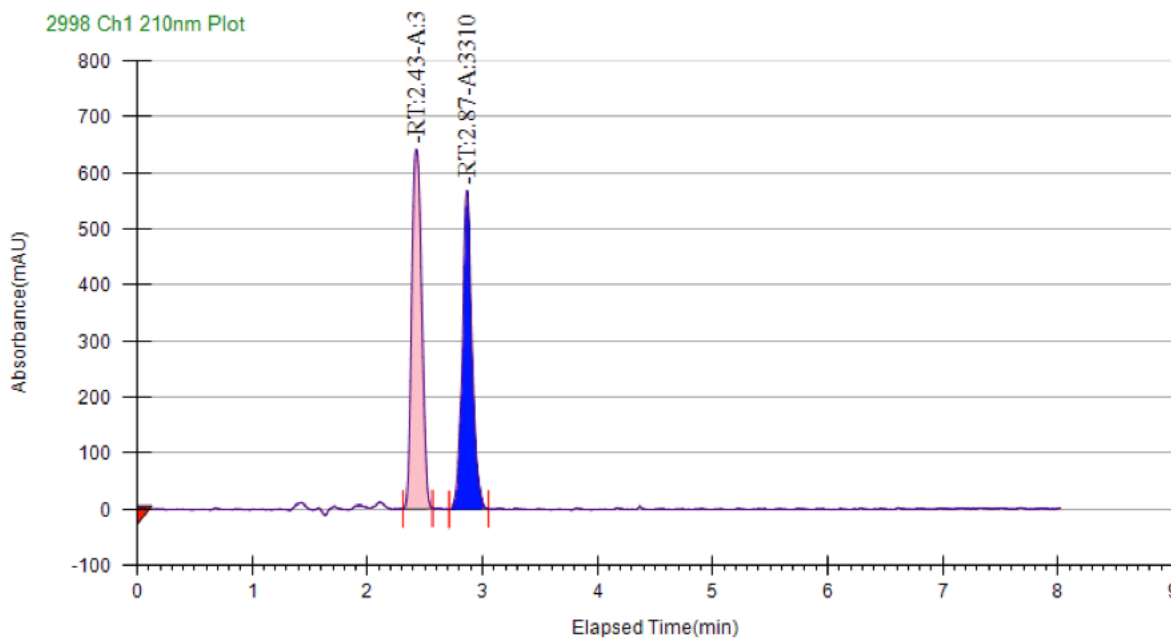
0.2 M Solvent was added to a solid mixture of CuCl (10 mol %), Ligand (12 mol %), and KO-*t*-Bu (1.5 equiv) under N_2 . The reaction was allowed to stir at rt for 10 minutes. B_2pin_2 (2.0 equiv) was added under N_2 and the reaction was allowed to stir for an additional 30 minutes at rt. 4-Phenyl-1-butene (1.0 equiv) and MeOH (2.0 equiv) were added to the mixture by syringe. The reaction mixture was allowed to stir at rt for 2 h and was then filtered through silica gel, eluting with 50% v/v EtOAc/hexanes. The solvent was removed *in vacuo*. The crude residue was purified via flash chromatography (100% hexanes- 96:4 hexanes: EtOAc) Following literature precedent, conversion of the secondary alkylborane to the secondary alcohol was performed for enantioselectivity determination.²⁶

Reaction using ligand 2-59



The general procedure was followed using CuCl (2.0 mg, 0.02 mmol), **2-59** (11.6 mg, 0.024 mmol), KO-*t*-Bu (34 mg, 0.3 mmol), B₂pin₂ (102 mg, 0.4 mmol), 4-phenyl-1-butene (26 mg, 0.2 mmol), MeOH (13 mg, 0.4 mmol) and 1.5 mL of acetonitrile. The crude residue was purified via flash chromatography (100% hexanes to 4% EtOAc in hexanes) to afford the desired product as an 86:14 mixture of regioisomers (29 mg, 0.11 mmol, 56% yield). The enantioselectivity was determined by SFC analysis: OD-H column, 3 mL/min, 20% *i*-PrOH, 120 bar, 40 °C, 24% ee.

Racemic

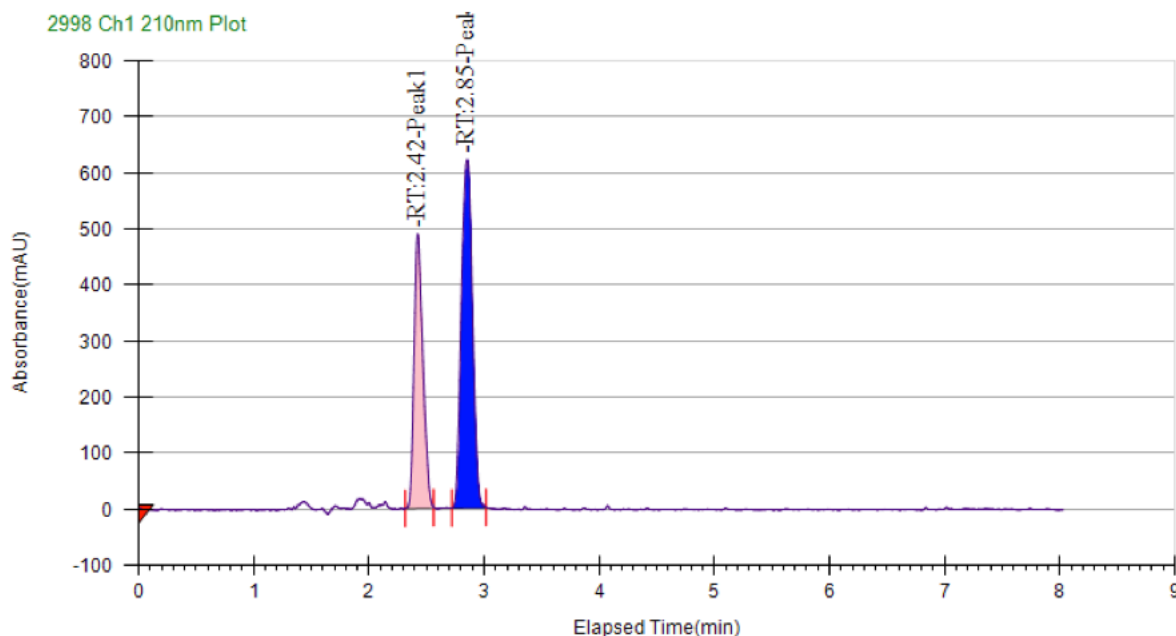


Peak Information

Peak No	% Area	Area	Ret. Time	Height	Cap. Factor
1	53.6287	3127.8146	2.4 min	497.9369	2402.3333
2	46.3713	2704.5425	2.84 min	440.7452	2842.3333

Table 6-1: Racemic SFC Trace for 4-Phenyl-2-butanol 3 Minute Run

Reaction with ligand 2-59

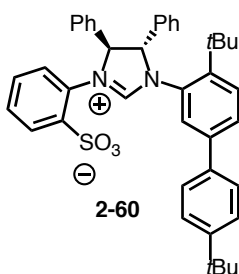


Peak Information

Peak No	% Area	Area	Ret. Time	Height	Cap. Factor
1	38.2337	2550.1034	2.42 min	488.6584	0
2	61.7663	4119.684	2.85 min	620.9428	0

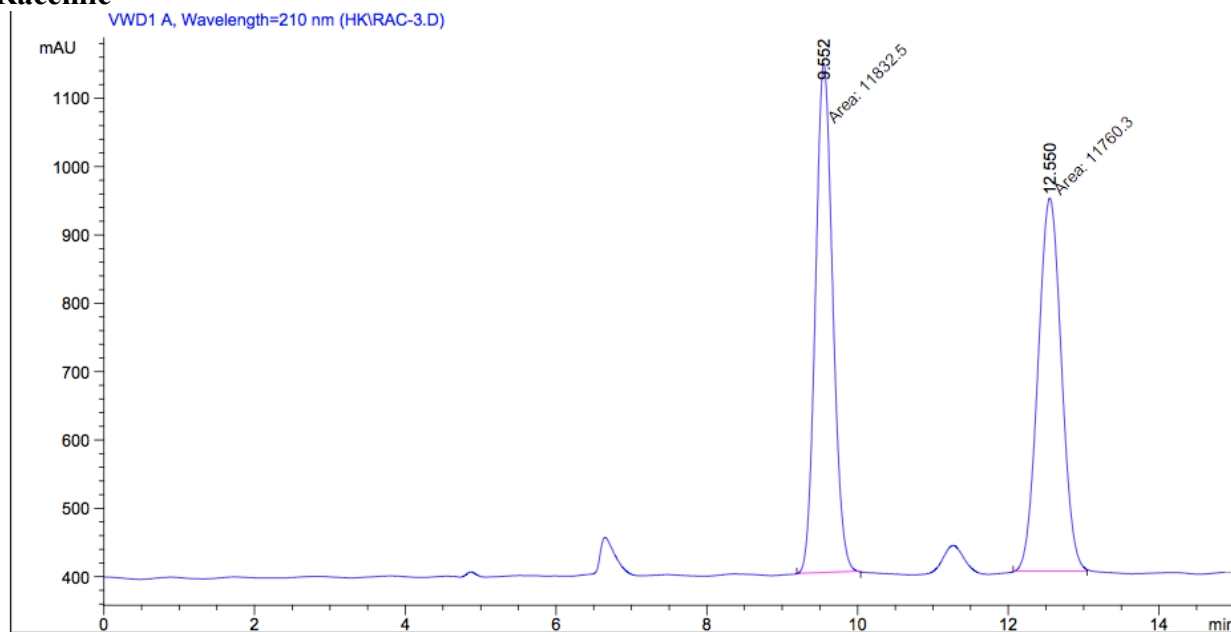
Table 6-2: SFC Trace for Reaction with Ligand 2-59

Reaction at room temperature with ligand 2-60



The general procedure was followed using CuCl (2.0 mg, 0.02 mmol), **2-60** (15.2 mg, 0.024 mmol), KO-*t*-Bu (34 mg, 0.3 mmol), B₂pin₂ (102 mg, 0.4 mmol), 4-phenyl-1-butene (26 mg, 0.2 mmol), MeOH (13 mg, 0.4 mmol) and 1.0 mL of tetrahydrofuran. The crude residue was purified via flash chromatography (100% hexanes to 4% EtOAc in hexanes) to afford the desired product as a 70:30 mixture of regioisomers (50.0 mg, 0.19 mmol, 96% yield). The enantioselectivity was determined by HPLC analysis: OD-H column, 0.75 mL/min, 10% *i*-PrOH 15% ee.

Racemic

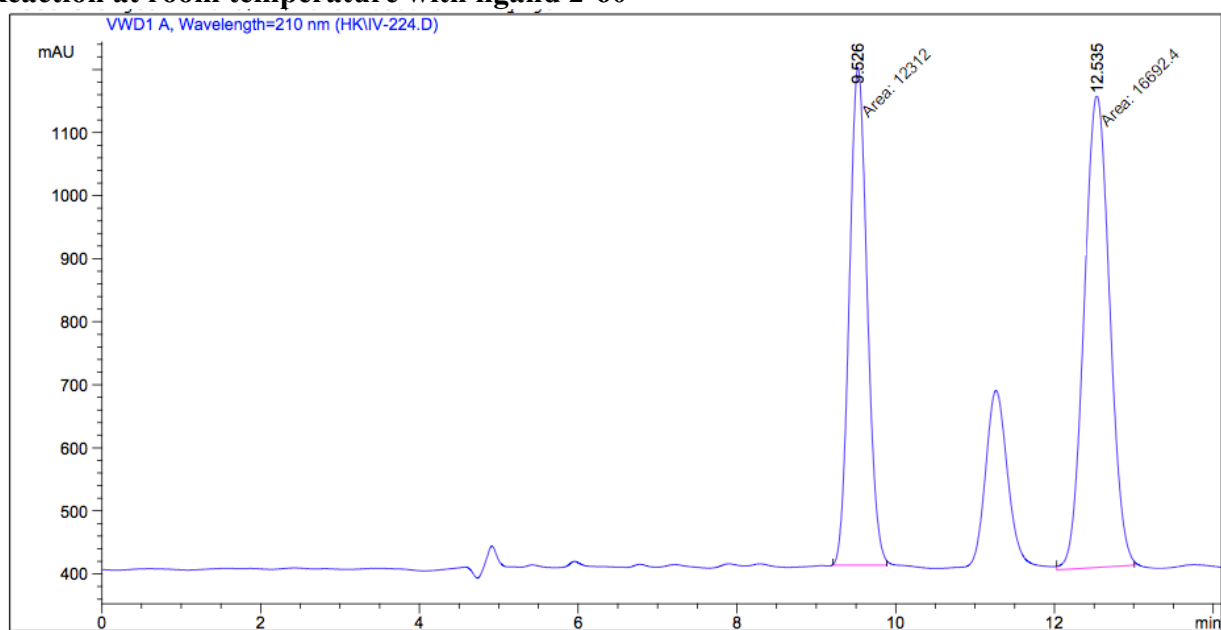


Signal 1: VWD1 A, Wavelength=210 nm

Peak #	RetTime [min]	Type	Width [min]	Area mAU *s	Height [mAU]	Area %
1	9.552	MM	0.2648	1.18325e4	744.70459	50.1531
2	12.550	MM	0.3595	1.17603e4	545.25323	49.8469

Table 6-3: Racemic SFC Trace for 4-Phenyl-2-butanol

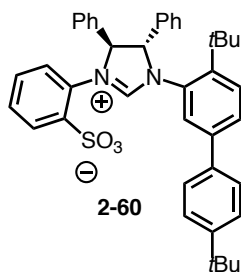
Reaction at room temperature with ligand 2-60



Peak #	RetTime [min]	Type	Width [min]	Area mAU *s	Height [mAU]	Area %
1	9.526	MM	0.2600	1.23120e4	789.32135	42.4488
2	12.535	MM	0.3719	1.66924e4	748.10834	57.5512

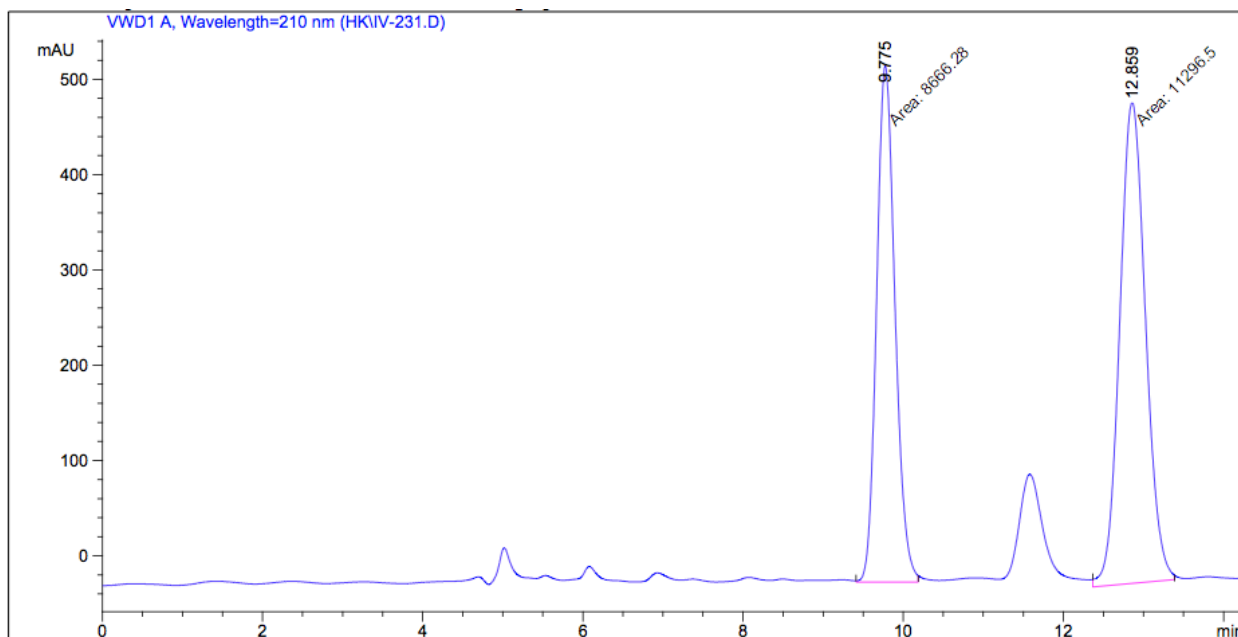
Table 6-4: HPLC Trace for Reaction with Ligand 2-60 at Room Temperature

Reaction at -35 °C with ligand 2-60



The general procedure was followed using CuCl (2.0 mg, 0.02 mmol), **2-60** (15.2 mg, 0.024 mmol), KO-*t*-Bu (34 mg, 0.3 mmol), B₂pin₂ (102 mg, 0.4 mmol) and 1.0 mL of tetrahydrofuran. The reaction was cooled to -35 °C before, 4-phenyl-1-butene (26 mg, 0.2 mmol), MeOH (13 mg, 0.4 mmol) were added. The crude residue was purified via flash chromatography (100% hexanes to 4% EtOAc in hexanes) to afford the desired product as a 70:30 mixture of regioisomers (17.1

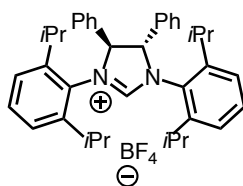
mg, 0.066 mmol, 33% yield). The enantioselectivity was determined by HPLC analysis: OD-H column, 0.75 mL/min, 10% *i*-PrOH, 13% ee.



Peak #	RetTime [min]	Type	Width [min]	Area mAU *s	Height [mAU]	Area %
1	9.775	MM	0.2666	8666.27734	541.84882	43.4122
2	12.859	MM	0.3728	1.12965e4	504.97388	56.5878

Table 6-5: HPLC Trace for Reaction with Ligand 2-60 at -35 °C

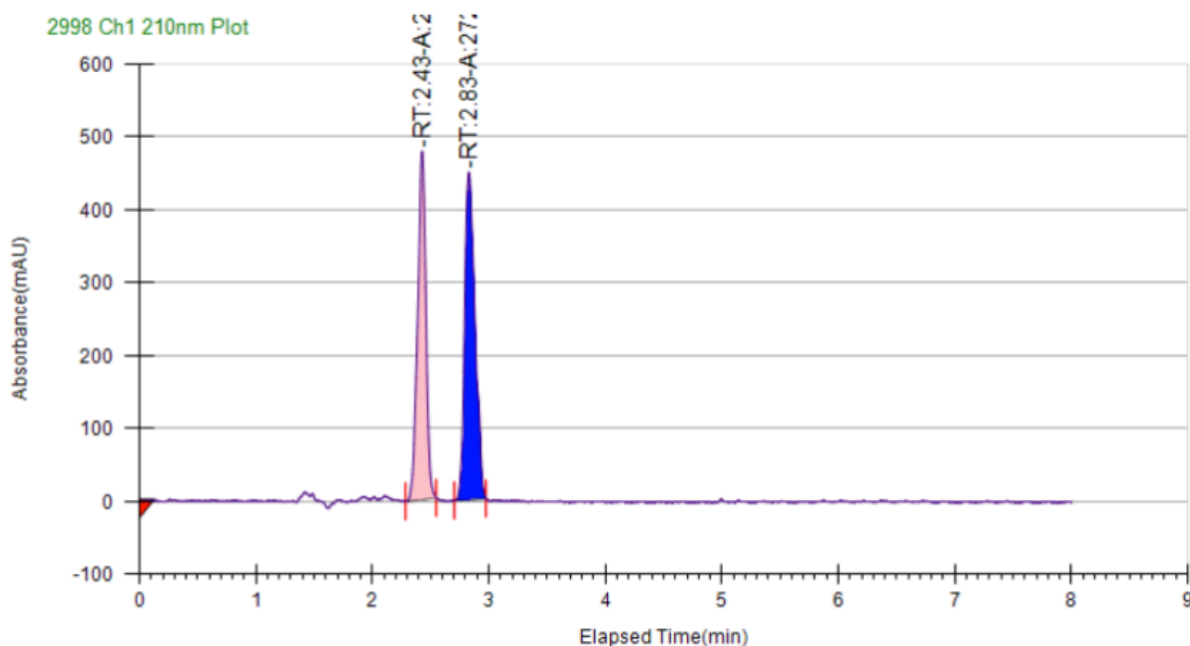
Reaction using ligand 2-61



2-61

The general procedure was followed using CuCl (2.0 mg, 0.02 mmol), **2-61** (15.0 mg, 0.024 mmol), KO-*t*-Bu (34 mg, 0.3 mmol), B₂pin₂ (102 mg, 0.4 mmol), 4-phenyl-1-butene (26 mg, 0.2 mmol), MeOH (13 mg, 0.4 mmol) and 1.5 mL of acetonitrile. The crude residue was purified via flash chromatography (100% hexanes to 4% EtOAc in hexanes) to afford the desired product as

a >98:2 mixture of regioisomers (44 mg, 0.17 mmol, 85% yield). The enantioselectivity was determined by SFC analysis: OD-H column, 3 mL/min, 20% *i*-PrOH, 120 bar, 40 °C, 8% ee.

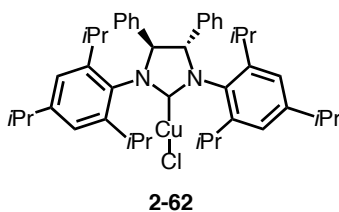


Peak Information

Peak No	% Area	Area	Ret. Time	Height	Cap. Factor
1	46.066	2331.0111	2.43 min	478.0202	2425.6667
2	53.934	2729.1442	2.83 min	449.1405	2829

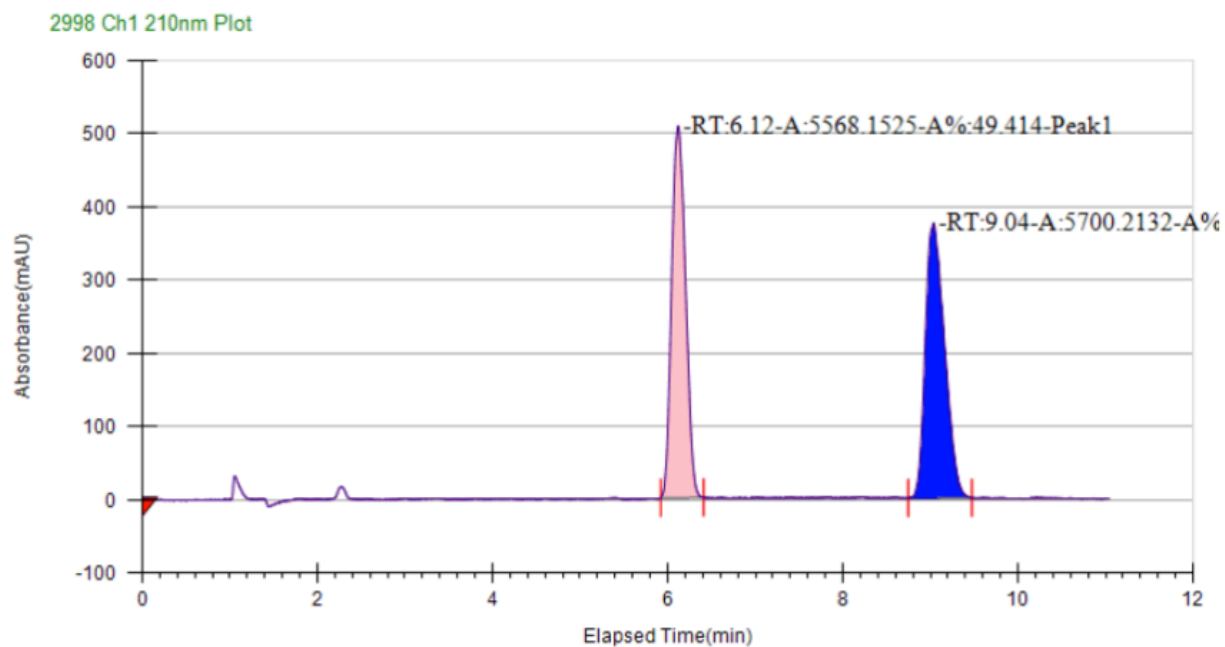
Table 6-6 SFC Trace for Reaction with Ligand 2-61

Reaction using catalyst 2-62 in tetrahydrofuran



The general procedure was followed using **2-62** (3.6 mg, 0.005 mmol), KO-*t*-Bu (16.8 mg, 0.15 mmol), B₂pin₂ (51 mg, 0.2 mmol), 4-phenyl-1-butene (13 mg, 0.1 mmol), MeOH (6.4 mg, 0.42mmol) and 0.5 mL of tetrahydrofuran. The crude residue was a mixture of regioisomers >98:2 and was directly oxidized (6.1 mg, 0.04 mmol, 41% yield). The enantioselectivity was determined by SFC analysis: OD-H column, 3 mL/min, 5% *i*-PrOH, 120 bar, 40 °C, 5% ee.

Racemic

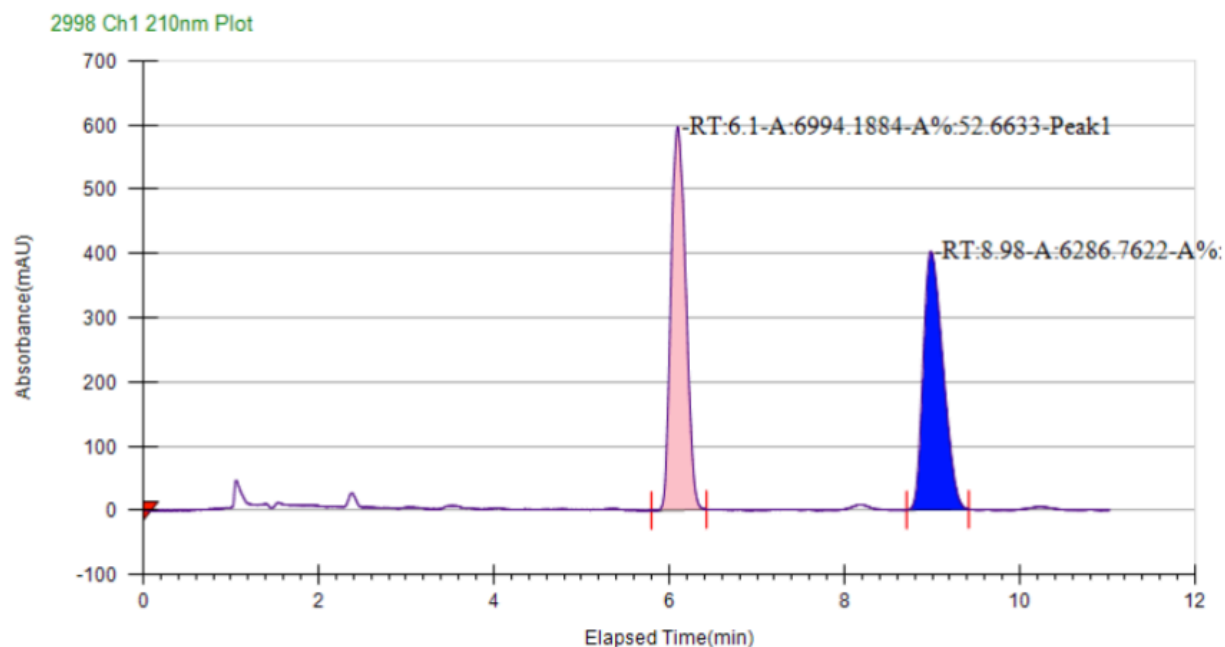


Peak Information

Peak No	% Area	Area	Ret. Time	Height	Cap. Factor
1	49.414	5568.1525	6.12 min	507.9188	6119
2	50.586	5700.2132	9.04 min	375.043	9035.6667

Table 6-7: Racemic SFC Trace for 4-Phenyl-2-butanol 10 Minute Run

Reaction using catalyst 2-62 in tetrahydrofuran

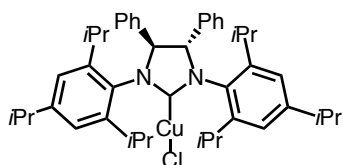


Peak Information

Peak No	% Area	Area	Ret. Time	Height	Cap. Factor
1	52.6633	6994.1884	6.1 min	596.7995	0
2	47.3367	6286.7622	8.98 min	402.3723	0

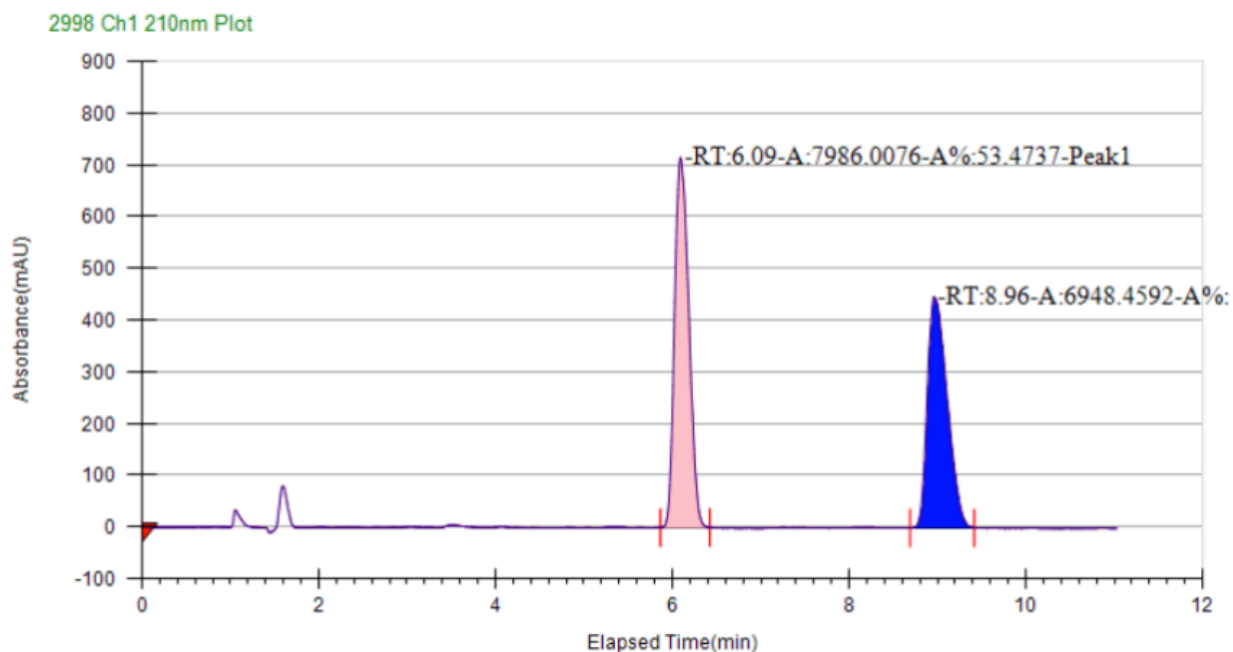
Table 6-8: Reaction Using Catalyst 2-62 in Tetrahydrofuran

Reaction using catalyst 2-62 in toluene



2-62

The general procedure was followed using **2-62** (3.6 mg, 0.005 mmol), KO-*t*-Bu (16.8 mg, 0.15 mmol), B₂pin₂ (51 mg, 0.2 mmol), 4-phenyl-1-butene (13 mg, 0.1 mmol), MeOH (6.4 mg, 0.42mmol) and 0.5 mL of toluene. The crude residue was a mixture of isomers >98:2 that was directly oxidized (7.6 mg, 0.05 mmol, 51% yield). The enantioselectivity was determined by SFC analysis: OD-H column, 3 mL/min, 5% *i*-PrOH, 120 bar, 40 °C, 7% ee.

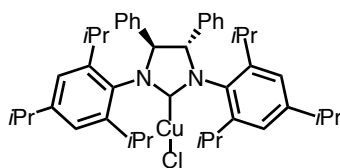


Peak Information

Peak No	% Area	Area	Ret. Time	Height	Cap. Factor
1	53.4737	7986.0076	6.09 min	714.648	0
2	46.5263	6948.4592	8.96 min	446.7041	0

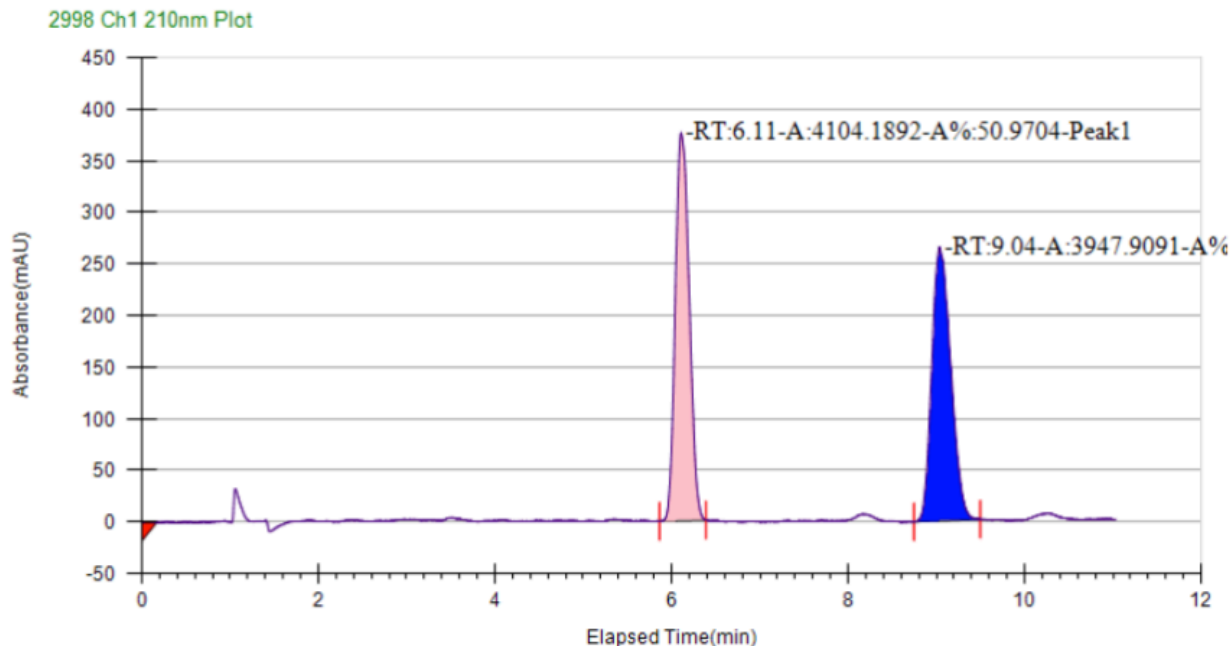
Table 6-9: Reaction Using Catalyst 2-62 in Toluene

Reaction using catalyst 2-62 in acetonitrile



2-62

The general procedure was followed using **2-62** (3.6 mg, 0.005 mmol), KO-*t*-Bu (16.8 mg, 0.15 mmol), B₂pin₂ (51 mg, 0.2 mmol), 4-phenyl-1-butene (13 mg, 0.1 mmol), MeOH (6.4 mg, 0.42mmol) and 0.5 mL of acetonitrile. The crude residue was a mixture of isomers 95:5 that were directly oxidized (7.6 mg, 0.05 mmol, 51% yield). The enantioselectivity was determined by SFC analysis: OD-H column, 3 mL/min, 5% *i*-PrOH, 120 bar, 40 °C, 2% ee.



Peak Information

Peak No	% Area	Area	Ret. Time	Height	Cap. Factor
1	50.9704	4104.1892	6.11 min	375.869	6105.6667
2	49.0296	3947.9091	9.04 min	265.1831	9035.6667

Table 6-10: Reaction Using Catalyst 2-62 in Tetrahydrofuran

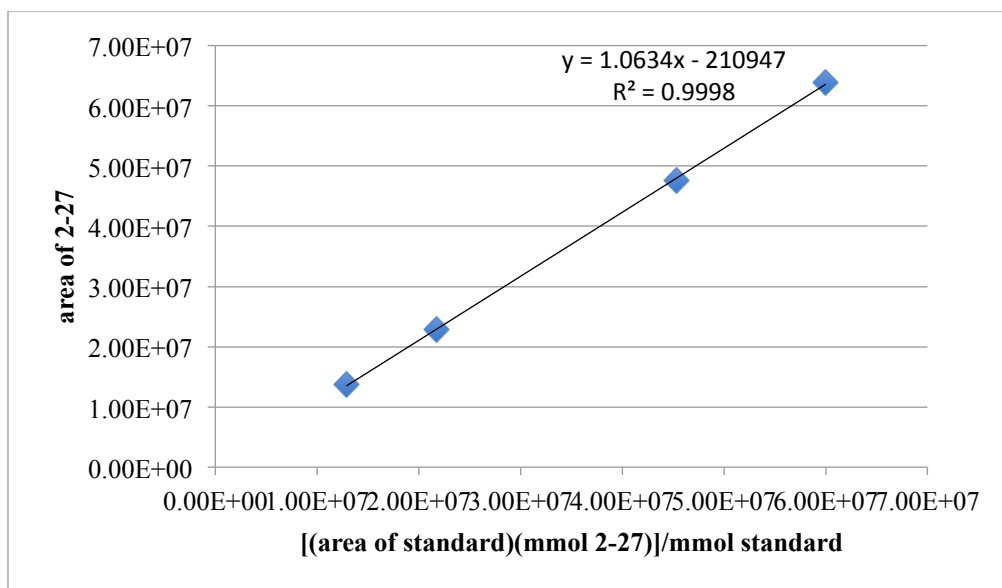
6.2.7 Hydroboration of 1,2-Disubstituted Olefins

6.2.7.1 GC-FID Calibration Curves

Solutions containing a constant amount of internal standard, tridecane, (0.200 mmol) and varying amounts of **2-27** (0.0485, 0.0970, 0.1455, 0.1940 mmol) were prepared in ethyl acetate. Each sample was analyzed by GC-FID and the response factor (F) was calculated via a linear regression to calculate the slope (F) of equation 1. Equation 2 was used to determine the amount of desired product.

$$\frac{\text{area of } \mathbf{2-27}}{\text{mmol of } \mathbf{2-27}} = F \frac{\text{area of standard}}{\text{mmol of standard}} \quad (\text{equation 1})$$

$$\text{mmol of } \mathbf{2-27} = \frac{(\text{mmol of standard})(\text{area of } \mathbf{2-27})}{F (\text{area of standard})} \quad (\text{equation 2})$$

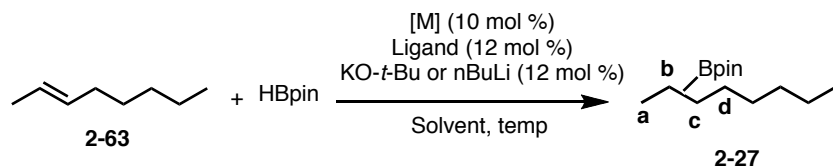


mmol 2-27	area 2-27	area IS	mmol IS
0.0485	13729811	53246861	0.2
0.0970	22790204	44791016	0.2
0.1455	47609265	62355222	0.2
0.1940	63872472	61831334	0.2

Table 6-11: Calibration Curve for 2-27

6.2.7.2 Tables of Reaction Screens for Hydroboration of Internal Olefins

Table 6-12 summarized the hydroboration of *trans*-2-octene with nickel and palladium catalysts and a variety of *N*-heterocyclic carbenes.



Entry	[M]	Ligand	Solvent	temp	a:b:c:d	Yield(GCFID)
1	Ni(cod) ₂	IPr·HCl	THF	rt	-	
2	Ni(cod) ₂	IMes·HCl	THF	rt	-	
3	Ni(cod) ₂	ICy·HBF ₄	THF	rt	-	
4	Ni(cod) ₂	DMIPr·HCl	THF	rt	-	
5	Pd ₂ (dba) ₃	IPr·HCl	THF	rt	-	
6	Pd ₂ (dba) ₃	IMes·HCl	THF	rt	-	
7	Pd ₂ (dba) ₃	ICy·HBF ₄	THF	rt	-	
8	Pd ₂ (dba) ₃	DMIPr·HCl	THF	rt	-	
9	Pd(OAc) ₂	IPr·HCl	Toluene	100 °C	100:0:0:0	trace
10	Pd(OAc) ₂	IMes·HCl	Toluene	100 °C	100:0:0:0	trace
11	Pd(OAc) ₂	DMIPr·HCl	Toluene	100 °C	-	
12	Pd(OAc) ₂	ICy·HBF ₄	Toluene	100 °C	-	
13	Pd(OAc) ₂	IPrBAC·HCl	Toluene	100 °C	39:37:24:0	9%:8%:5%:0%
14	Pd(OAc) ₂	IPr*OMe	Toluene	100 °C	-	
15	Pd(OAc) ₂	<i>i</i> prNHC·HCl	Toluene	100 °C	55:24:20:1	7%:3%:2%:<1%
16	Pd(OAc) ₂	BMIMCl	Toluene	100 °C	19:39:40:3	11%:23%:24%:2%
17	Pd(OAc) ₂	MeNHC·HCl	Toluene	100 °C	-	

Table 6-12 Hydroboration of Internal Olefins with Nickel and Palladium

Table 6-13 summarizes the hydroboration of *trans*-2-octene with an iron catalyst in several solvents.

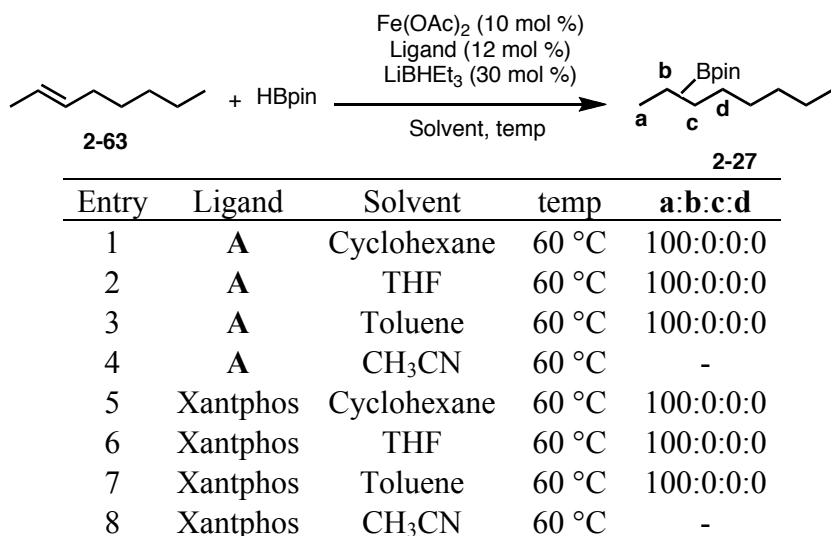


Table 6-13 Hydroboration of Internal Olefins with Iron

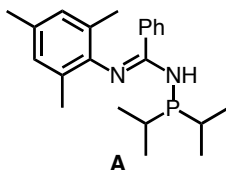


Table 6-14 summarizes the hydroboration of *trans*-2-octene with cobalt and LiBHET₃.

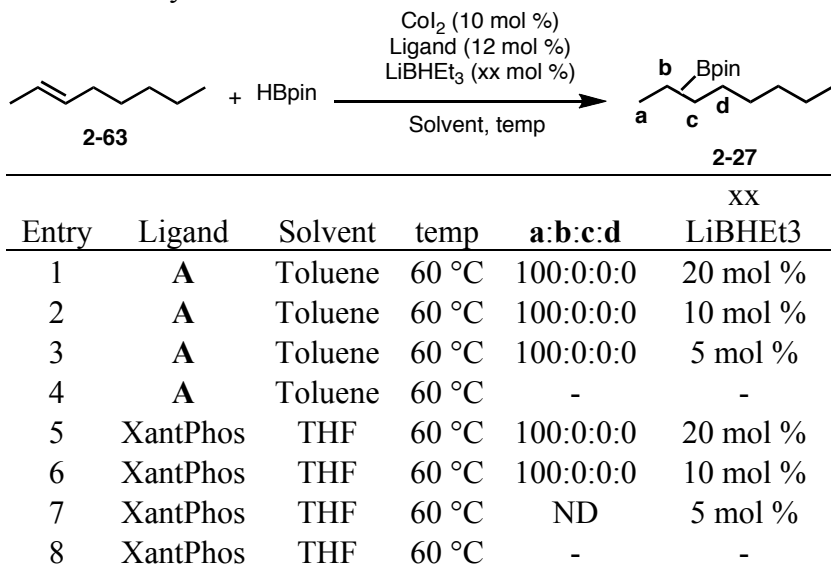
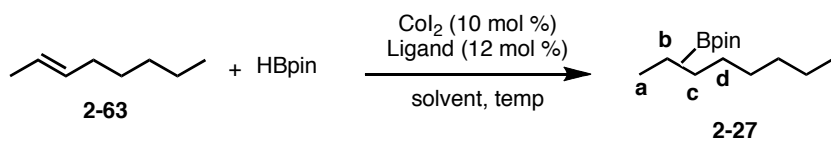


Table 6-14 Hydroboration of Internal Olefins with Cobalt and Additive

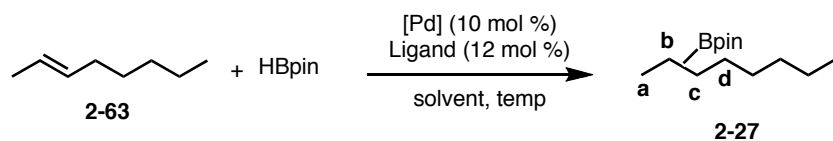
Table 6-15 summarizes hydroboration of *trans*-2-octene with cobalt and no additive in a variety of solvents.



Entry	Ligand	Solvent	temp	a:b:c:d	Note
1	A	Cyclohexane	60 °C	100:0:0:0	
2	A	THF	60 °C	100:0:0:0	
3	A	Toluene	60 °C	100:0:0:0	55% isolated
4	A	CH ₃ CN	60 °C	-	
5	Xantphos	Cyclohexane	60 °C	100:0:0:0	
6	Xantphos	THF	60 °C	ND	product unable to analyze
7	Xantphos	Toluene	60 °C	ND	product unable to analyze
8	Xantphos	CH ₃ CN	60 °C	-	

Table 6-15 Hydroboration of Internal Olefin with Cobalt and No Additive

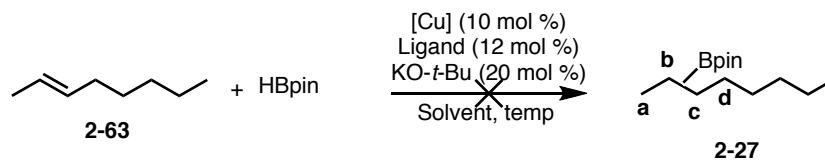
Table 6-16 summarizes the hydroboration of *trans*-2-octene with palladium and phosphine ligands.



Entry	[Pd]	Ligand	Solvent	temp	a:b:c:d	Notes
1	Pd(OAc) ₂	XantPhos	THF	60 °C	-	
2	Pd(OAc) ₂	S-Phos	THF	60 °C	100:0:0:0	
3	Pd(OAc) ₂	A	THF	60 °C	-	
4	Pd(OAc) ₂	S-Phos	Toluene	100 °C	100:0:0:0	
5	Pd(OAc) ₂	Trinaph	Toluene	100 °C	-	
6	Pd(OAc) ₂	Ru-Phos	Toluene	100 °C	100:0:0:0	
7	Pd(OAc) ₂	TTMPP	Toluene	100 °C	-	
8	Pd(OAc) ₂	BrettPhos	Toluene	100 °C	-	
9	Pd(OAc) ₂	Xantphos	Toluene	100 °C	100:0:0:0	trace isomers
10	Pd(OAc) ₂	rac-BINAP	Toluene	100 °C	100:0:0:0	trace isomers
11	Pd(OAc) ₂	DPEPhos	Toluene	100 °C	100:0:0:0	
12	Pd(OAc) ₂	(S)-DTBM-SEGPHOS	Toluene	100 °C	100:0:0:0	
13	Pd(OAc) ₂	PhDavePhos	Toluene	100 °C	100:0:0:0	trace isomers
14	Pd(OAc) ₂	DiPhos	Toluene	100 °C	100:0:0:0	trace isomers
15	Pd(OAc) ₂	BiPhos	Toluene	100 °C	-	trace isomer
16	Pd ₂ (dba) ₃	S-Phos	Toluene	100 °C	-	
17	Pd ₂ (dba) ₃	Trinaph	Toluene	100 °C	-	
18	Pd ₂ (dba) ₃	Ru-Phos	Toluene	100 °C	-	
19	Pd ₂ (dba) ₃	TTMPP	Toluene	100 °C	-	
20	Pd ₂ (dba) ₃	BrettPhos	Toluene	100 °C	-	

Table 6-16 Hydroboration of Internal Olefins with Palladium and Phosphine Ligands

Table 6-17 summarizes the failed hydroboration reactions of *trans*-2-octene with copper catalysts.



Entry	[Cu]	Ligand	Solvent	temp
1	IPrCuCl	-	nhexane	rt
2	IMesCuCl	-	nhexane	rt
3	ICyCuCl	-	nhexane	rt
4	CuCl	BIPHEP	nhexane	rt
5	CuCl	BIPHEP	THF	rt
6	CuCl	BIPHEP	Toluene	rt
7	CuCl	A	nhexane	rt
8	CuCl	A	THF	rt
9	CuCl	A	Toluene	rt
10	CuCl	A	nhexane	60 °C
11	CuCl	A	THF	60 °C
12	CuCl	A	Toluene	60 °C
13	CuCl	A	CH ₃ CN	60 °C
14	CuCl	XantPhos	nhexane	rt
15	CuCl	XantPhos	THF	rt
16	CuCl	XantPhos	Toluene	rt
17	CuCl	XantPhos	nhexane	60 °C
18	CuCl	XantPhos	THF	60 °C
19	CuCl	XantPhos	Toluene	60 °C
20	CuCl	XantPhos	MeCN	60 °C

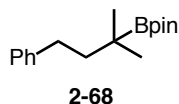
Table 6-17 Hydroboration of Internal Olefins with Copper

6.2.8 Synthesis of Tertiary Alkylboranes

General procedures for copper-catalyzed hydroboration of trisubstituted olefins:

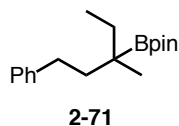
1.5 mL of dichloromethane was added to a solid mixture of IPrCuCl (0.03 mmol) and NaO-*t*-Bu (0.3 mmol) under N₂. The reaction was allowed to stir at rt for 10 minutes. B₂pin₂ (0.6 mmol) was added under N₂ and the reaction was allowed to stir for an additional 30 minutes at rt. The alkene (0.3 mmol) and MeOH (0.6 mmol) were added to the mixture by syringe. The reaction mixture was allowed to stir at rt for 2 h and was then filtered through silica gel, eluting with 50% v/v EtOAc/hexanes. The solvent was removed *in vacuo*, and the crude residue was purified via flash chromatography on silica gel to afford the desired product.

4,4,5,5-tetramethyl-2-(2-methyl-4-phenylbutan-2-yl)-1,3,2-dioxaborolane (2-68)



The title compound was prepared from IPrCuCl (14.6 mg, 0.03 mmol), NaO-*t*-Bu (29 mg, 0.3 mmol), B₂pin₂ (152 mg, 0.6 mmol), (3-methylbut-3-enyl)benzene (44 mg, 0.3 mmol) and MeOH (19 mg, 0.6 mmol) by following the general procedure. The crude residue was purified via flash chromatography (100% hexanes to 4% EtOAc in hexanes) to afford the desired product as a 91:9 mixture of regioisomers (72 mg, 0.26 mmol, 87% yield). ¹H NMR (500 MHz, CDCl₃): δ 7.34 – 7.24 (m, 2H), 7.22 – 7.14 (m, 3H), 2.61 – 2.54 (m, 2H), 1.63 – 1.56 (m, 2H), 1.27 (s, 12H), 1.02 (s, 6H). ¹³C NMR (126 MHz, CDCl₃): δ 143.63, 128.31, 128.19, 125.42, 82.96, 43.50, 33.06, 24.76, 24.74. ¹¹B NMR (128 MHz, CDCl₃): δ 34.80. IR (thin film): ν 2937, 2861, 1474, 1388, 1365, 1306, 1134, 854, 693 cm⁻¹. HRMS (EI) (m/z): [M+H⁺] calculated for C₁₇H₂₇BO₂, 274.2104 found, 274.2110.

4,4,5,5-tetramethyl-2-(3-methyl-1-phenylpentan-3-yl)-1,3,2-dioxaborolane (2-71)

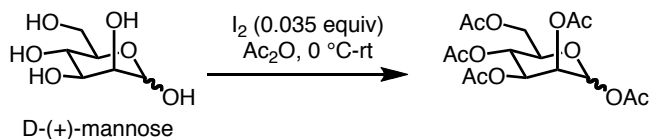


The title compound was prepared from IPrCuCl (14.6 mg, 0.03 mmol), NaO-*t*-Bu (29 mg, 0.3 mmol), B₂pin₂ (152 mg, 0.6 mmol), (3-methylenepentyl)benzene (48 mg, 0.3 mmol) and MeOH (19 mg, 0.6 mmol) by following the general procedure. The crude residue was purified via flash chromatography (100% hexanes to 4% EtOAc in hexanes) to afford the desired product as a 93:7 mixture of regioisomers (51 mg, 0.26 mmol, 59% yield). ¹H NMR (700 MHz, CDCl₃): δ 7.28 – 7.25 (m, 2H), 7.20 – 7.18 (m, 2H), 7.16 (td, *J* = 7.2, 1.4 Hz, 1H), 2.58 (td, *J* = 13.0, 5.0 Hz, 1H), 2.52 (td, *J* = 13.0, 4.7 Hz, 1H), 1.71 (td, *J* = 13.0, 4.7 Hz, 1H), 1.56 – 1.45 (m, 2H), 1.33 – 1.23 (m, 13H), 0.98 (s, 3H), 0.88 (t, *J* = 7.5 Hz, 3H). ¹³C NMR (176 MHz, CDCl₃): δ 143.76, 128.32, 128.20, 125.42, 82.98, 41.35, 32.43, 31.38, 24.90, 24.84, 20.83, 10.05. ¹¹B NMR (128 MHz, CDCl₃): δ 34.49. IR (thin film): ν 2974, 2931, 1456, 1370, 1306, 1260, 1138, 852, 698 cm⁻¹. HRMS (EI) (*m/z*): [M+H⁺] calculated for C₁₈H₂₀BO₂, 289.2333 found, 289.2335.

6.3 Chapter 4 Experimental

6.3.1 Synthesis of 2-Hydroxy Mannose 4-28

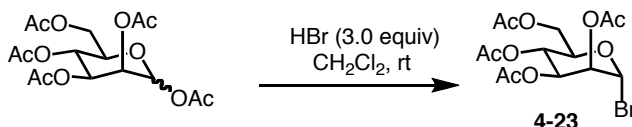
α/β-D-Mannose pentaacetate



D-(+)-mannose (5.0 g, 27.8 mmol) and I₂ (247 mg, 0.973 mmol) were added to a flask and backfilled with N₂ before being cooled to 0 °C. Ac₂O (25 mL, 1.1 M) was added via syringe. The reaction was allowed to stir overnight gradually warming to room temperature. 50 mL Na₂S₂O₃

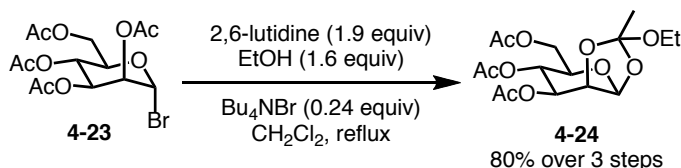
was added. The reaction was extracted 3x50 mL CH₂Cl₂. The combined organic layers were dried over MgSO₄ and filtered. The solvent was removed *in vacuo* and the crude material was used without further purification.

(2*R*,3*R*,4*S*,5*S*,6*R*)-2-(acetoxymethyl)-6-bromotetrahydro-2*H*-pyran-3,4,5-triyl triacetate (4-23)



α/β -D-Mannose pentaacetate (10.8 g, 27.8 mmol) was dissolved in CH₂Cl₂ (28 mL, 1.0 M). HBr (20 mL, 83.4 mmol, 33% weight in AcOH) was carefully added. The flask was capped with a septum and a balloon. The reaction was allowed to stir at room temperature for 4 h. The reaction was poured over ice. After ~5 minutes, the reaction was diluted with 200 mL CH₂Cl₂. Saturated NaHCO₃ was carefully added until gas formation ceased. The reaction continued to stir for 30 minutes. The layers were separated. The aqueous layer was washed 2x200 mL CH₂Cl₂. The combined organic layers were washed 2x200 mL saturated NaHCO₃, dried over MgSO₄ and filtered. The solvent was removed *in vacuo* and the crude material was used without further purification.

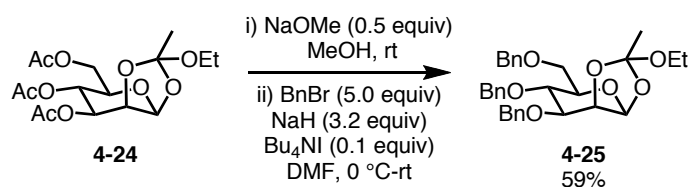
(3*aS*,5*R*,6*R*,7*S*,7*aS*)-5-(acetoxymethyl)-2-ethoxy-2-methyltetrahydro-3*aH*-[1,3]dioxolo[4,5-*b*]pyran-6,7-diyl diacetate (4-24)



CH₂Cl₂ (140 mL, 0.2 M) was added via syringe to a stirring solution of **4-23** (11.4 g, 27.8 mmol) and tetrabutyl ammonium bromide (2.2 g 6.7 mmol). Distilled 2,6-lutidine (6.1 mL, 52.8 mmol)

and dry ethanol (2.6 mL, 44.5 mmol) were added via syringe. The reaction was heated to reflux and allowed to stir overnight. The reaction was cooled to room temperature and diluted with 200 mL CH₂Cl₂. The reaction was washed 2x200 mL water, 1x200 mL saturated NaHCO₃, dried over MgSO₄, and filtered. The solvent was removed *in vacuo* and the crude residue was recrystallized from CH₂Cl₂/pentanes affording a white crystalline solid (8.35 g, 22.2 mmol, 80%). ¹H NMR (700 MHz, CDCl₃): δ 5.30 (d, *J* = 2.5 Hz, 1H), 5.03 (t, *J* = 9.7 Hz, 1H), 4.96 (dd, *J* = 9.9, 3.9 Hz, 1H), 4.35 (dd, *J* = 4.0, 2.5 Hz, 1H), 4.00 (dd, *J* = 12.2, 4.7 Hz, 1H), 3.89 (dd, *J* = 12.2, 2.6 Hz, 1H), 3.53 – 3.48 (m, 1H), 3.37 – 3.22 (m, 2H), 1.87 (s, 3H), 1.83 (s, 3H), 1.81 (s, 3H), 1.49 (s, 3H), 0.93 (t, *J* = 7.1 Hz, 3H). ¹³C NMR (176 MHz, CDCl₃): δ 169.98, 169.72, 168.93, 123.76, 96.89, 76.25, 70.61, 70.16, 65.17, 61.77, 57.36, 24.53, 20.18, 20.14, 20.12, 14.56. HRMS (ESI) (*m/z*): [M+Na⁺] calculated for NaC₁₆H₂₄O₁₀, 399.1262 found, 399.1261.

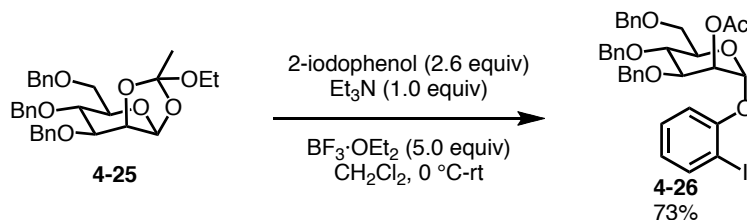
(3a*S*,5*R*,6*R*,7*S*,7a*S*)-6,7-bis(benzyloxy)-5-(benzyloxymethyl)-2-ethoxy-2-methyltetrahydro-3a*H*-[1,3]dioxolo[4,5-*b*]pyran (4-25)



4-24 (10.4 g, 27.6 mmol) was added to a flask and dissolved in MeOH (276 mL, 0.1 M). NaOMe (746 mg, 13.8 mmol, 95%) was added. The reaction was allowed to stir until full conversion via TLC. The solvent was removed *in vacuo*. Bu₄NI (1.02 g, 2.76 mmol) was added and the flask was backfilled with N₂. DMF (138 mL, 0.2 M) and BnBr (16.4 mL, 138 mmol) were added via syringe. The flask was cooled to 0 °C. NaH (3.2 g, 88.3 mmol, 95%) was added slowly under a stream of N₂. The reaction was allowed to stir for 4 h gradually warming to room temperature.

20 mL MeOH was added to quench the reaction. 200 mL NaHCO₃ was added and the reaction was allowed to stir an additional 30 minutes at room temperature. The reaction was extracted 3x200 mL Et₂O. The combined organic layers were washed 5x200 mL brine, dried over MgSO₄ and filtered. The solvent was removed *in vacuo*. The crude residue was purified via flash chromatography (80:20-70:30 hexanes: EtOAc) then recrystallized from dichloromethane/pentanes to afford the desired product (8.51 g, 16.3 mmol, 59%). ¹H NMR (700 MHz, CDCl₃): δ 7.42 – 7.37 (m, 2H), 7.35 – 7.25 (m, 10H), 7.25 – 7.23 (m, 2H), 5.33 (d, *J* = 2.5 Hz, 1H), 4.90 (d, *J* = 10.8 Hz, 1H), 4.81 – 4.74 (m, 2H), 4.62 (d, *J* = 1.9 Hz, 1H), 4.60 (d, *J* = 3.3 Hz, 1H), 4.56 (s, 1H), 4.54 (s, 1H), 4.38 (dd, *J* = 4.0, 2.6 Hz, 1H), 3.92 (t, *J* = 9.3 Hz, 1H), 3.77 – 3.68 (m, 3H), 3.61 – 3.51 (m, 2H), 3.42 (ddd, *J* = 9.5, 4.6, 2.2 Hz, 1H), 1.75 (s, 3H), 1.22 (t, *J* = 7.0 Hz, 3H). ¹³C NMR (176 MHz, CDCl₃): δ 138.33, 137.95, 128.57, 128.47, 128.37, 128.13, 128.11, 128.05, 127.83, 127.60, 127.57, 123.81, 97.59, 79.13, 76.98, 75.31, 74.34, 74.26, 73.44, 72.46, 69.12, 58.02, 24.82, 15.34. HRMS (ESI) (*m/z*): [M+NH₄⁺] calculated for C₃₁H₄₀NO₇, 538.2799 found, 538.2794.

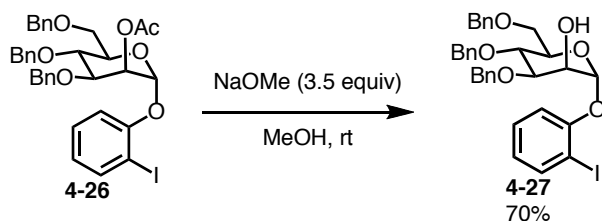
(2*R*,3*S*,4*S*,5*S*,6*R*)-4,5-bis(benzyloxy)-6-(benzyloxymethyl)-2-(2-iodophenoxy)tetrahydro-2*H*-pyran-3-yl acetate (4-26)



4-25 (1.0 g, 1.92 mmol) and 2-iodophenol (1.1 g, 4.99 mmol) were added to a flask before being backfilled 2xN₂. CH₂Cl₂ (13 mL, 0.15 M) and distilled Et₃N (0.27 mL, 1.92 mmol) were added via syringe. The reaction was allowed to stir at room temperature for 20 minutes before being cooled to 0 °C. BF₃·OEt₂ (1.2 mL, 9.6 mmol) was added dropwise via syringe. The reaction was

allowed to stir gradually warming to room temperature. After full conversion via mass spectroscopy Et₃N was added to quench the reaction. The solvent was removed in vacuo. The reaction was filtered through silica gel, eluting with 50% v/v EtOAc/hexanes. The solvent was removed *in vacuo*. The crude material was purified via flash chromatography, Biotage (100% hexanes-80:20 hexanes: EtOAc) to afford product that was used without further purification (988 mg, 1.42 mmol, 73%). **¹H NMR (700 MHz, CDCl₃):** δ 7.75 (dd, J = 7.8, 1.4 Hz, 1H), 7.40 (d, J = 7.4 Hz, 2H), 7.35 – 7.24 (m, 12H), 7.19 (d, J = 7.2 Hz, 2H), 7.13 (d, J = 8.2 Hz, 1H), 6.77 (t, J = 7.6 Hz, 1H), 5.59 (d, J = 11.9 Hz, 2H), 4.92 (d, J = 10.8 Hz, 1H), 4.80 (d, J = 11.4 Hz, 1H), 4.67 (dd, J = 18.4, 11.7 Hz, 2H), 4.53 (d, J = 10.7 Hz, 1H), 4.45 (d, J = 12.0 Hz, 1H), 4.34 (dd, J = 9.5, 3.2 Hz, 1H), 4.06 (t, J = 9.7 Hz, 1H), 3.92 – 3.88 (m, 1H), 3.81 (dd, J = 11.0, 4.2 Hz, 1H), 3.66 (dd, J = 11.0, 1.8 Hz, 1H), 2.21 (s, 3H). **¹³C NMR (176 MHz, CDCl₃):** δ 170.44, 154.87, 139.45, 138.39, 138.14, 137.82, 129.62, 128.56, 128.43, 128.39, 128.37, 128.36, 127.94, 127.82, 127.72, 127.67, 124.29, 114.96, 96.73, 87.15, 77.51, 75.27, 74.06, 73.41, 72.61, 72.12, 68.78, 68.61, 21.18. **HRMS (ESI) (m/z):** [M+Na⁺] calculated for NaC₃₅H₃₅IO₇, 717.1320 found, 717.1313.

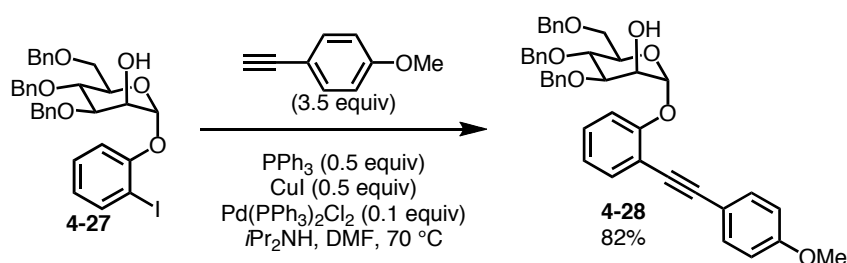
(2*R*,3*S*,4*R*,5*S*,6*R*)-4,5-bis(benzyloxy)-6-(benzyloxymethyl)-2-(2-iodophenoxy)tetrahydro-2H-pyran-3-ol (4-27)



4-26 (1.72 g, 2.49 mmol) was added to a flask and dissolved in MeOH (25 mL, 0.1 M). NaOMe (471 mg, 8.72 mmol, 95%) was added to the reaction. The reaction was allowed to stir at room temperature until full conversion of starting material was seen by TLC. The reaction was diluted

with 100 mL sat. NH_4Cl and acidified to pH=3 with 2 M HCl. The reaction was extracted 3x75 mL EtOAc. The combined organic layers were dried over Na_2SO_4 and filtered. The solvent was removed *in vacuo*. The reaction was purified via flash chromatography, Biotage (95:5-70:30 hexanes: EtOAc) to afford the desired product (1.10 g, 1.69 mmol, 70%). $^1\text{H NMR}$ (700 MHz, CDCl_3): δ 7.71 – 7.66 (m, 1H), 7.37 (dd, $J = 7.4, 1.9$ Hz, 2H), 7.31 (t, $J = 7.6, 1.9$ Hz, 2H), 7.28 – 7.18 (m, 9H), 7.17 – 7.13 (m, 4H), 6.71 (t, $J = 7.5$ Hz, 1H), 5.57 (s, 1H), 4.82 (d, $J = 10.4$ Hz, 1H), 4.77 – 4.70 (m, 3H), 4.56 (d, $J = 11.7$ Hz, 1H), 4.51 (d, $J = 10.1$ Hz, 1H), 4.40 (d, $J = 11.5$ Hz, 1H), 4.21 – 4.18 (m, 1H), 4.18 – 4.13 (m, 1H), 3.96 (t, $J = 9.2$ Hz, 1H), 3.85 – 3.79 (m, 1H), 3.71 (dt, $J = 11.0, 3.0$ Hz, 1H), 3.59 (d, $J = 10.6$ Hz, 1H). $^{13}\text{C NMR}$ (176 MHz, CDCl_3): δ 155.02, 139.34, 138.34, 138.17, 137.83, 129.65, 128.68, 128.40, 128.34, 128.27, 128.13, 127.98, 127.88, 127.75, 127.61, 124.12, 115.28, 98.30, 87.26, 79.54, 75.21, 74.01, 73.39, 72.44, 72.29, 68.70, 68.51. HRMS (ESI) (m/z): $[\text{M}+\text{Na}^+]$ calculated for $\text{NaC}_{33}\text{H}_{33}\text{IO}_6$, 675.1214 found, 675.1209.

(2R,3S,4R,5S,6R)-4,5-bis(benzyloxy)-6-(benzyloxymethyl)-2-(2-((4-methoxyphenyl)ethynyl)phenoxy)tetrahydro-2H-pyran-3-ol (4-28)

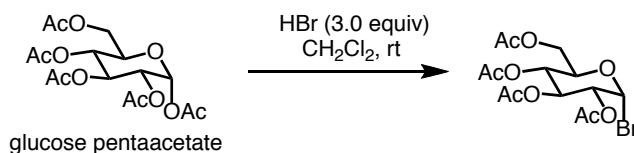


Following a modified procedure,¹⁶⁶ **4-27** (1.1 g, 1.69 mmol), *para*-methoxyphenylacetylene (780 mg, 5.90 mmol), $\text{Pd}(\text{PPh}_3)_2\text{Cl}_2$ (119 mg, 0.169 mmol), CuI (161 mg, 0.845 mmol), and PPh_3 (222 mg, 0.845 mmol) were added to a 2-neck round bottom flask with reflux condenser before being back filled $2\times\text{N}_2$. DMF (28 mL, 0.06 M) and distilled $i\text{Pr}_2\text{NH}$ (47 mL, 0.036 M) were added via syringe. The reaction was heated to 70 °C and allowed to stir overnight. The reaction

was cooled to room temperature and 60 mL saturated NH_4Cl was added. The reaction was extracted 3x60 mL EtOAc. The combined organic layers were washed 2x60 mL H_2O , 5x 60 mL brine, dried over Na_2SO_4 and filtered. The solvent was removed *in vacuo*. The reaction was filtered through silica gel, eluting with 50% v/v EtOAc/hexanes. The solvent was removed *in vacuo*. The reaction was purified via flash chromatography, Biotage (97:3-70:30 hexanes: EtOAc) to afford the desired product (909 mg, 1.38 mmol, 82%). **^1H NMR (700 MHz, CDCl_3):** δ 7.55 (d, $J = 8.3$ Hz, 3H), 7.40 – 7.28 (m, 14H), 7.26 (t, $J = 8.1$ Hz, 3H), 7.07 (t, $J = 7.4$ Hz, 1H), 6.73 (d, $J = 8.4$ Hz, 2H), 5.88 (s, 1H), 4.93 (d, $J = 10.8$ Hz, 1H), 4.78 – 4.70 (m, 2H), 4.68 (d, $J = 12.0$ Hz, 1H), 4.62 (d, $J = 10.8$ Hz, 1H), 4.48 (d, $J = 12.0$ Hz, 1H), 4.40 (s, 1H), 4.34 (dd, $J = 9.3, 3.2$ Hz, 1H), 4.25 (dd, $J = 10.3, 2.7$ Hz, 2H), 4.12 (t, $J = 9.6$ Hz, 1H), 3.87 (dd, $J = 11.1, 4.3$ Hz, 1H), 3.78 (s, 3H), 3.72 (dd, $J = 11.2, 1.9$ Hz, 1H), 3.00 (s, 1H). **^{13}C NMR (176 MHz, CDCl_3):** δ 159.52, 156.14, 138.46, 138.09, 137.95, 132.97, 132.93, 129.31, 128.43, 128.22, 127.87, 127.84, 127.81, 127.79, 127.70, 127.50, 127.48, 122.43, 115.81, 115.37, 114.73, 113.91, 97.90, 93.76, 84.03, 80.41, 75.03, 74.07, 73.17, 72.26, 72.12, 68.60, 68.29, 55.19. **HRMS (ESI) (m/z):** $[\text{M}+\text{NH}_4^+]$ calculated for $\text{C}_{42}\text{H}_{37}\text{NO}_7$, 674.3112 found, 674.3104.

6.3.2 Synthesis of 2-Hydroxy Glucose Sugar 4-36 and 4-38

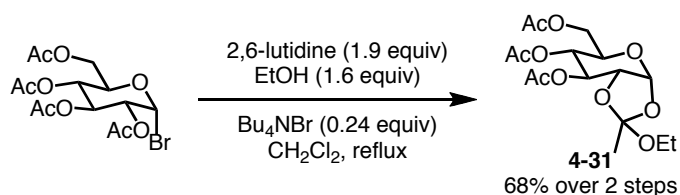
(2R,3R,4S,5R,6R)-2-(acetoxymethyl)-6-bromotetrahydro-2H-pyran-3,4,5-triyl triacetate



β -D-glucose pentaacetate (10.8 g, 27.8 mmol) was dissolved in CH_2Cl_2 (28 mL, 1.0 M). HBr (20 mL, 83.4 mmol, 33% weight in AcOH) was carefully added. The flask was capped with a septum and a balloon. The reaction was allowed to stir at room temperature for 4 h. The reaction was

poured over ice. After ~5 minutes, the reaction was diluted with 200 mL CH₂Cl₂. Saturated NaHCO₃ was carefully added until gas formation ceased. The reaction continued to stir for 30 minutes. The layers were separated. The aqueous layer was washed 2x200 mL CH₂Cl₂. The combined organic layers were washed 2x200 mL saturated NaHCO₃, dried over MgSO₄ and filtered. The solvent was removed *in vacuo* and the crude material was used without further purification.

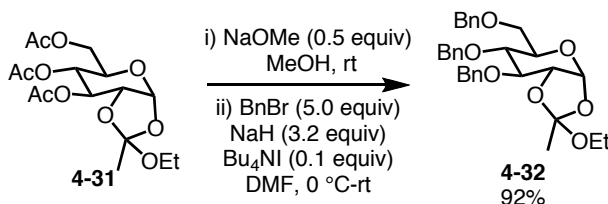
(3aR,5R,6R,7S,7aR)-5-(acetoxymethyl)-2-ethoxy-2-methyltetrahydro-3aH-[1,3]dioxolo[4,5-b]pyran-6,7-diyl diacetate (4-31)



CH₂Cl₂ (140 mL, 0.2 M) was added via syringe to a stirring solution of (2R,3R,4S,5R,6R)-2-(acetoxymethyl)-6-bromotetrahydro-2H-pyran-3,4,5-triyl triacetate (11.4 g, 27.8 mmol) and tetrabutyl ammonium bromide (2.2 g 6.7 mmol). Distilled 2,6-lutidine (6.1 mL, 52.8 mmol) and dry ethanol (2.6 mL, 44.5 mmol) were added via syringe. The reaction was heated to reflux and allowed to stir overnight. The reaction was cooled to room temperature and diluted with 200 mL CH₂Cl₂. The reaction was washed 2x200 mL water, 1x200 mL saturated NaHCO₃, dried over MgSO₄, and filtered. The solvent was removed *in vacuo* and the crude residue was recrystallized from CH₂Cl₂/pentanes affording a white crystalline solid that was used without further purification (7.03 g, 18.7 mmol, 68%). ¹H NMR (700 MHz, CDCl₃): δ 5.70 (d, *J* = 5.2 Hz, 1H), 5.17 (t, *J* = 2.8 Hz, 1H), 4.92 – 4.83 (m, 1H), 4.34 – 4.28 (m, 1H), 4.22 – 4.14 (m, 2H), 3.95 – 3.91 (m, 1H), 3.55 – 3.47 (m, 2H), 2.09 (s, 3H), 2.08 (s, 3H), 2.07 (s, 3H), 1.70 (s, 2H), 1.16 (t, *J* = 7.1 Hz, 3H). ¹³C NMR (176 MHz, CDCl₃): δ 170.67, 169.64, 169.16, 121.24, 96.88, 73.04,

70.12, 68.21, 66.92, 63.06, 59.16, 20.79, 20.78, 20.75, 20.74, 15.26. HRMS (ESI) (m/z): [M+Na⁺] calculated for NaC₁₆H₂₄O₁₀, 399.1262 found, 399.1266.

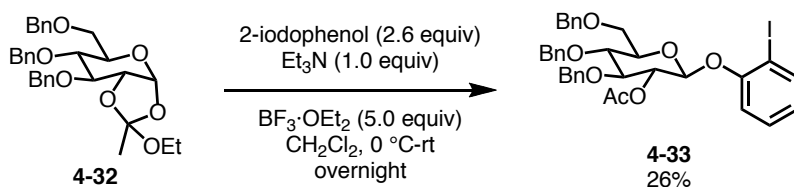
(3aR,5R,6R,7S,7aR)-6,7-bis(benzyloxy)-5-(benzyloxymethyl)-2-ethoxy-2-methyltetrahydro-3aH-[1,3]dioxolo[4,5-b]pyran (4-32)



4-31 (7.0 g, 18.6 mmol) was added to a flask and dissolved in MeOH (186 mL, 0.1 M). NaOMe (502 mg, 9.3 mmol, 95%) was added. The reaction was allowed to stir until full conversion via TLC. The solvent was removed *in vacuo*. Bu₄NI (687 mg, 1.86 mmol) was added and the flask was backfilled with N₂. DMF (93 mL, 0.2 M) and BnBr (11.0 mL, 93.0 mmol) were added via syringe. The flask was cooled to 0 °C. NaH (2.2 g, 59.5 mmol, 95%) was added slowly under a stream of N₂. The reaction was allowed to stir for 4 h gradually warming to room temperature. 15 mL MeOH was added to quench the reaction. 200 mL NaHCO₃ was added and the reaction was allowed to stir an additional 30 minutes at room temperature. The reaction was extracted 3x150 mL Et₂O. The combined organic layers were washed 5x200 mL brine, dried over MgSO₄ and filtered. The solvent was removed *in vacuo*. The crude residue was purified via flash chromatography (80:20-hexanes: EtOAc) to afford the desired product that was used without further purification (9.2 g, 17.7 mmol, 95%). ¹H NMR (500 MHz, CDCl₃): δ 7.41 – 7.24 (m, 13H), 7.18 (dd, *J* = 7.4, 2.2 Hz, 2H), 5.77 (d, *J* = 5.2 Hz, 1H), 4.73 – 4.69 (m, 1H), 4.59 (dd, *J* = 12.0, 9.0 Hz, 4H), 4.53 – 4.48 (m, 2H), 4.43 – 4.39 (m, 2H), 3.88 (t, *J* = 4.0 Hz, 1H), 3.79 (dt, *J* = 9.5, 3.1 Hz, 1H), 3.71 (dd, *J* = 9.5, 4.6 Hz, 1H), 3.66 (t, *J* = 3.7 Hz, 2H), 3.59 – 3.50 (m, 2H), 1.67 (d, *J* = 2.3 Hz, 3H), 1.20 (t, *J* = 7.1 Hz, 4H). ¹³C NMR (126 MHz, CDCl₃): δ 138.19,

138.03, 137.83, 129.10, 128.87, 128.52, 128.49, 128.47, 128.42, 128.41, 128.10, 128.08, 127.96, 127.92, 127.85, 127.80, 127.72, 127.67, 121.05, 97.87, 78.93, 75.89, 75.01, 73.49, 73.03, 72.00, 70.57, 69.22, 58.77, 21.95, 15.43. **HRMS (ESI) (m/z):** $[M+Na^+]$ calculated for $NaC_{31}H_{36}O_7$, 543.2353 found, 543.2350.

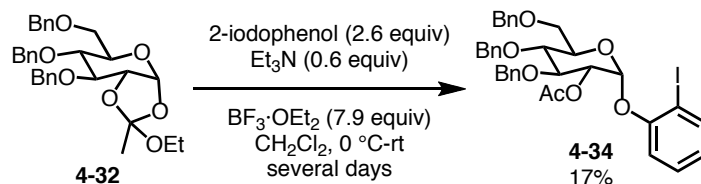
(2*S*,3*R*,4*S*,5*R*,6*R*)-4,5-bis(benzyloxy)-6-(benzyloxymethyl)-2-(2-iodophenoxy)tetrahydro-2*H*-pyran-3-yl acetate (4-33)



4-32 (1.0 g, 1.92 mmol) and 2-iodophenol (1.1 g, 4.99 mmol) were added to a flask before being backfilled $2 \times N_2$. CH_2Cl_2 (13 mL, 0.15 M) and distilled Et_3N (0.27 mL, 1.92 mmol) were added via syringe. The reaction was allowed to stir at room temperature for 20 minutes before being cooled to 0 °C. $BF_3 \cdot OEt_2$ (1.2 mL, 9.6 mmol) was added dropwise via syringe. The reaction was allowed to stir gradually warming to room temperature overnight. Et_3N was added to quench the reaction. The solvent was removed *in vacuo*. The reaction was filtered through silica gel, eluting with 50% v/v $EtOAc$ /hexanes. The solvent was removed *in vacuo*. The crude material was purified via flash chromatography, Biotage (97:3 hexanes: $EtOAc$ -70:30 hexanes: $EtOAc$) followed by recrystallization from CH_2Cl_2 /pentane to afford the desired product (320 mg, 0.49 mmol, 26%). **1H NMR (700 MHz, $CDCl_3$):** 7.73 (dd, $J = 7.8, 1.5$ Hz, 1H), 7.34 – 7.25 (m, 12H), 7.20 (d, $J = 7.5$ Hz, 3H), 7.10 (d, $J = 8.2$ Hz, 1H), 6.76 (t, $J = 7.5$ Hz, 1H), 5.37 (t, $J = 8.5$ Hz, 1H), 4.90 (d, $J = 7.9$ Hz, 1H), 4.81 (dd, $J = 11.1, 4.7$ Hz, 2H), 4.70 (d, $J = 11.4$ Hz, 1H), 4.61 – 4.56 (m, 2H), 4.53 (d, $J = 12.0$ Hz, 1H), 3.82 – 3.71 (m, 4H), 3.71 – 3.63 (m, 2H), 2.01 (s, 3H). **^{13}C NMR (176 MHz, $CDCl_3$):** δ 169.45, 156.47, 139.55, 138.10, 138.07, 137.81, 129.64,

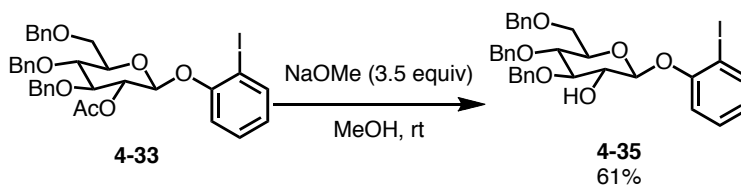
128.57, 128.55, 128.46, 128.13, 128.05, 128.03, 127.91, 127.77, 127.73, 124.55, 116.01, 100.09, 86.86, 82.88, 77.88, 75.69, 75.21, 75.18, 73.64, 72.38, 68.83, 21.60. HRMS (ESI) (m/z): [M+Na⁺] calculated for NaC₃₅H₃₅IO₇, 717.1320 found, 717.1310.

(2R,3R,4S,5R,6R)-4,5-bis(benzyloxy)-6-(benzyloxymethyl)-2-(2-iodophenoxy)tetrahydro-2H-pyran-3-yl acetate (4-34)



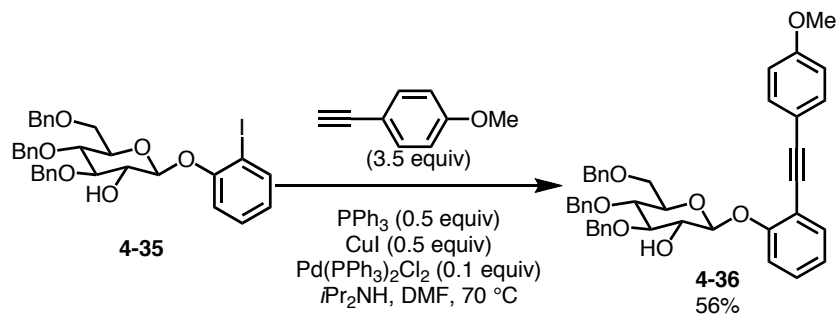
4-32 (7.9 g, 15.2 mmol) and 2-iodophenol (6.7 g, 430.4 mmol) were added to a flask before being backfilled 2xN₂. CH₂Cl₂ (100 mL, 0.15 M) and distilled Et₃N (1.34 mL, 9.6 mmol) were added via syringe. The reaction was allowed to stir at room temperature for 20 minutes before being cooled to 0 °C. BF₃·OEt₂ (14.9 mL, 120 mmol) was added dropwise via syringe. The reaction was allowed to stir gradually warming to room temperature for several days. Et₃N was added to quench the reaction. The solvent was removed *in vacuo*. The reaction was filtered through silica gel, eluting with 50% v/v EtOAc/hexanes. The solvent was removed *in vacuo*. The crude material was purified via flash chromatography (97:3 hexanes-70:30 hexanes: EtOAc) to afford the desired product that was used with out further purification (1.76 mg, 2.53 mmol, 17%).

(2S,3R,4S,5R,6R)-4,5-bis(benzyloxy)-6-(benzyloxymethyl)-2-(2-iodophenoxy)tetrahydro-2H-pyran-3-ol (4-35)



4-33 (320 mg, 0.46 mmol) was added to a flask and dissolved in MeOH (4.6 mL, 0.1 M) and THF (1.0 mL). NaOMe (87 mg, 1.61 mmol, 95%) was added to the reaction. The reaction was allowed to stir at room temperature until full conversion of starting material was seen by TLC. The reaction was diluted with 10 mL sat. NH₄Cl and acidified to pH=3 with 2 M HCl. The reaction was extracted 3x10 mL CH₂Cl₂. The combined organic layers were dried over MgSO₄ and filtered. The solvent was removed *in vacuo*. The crude material was purified recrystallization from CH₂Cl₂/pentanes (184 mg, 0.28 mmol, 61%). ¹H NMR (700 MHz, CDCl₃): δ 7.77 (d, *J* = 7.9 Hz, 1H), 7.42 (d, *J* = 7.5 Hz, 2H), 7.38 – 7.27 (m, 10H), 7.26 (d, *J* = 6.6 Hz, 1H), 7.24 – 7.19 (m, 3H), 6.83 (t, *J* = 7.5 Hz, 1H), 5.05 (d, *J* = 11.2 Hz, 1H), 4.89 (dd, *J* = 22.3, 11.0 Hz, 2H), 4.80 (d, *J* = 7.7 Hz, 1H), 4.66 – 4.55 (m, 3H), 3.98 (t, *J* = 8.2 Hz, 1H), 3.83 (d, *J* = 10.7 Hz, 1H), 3.76 – 3.64 (m, 5H), 2.82 – 2.78 (m, 1H). ¹³C NMR (176 MHz, CDCl₃): δ 156.28, 139.16, 138.63, 138.15, 138.07, 129.95, 128.51, 128.46, 128.40, 128.08, 128.07, 127.92, 127.80, 127.73, 124.94, 116.85, 103.00, 87.76, 84.01, 75.64, 75.32, 75.22, 74.93, 73.60, 68.97. HRMS (ESI) (*m/z*): [M+Na⁺] calculated for NaC₃₃H₃₃O₇, 675.1214 found, 675.1204.

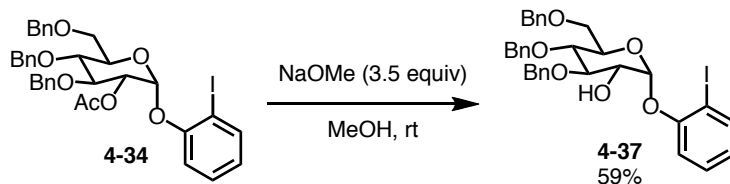
(2*S*,3*R*,4*S*,5*R*,6*R*)-4,5-bis(benzyloxy)-6-(benzyloxymethyl)-2-(2-((4-methoxyphenyl)ethynyl)phenoxy)tetrahydro-2*H*-pyran-3-ol (4-36)



Following a modified procedure,¹⁶⁶ **4-35** (503 mg, 0.77 mmol), *para*-methoxyphenylacetylene (357 mg, 2.7 mmol), Pd(PPh₃)₂Cl₂ (54 mg, 0.077 mmol), CuI (73 mg, 0.385 mmol), and PPh₃ (101 mg, 0.385 mmol) were added to a 2-neck round bottom flask with reflux condenser before

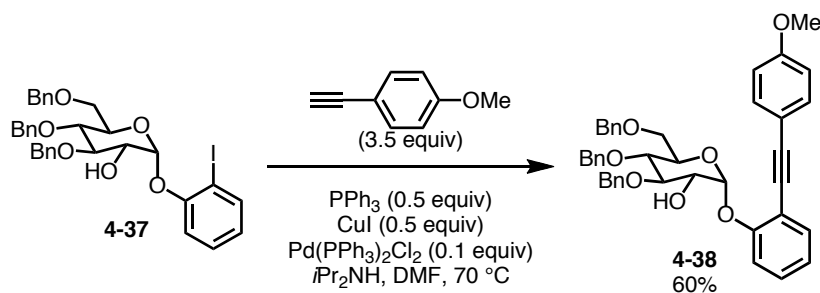
being back filled 2xN₂. DMF (13 mL, 0.06 M) and distilled *i*Pr₂NH (21 mL, 0.036 M) were added via syringe. The reaction was heated to 70 °C and allowed to stir overnight. The reaction was cooled to room temperature and 50 mL saturated NH₄Cl was added. The reaction was extracted 3x30 mL EtOAc. The combined organic layers were washed 2x50 mL H₂O, 5x 50 mL brine, dried over Na₂SO₄ and filtered. The solvent was removed *in vacuo*. The reaction was filtered through silica gel, eluting with 50% v/v EtOAc/hexanes. The solvent was removed *in vacuo*. The reaction was purified via flash chromatography, Biotage (100% hexanes-80:20 hexanes: EtOAc) to afford the desired product (281 mg, 0.43 mmol, 56%). ¹H NMR (700 MHz, CDCl₃): δ 7.49 (d, *J* = 8.0 Hz, 3H), 7.41 (d, *J* = 7.5 Hz, 2H), 7.36 – 7.24 (m, 13H), 7.21 (d, *J* = 7.3 Hz, 2H), 7.09 – 7.05 (m, 1H), 6.89 (d, *J* = 8.4 Hz, 2H), 5.04 (d, *J* = 11.2 Hz, 1H), 4.89 (d, *J* = 10.8 Hz, 1H), 4.85 (d, *J* = 11.3 Hz, 1H), 4.82 (d, *J* = 7.8 Hz, 1H), 4.63 (d, *J* = 12.1 Hz, 1H), 4.58 (dd, *J* = 13.8, 11.5 Hz, 2H), 3.94 (t, *J* = 8.0 Hz, 1H), 3.82 (d, *J* = 18.2 Hz, 4H), 3.75 (dd, *J* = 11.0, 5.2 Hz, 1H), 3.71 (dd, *J* = 10.7, 6.2 Hz, 2H), 3.66 – 3.61 (m, 1H), 2.99 (s, 1H). (176 MHz, CDCl₃): δ 159.87, 157.56, 138.74, 138.24, 138.15, 133.18, 132.98, 129.58, 128.47, 128.45, 128.43, 128.09, 128.05, 127.86, 127.79, 127.71, 127.68, 123.53, 118.13, 115.17, 115.16, 114.17, 103.17, 94.32, 84.18, 84.00, 75.65, 75.20, 75.18, 75.08, 73.57, 68.95, 55.41, 17.16, 17.13, 13.12. HRMS (ESI) (*m/z*): [M+Na⁺] calculated for NaC₄₂H₄₀O₇, 679.2666 found, 679.2662.

(2*R*,3*R*,4*R*,5*S*,6*R*)-4,5-bis(benzyloxy)-6-(benzyloxymethyl)-2-(2-iodophenoxy)tetrahydro-2*H*-pyran-3-ol (4-37)



4-34 (1.76 g, 2.53 mmol) was added to a flask and dissolved in MeOH (25 mL, 0.1 M) and THF (2.0 mL). NaOMe (479 mg, 8.87 mmol, 95%) was added to the reaction. The reaction was allowed to stir at room temperature until full conversion of reaction was seen by TLC. The reaction was diluted with 50 mL sat. NH₄Cl and acidified to pH=3 with 2 M HCl. The reaction was extracted 3x30 mL EtOAc. The combined organic layers were dried over MgSO₄ and filtered. The solvent was removed *in vacuo*. The crude material was purified via flash chromatography, Biotage (95:5-70:30 hexanes:EtOAc) to afford the desired product (975 mg, 1.50 mmol, 59%). ¹H NMR (700 MHz, CDCl₃): δ 7.73 (dd, *J* = 7.8, 1.5 Hz, 1H), 7.43 (d, *J* = 7.2 Hz, 2H), 7.34 (dd, *J* = 8.2, 6.8 Hz, 2H), 7.32 – 7.19 (m, 8H), 7.19 – 7.15 (m, 2H), 6.79 (td, *J* = 7.5, 1.6 Hz, 1H), 5.54 (d, *J* = 3.7 Hz, 1H), 5.03 (d, *J* = 11.2 Hz, 1H), 4.92 (d, *J* = 11.1 Hz, 1H), 4.88 (d, *J* = 10.8 Hz, 1H), 4.61 (d, *J* = 12.0 Hz, 1H), 4.54 (d, *J* = 10.7 Hz, 1H), 4.46 (d, *J* = 12.0 Hz, 1H), 4.04 (t, *J* = 9.2 Hz, 1H), 3.91 (ddd, *J* = 10.1, 3.8, 2.1 Hz, 1H), 3.84 (td, *J* = 10.0, 3.7 Hz, 1H), 3.79 – 3.75 (m, 2H), 3.64 (dd, *J* = 10.8, 2.0 Hz, 1H), 2.30 (d, *J* = 10.7 Hz, 1H). ¹³C NMR (176 MHz, CDCl₃): δ 155.30, 139.13, 138.57, 138.18, 137.84, 129.95, 128.53, 128.52, 128.46, 128.46, 128.39, 127.97, 127.94, 127.92, 127.85, 127.83, 127.82, 124.51, 115.46, 99.40, 87.48, 82.84, 75.47, 75.19, 73.55, 73.17, 71.74, 68.35. HRMS (ESI) (*m/z*): [M+Na⁺] calculated for NaC₃₃H₃₃IO₆, 675.1214 found, 675.1206.

(2*R*,3*R*,4*R*,5*S*,6*R*)-4,5-bis(benzyloxy)-6-(benzyloxymethyl)-2-(2-((4-methoxyphenyl)ethynyl)phenoxy)tetrahydro-2*H*-pyran-3-ol (4-37)



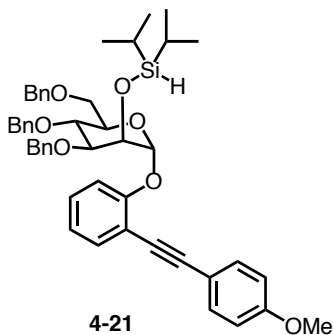
Following a modified procedure¹⁶⁶, **4-36** (900 mg, 1.38 mmol), *para*-methoxyphenylacetylene (638 mg, 4.83 mmol), Pd(PPh₃)₂Cl₂ (97 mg, 0.138 mmol), CuI (131 mg, 0.690 mmol), and PPh₃ (181 mg, 0.690 mmol) were added to a 2-neck round bottom flask with reflux condenser before being back filled 2xN₂. DMF (23 mL, 0.06 M) and distilled *i*Pr₂NH (38 mL, 0.036 M) were added via syringe. The reaction was heated to 70 °C and allowed to stir overnight. The reaction was cooled to room temperature and 100 mL saturated NH₄Cl was added. The reaction was extracted 3x50 mL EtOAc. The combined organic layers were washed 2x50 mL H₂O, 5x 50 mL brine, dried over Na₂SO₄ and filtered. The solvent was removed *in vacuo*. The reaction was filtered through silica gel, eluting with 50% v/v EtOAc/hexanes. The solvent was removed *in vacuo*. The reaction was purified via flash chromatography, Biotage (95:5-70:30 hexanes: EtOAc) to afford the desired product (546 mg, 0.83 mmol, 60%). **¹H NMR (700 MHz, CDCl₃):** δ 7.50 (t, *J* = 9.0 Hz, 3H), 7.36 (d, *J* = 7.8 Hz, 2H), 7.34 – 7.25 (m, 13H), 7.18 – 7.14 (m, 2H), 7.07 (ddt, *J* = 8.0, 5.5, 2.2 Hz, 1H), 6.77 – 6.72 (m, 2H), 5.65 – 5.57 (m, 1H), 4.97 (d, *J* = 11.0 Hz, 1H), 4.87 (d, *J* = 10.6 Hz, 1H), 4.81 (d, *J* = 11.1 Hz, 1H), 4.64 (dd, *J* = 12.0, 1.5 Hz, 1H), 4.54 (d, *J* = 10.7 Hz, 1H), 4.48 (dd, *J* = 12.0, 1.6 Hz, 1H), 4.18 (d, *J* = 9.5 Hz, 1H), 4.07 (td, *J* = 9.2, 1.6 Hz, 1H), 3.96 – 3.89 (m, 1H), 3.82 – 3.76 (m, 2H), 3.75 (d, *J* = 1.6 Hz, 3H), 3.70 (d, *J* = 10.8 Hz, 1H), 2.68 (d, *J* = 10.5 Hz, 1H). **¹³C NMR (176 MHz, CDCl₃):** δ 159.85, 157.11, 138.82, 138.35, 137.93, 133.12, 132.81, 129.68, 128.44, 128.39, 127.95, 127.89, 127.77, 127.70, 127.66, 123.19, 116.84, 115.11, 115.03, 114.11, 99.74, 94.44, 83.97, 77.04, 75.67, 75.10, 73.52, 73.35, 71.70, 68.45, 55.35. **HRMS (ESI) (m/z):** [M+NH₄⁺] calculated for C₄₂H₄₄NO₇, 674.3112 found, 674.3060.

6.3.3 Synthesis of Sugar Silane from 2-Hydroxy Sugars

General Procedure:

Dry CH₂Cl₂ (0.2 M) was added to the prospective 2-hydroxy sugar (1.0 equiv.) under N₂. The reaction was cooled to 0 °C. Freshly distilled Et₃N (2.0 equiv.) was added dropwise via syringe. After ~5 minutes distilled R₂Si(H)Cl (1.3 equiv.) was added dropwise via syringe. The reaction was allowed to stir at 0 °C for 4 hours. Sat. NaHCO₃ was added. The reaction was extracted 3xCH₂Cl₂. The combined organic layers were washed 1xH₂O, 1xbrine, dried over MgSO₄ and filtered. The solvent was removed *in vacuo*. The material was either used as was or purified.

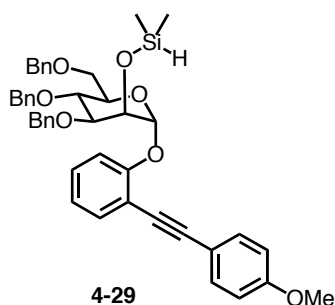
((2*R*,3*S*,4*S*,5*S*,6*R*)-4,5-bis(benzyloxy)-6-(benzyloxymethyl)-2-(2-((4-methoxyphenyl)ethynyl)phenoxy)tetrahydro-2*H*-pyran-3-yloxy)diisopropylsilane (4-21)



The title compound was prepared from **4-28** (2.85 g, 4.34 mmol), *i*Pr₂Si(H)Cl (0.96 mL, 5.64 mmol), Et₃N (1.2 mL, 8.68 mmol) in 22 mL CH₂Cl₂ by following the general procedure. The crude residue was purified via flash chromatography, Biotage (100% hexanes-90:10 hexanes: EtOAc) to afford the desired product as a white solid (2.85 g, 3.70 mmol, 85%). ¹H NMR (700 MHz, CDCl₃): δ 7.49 – 7.44 (m, 3H), 7.33 – 7.30 (m, 2H), 7.30 – 7.22 (m, 12H), 7.16 (dd, *J* = 7.2, 2.4 Hz, 2H), 7.01 (td, *J* = 7.4, 1.2 Hz, 1H), 6.68 – 6.62 (m, 2H), 5.67 (d, *J* = 2.0 Hz, 1H), 4.85 (d, *J* = 10.8 Hz, 1H), 4.75 (d, *J* = 11.4 Hz, 1H), 4.62 (d, *J* = 12.0 Hz, 1H), 4.56 (d, *J* = 11.4 Hz, 1H), 4.52 (d, *J* = 10.7 Hz, 1H), 4.45 (t, *J* = 2.4 Hz, 1H), 4.43 (d, *J* = 12.0 Hz, 1H), 4.35 (s,

1H), 4.26 (dd, $J = 8.7, 2.7$ Hz, 1H), 4.12 – 4.06 (m, 2H), 3.80 (dd, $J = 11.1, 4.1$ Hz, 1H), 3.73 (s, 3H), 3.69 (dd, $J = 11.1, 1.6$ Hz, 1H), 1.12 – 1.08 (m, 1H), 1.06 – 1.00 (m, 14H). ^{13}C NMR (176 MHz, CDCl_3): δ 159.62, 156.42, 138.69, 138.64, 138.55, 133.13, 133.06, 129.36, 128.29, 128.24, 128.23, 128.11, 127.69, 127.65, 127.63, 127.54, 127.42, 127.39, 122.39, 115.84, 115.56, 114.76, 113.99, 98.75, 93.75, 84.15, 81.07, 75.09, 74.23, 73.07, 73.04, 72.55, 71.64, 69.06, 55.35, 17.56, 17.55, 17.53, 17.42, 12.81, 12.76. HRMS (ESI) (m/z): $[\text{M}+\text{NH}_4^+]$ calculated for $\text{C}_{48}\text{H}_{58}\text{NO}_7\text{Si}$, 788.3977 found, 788.3973.

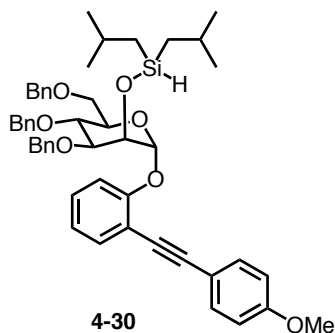
((2*R*,3*S*,4*S*,5*S*,6*R*)-4,5-bis(benzyloxy)-6-(benzyloxymethyl)-2-((4-methoxyphenyl)ethynyl)phenoxy)tetrahydro-2*H*-pyran-3-yloxy)dimethylsilane (4-29)



The title compound was prepared from **4-28** (1.06 mg, 1.61 mmol), $\text{Me}_2\text{Si}(\text{H})\text{Cl}$ (0.27 mL, 2.42 mmol), Et_3N (0.45 mL, 3.22 mmol) in 8 mL CH_2Cl_2 by following the general procedure. The crude yellow viscous oil was used as was (970 mg, 1.36 mmol, 84%). ^1H NMR (700 MHz, CDCl_3): δ 7.44 (t, $J = 8.9$ Hz, 4H), 7.31 – 7.25 (m, 9H), 7.24 – 7.21 (m, 5H), 7.18 (d, $J = 8.3$ Hz, 1H), 7.14 – 7.11 (m, 2H), 6.99 (t, $J = 7.4$ Hz, 1H), 6.64 (d, $J = 8.3$ Hz, 2H), 5.63 (s, 1H), 4.83 (d, $J = 10.7$ Hz, 1H), 4.79 – 4.76 (m, 1H), 4.71 (d, $J = 11.4$ Hz, 1H), 4.62 (d, $J = 12.1$ Hz, 1H), 4.57 (d, $J = 11.4$ Hz, 1H), 4.50 (d, $J = 10.7$ Hz, 1H), 4.40 (d, $J = 12.0$ Hz, 2H), 4.21 (dd, $J = 8.9, 2.8$ Hz, 1H), 4.07 (dd, $J = 10.0, 4.0$ Hz, 1H), 3.78 (dd, $J = 11.2, 4.3$ Hz, 1H), 3.72 – 3.69 (m, 3H), 3.66 (d, $J = 11.4$ Hz, 1H), 0.25 (d, $J = 2.7$ Hz, 3H), 0.21 (d, $J = 2.8$ Hz, 3H). ^{13}C NMR (176 MHz, CDCl_3): δ 159.64, 156.43, 138.67, 138.47, 133.11, 133.08, 133.05, 129.39, 128.62,

128.37, 128.33, 128.30, 128.28, 128.01, 127.96, 127.85, 127.82, 127.73, 127.66, 127.59, 127.54, 127.48, 122.43, 115.89, 115.53, 114.74, 114.02, 114.00, 98.85, 93.77, 84.14, 80.84, 75.06, 74.31, 73.20, 73.05, 72.81, 71.16, 68.97, 55.35, -0.42, -0.54. **HRMS (ESI) (m/z):** $[M+Na^+]$ calculated for $NaC_{44}H_{46}O_7Si$, 737.2905 found, 737.2895.

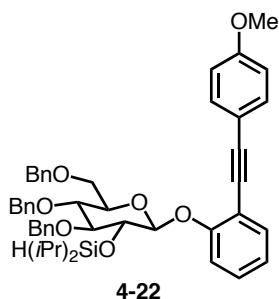
((2*R*,3*S*,4*S*,5*S*,6*R*)-4,5-bis(benzyloxy)-6-(benzyloxymethyl)-2-(2-((4-methoxyphenyl)ethynyl)phenoxy)tetrahydro-2*H*-pyran-3-yloxy)diisobutylsilane (4-30)



The title compound was prepared from **4-28** (342 mg, 0.52 mmol), $iBu_2Si(H)Cl$ (0.34 mL, 0.68 mmol), Et_3N (0.15 mL, 1.04 mmol) in 3 mL CH_2Cl_2 by following the general procedure. The crude residue was purified via flash chromatography, Biotage (97:3-70:30 hexanes: EtOAc) to afford the desired product as a colorless viscous oil (197 mg, 0.25 mmol, 47%). **1H NMR (700 MHz, $CDCl_3$):** δ 7.47 (t, $J = 7.6$ Hz, 3H), 7.33 (d, $J = 6.7$ Hz, 2H), 7.30 – 7.24 (m, 12H), 7.22 (d, $J = 8.3$ Hz, 1H), 7.17 (dd, $J = 7.3, 2.2$ Hz, 2H), 7.02 (td, $J = 7.5, 1.1$ Hz, 1H), 6.69 – 6.65 (m, 2H), 5.65 (d, $J = 2.0$ Hz, 1H), 4.86 (d, $J = 10.7$ Hz, 1H), 4.77 (p, $J = 2.6$ Hz, 1H), 4.74 (d, $J = 11.4$ Hz, 1H), 4.61 (dd, $J = 17.8, 11.7$ Hz, 2H), 4.53 (d, $J = 10.7$ Hz, 1H), 4.45 – 4.40 (m, 2H), 4.27 – 4.24 (m, 1H), 4.09 – 4.07 (m, 2H), 3.79 (dd, $J = 11.1, 3.9$ Hz, 1H), 3.74 (s, 3H), 3.71 – 3.67 (m, 1H), 1.87 (dhept, $J = 20.2, 6.7$ Hz, 2H), 0.97 – 0.91 (m, 12H), 0.79 (dddd, $J = 21.1, 14.9, 6.8, 2.7$ Hz, 2H), 0.72 (ddd, $J = 14.8, 7.3, 2.6$ Hz, 1H), 0.63 (ddd, $J = 14.9, 7.5, 2.3$ Hz, 1H). **^{13}C NMR (176 MHz, $CDCl_3$):** δ 159.62, 156.39, 138.68, 138.58, 138.51, 133.12, 133.05,

129.37, 128.30, 128.27, 128.25, 128.09, 127.73, 127.70, 127.56, 127.46, 127.42, 122.36, 115.78, 115.55, 114.73, 113.99, 98.71, 93.75, 84.15, 80.93, 75.07, 74.33, 73.11, 73.01, 72.71, 71.46, 69.01, 55.34, 26.21, 26.11, 25.98, 25.83, 25.54, 25.19, 24.55, 24.45. **HRMS (ESI) (m/z):** $[M+NH_4^+]$ calculated for $C_{50}H_{62}NO_7Si$, 816.4290 found, 816.4285.

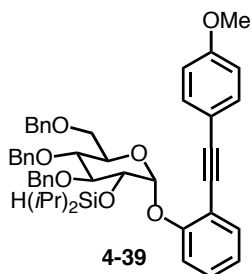
((2*S*,3*R*,4*R*,5*R*,6*R*)-4,5-bis(benzyloxy)-6-(benzyloxymethyl)-2-(2-((4-methoxyphenyl)ethynyl)phenoxy)tetrahydro-2*H*-pyran-3-yloxy)diisopropylsilane (4-22)



The title compound was prepared from **4-35** (280 mg, 0.43 mmol), $iPr_2Si(H)Cl$ (96 μL , 0.85 mmol), Et_3N (119 μL , 0.56 mmol) in 2.2 mL CH_2Cl_2 by following the general procedure. The crude residue was purified via flash chromatography, Biotage (100% hexanes-80:20 hexanes: EtOAc) to afford the desired product as light yellow viscous oil (191 mg, 0.25 mmol, 57%). **1H NMR (700 MHz, $CDCl_3$):** δ 7.50 (d, $J = 7.4$ Hz, 1H), 7.49 – 7.46 (m, 2H), 7.37 (d, $J = 7.9$ Hz, 2H), 7.34 – 7.30 (m, 2H), 7.29 – 7.23 (m, 10H), 7.17 – 7.14 (m, 2H), 7.00 – 6.96 (m, 2H), 6.84 (d, $J = 8.7$ Hz, 2H), 5.14 (td, $J = 7.3, 1.4$ Hz, 1H), 4.98 (d, $J = 11.1$ Hz, 1H), 4.87 (d, $J = 11.1$ Hz, 1H), 4.80 (d, $J = 10.8$ Hz, 1H), 4.56 (d, $J = 10.9$ Hz, 1H), 4.54 – 4.45 (m, 3H), 4.07 (t, $J = 7.3$ Hz, 1H), 3.82 (s, 3H), 3.76 (d, $J = 10.1$ Hz, 1H), 3.71 – 3.69 (m, 2H), 3.67 – 3.64 (m, 2H), 1.11 (m, 2H), 0.94 (t, $J = 6.9$ Hz, 9H), 0.88 (dd, $J = 7.4, 1.4$ Hz, 3H). **^{13}C NMR (176 MHz, $CDCl_3$):** δ 159.49, 156.79, 138.68, 138.22, 138.13, 133.79, 133.13, 129.10, 128.46, 128.35, 127.95, 127.82, 127.79, 127.70, 127.57, 127.54, 121.84, 116.16, 114.24, 114.11, 113.87, 99.80, 93.60, 86.27, 84.97, 77.83, 76.45, 75.70, 75.55, 75.01, 73.56, 68.86, 55.38, 17.61, 17.52, 17.37, 17.32,

12.65, 12.22. **HRMS (ESI) (m/z):** $[M+NH_4^+]$ calculated for $C_{48}H_{58}NO_7Si$, 788.3977 found, 788.3968.

((2R,3R,4S,5S,6R)-4,5-bis(benzyloxy)-6-(benzyloxymethyl)-2-(2-((4-methoxyphenyl)ethynyl)phenoxy)tetrahydro-2H-pyran-3-yloxy)diisopropylsilane (4-39)



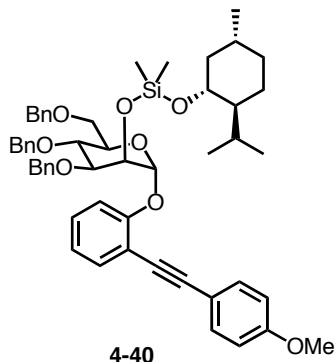
The title compound was prepared from **4-38** (546 mg, 0.83 mmol), $iPr_2Si(H)Cl$ (184 μ L, 1.66 mmol), Et_3N (234 μ L, 0.56 mmol) in 4.2 mL CH_2Cl_2 by following the general procedure. The crude residue was purified via flash chromatography, Biotage (100% hexanes-80:20 hexanes: EtOAc) to afford the desired product as a colorless viscous oil (447 mg, 6.29 mmol, 70%). 1H NMR (700 MHz, $CDCl_3$): δ 7.51 (d, $J = 8.0$ Hz, 2H), 7.47 (d, $J = 7.6$ Hz, 1H), 7.35 (d, $J = 8.0$ Hz, 2H), 7.33 – 7.22 (m, 12H), 7.19 (d, $J = 8.4$ Hz, 1H), 7.09 – 7.05 (m, 2H), 6.99 (t, $J = 7.4$ Hz, 1H), 6.65 (d, $J = 8.0$ Hz, 2H), 5.74 (d, $J = 3.3$ Hz, 1H), 4.99 (d, $J = 11.1$ Hz, 1H), 4.81 (dd, $J = 13.6, 11.2$ Hz, 2H), 4.61 (d, $J = 12.0$ Hz, 1H), 4.48 (d, $J = 10.7$ Hz, 1H), 4.41 (d, $J = 12.1$ Hz, 1H), 4.33 (s, 1H), 4.30 (td, $J = 9.3, 1.4$ Hz, 1H), 4.16 (dd, $J = 10.1, 2.5$ Hz, 1H), 4.06 (dd, $J = 9.5, 3.0$ Hz, 1H), 3.85 – 3.79 (m, 1H), 3.76 (dd, $J = 11.0, 2.9$ Hz, 1H), 3.73 (s, 3H), 3.59 (d, $J = 10.9$ Hz, 1H), 1.05 – 0.94 (m, 14H). ^{13}C NMR (176 MHz, $CDCl_3$): δ 159.48, 157.12, 139.07, 138.50, 137.93, 133.14, 132.87, 129.21, 128.40, 128.33, 128.30, 128.06, 127.87, 127.74, 127.71, 127.56, 127.44, 121.92, 115.93, 114.75, 114.40, 113.87, 97.12, 93.93, 84.51, 77.50, 75.84, 75.41, 75.07, 73.45, 71.49, 68.32, 55.33, 17.42, 17.39, 17.37, 17.26, 17.20, 17.03, 12.86, 12.27. **HRMS (ESI) (m/z):** $[M+NH_4^+]$ calculated for $C_{48}H_{58}NO_7Si$, 788.3977 found, 788.3969.

6.3.4 Tethering Alcohols to Sugar Silanes

General Procedure:

Dry toluene (0.1 M) was added via syringe to the respective sugar silane (1.1 equiv.) and alcohol (1.0 equiv.) under N₂. B(C₆F₅)₃ (4 mol %) in minimal toluene was added via syringe. The reaction was allowed to stir at room temperature for 3-5 hours. B(C₆F₅)₃ (4 mol %) in minimal toluene was added via syringe. The reaction was allowed to stir at room temperature overnight. The reaction was directly purified via flash chromatography, Biotage.

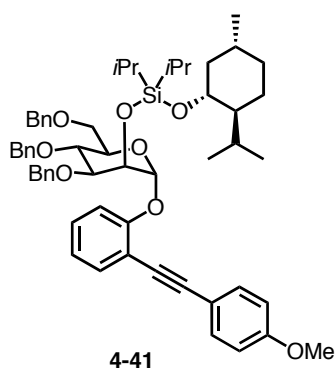
((2*R*,3*S*,4*S*,5*S*,6*R*)-4,5-bis(benzyloxy)-6-(benzyloxymethyl)-2-((4-methoxyphenyl)ethynyl)phenoxy)tetrahydro-2*H*-pyran-3-ylxy)((1*R*,2*S*,5*R*)-2-isopropyl-5-methylcyclohexyloxy)dimethylsilane (4-40)



The title compound was prepared from **4-29** (79 mg, 0.11 mmol), (-)-menthol (16 mg, 0.1 mmol), B(C₆F₅)₃ (4.0 mg, 0.008 mmol) in 1.5 mL toluene by following the general procedure. The reaction was directly purified via flash chromatography, Biotage (100% hexanes-90:10 hexanes: EtOAc) to afford the desired product as a colorless viscous oil (53 mg, 0.061 mmol, 60%). ¹H NMR (700 MHz, CDCl₃): δ 7.46 – 7.42 (m, 3H), 7.29 – 7.17 (m, 16H), 7.14 (dd, *J* = 7.3, 2.3 Hz, 2H), 6.98 (td, *J* = 7.5, 1.1 Hz, 1H), 6.62 (d, *J* = 8.7 Hz, 2H), 5.66 (d, *J* = 2.0 Hz, 1H), 4.84 (d, *J* = 10.7 Hz, 1H), 4.69 (d, *J* = 11.4 Hz, 1H), 4.61 (d, *J* = 11.9 Hz, 1H), 4.57 (d, *J* = 11.5 Hz, 1H), 4.53 (d, *J* = 10.7 Hz, 1H), 4.48 (t, *J* = 2.5 Hz, 1H), 4.42 (d, *J* = 11.9 Hz, 1H), 4.22 (dd, *J*

= 9.3, 2.9 Hz, 1H), 4.09 (ddd, $J = 9.9, 5.0, 1.8$ Hz, 1H), 4.04 (t, $J = 9.6$ Hz, 1H), 3.79 (dd, $J = 11.3, 4.8$ Hz, 1H), 3.70 (s, 3H), 3.68 (dd, $J = 11.4, 1.8$ Hz, 1H), 3.53 (td, $J = 10.4, 4.3$ Hz, 1H), 2.11 (pd, $J = 7.0, 2.6$ Hz, 1H), 1.99 – 1.94 (m, 1H), 1.60 – 1.55 (m, 1H), 1.56 – 1.49 (m, 1H), 1.33 – 1.26 (m, 1H), 1.10 (ddt, $J = 12.8, 10.0, 3.1$ Hz, 1H), 1.02 (td, $J = 12.2, 10.7$ Hz, 1H), 0.86 (dt, $J = 13.2, 2.9$ Hz, 1H), 0.82 (d, $J = 6.5$ Hz, 3H), 0.78 (d, $J = 7.1$ Hz, 3H), 0.68 (d, $J = 6.9$ Hz, 3H), 0.16 (s, 3H), 0.13 (s, 3H). ^{13}C NMR (176 MHz, CDCl_3): δ 159.62, 156.58, 138.76, 138.70, 138.61, 133.13, 133.03, 129.37, 128.31, 128.30, 128.27, 127.99, 127.76, 127.66, 127.52, 127.46, 127.41, 122.28, 115.63, 114.74, 113.99, 99.01, 93.70, 84.24, 80.55, 75.04, 74.66, 73.20, 73.12, 72.81, 72.73, 69.48, 69.21, 55.35, 50.00, 45.49, 34.59, 31.73, 25.47, 22.94, 22.33, 21.20, 15.96, -1.28, -1.35. HRMS (ESI) (m/z): $[\text{M}+\text{NH}_4^+]$ calculated for $\text{C}_{54}\text{H}_{68}\text{NO}_8\text{Si}$, 886.4709 found, 886.4707.

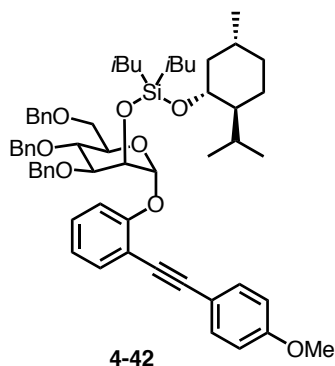
((2*R*,3*S*,4*S*,5*S*,6*R*)-4,5-bis(benzyloxy)-6-(benzyloxymethyl)-2-((4-methoxyphenyl)ethynyl)phenoxy)tetrahydro-2*H*-pyran-3-yloxy)diisopropyl((1*R*,2*S*,5*R*)-2-isopropyl-5-methylcyclohexyloxy)silane (4-40)



The title compound was prepared from **4-21** (85 mg, 0.11 mmol), (-)-menthol (16 mg, 0.1 mmol), $\text{B}(\text{C}_6\text{F}_5)_3$ (4.0 mg, 0.008 mmol) in 1.5 mL toluene by following the general procedure. The reaction was directly purified via flash chromatography, Biotage (97:3-85:15 hexanes: EtOAc) to afford the desired product as a colorless viscous oil (78 mg, 0.085 mmol, 85%). ^1H

NMR (700 MHz, CDCl₃): δ 7.51 – 7.45 (m, 3H), 7.32 – 7.22 (m, 17H), 7.19 (dd, $J = 7.3, 2.2$ Hz, 2H), 7.01 (td, $J = 7.4, 1.1$ Hz, 1H), 6.68 – 6.59 (m, 2H), 5.70 (d, $J = 2.0$ Hz, 1H), 4.88 (d, $J = 10.8$ Hz, 1H), 4.74 (d, $J = 11.5$ Hz, 1H), 4.64 (t, $J = 2.4$ Hz, 1H), 4.63 – 4.57 (m, 4H), 4.46 (d, $J = 12.0$ Hz, 1H), 4.28 (dd, $J = 8.9, 2.7$ Hz, 1H), 4.16 – 4.09 (m, 2H), 3.80 (dd, $J = 11.2, 4.6$ Hz, 1H), 3.74 – 3.70 (m, 4H), 3.68 (td, $J = 10.3, 4.2$ Hz, 1H), 2.28 (pd, $J = 7.0, 2.6$ Hz, 1H), 2.06 (dtd, $J = 12.0, 3.8, 1.9$ Hz, 1H), 1.59 (dq, $J = 12.4, 3.0$ Hz, 1H), 1.55 (dq, $J = 13.1, 3.3$ Hz, 1H), 1.36 – 1.28 (m, 1H), 1.17 – 0.99 (m, 14H), 0.91 – 0.87 (m, 1H), 0.84 (d, $J = 6.5$ Hz, 3H), 0.80 (d, $J = 7.1$ Hz, 3H), 0.73 (d, $J = 6.9$ Hz, 3H). **¹³C NMR (176 MHz, CDCl₃):** δ 159.57, 156.76, 138.85, 138.75, 138.68, 133.12, 132.97, 129.34, 128.29, 128.21, 128.16, 128.08, 127.58, 127.54, 127.50, 127.31, 127.29, 122.19, 115.66, 115.53, 114.78, 113.95, 99.19, 93.66, 84.29, 80.76, 75.04, 74.66, 73.23, 73.04, 72.94, 72.81, 69.69, 69.33, 55.33, 50.44, 45.90, 34.56, 31.73, 25.22, 22.70, 22.33, 21.31, 17.80, 17.75, 17.72, 15.88, 13.68, 13.45. **HRMS (ESI) (m/z):** [M+NH₄⁺] calculated for C₅₈H₇₆NO₈Si, 942.5335 found, 942.5336.

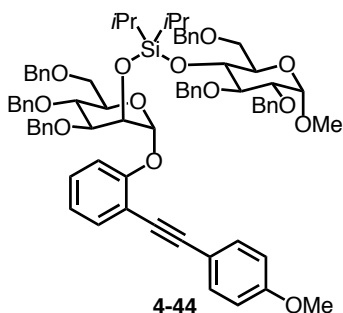
((2*R*,3*S*,4*S*,5*S*,6*R*)-4,5-bis(benzyloxy)-6-(benzyloxymethyl)-2-(2-((4-methoxyphenyl)ethynyl)phenoxy)tetrahydro-2*H*-pyran-3-yloxy)diisobutyl((1*R*,2*S*,5*R*)-2-isopropyl-5-methylcyclohexyloxy)silane (4-42)



The title compound was prepared from **4-30** (67 mg, 0.084 mmol), (-)-menthol (12 mg, 0.076 mmol), B(C₆F₅)₃ (3.1 mg, 0.006 mmol) in 1.2 mL toluene by following the general procedure.

The reaction was directly purified via flash chromatography, Biotage (100% hexanes-80:20 hexanes: EtOAc) to afford the desired product as a colorless viscous oil (52 mg, 0.055 mmol, 65%). **¹H NMR (700 MHz, CDCl₃):** δ 7.49 (dd, *J* = 7.6, 5.5 Hz, 3H), 7.32 (d, *J* = 7.5 Hz, 2H), 7.31 – 7.25 (m, 12H), 7.22 (d, *J* = 8.3 Hz, 1H), 7.20 – 7.18 (m, 2H), 7.02 (t, *J* = 7.5 Hz, 1H), 6.67 (d, *J* = 8.4 Hz, 2H), 5.71 (d, *J* = 2.1 Hz, 1H), 4.88 (d, *J* = 10.7 Hz, 1H), 4.72 (d, *J* = 11.5 Hz, 1H), 4.66 – 4.61 (m, 2H), 4.61 – 4.56 (m, 2H), 4.46 (d, *J* = 12.0 Hz, 1H), 4.27 (dd, *J* = 9.3, 2.7 Hz, 1H), 4.14 (dd, *J* = 10.2, 4.6 Hz, 1H), 4.09 (t, *J* = 9.6 Hz, 1H), 3.81 (dd, *J* = 11.4, 4.9 Hz, 1H), 3.74 (s, 3H), 3.73 – 3.69 (m, 1H), 3.61 (td, *J* = 10.4, 4.2 Hz, 1H), 2.22 (pd, *J* = 7.1, 2.2 Hz, 1H), 2.05 (d, *J* = 12.1 Hz, 1H), 1.96 (hept, *J* = 6.7 Hz, 1H), 1.87 (hept, *J* = 6.7 Hz, 1H), 1.59 (ddd, *J* = 31.7, 14.5, 3.7 Hz, 3H), 1.37 – 1.30 (m, 1H), 1.16 – 1.10 (m, 1H), 1.10 – 1.04 (m, 1H), 1.00 (dd, *J* = 11.2, 6.6 Hz, 6H), 0.91 (d, *J* = 6.5 Hz, 3H), 0.89 (d, *J* = 6.5 Hz, 3H), 0.85 (d, *J* = 6.6 Hz, 3H), 0.82 (d, *J* = 7.2 Hz, 3H), 0.78 (dd, *J* = 12.8, 3.2 Hz, 1H), 0.73 (d, *J* = 6.9 Hz, 3H), 0.66 (m, 4H). **¹³C NMR (176 MHz, CDCl₃):** δ 159.58, 156.70, 138.81, 138.73, 138.68, 133.13, 132.97, 129.34, 128.30, 128.24, 128.20, 128.09, 127.63, 127.53, 127.50, 127.34, 127.31, 122.19, 115.65, 115.48, 114.73, 113.97, 99.00, 93.69, 84.28, 80.63, 75.06, 74.70, 73.24, 73.01, 72.82, 72.68, 69.46, 69.29, 55.32, 50.23, 45.76, 34.54, 31.75, 26.58, 26.47, 26.40, 26.27, 25.16, 25.14, 25.06, 24.02, 23.94, 22.70, 22.34, 21.30, 15.85. **HRMS (ESI) (m/z):** [M+NH₄⁺] calculated for C₆₀H₈₀NO₈Si, 970.5648 found, 970.5640.

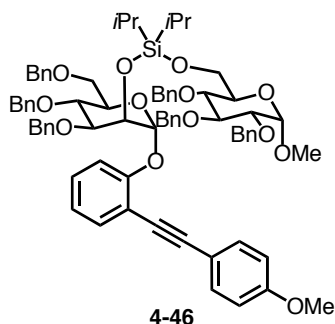
((2*R*,3*R*,4*R*,5*R*,6*S*)-4,5-bis(benzyloxy)-2-(benzyloxymethyl)-6-methoxytetrahydro-2*H*-pyran-3-yloxy)((2*R*,3*S*,4*S*,5*S*,6*R*)-4,5-bis(benzyloxy)-6-(benzyloxymethyl)-2-(2-((4-methoxyphenyl)ethynyl)phenoxy)tetrahydro-2*H*-pyran-3-yloxy)diisopropylsilane (4-44)



The title compound was prepared from **4-21** (85 mg, 0.11 mmol), (2*R*,3*R*,4*S*,5*R*,6*S*)-4,5-bis(benzyloxy)-2-(benzyloxymethyl)-6-methoxytetrahydro-2*H*-pyran-3-ol¹⁵⁹ (46 mg, 0.1 mmol), B(C₆F₅)₃ (4.0 mg, 0.008 mmol) in 1.5 mL toluene by following the general procedure. The reaction was directly purified via flash chromatography, Biotage (97:3-70:3- hexanes: EtOAc) to afford the desired product as a colorless viscous oil (39 mg, 0.032 mmol, 32%). ¹H NMR (700 MHz, CDCl₃): δ 7.47 (dd, *J* = 7.8, 1.7 Hz, 1H), 7.46 – 7.43 (m, 2H), 7.32 – 7.15 (m, 30H), 7.12 (dd, *J* = 6.6, 3.0 Hz, 2H), 6.99 (td, *J* = 7.3, 1.4 Hz, 1H), 6.60 – 6.56 (m, 2H), 5.72 (d, *J* = 1.9 Hz, 1H), 5.12 (d, *J* = 11.6 Hz, 1H), 4.82 (d, *J* = 10.7 Hz, 1H), 4.69 (d, *J* = 11.6 Hz, 1H), 4.61 – 4.55 (m, 4H), 4.52 – 4.44 (m, 6H), 4.37 (d, *J* = 12.0 Hz, 1H), 4.23 (dd, *J* = 9.3, 2.8 Hz, 1H), 4.10 (ddd, *J* = 10.1, 4.9, 1.7 Hz, 1H), 4.05 (dd, *J* = 11.4, 7.9 Hz, 1H), 3.92 (t, *J* = 9.0 Hz, 1H), 3.82 – 3.76 (m, 4H), 3.75 – 3.72 (m, 1H), 3.71 (s, 3H), 3.64 (dd, *J* = 11.2, 1.8 Hz, 1H), 3.46 (dd, *J* = 9.5, 3.6 Hz, 1H), 3.35 (s, 3H), 1.05 (dt, *J* = 19.2, 6.6 Hz, 2H), 0.99 (s, 9H), 0.98 – 0.95 (m, 3H). ¹³C NMR (176 MHz, CDCl₃): δ 159.56, 156.25, 139.42, 138.85, 138.69, 138.48, 138.36, 138.11, 133.14, 133.12, 133.04, 129.43, 128.69, 128.46, 128.31, 128.24, 128.22, 128.19, 128.15, 128.10, 128.04, 127.91, 127.76, 127.65, 127.62, 127.58, 127.47, 127.44, 127.41, 127.39, 127.36, 127.20, 127.05, 126.97, 122.22, 115.58, 115.31, 114.71, 114.07, 113.94, 98.40, 97.62, 93.74,

84.29, 81.49, 80.99, 80.81, 74.98, 74.51, 74.50, 73.38, 73.05, 72.94, 72.84, 72.60, 71.46, 71.24, 69.89, 69.83, 69.22, 55.33, 55.23, 17.77, 17.73, 17.72, 17.56, 12.89, 12.78. **HRMS (ESI) (m/z):** $[M+NH_4^+]$ calculated for $C_{76}H_{88}NO_{13}Si$, 1250.6019 found, 1250.6020.

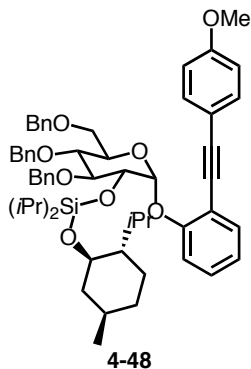
((2R,3S,4S,5S,6R)-4,5-bis(benzyloxy)-6-(benzyloxymethyl)-2-(2-((4-methoxyphenyl)ethynyl)phenoxy)tetrahydro-2H-pyran-3-yloxy)diisopropyl(((2R,3R,4S,5S,6R)-3,4,5-tris(benzyloxy)-6-methoxytetrahydro-2H-pyran-2-yl)methoxy)silane (4-46)



The title compound was prepared from **4-21** (85 mg, 0.11 mmol), ((2R,3R,4S,5S,6R)-3,4,5-tris(benzyloxy)-6-methoxytetrahydro-2H-pyran-2-yl)¹⁷⁸ (46 mg, 0.1 mmol), $B(C_6F_5)_3$ (8.0 mg, 0.016 mmol) in 1.5 mL toluene by following a modified general procedure. The reaction was directly purified via flash chromatography, Biotage (100% hexanes-70:30 hexanes: EtOAc) to afford the desired product as a colorless viscous oil (96 mg, 0.078 mmol, 77%). **¹H NMR (700 MHz, $CDCl_3$):** δ 7.44 (dd, $J = 7.7, 5.6$ Hz, 3H), 7.37 – 7.20 (m, 29H), 7.19 – 7.14 (m, 3H), 6.93 (t, $J = 7.5$ Hz, 1H), 6.64 (d, $J = 8.5$ Hz, 2H), 5.75 (d, $J = 2.0$ Hz, 1H), 4.90 (d, $J = 10.8$ Hz, 1H), 4.86 (d, $J = 10.8$ Hz, 1H), 4.83 (d, $J = 11.0$ Hz, 1H), 4.75 (d, $J = 10.8$ Hz, 1H), 4.73 – 4.69 (m, 2H), 4.62 (d, $J = 11.6$ Hz, 1H), 4.60 (d, $J = 3.3$ Hz, 1H), 4.58 (d, $J = 4.4$ Hz, 1H), 4.55 (d, $J = 10.7$ Hz, 1H), 4.47 (d, $J = 3.3$ Hz, 1H), 4.44 (dd, $J = 12.7, 11.1$ Hz, 3H), 4.28 (dd, $J = 9.4, 2.6$ Hz, 1H), 4.12 (t, $J = 9.6$ Hz, 1H), 4.04 (ddd, $J = 10.0, 4.8, 1.7$ Hz, 1H), 4.00 (dd, $J = 11.2, 1.8$ Hz, 1H), 3.95 – 3.89 (m, 2H), 3.79 (dd, $J = 11.3, 4.7$ Hz, 1H), 3.72 (s, 3H), 3.68 (dd, $J = 11.3, 1.8$ Hz, 1H), 3.63 (dd, $J = 10.3, 4.5$ Hz, 1H), 3.47 (t, $J = 9.5$ Hz, 1H), 3.29 (dd, $J = 9.6, 3.5$ Hz,

1H), 3.21 (s, 3H), 1.06 (dq, $J = 11.6, 5.8, 4.7$ Hz, 14H). ^{13}C NMR (176 MHz, CDCl_3): δ 159.63, 156.48, 138.85, 138.82, 138.68, 138.61, 138.41, 138.33, 133.07, 133.05, 129.44, 128.49, 128.47, 128.44, 128.42, 128.35, 128.30, 128.28, 128.23, 128.16, 128.11, 127.95, 127.92, 127.78, 127.75, 127.66, 127.56, 127.54, 127.40, 127.35, 121.96, 115.57, 114.95, 114.20, 114.01, 98.47, 97.48, 93.79, 84.33, 82.07, 80.85, 80.75, 77.76, 75.88, 75.14, 75.09, 74.50, 73.09, 73.02, 72.94, 72.74, 71.41, 69.48, 69.19, 62.53, 55.34, 54.87, 17.54, 17.48, 17.46, 12.75, 12.72, 1.11. HRMS (ESI) (m/z): $[\text{M}+\text{K}^+]$ calculated for $\text{KC}_76\text{H}_{84}\text{O}_{13}\text{Si}$, 1271.5313 found, 1271.5305.

((2R,3R,4S,5S,6R)-4,5-bis(benzyloxy)-6-(benzyloxymethyl)-2-(2-((4-methoxyphenyl)ethynyl)phenoxy)tetrahydro-2H-pyran-3-yloxy)diisopropyl((1R,2S,5R)-2-isopropyl-5-methylcyclohexyloxy)silane (4-48)



The title compound was prepared from **4-39** (85 mg, 0.11 mmol), (-)-menthol (16 mg, 0.1 mmol), $\text{B}(\text{C}_6\text{F}_5)_3$ (4.0 mg, 0.008 mmol) in 1.5 mL toluene by following the general procedure. The reaction was directly purified via flash chromatography, Biotage (100% hexanes-80:20 hexanes: EtOAc) to afford the desired product as a colorless viscous oil (81 mg, 0.087 mmol, 87%). ^1H NMR (700 MHz, CDCl_3): δ 7.57 – 7.52 (m, 2H), 7.47 (dd, $J = 7.7, 1.8$ Hz, 1H), 7.36 (d, $J = 8.1$ Hz, 2H), 7.34 – 7.20 (m, 13H), 7.07 (dd, $J = 5.3, 2.6$ Hz, 2H), 6.98 (t, $J = 7.4$ Hz, 1H), 6.70 – 6.64 (m, 2H), 5.84 (d, $J = 7.2$ Hz, 1H), 5.03 (d, $J = 11.3$ Hz, 1H), 4.81 (dd, $J = 11.0, 9.1$ Hz, 2H), 4.61 (dd, $J = 12.1, 1.6$ Hz, 1H), 4.50 (d, $J = 10.6$ Hz, 1H), 4.42 (dd, $J = 12.1, 1.6$ Hz,

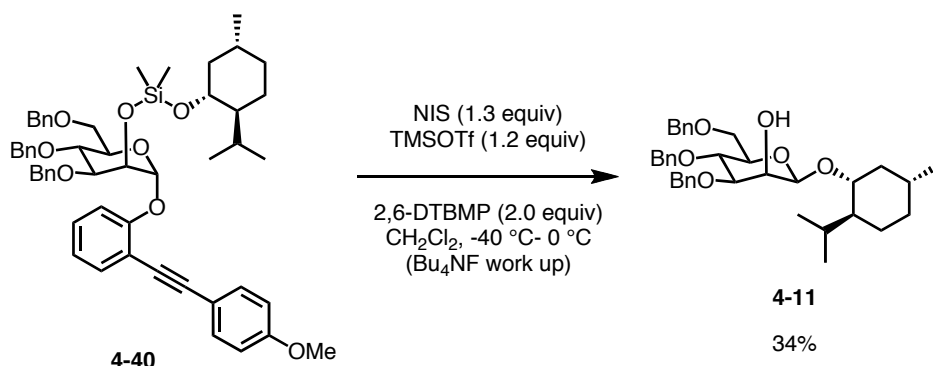
1H), 4.33 (td, $J = 9.3, 1.6$ Hz, 1H), 4.22 (dt, $J = 9.6, 2.4$ Hz, 1H), 4.12 (ddd, $J = 10.3, 3.6, 1.9$ Hz, 1H), 3.81 – 3.76 (m, 2H), 3.74 (d, $J = 1.7$ Hz, 3H), 3.60 (dd, $J = 11.1, 2.1$ Hz, 1H), 3.53 (td, $J = 10.3, 4.1$ Hz, 1H), 2.28 – 2.23 (m, 1H), 2.09 – 2.05 (m, 1H), 1.57 – 1.50 (m, 2H), 1.13 – 1.02 (m, 11H), 1.03 – 0.99 (m, 3H), 0.98 (d, $J = 6.4$ Hz, 2H), 0.96 – 0.89 (m, 1H), 0.84 (dd, $J = 7.1, 1.6$ Hz, 3H), 0.83 – 0.78 (m, 4H), 0.79 – 0.73 (m, 1H), 0.69 (dd, $J = 6.9, 1.6$ Hz, 3H). **^{13}C NMR (176 MHz, CDCl_3):** δ 159.44, 156.92, 139.28, 138.52, 138.01, 133.16, 132.77, 129.08, 128.37, 128.27, 128.23, 127.99, 127.87, 127.67, 127.52, 127.49, 127.26, 121.61, 116.04, 114.50, 114.08, 113.83, 97.17, 93.90, 84.56, 82.97, 77.77, 75.79, 75.03, 73.63, 73.34, 73.29, 71.33, 68.50, 55.32, 50.47, 45.49, 34.52, 31.66, 25.14, 22.68, 22.24, 21.43, 17.87, 17.74, 17.59, 17.42, 15.87, 13.67, 13.54. **HRMS (ESI) (m/z):** $[\text{M}+\text{NH}_4^+]$ calculated for $\text{C}_{58}\text{H}_{76}\text{NO}_8\text{Si}$, 942.5335 found, 942.5331.

6.3.5 Aglycone Delivery

General Procedure:

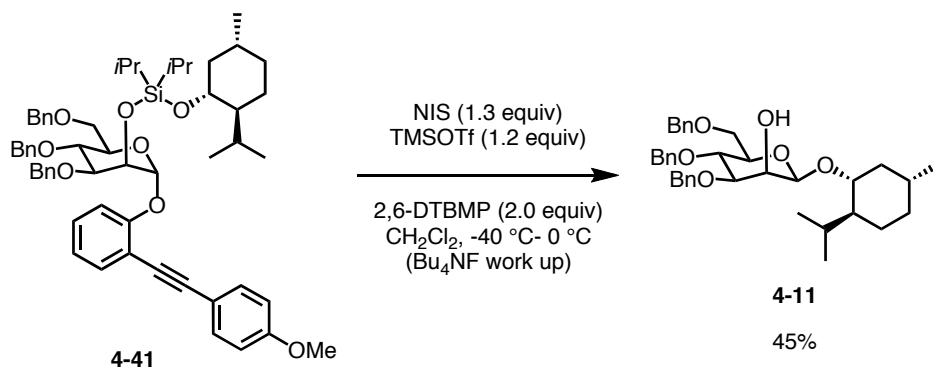
CH_2Cl_2 (0.02 M) was added to the respective tethered sugar silane (1.0 equiv.) under N_2 . The reaction was cooled to -40 °C. A slurry of *N*-iodosuccinimide (1.3 equiv) and 2,6-DTBMP (2.0 equiv.) in minimal CH_2Cl_2 was added via syringe. The reaction was allowed to stir ~5 minutes before TMSOTf (1.2 equiv.) was added via syringe. The reaction as allowed to stir 20 minutes before being warmed to 0 °C. The reaction was allowed to stir at 0 °C for 7-8 hours before being quenched with Bu_4NF (5.0 equiv.) The reaction was allowed to stir at room temperature overnight. Saturated $\text{Na}_2\text{S}_2\text{O}_3$ and NH_4Cl were added. The reaction was extracted 3x5 mL CH_2Cl_2 . The combined organic layers were dried over MgSO_4 and filtered. The solvent was removed *in vacuo*. The crude residue was purified via flash chromatography, Biotage.

(2*R*,3*S*,4*R*,6*R*)-4,5-bis(benzyloxy)-6-(benzyloxymethyl)-2-((1*R*,2*S*,5*R*)-2-isopropyl-5-methylcyclohexyloxy)tetrahydro-2*H*-pyran-3-ol (4-11)



The title compound was prepared from **4-40** (52 mg, 0.060 mmol), NIS (17.5 mg, 0.078 mmol), TMSOTf (13 μ L, 0.072 mmol), 2,6-DTBMP (25 mg, 0.12 mmol) in 3.0 mL CH₂Cl₂ by following the general procedure. The crude residue was purified via flash chromatography, Biotage (97:3-70:30 hexanes: EtOAc) to give the desired product as a white solid (12 mg, 0.021 mmol, 34%). The spectral data matched the literature.¹⁶¹

(2*R*,3*S*,4*R*,6*R*)-4,5-bis(benzyloxy)-6-(benzyloxymethyl)-2-((1*R*,2*S*,5*R*)-2-isopropyl-5-methylcyclohexyloxy)tetrahydro-2*H*-pyran-3-ol (4-11)

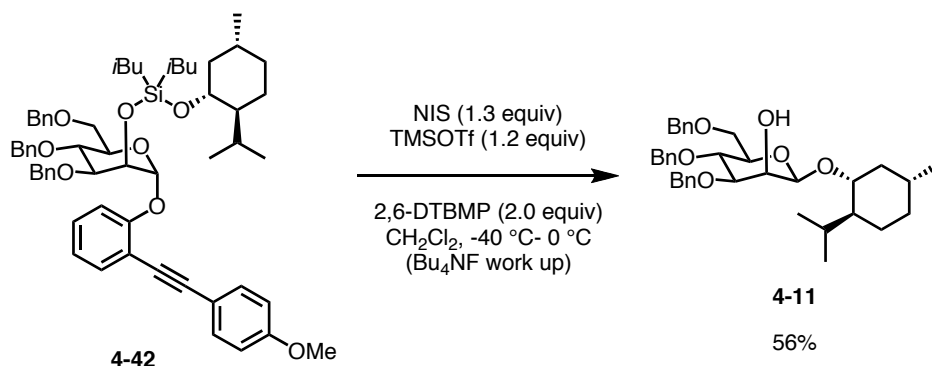


The title compound was prepared from **4-41** (63 mg, 0.068 mmol), NIS (32.5 mg, 0.089 mmol), TMSOTf (14 μ L, 0.082 mmol), 2,6-DTBMP (28 mg, 0.14 mmol) in 3.4 mL CH₂Cl₂ by following the general procedure. The crude residue was purified via flash chromatography, Biotage (97:3-

70:30 hexanes: EtOAc) to give the desired product as a white solid (18 mg, 0.030 mmol, 44%).

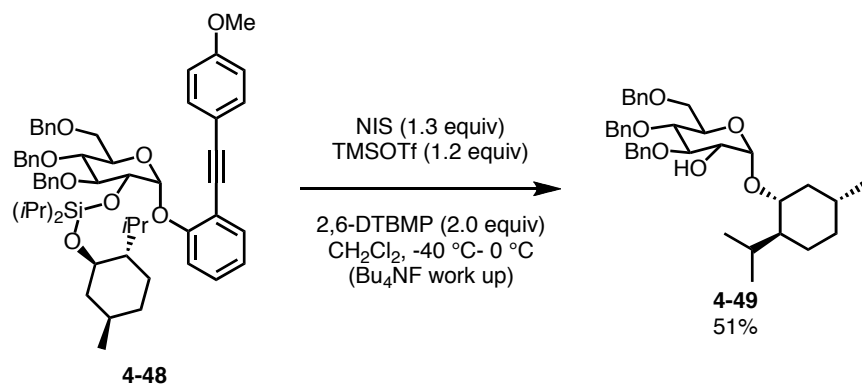
The spectral data matched the literature.¹⁶¹

(2*R*,3*S*,4*R*,6*R*)-4,5-bis(benzyloxy)-6-(benzyloxymethyl)-2-((1*R*,2*S*,5*R*)-2-isopropyl-5-methylcyclohexyloxy)tetrahydro-2*H*-pyran-3-ol (4-11)



The title compound was prepared from **4-41** (52 mg, 0.055 mmol), NIS (16.0 mg, 0.071 mmol), TMSOTf (12 μ L, 0.066 mmol), 2,6-DTBMP (23 mg, 0.11 mmol) in 2.8 mL CH₂Cl₂ by following the general procedure. The crude residue was purified via flash chromatography, Biotage (100% hexanes-80:20 hexanes: EtOAc) to give the desired product as a white solid (18 mg, 0.030 mmol, 56%). The spectral data matched the literature.¹⁶¹

(2*S*,3*R*,4*R*,6*R*)-4,5-bis(benzyloxy)-6-(benzyloxymethyl)-2-((1*R*,2*S*,5*R*)-2-isopropyl-5-methylcyclohexyloxy)tetrahydro-2*H*-pyran-3-ol (4-49)



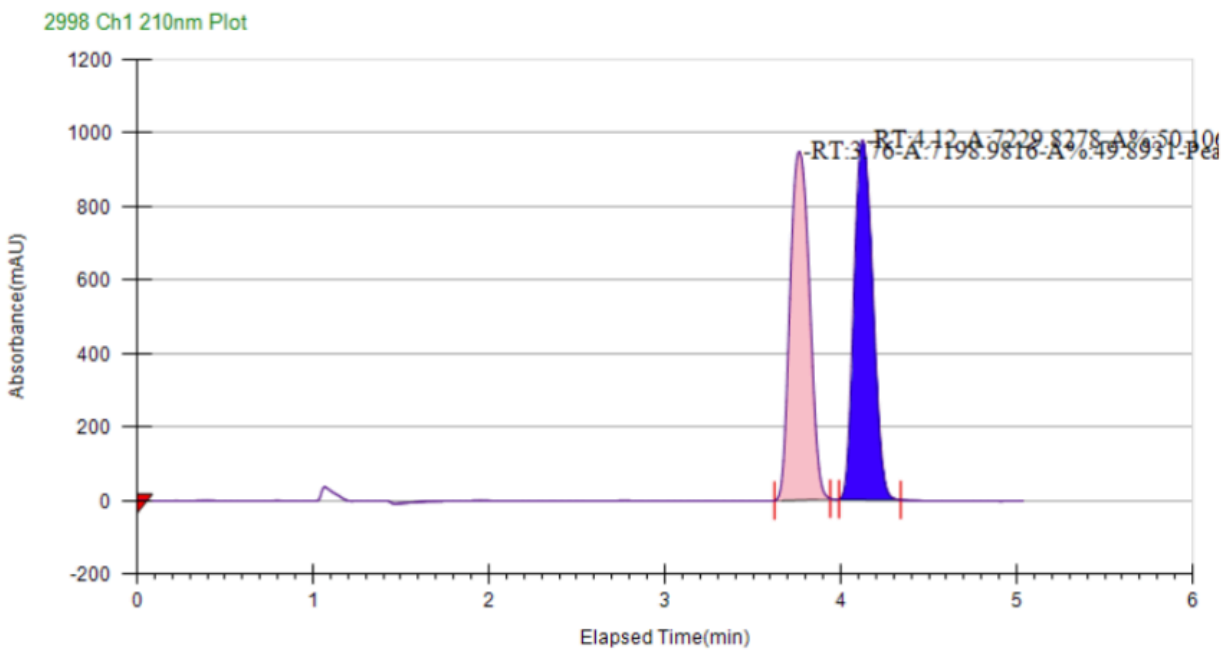
The title compound was prepared from **4-48** (80 mg, 0.086 mmol), NIS (25.3 mg, 0.11 mmol), TMSOTf (19 μ L, 0.10 mmol), 2,6-DTBMP (35 mg, 0.17 mmol) in 4.3 mL CH₂Cl₂ by following the general procedure. The crude residue was purified via flash chromatography, Biotage (100% hexanes-80:20 hexanes: EtOAc) to give the desired product as a white solid (26 mg, 0.044 mmol, 51%). The spectral data matched the literature.¹⁶¹

6.3.6 Asymmetric Hydrosilylation of Ketones

General Procedure:

Dry THF (0.2 M) was added to a solid mixture of Ni(cod)₂ (0.10 equiv.), Ligand (0.11 equiv.), KO-*t*-Bu (0.12 equiv.) under N₂. The reaction was allowed to premix at room temperature for 20 minutes. Silane (2.0 equiv.) was added to the reaction under N₂. The reaction was allowed to stir at room temperature for 5 minutes before acetophenone (1.0 equiv.) was added under N₂. The reaction was allowed to stir at room temperature for 7-9 hours and was then filtered through silica gel, eluting with 50% v/v EtOAc/hexanes. The solvent was removed *in vacuo*. Dry THF (0.2 M) was added to the crude residue via under N₂. Bu₄NF (2.0 equiv) was added dropwise via syringe to the reaction. The reaction was allowed to stir at room temperature over night. The reaction was quenched with NH₄Cl and extracted 3x Et₂O. The combined organic layers were dried over MgSO₄ and filtered. The solvent was removed *in vacuo* and the crude residue was purified via flash chromatography, Biotage (100% hexanes-80:20 hexanes: EtOAc). The enantioselectivity was determined by SFC analysis: OD-H column, 3 mL/min, 5% *i*-PrOH, 120 bar, 40 °C.

Racemic:

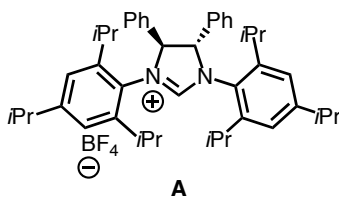


Peak Information

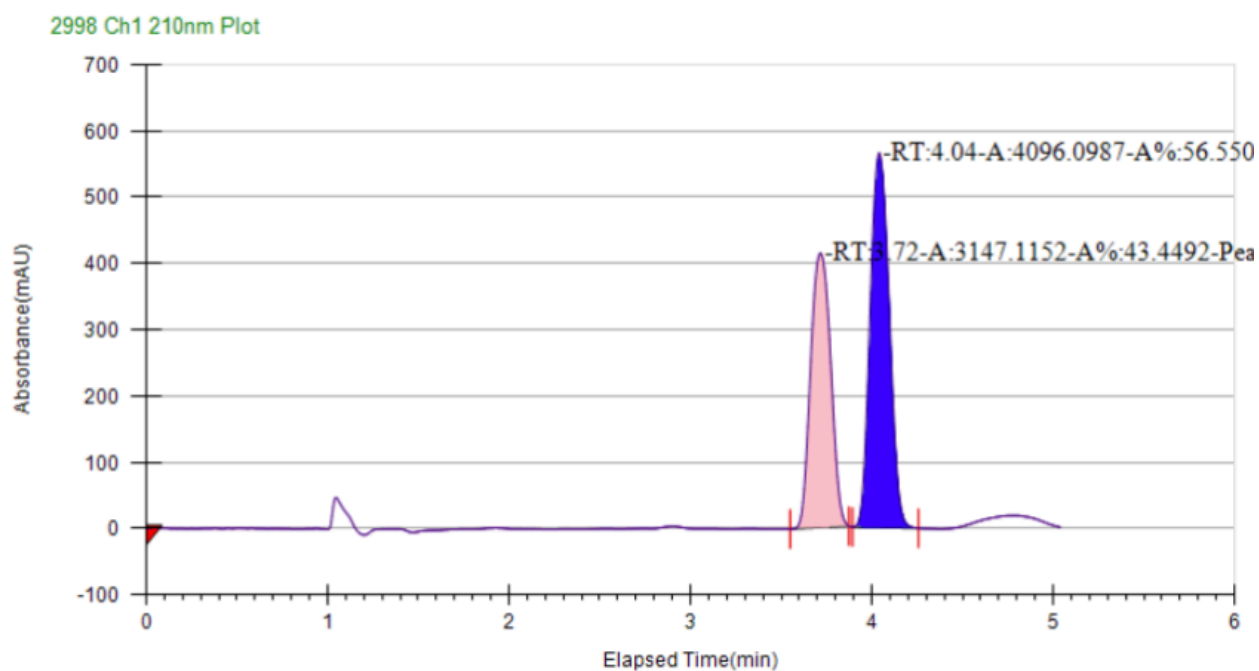
Peak No	% Area	Area	Ret. Time	Height	Cap. Factor
1	49.8931	7198.9816	3.76 min	948.1887	0
2	50.1069	7229.8278	4.12 min	978.1519	0

Table 6-18: Racemic SFC Trace for 4-53

Reaction using ligand A



The general procedure was followed using Ni(cod)₂ (5.5 mg, 0.02 mmol), Ligand A (15.1 mg, 0.022 mmol), KO-*t*-Bu (2.7 mg, 0.024 mmol), Et₃SiH (64 μL, 0.4 mmol), acetophenone (23 μL, 0.2 mmol) and 1.0 mL of THF. The crude residue was purified via flash chromatography, Biotage (100% hexanes-80:20 hexanes: EtOAc) to afford the desired product (3.5 mg, 0.029 mmol, 14%, 13% ee).

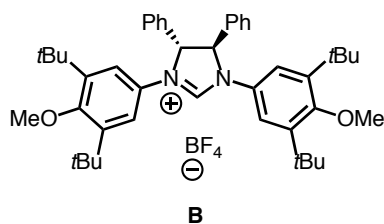


Peak Information

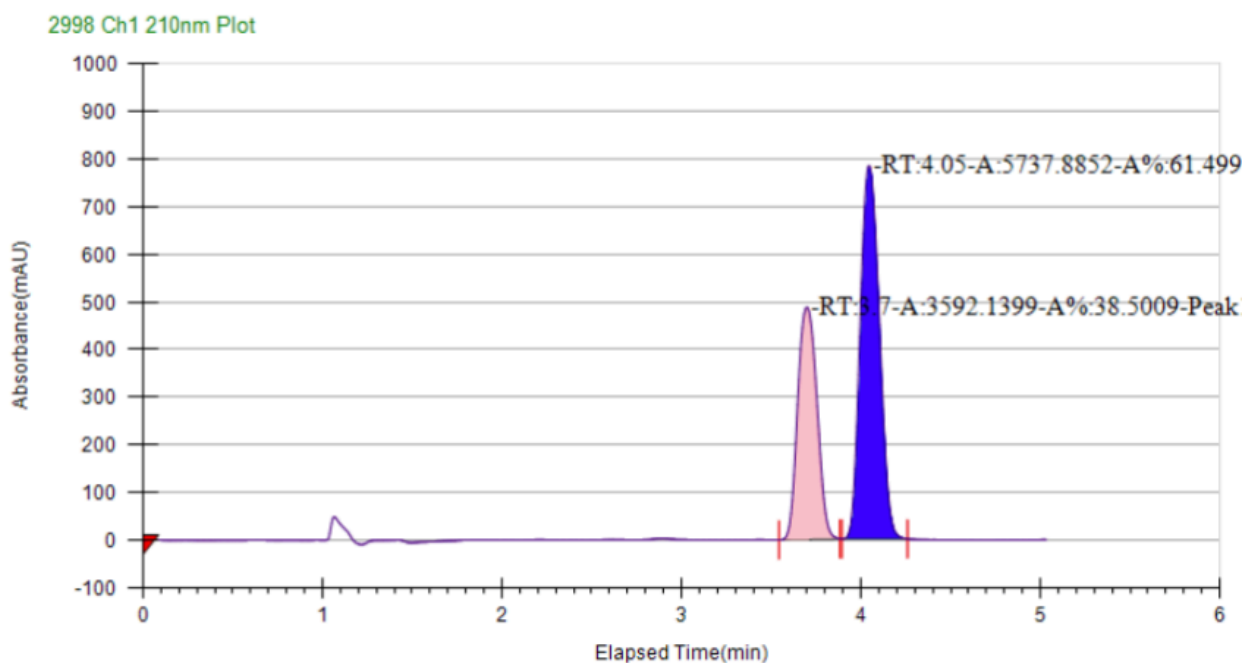
Peak No	% Area	Area	Ret. Time	Height	Cap. Factor
1	43.4492	3147.1152	3.72 min	414.1384	3715.6667
2	56.5508	4096.0987	4.04 min	565.0024	4039

Table 6-19: SFC Trace for Reaction with Ligand A

Reaction using ligand B



The general procedure was followed using Ni(cod)₂ (5.5 mg, 0.02 mmol), Ligand **B** (16.4 mg, 0.022 mmol), KO-*t*-Bu (2.7 mg, 0.024 mmol), Et₃SiH (64 μL, 0.4 mmol), acetophenone (23 μL, 0.2 mmol) and 1.0 mL of THF. The crude residue was purified via flash chromatography, Biotage (100% hexanes-80:20 hexanes: EtOAc) to afford the desired product (17.0 mg, 0.129 mmol, 70%, 23% ee).

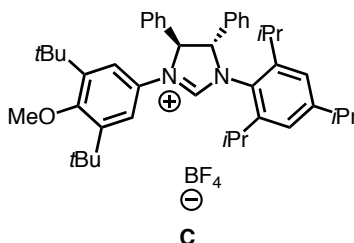


Peak Information

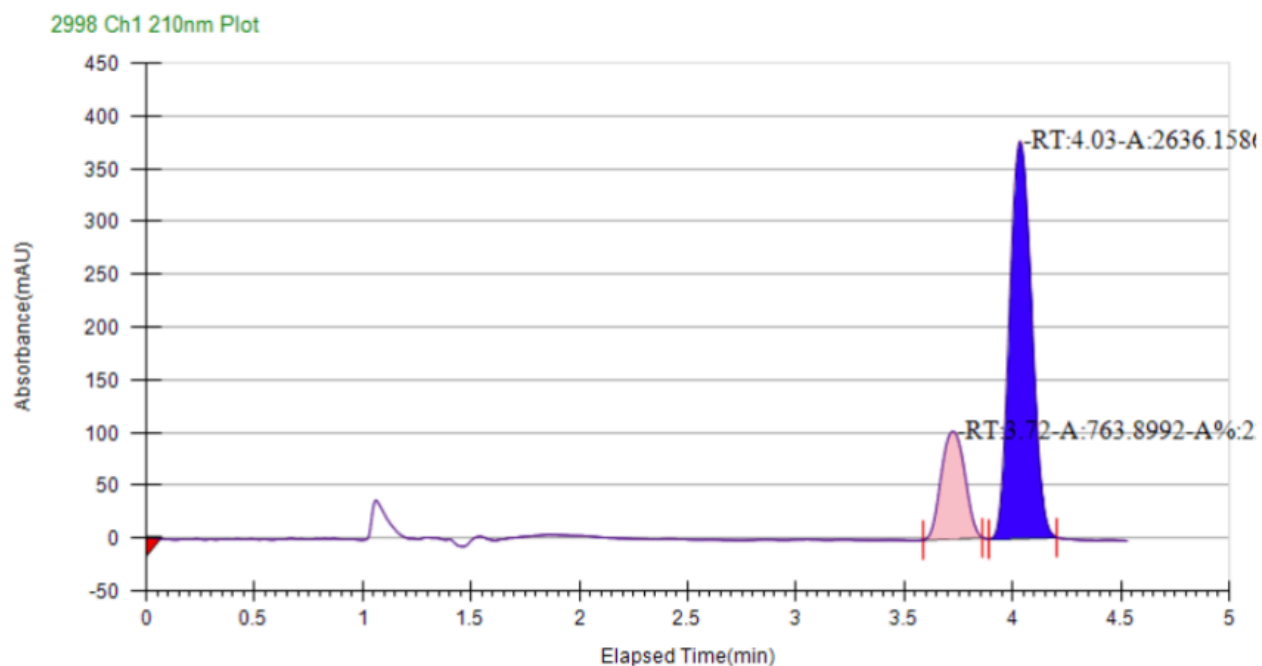
Peak No	% Area	Area	Ret. Time	Height	Cap. Factor
1	38.5009	3592.1399	3.7 min	487.0669	0
2	61.4991	5737.8852	4.05 min	782.8365	0

Table 6-20: SFC Trace for Reaction with Ligand B

Reaction using ligand C at room temperature



The general procedure was followed using Ni(cod)₂ (2.8 mg, 0.01 mmol), Ligand C (7.7 mg, 0.011 mmol), KO-*t*-Bu (1.3 mg, 0.012 mmol), *t*BuMe₂SiH (33 μL, 0.2 mmol), acetophenone (12 μL, 0.1 mmol) and 0.5 mL of THF. The crude residue was purified via flash chromatography, Biotage (100% hexanes-80:20 hexanes: EtOAc) to afford the desired product (1.1 mg, 0.009 mmol, 9%, 55% ee).

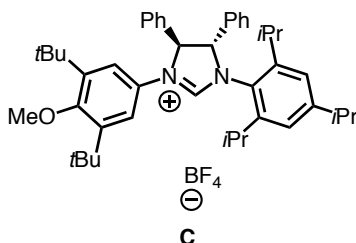


Peak Information

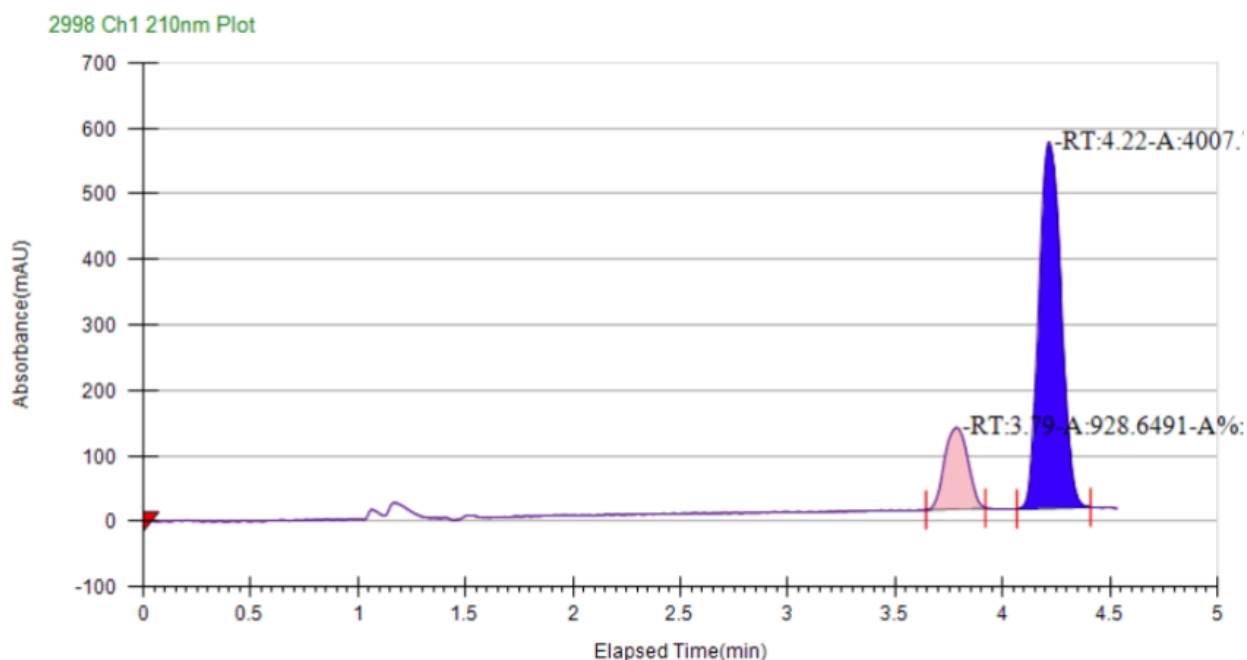
Peak No	% Area	Area	Ret. Time	Height	Cap. Factor
1	22.4672	763.8992	3.72 min	101.736	0
2	77.5328	2636.1586	4.03 min	376.1384	0

Table 6-21: SFC Trace for Reaction with Ligand C

Reaction using ligand C at 0 °C



A modified general procedure was followed using Ni(cod)₂ (2.8 mg, 0.01 mmol), Ligand C (7.7 mg, 0.011 mmol), KO-*t*-Bu (1.3 mg, 0.012 mmol), *t*BuMe₂SiH (33 μL, 0.2 mmol), acetophenone (12 μL, 0.1 mmol) and 0.5 mL of THF. The reaction was cooled to 0 °C before acetophenone was added. The reaction was run at 0 °C until the reaction was filtered through a plug of silica. The crude residue was purified via flash chromatography, Biotage (100% hexanes-80:20 hexanes: EtOAc) to afford the desired product (2.4 mg, 0.020 mmol, 20%, 63% ee).

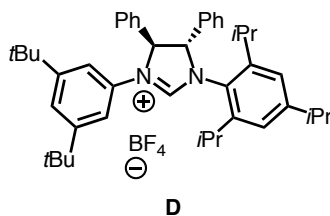


Peak Information

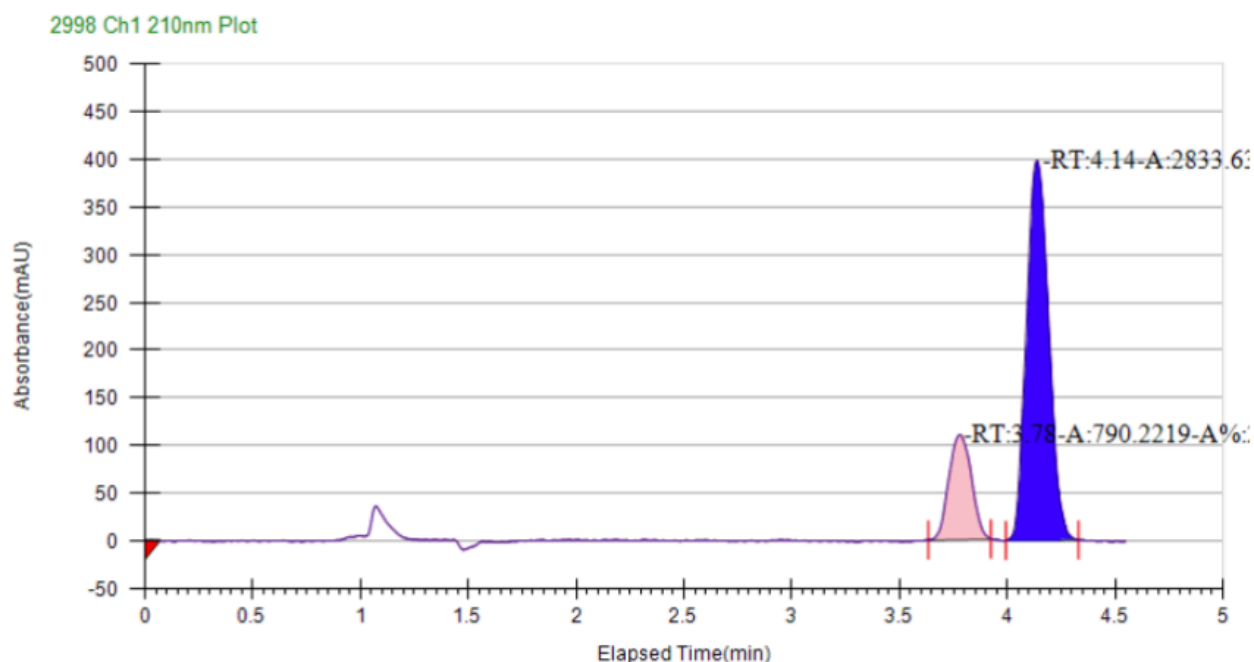
Peak No	% Area	Area	Ret. Time	Height	Cap. Factor
1	18.8124	928.6491	3.79 min	124.1541	3785.6667
2	81.1876	4007.7189	4.22 min	559.7236	4215.6667

Table 6-22: SFC Trace for Reaction with Ligand D at 0 °C

Reaction using ligand **D** and *t*BuMe₂SiH



The general procedure was followed using Ni(cod)₂ (2.8 mg, 0.01 mmol), Ligand **D** (8.0 mg, 0.011 mmol), KO-*t*-Bu (1.3 mg, 0.012 mmol), *t*BuMe₂SiH (33 μL, 0.2 mmol), acetophenone (12 μL, 0.1 mmol) and 0.5 mL of THF. The crude residue was purified via flash chromatography, Biotage (100% hexanes-80:20 hexanes: EtOAc) to afford the desired product (5.9 mg, 0.048 mmol, 48%, 56% ee).

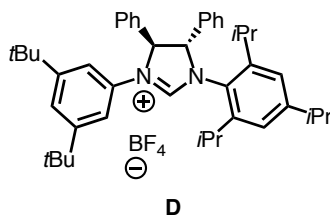


Peak Information

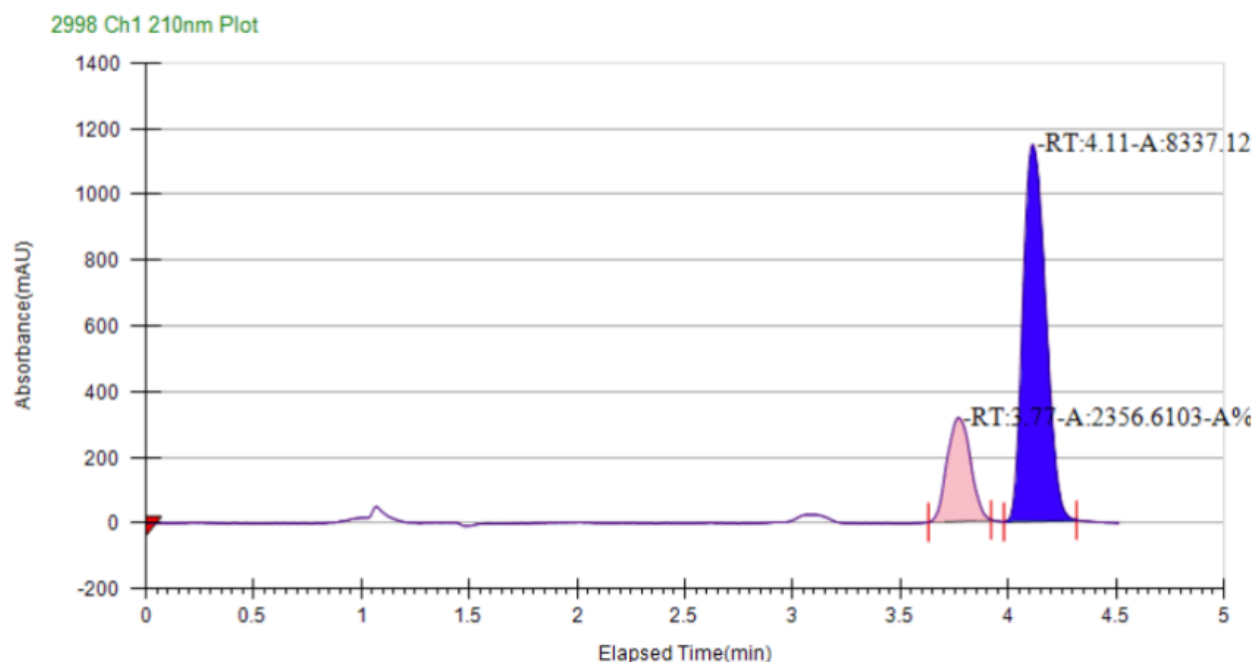
Peak No	% Area	Area	Ret. Time	Height	Cap. Factor
1	21.8061	790.2219	3.78 min	109.7664	3779
2	78.1939	2833.6399	4.14 min	397.7481	4135.6667

Table 6-23: SFC Trace for Reaction with Ligand **D** and *t*BuMe₂SiH

Reaction using ligand **D** and PhMe₂SiH



The general procedure was followed using Ni(cod)₂ (2.8 mg, 0.01 mmol), Ligand **D** (8.0 mg, 0.011 mmol), KO-*t*-Bu (1.3 mg, 0.012 mmol), PhMe₂SiH (31 μL, 0.2 mmol), acetophenone (12 μL, 0.1 mmol) and 0.5 mL of THF. The crude residue was purified via flash chromatography, Biotage (100% hexanes-80:20 hexanes: EtOAc) to afford the desired product (5.3 mg, 0.043 mmol, 43%, 56% ee).

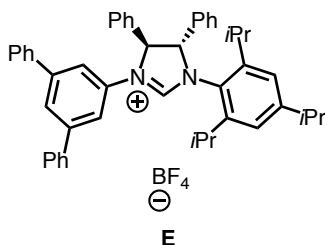


Peak Information

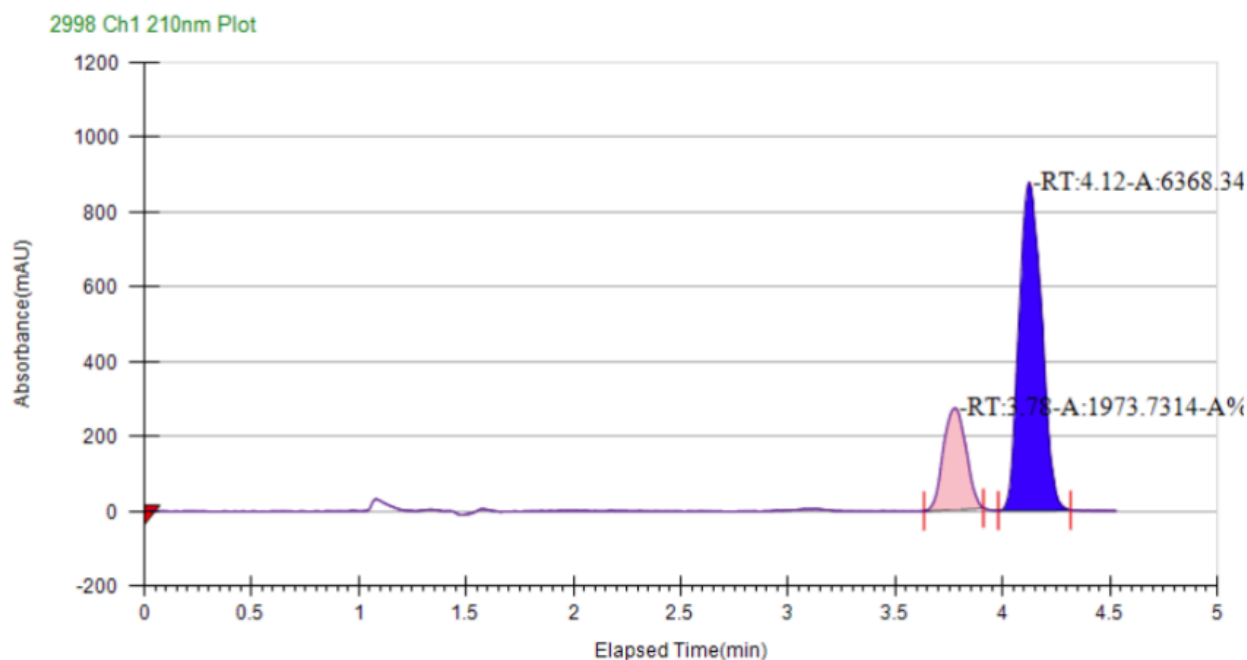
Peak No	% Area	Area	Ret. Time	Height	Cap. Factor
1	22.0373	2356.6103	3.77 min	315.0241	0
2	77.9627	8337.1256	4.11 min	1147.8227	0

Table 6-24: SFC Trace for Reaction with Ligand **D** and PhMe₂Si

Reaction using ligand E



The general procedure was followed using Ni(cod)₂ (2.8 mg, 0.01 mmol), Ligand **E** (8.1 mg, 0.011 mmol), KO-*t*-Bu (1.3 mg, 0.012 mmol), Bn₃SiH (60 mg, 0.2 mmol), acetophenone (12 μL, 0.1 mmol) and 0.5 mL of THF. The crude residue was purified via flash chromatography, Biotage (100% hexanes-80:20 hexanes: EtOAc) to afford the desired product (2.3 mg, 0.019 mmol, 19%, 53% ee).

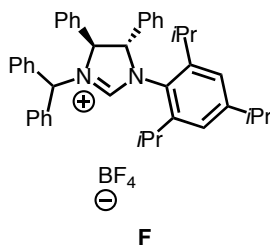


Peak Information

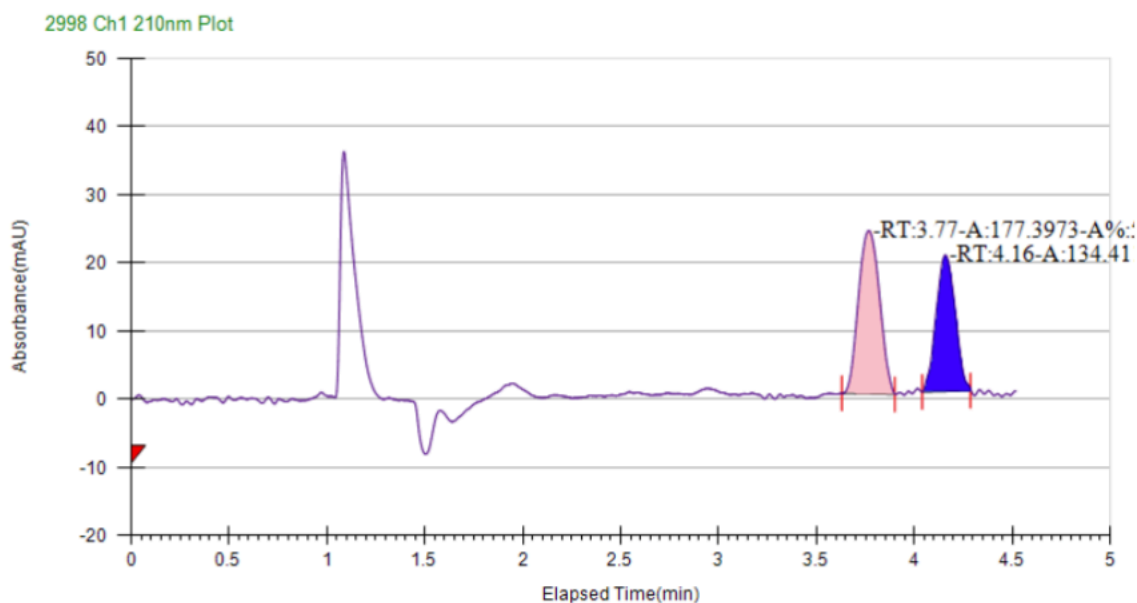
Peak No	% Area	Area	Ret. Time	Height	Cap. Factor
1	23.6599	1973.7314	3.78 min	271.2243	0
2	76.3401	6368.3466	4.12 min	878.1671	0

Table 6-25: SFC Trace for Reaction with Ligand E

Reaction using ligand F



The general procedure was followed using Ni(cod)₂ (2.8 mg, 0.01 mmol), Ligand **F** (7.5 mg, 0.011 mmol), KO-*t*-Bu (1.3 mg, 0.012 mmol), Et₃SiH (32 μL, 0.2 mmol), acetophenone (12 μL, 0.1 mmol) and 0.5 mL of THF. The crude residue was purified via flash chromatography, Biotage (100% hexanes-80:20 hexanes: EtOAc) to afford the desired product (0.9 mg, 0.007 mmol, 7%, 14% ee).



Peak Information

Peak No	% Area	Area	Ret. Time	Height	Cap. Factor
1	56.8931	177.3973	3.77 min	23.9594	0
2	43.1069	134.4111	4.16 min	19.9933	0

Table 6-26: SFC Trace for Reaction with Ligand **F**

6.4 NMR Spectra

1-Allyl-2-methylenecyclohexane

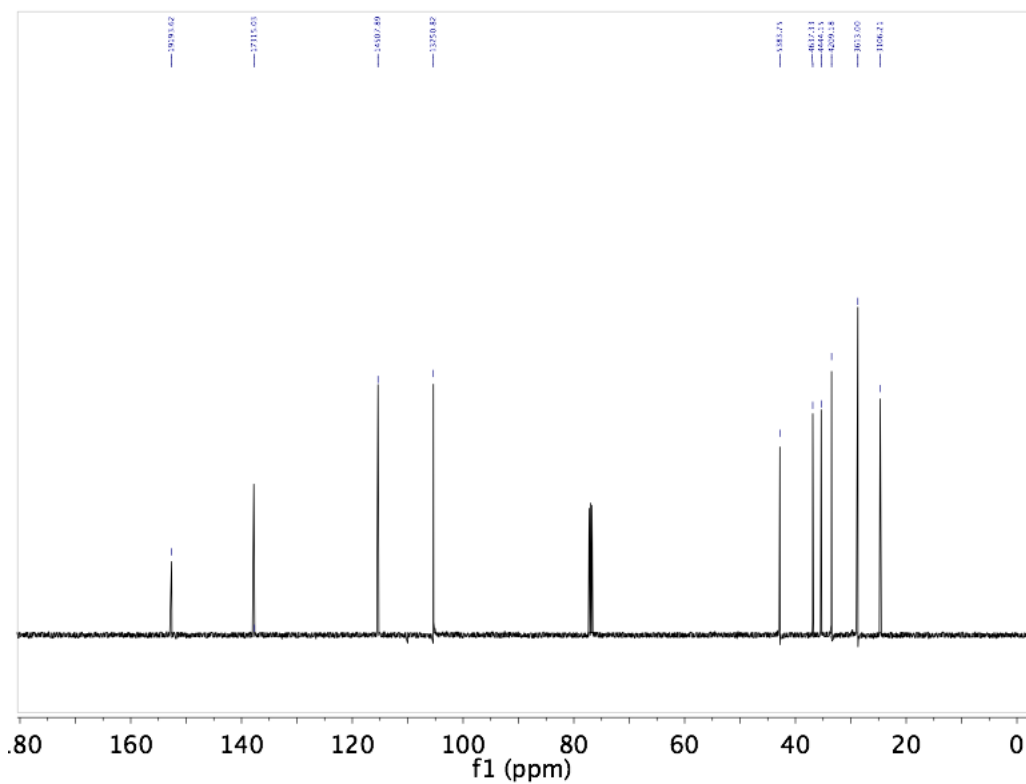
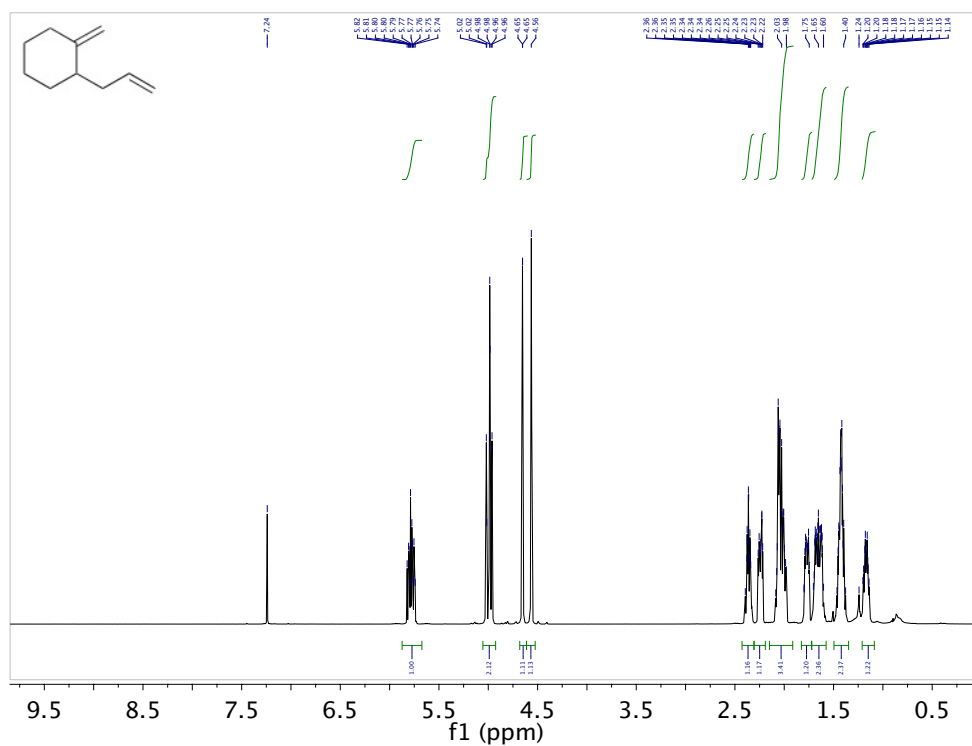


Figure 6-1: Spectra for 1-Allyl-2-methylenecyclohexane

hex-5-enyl pivalate

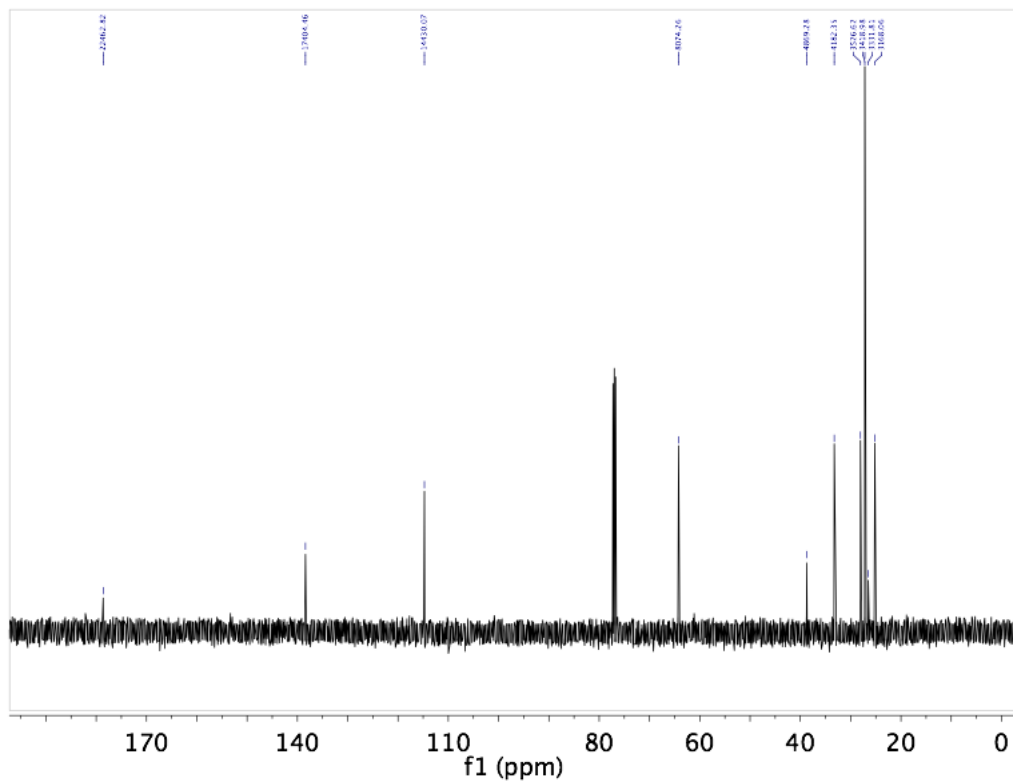
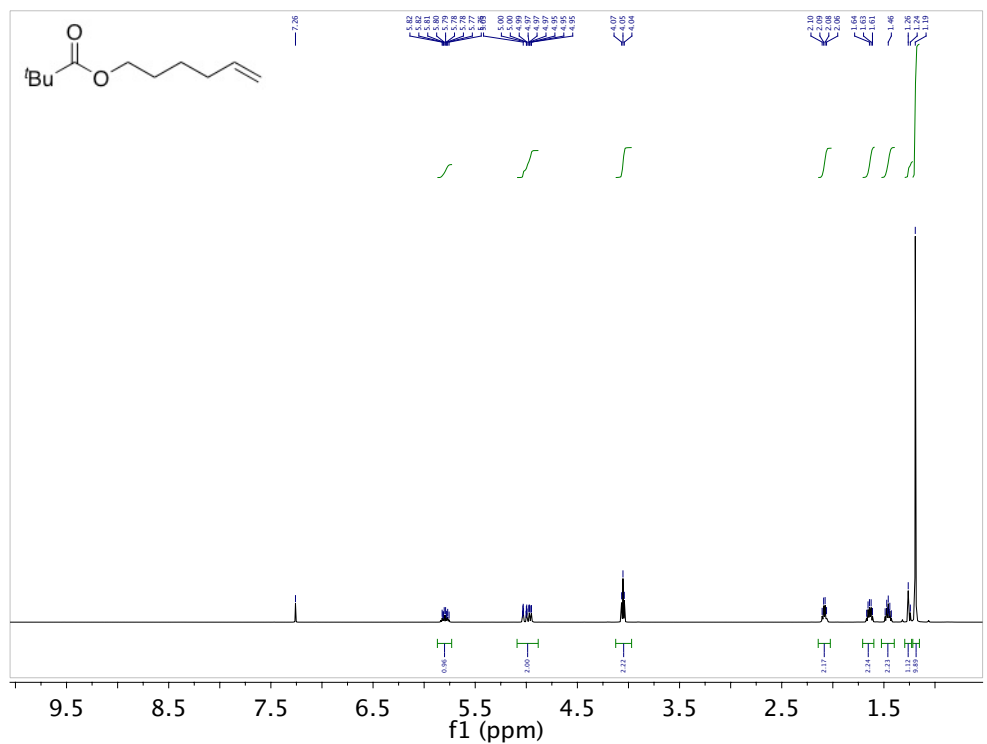


Figure 6-2: Spectra for Hex-5-enyl Pivalate

1-(but-3-enyl)-1H-indole

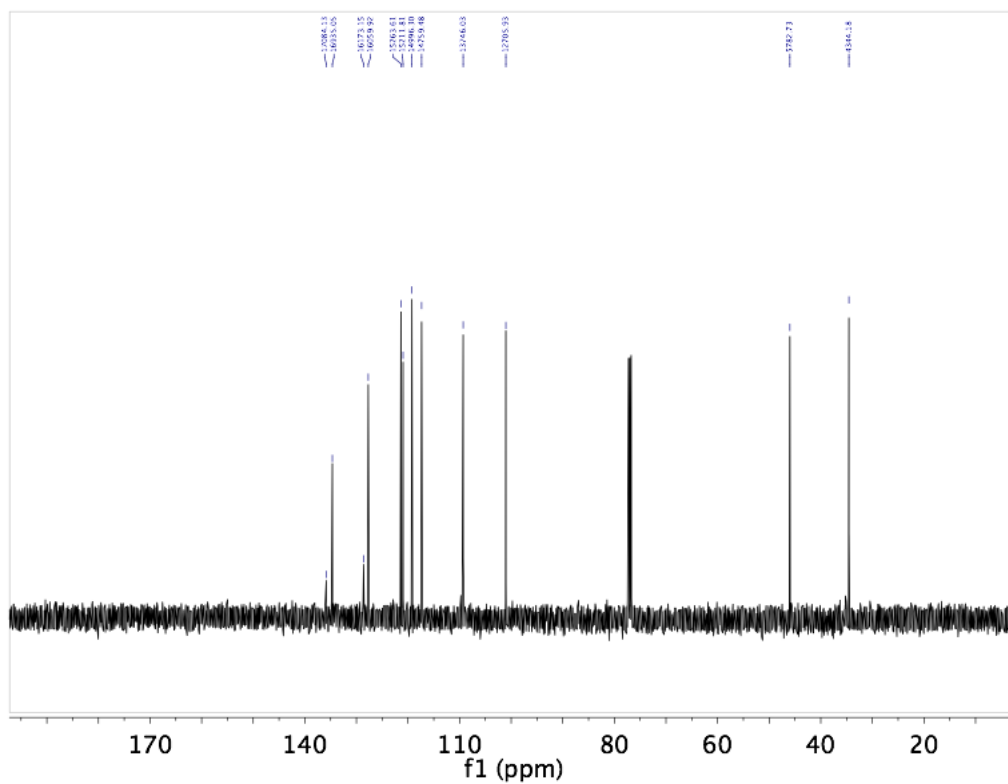
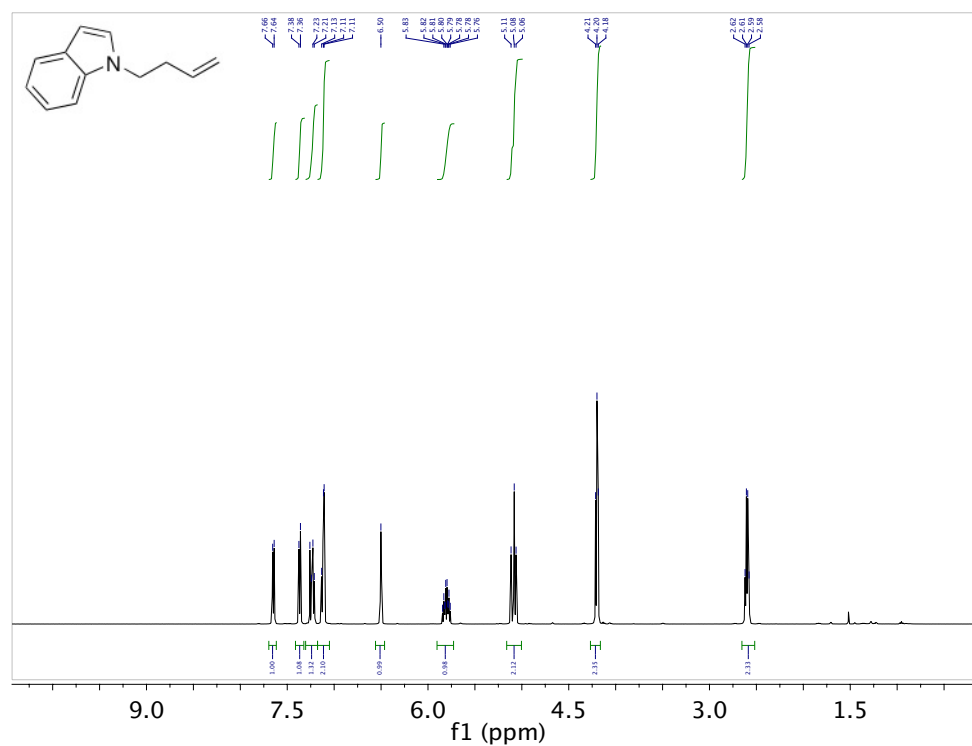


Figure 6-3: Spectra for 1-(But-3-enyl)-1H-indole

4,4,5,5-tetramethyl-2-(4-phenylbutan-2-yl)-1,3,2-dioxaborolane (2-1)

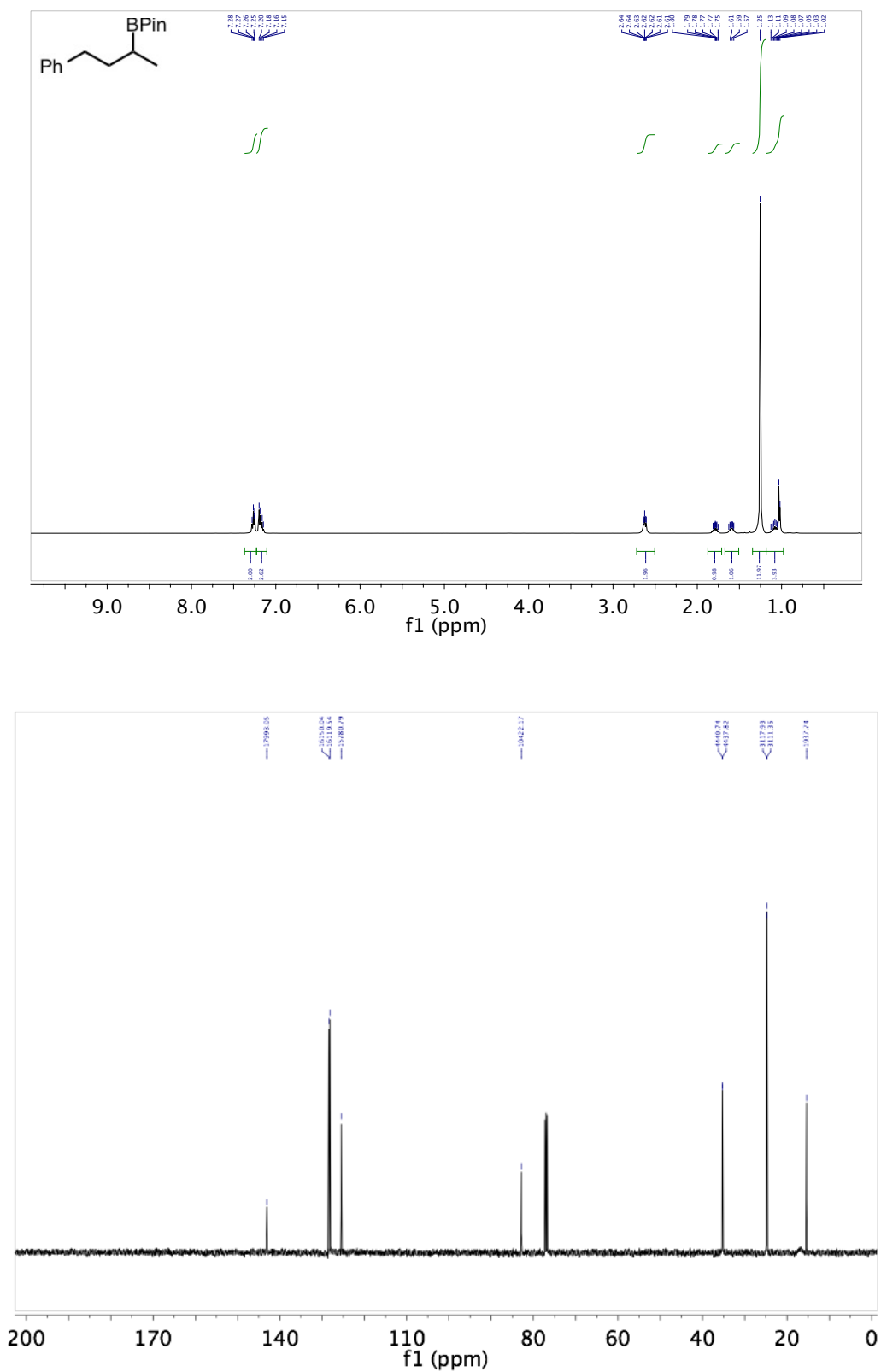


Figure 6-4: Spectra for Compound 2-1

4,4,5,5-tetramethyl-2-(octan-2-yl)-1,3,2-dioxaborolane (2-27)

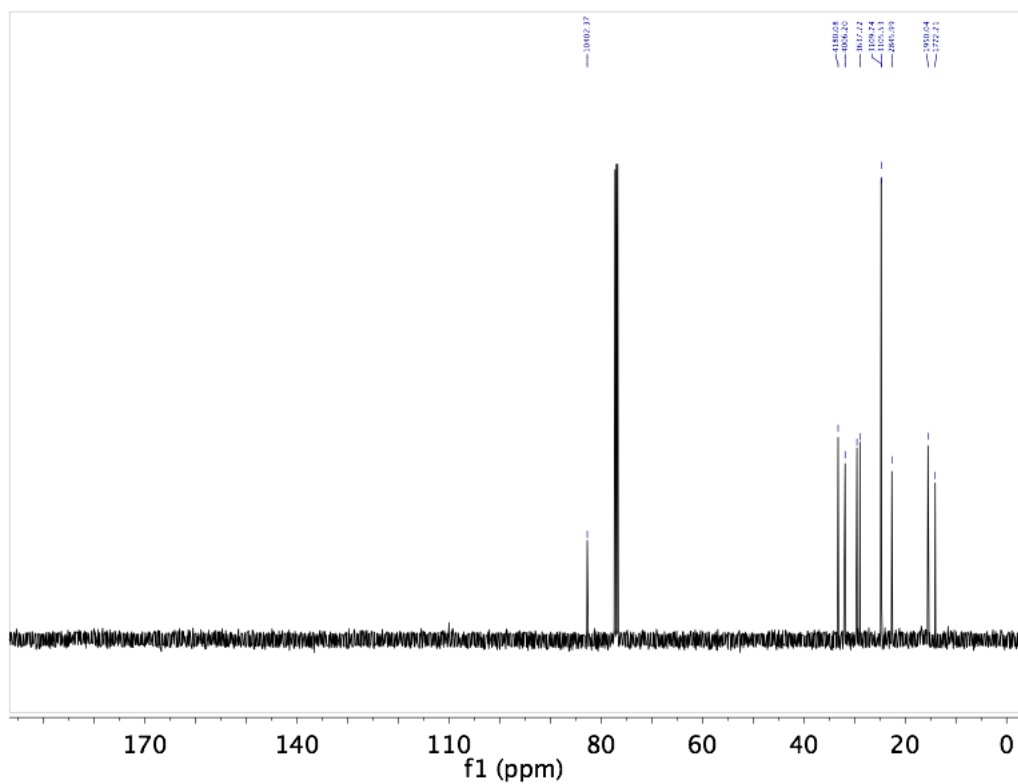
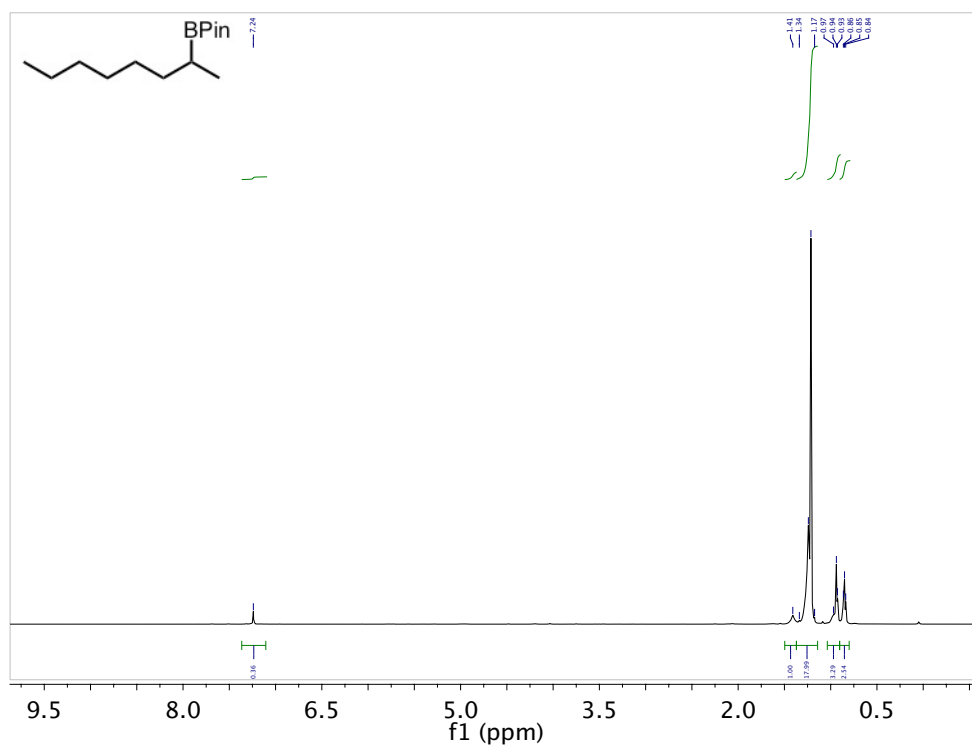


Figure 6-5: Spectra for Compound 2-27

2-(1-cyclohexylethyl)-4,4,5,5-tetramethyl-1,3,2-dioxaborolane (2-28)

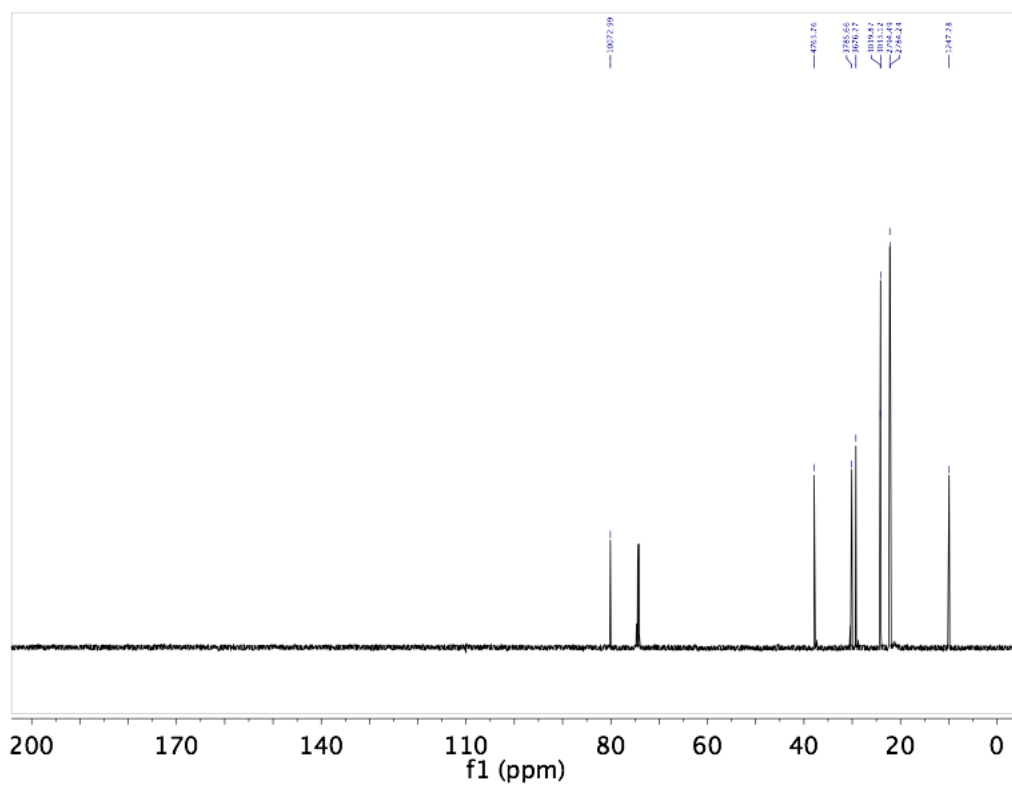
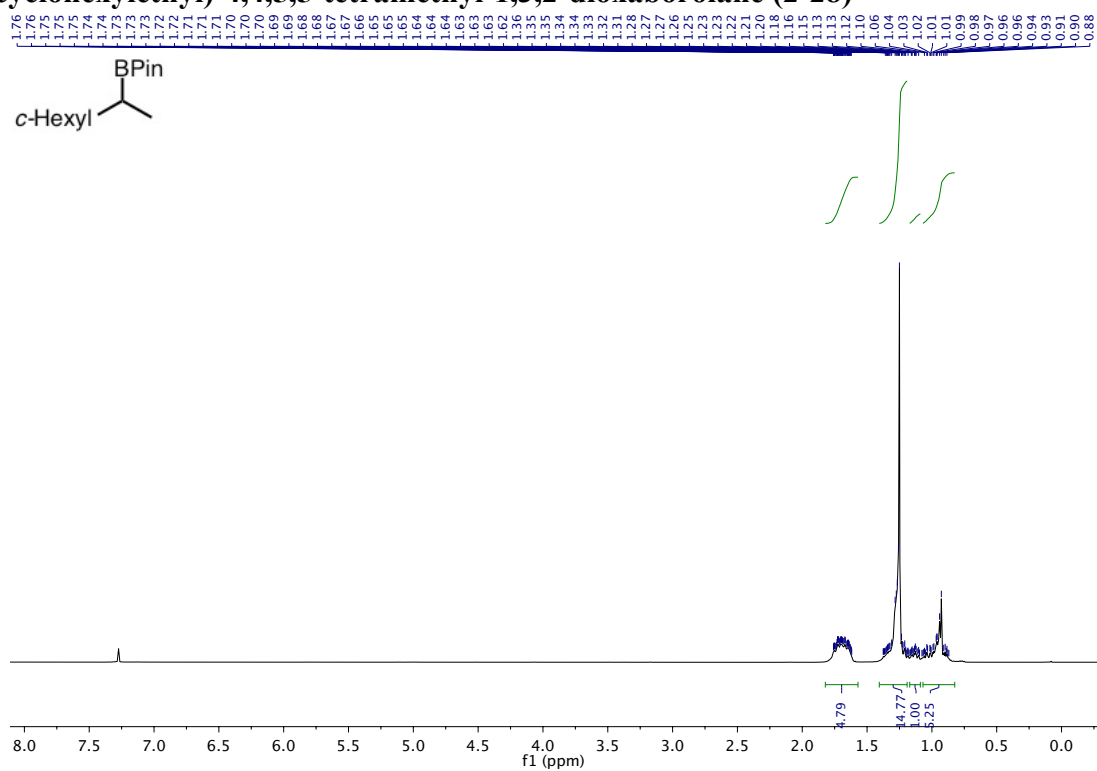


Figure 6-6: Spectra for Compound 2-28

2-(4,8-dimethylnon-7-en-2-yl)-4,4,5,5-tetramethyl-1,3,2-dioxaborolane (2-29)

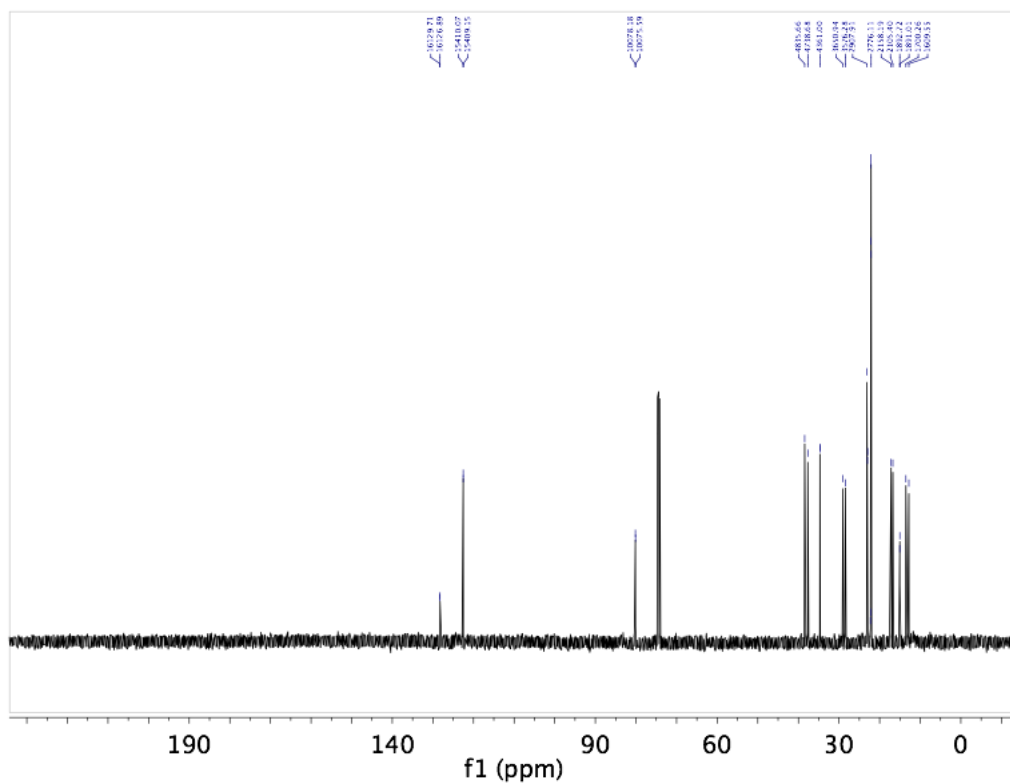
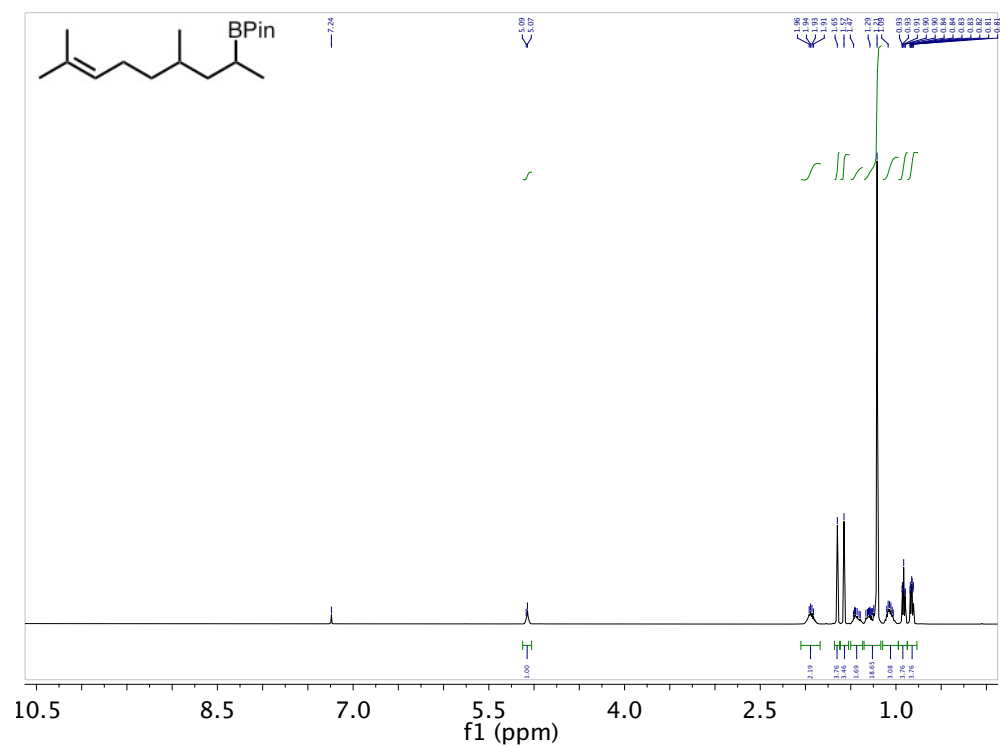


Figure 6-7: Spectra for Compound 2-29

4,4,5,5-tetramethyl-2-(1-(2-methylenecyclohexyl)propan-2-yl)-1,3,2-dioxaborolane (2-30)

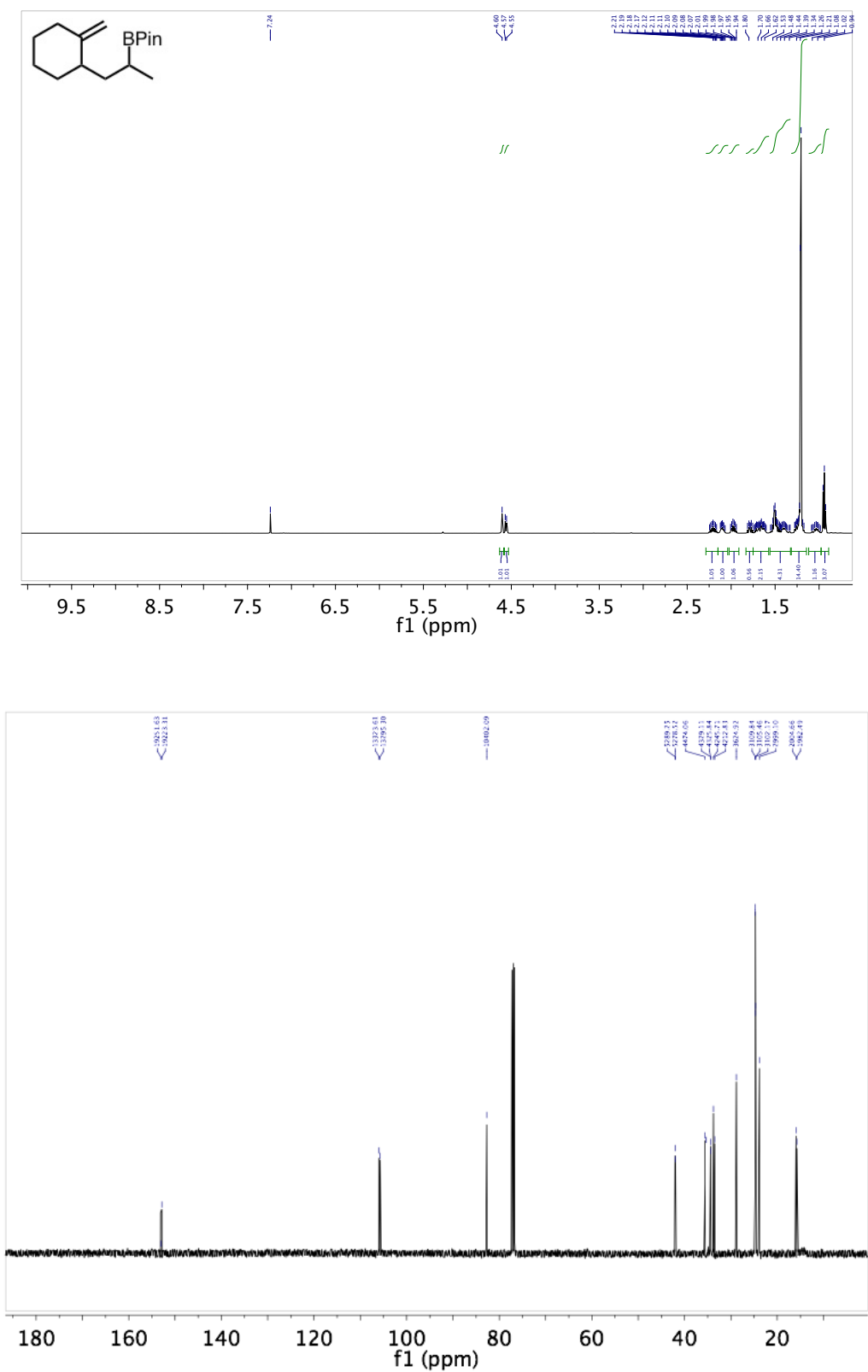


Figure 6-8: Spectra for Compound 2-30

2-(6-(benzyloxy)hexan-2-yl)-4,4,5,5-tetramethyl-1,3,2-dioxaborolane (2-31)

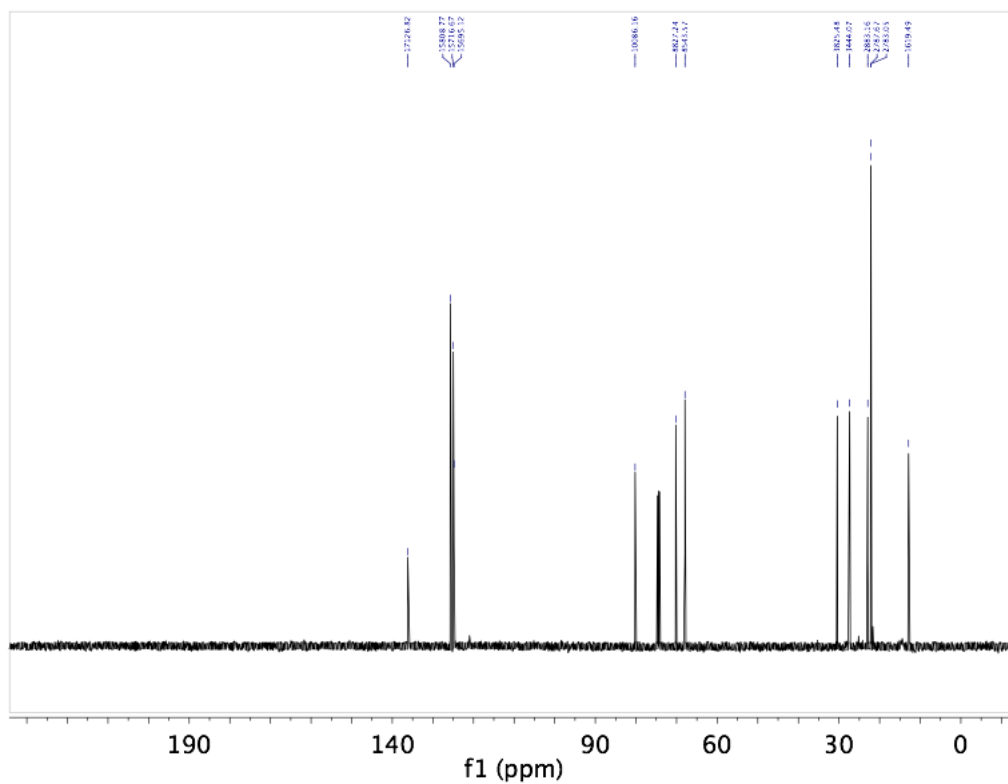
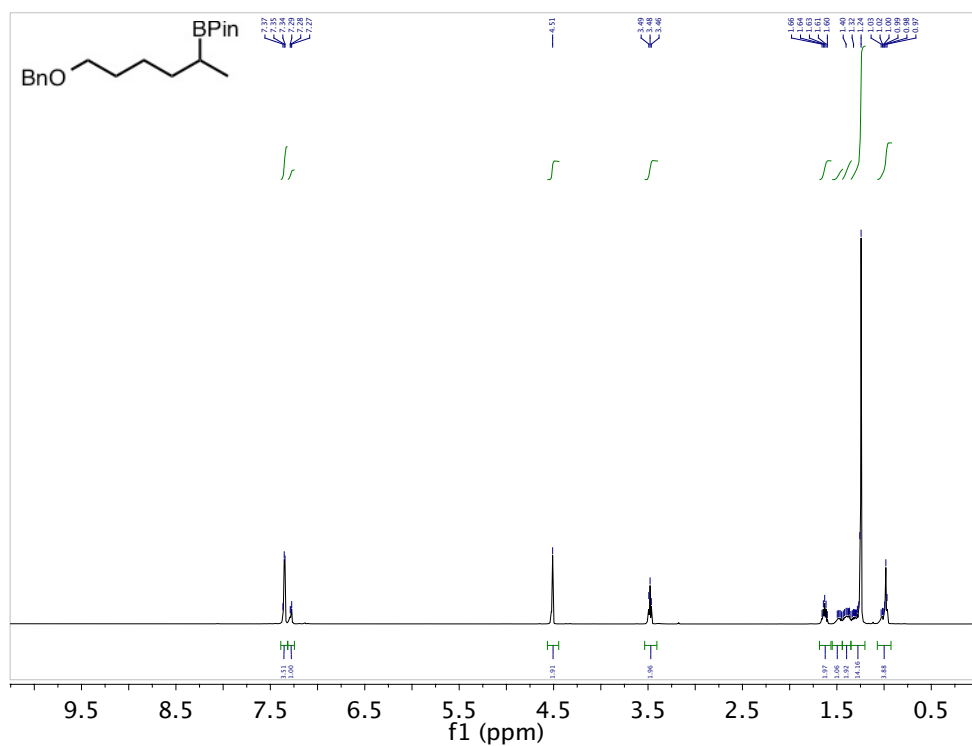


Figure 6-9: Spectra for Compound 2-32

tert-butyldimethyl(4-(4,4,5,5-tetramethyl-1,3,2-dioxaborolan-2-yl)pentyl)oxy)silane (2-32)

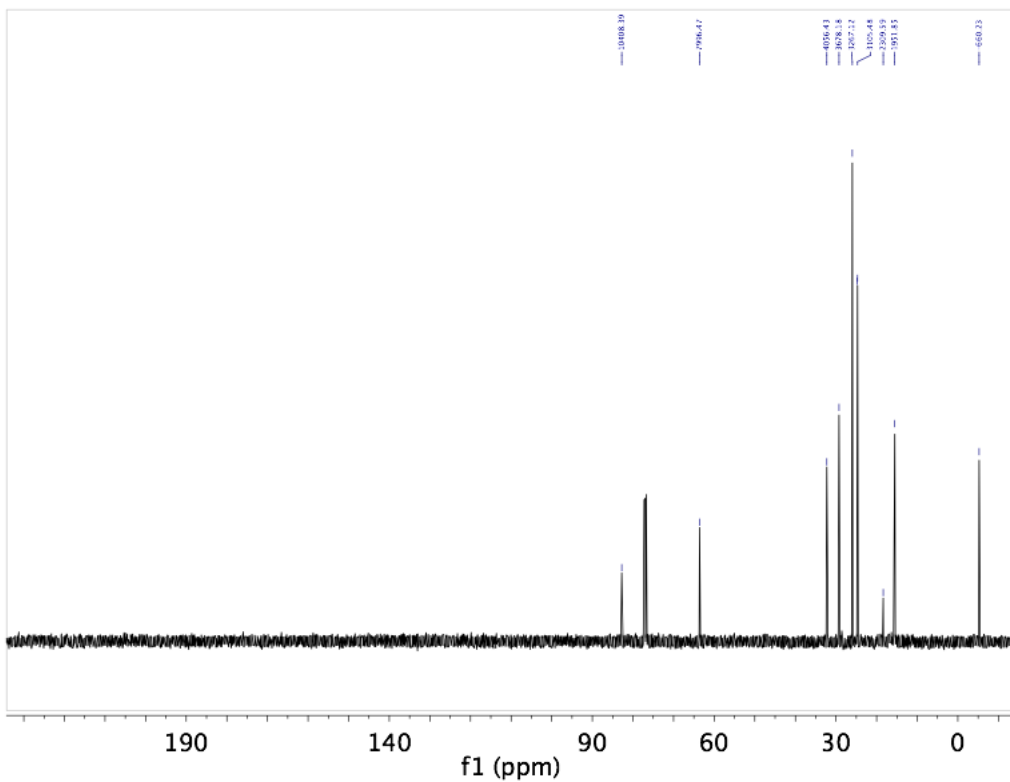
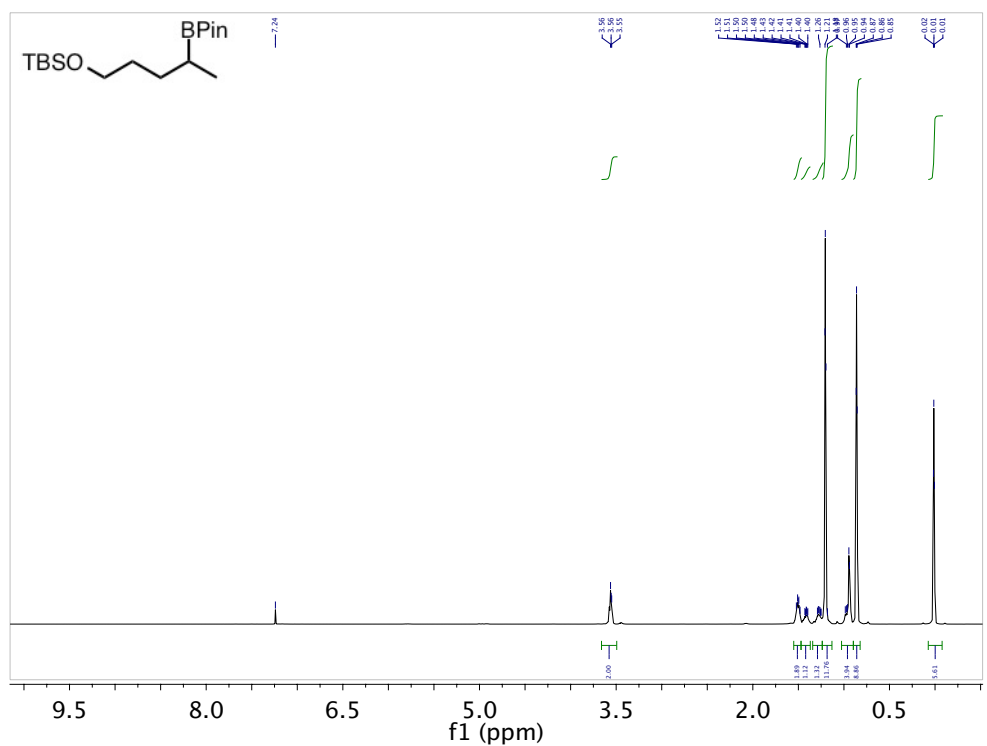


Figure 6-10: Spectra for Compound 2-32

5-(4,4,5,5-tetramethyl-1,3,2-dioxaborolan-2-yl)hexan-1-ol (2-33)

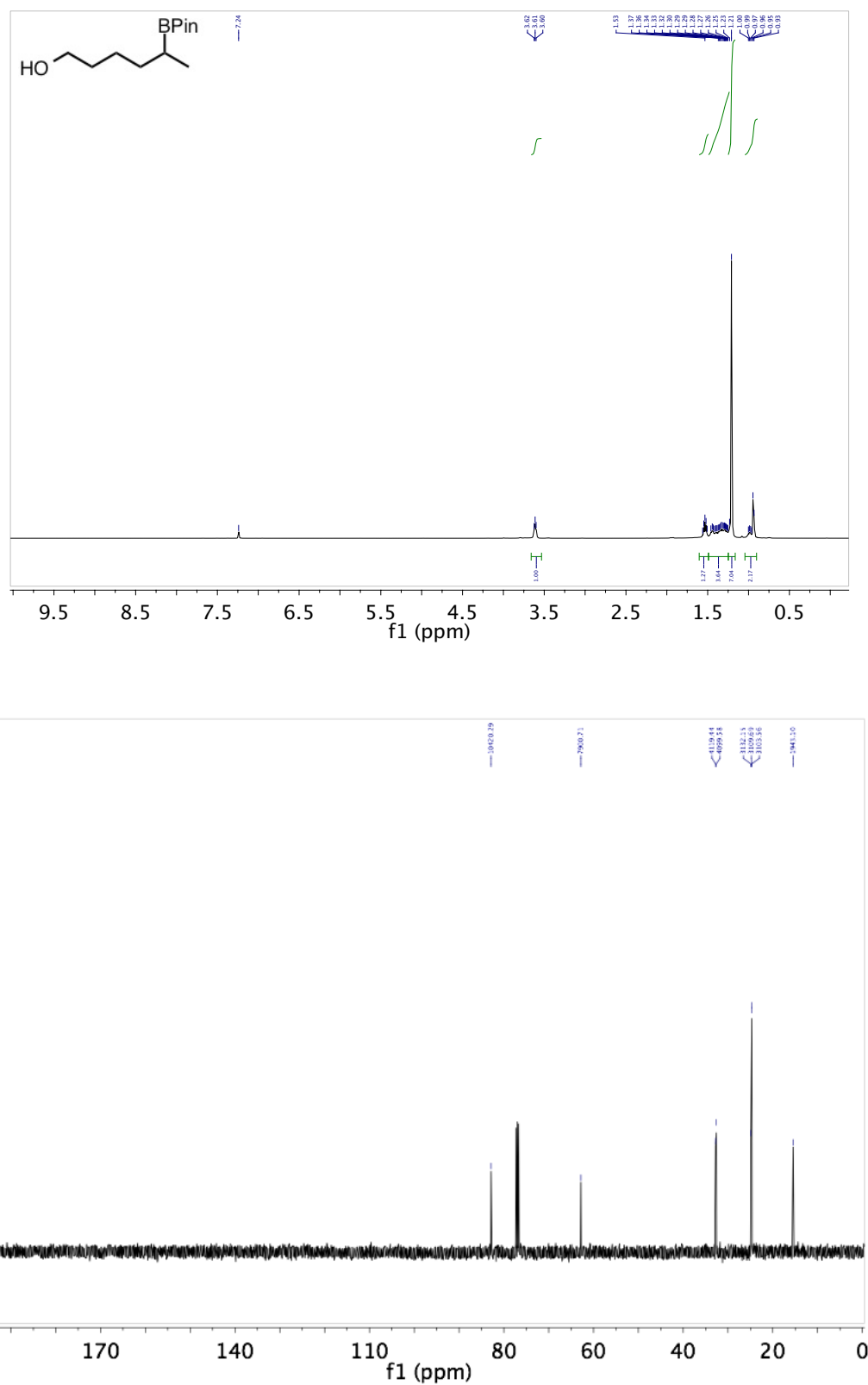


Figure 6-11: Spectra for Compound 2-33

5-(4,4,5,5-tetramethyl-1,3,2-dioxaborolan-2-yl)hexyl pivalate (2-34)

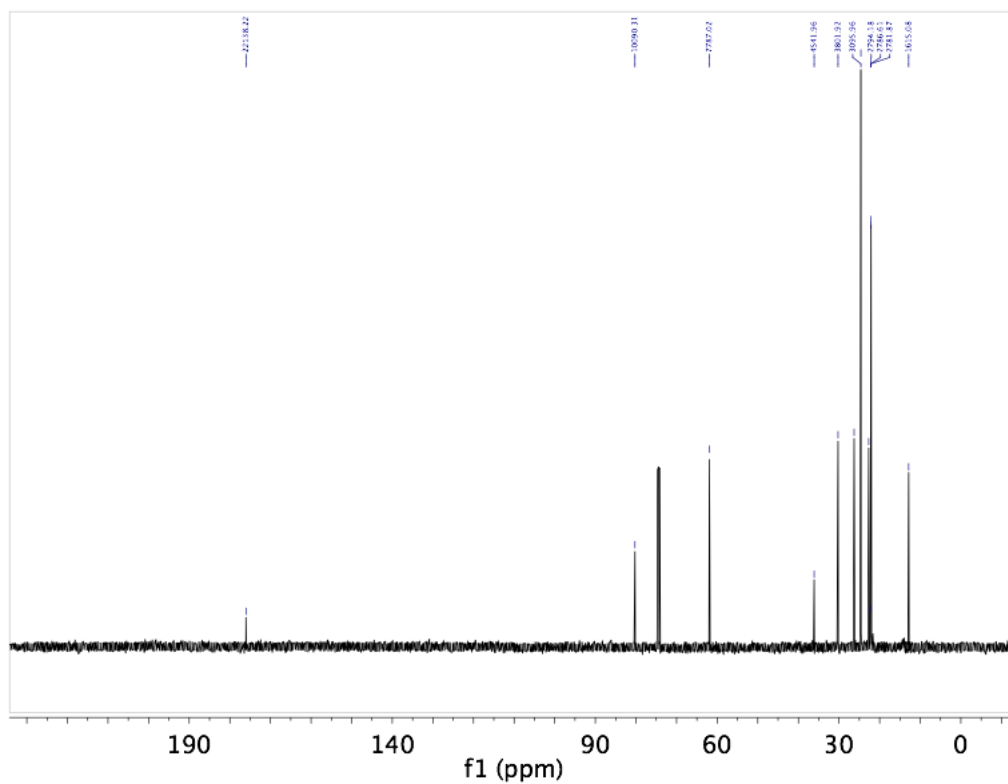
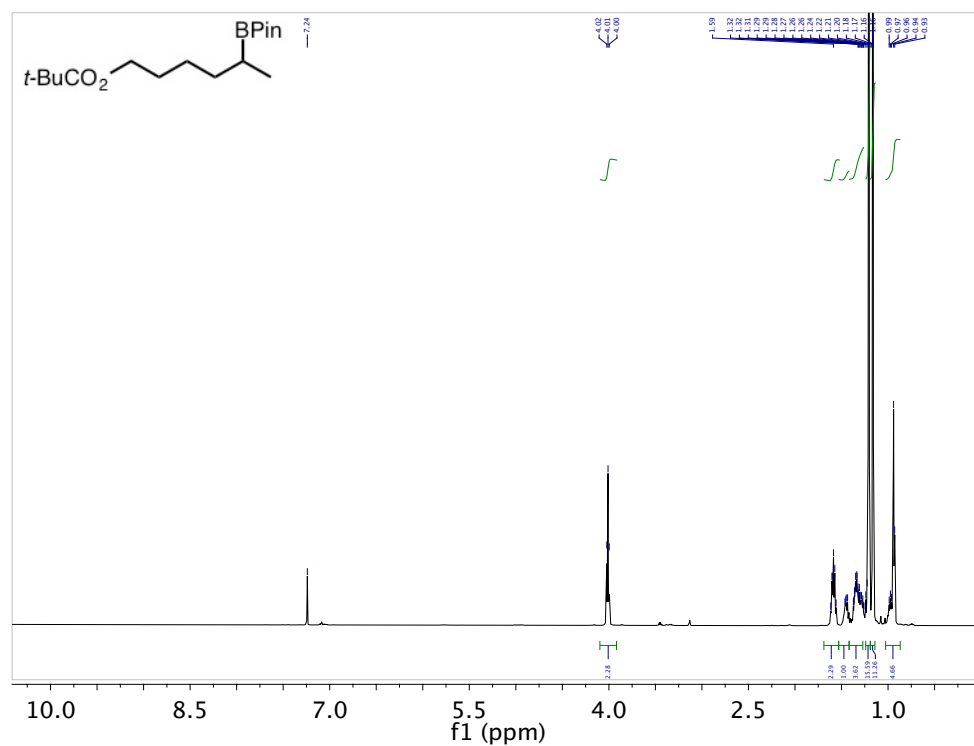


Figure 6-12: Spectra for Compound 2-34

2-(4-(2-bromophenyl)butan-2-yl)-4,4,5,5-tetramethyl-1,3,2-dioxaborolane (2-35)

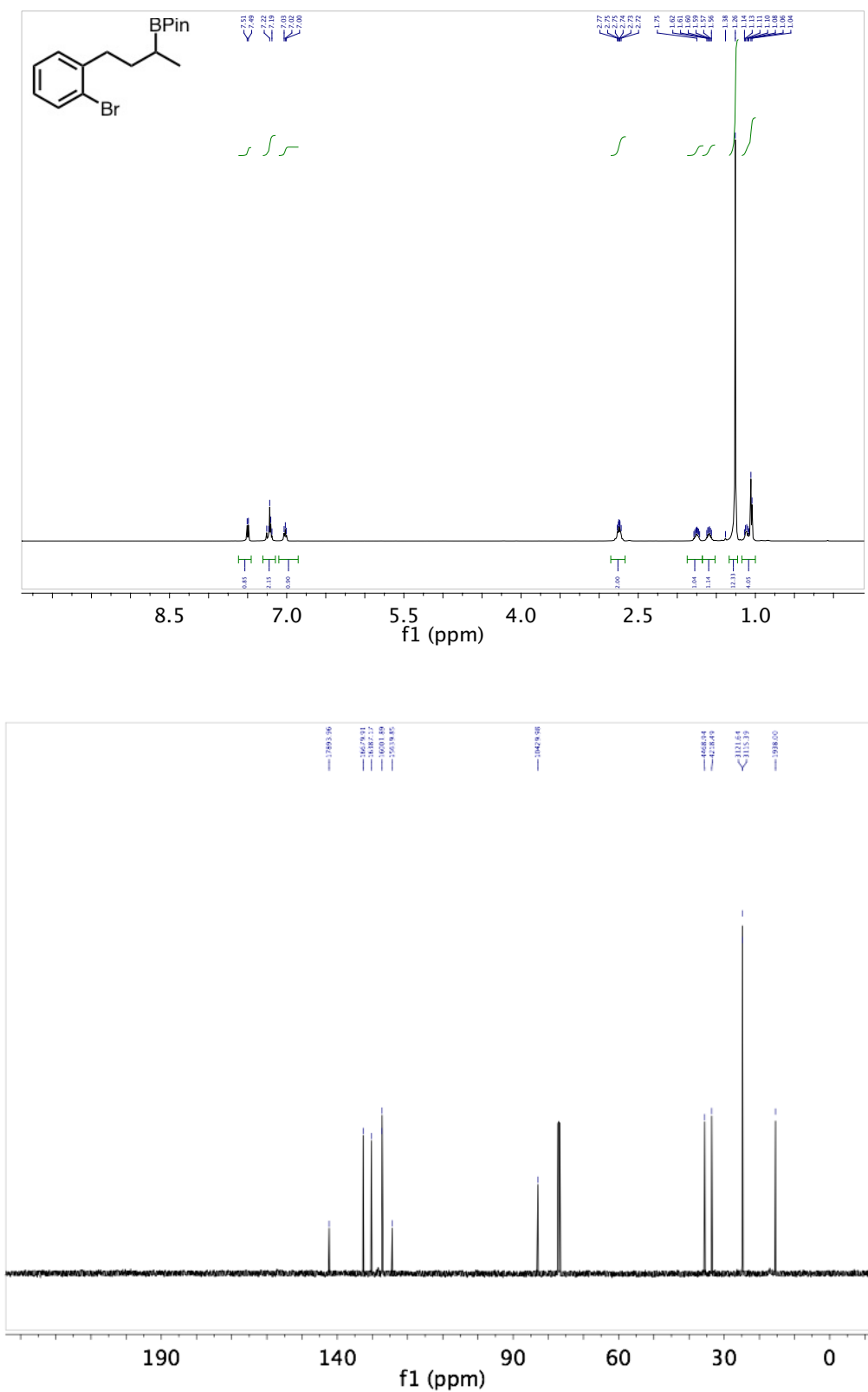


Figure 6-13: Spectra for Compound 2-35

4,4,5,5-tetramethyl-2-(1-phenylpropan-2-yl)-1,3,2-dioxaborolane (2-36)

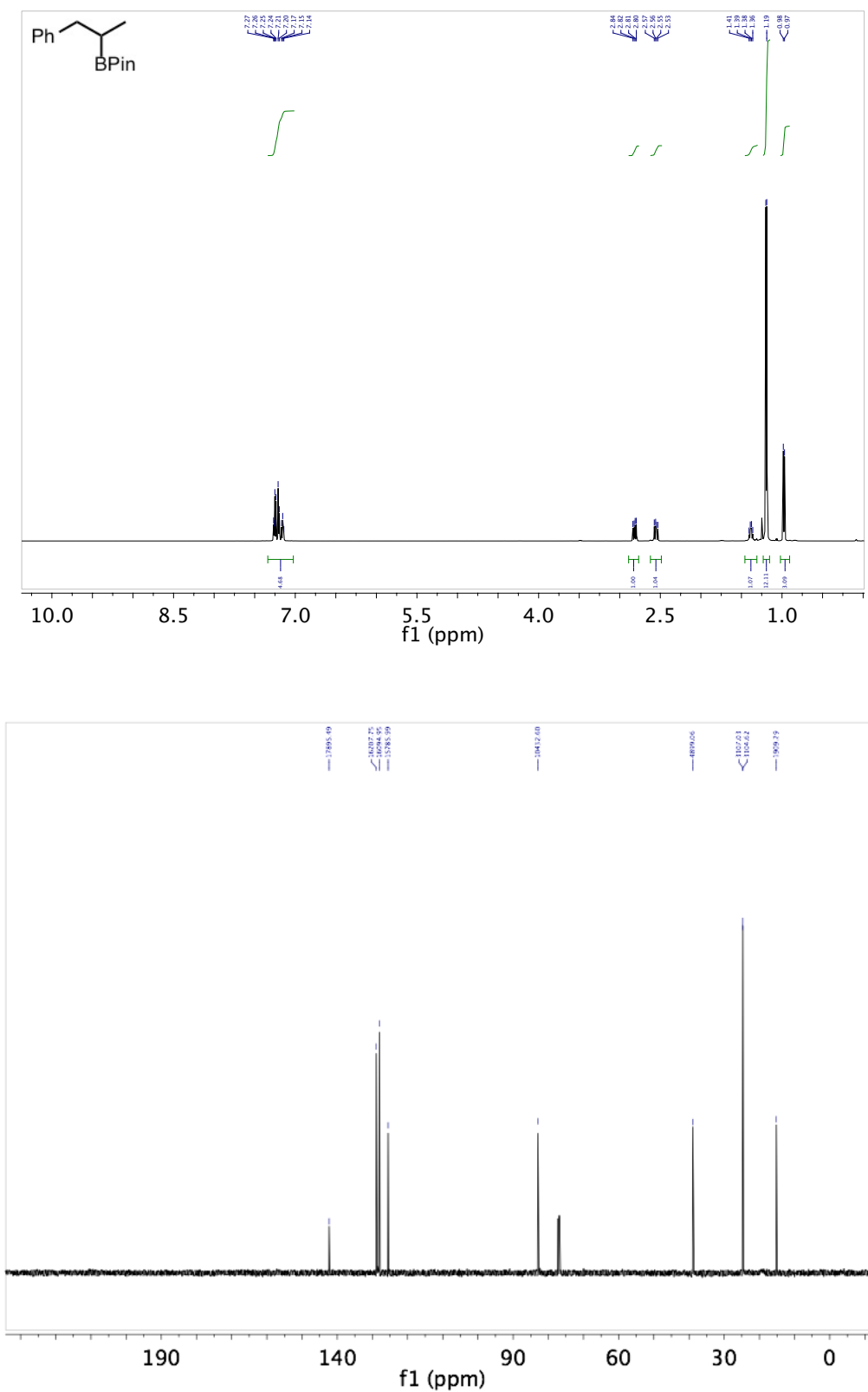


Figure 6-14: Spectra for Compound 2-36

trimethyl(2-(4,4,5,5-tetramethyl-1,3,2-dioxaborolan-2-yl)propyl)silane (2-37)

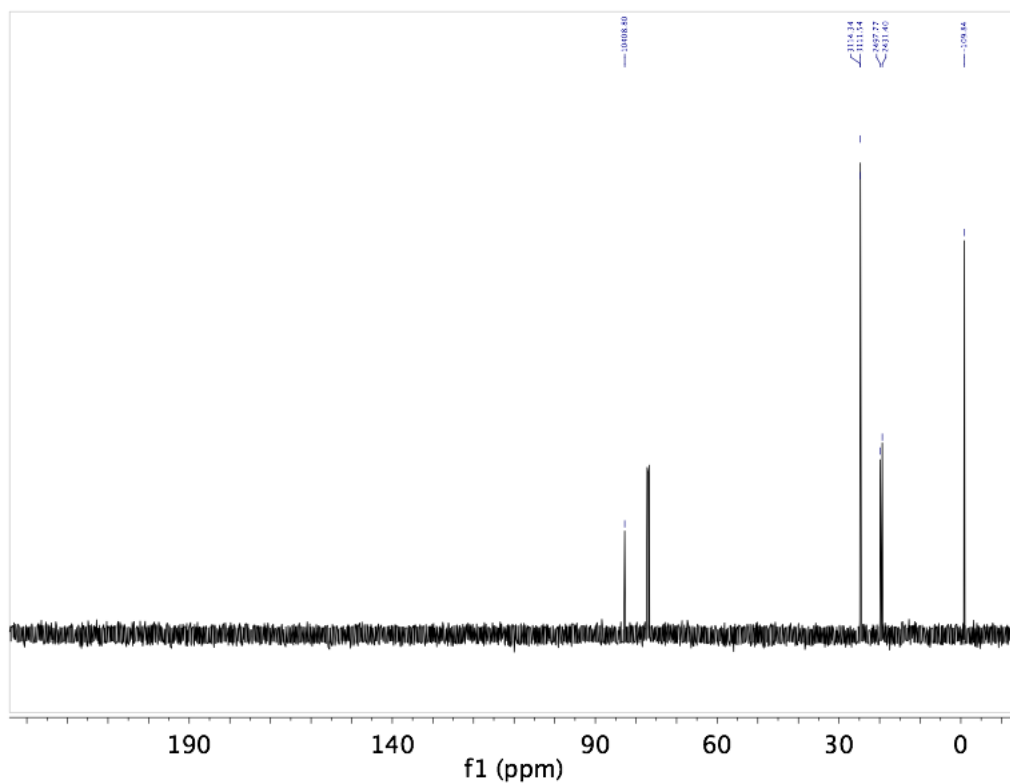
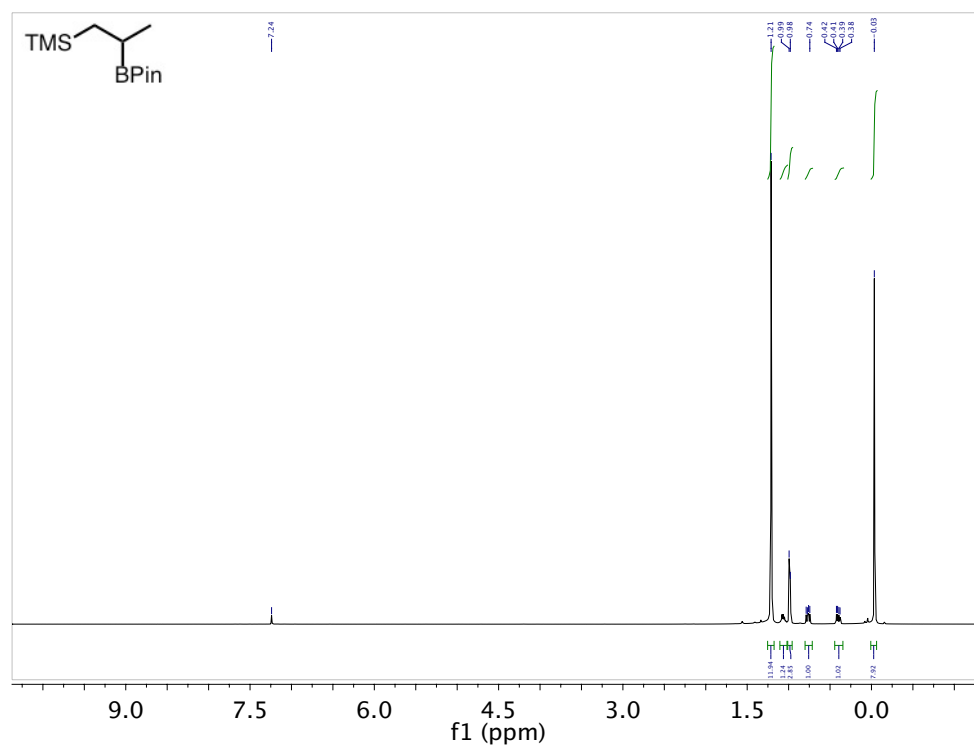


Figure 6-15: Spectra for Compound 2-37

1-(2-(4,4,5,5-tetramethyl-1,3,2-dioxaborolan-2-yl)propyl)-1*H*-indole (2-38)

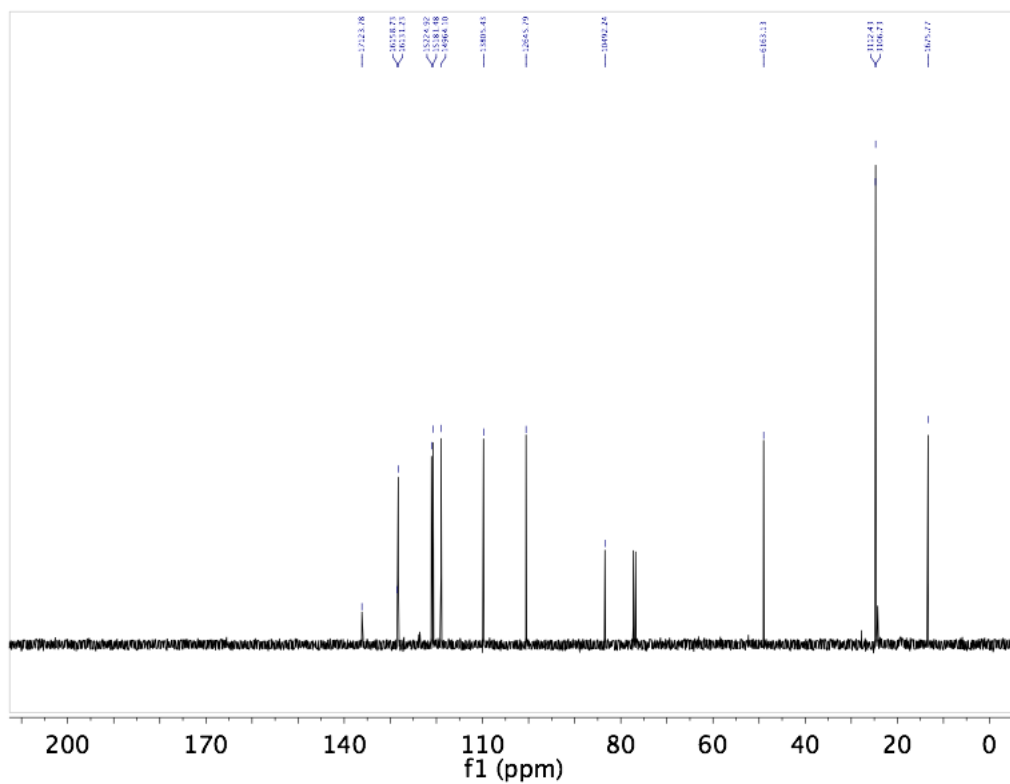
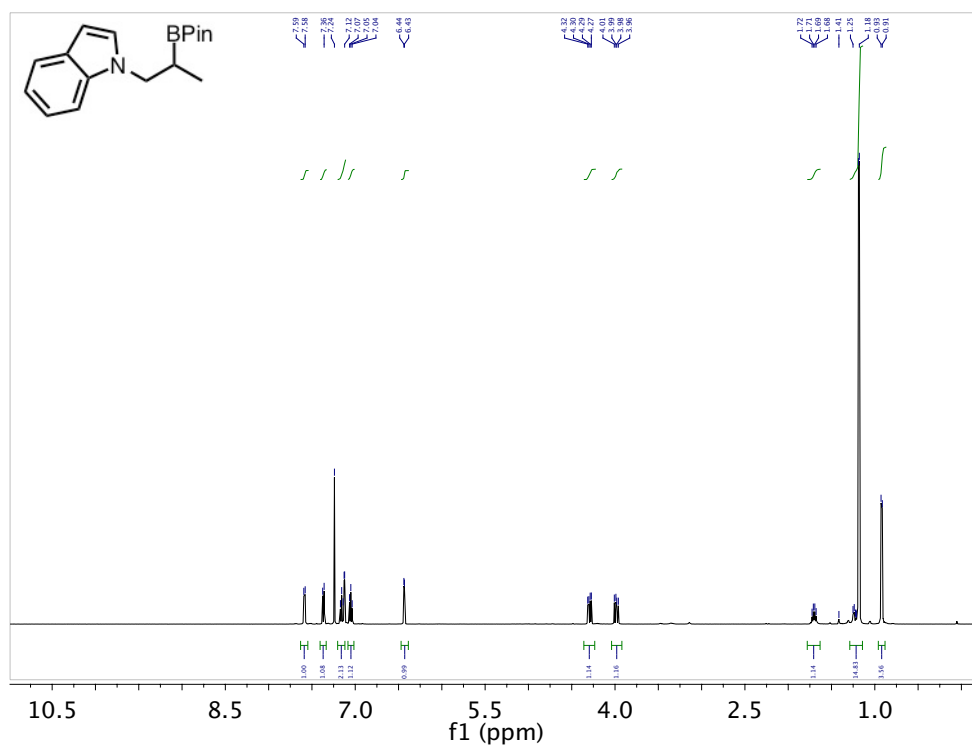


Figure 6-16: Spectra for Compound 2-38

1-(3-(4,4,5,5-tetramethyl-1,3,2-dioxaborolan-2-yl)propyl)-1*H*-indole

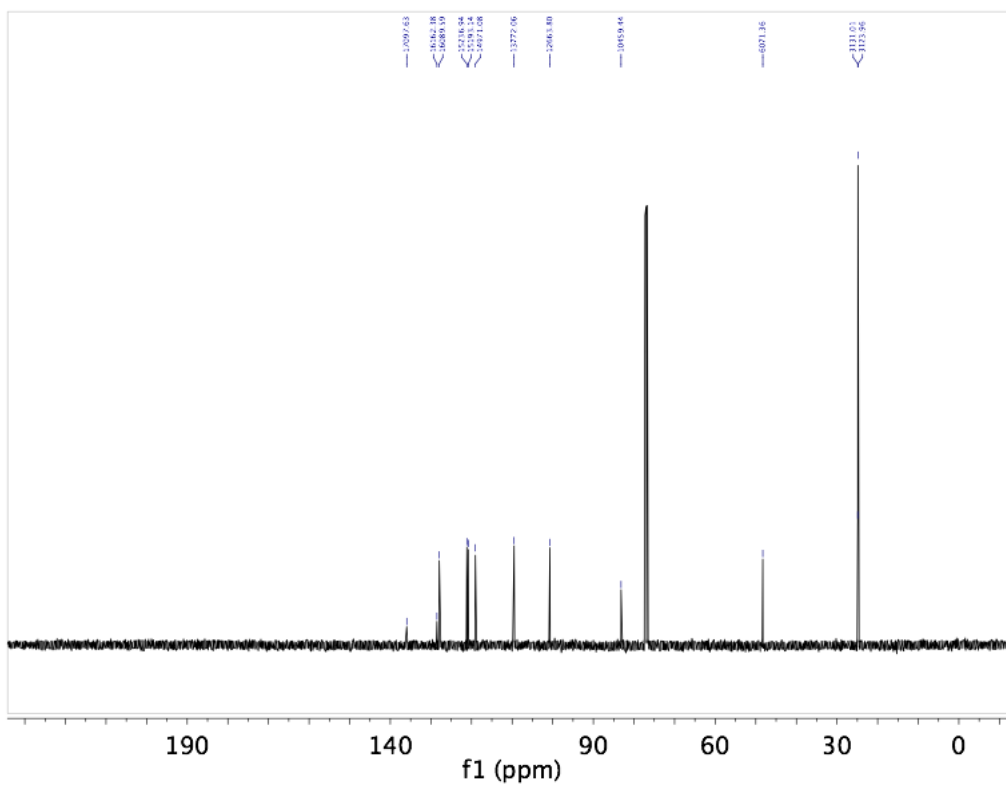
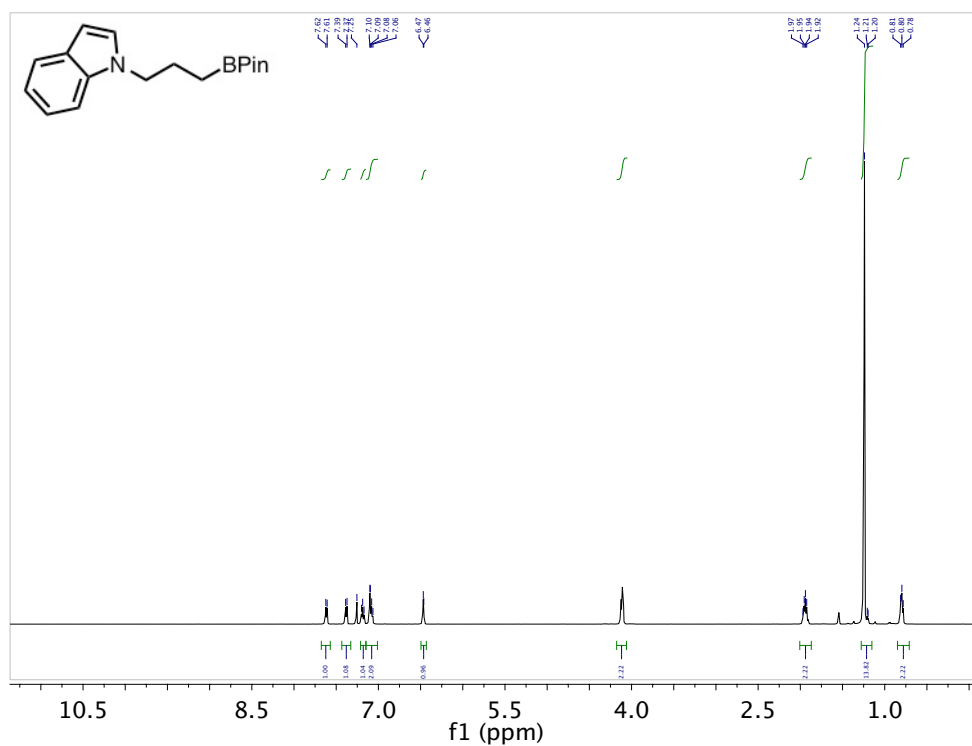


Figure 6-17: Spectra for 1-(3-(4,4,5,5-Tetramethyl-1,3,2-dioxaborolan-2-yl)propyl)-1*H*-indole

1-(3-(4,4,5,5-tetramethyl-1,3,2-dioxaborolan-2-yl)butyl)-1H-indole (2-39)

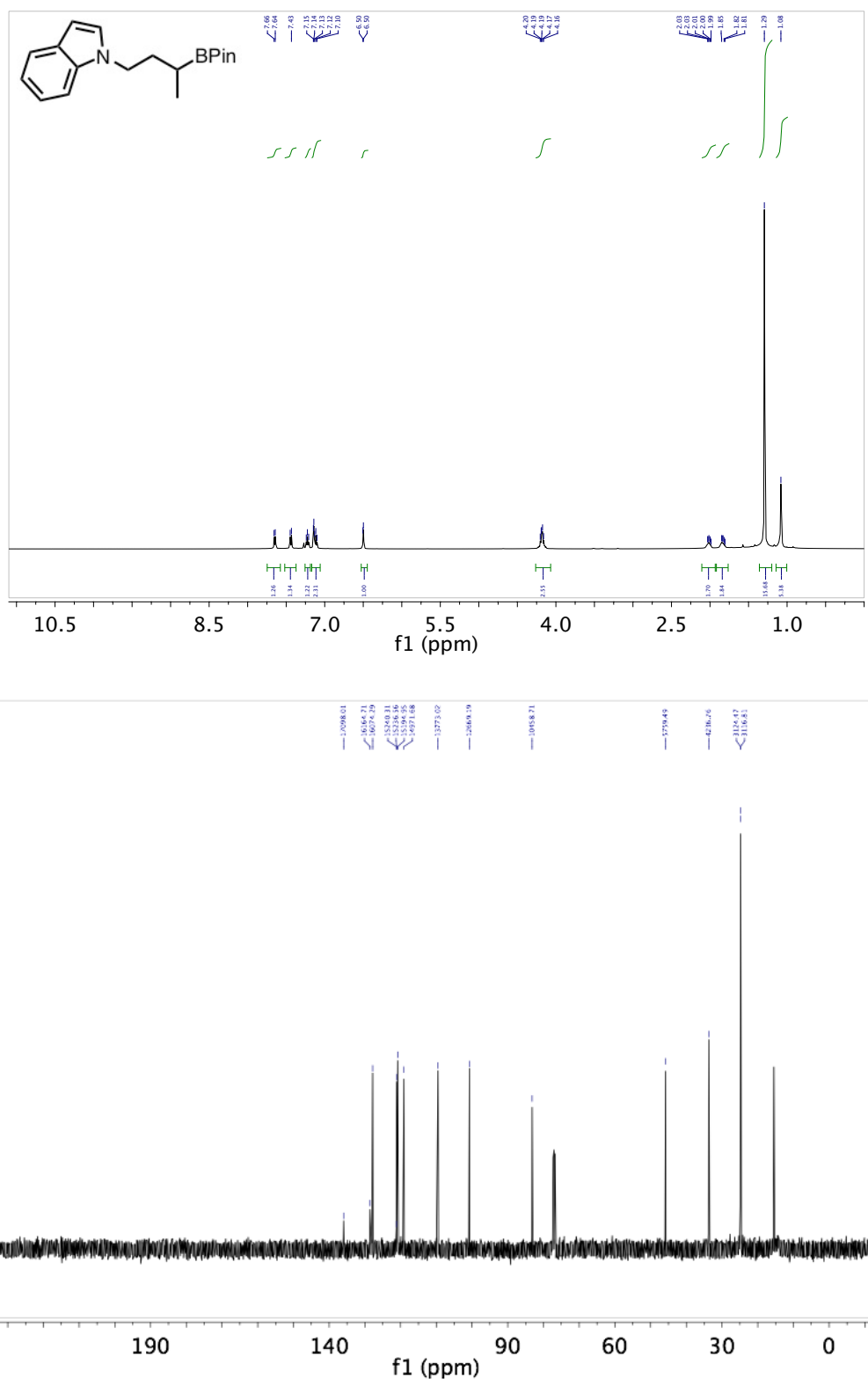


Figure 6-18: Spectra for Compound 2-39

Potassium (4-phenylbutan-2-yl)trifluoroborate

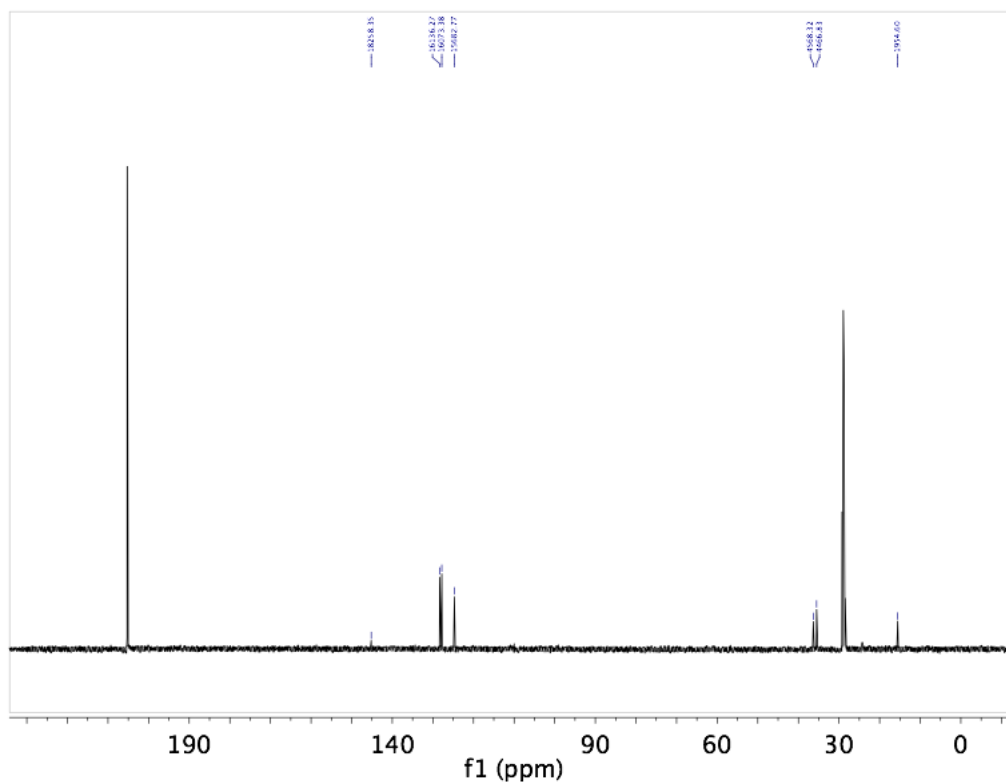
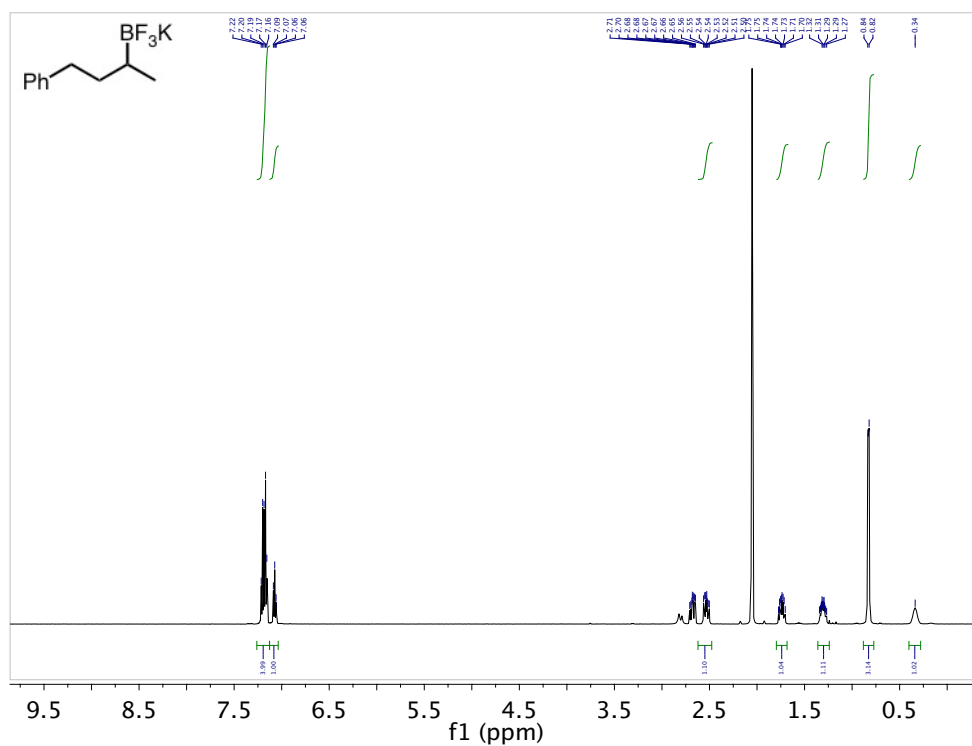


Figure 6-19: Spectra for Potassium (4-Phenylbutan-2-yl)trifluoroborate

Potassium trifluoro(6-hydroxyhexan-2-yl)borate

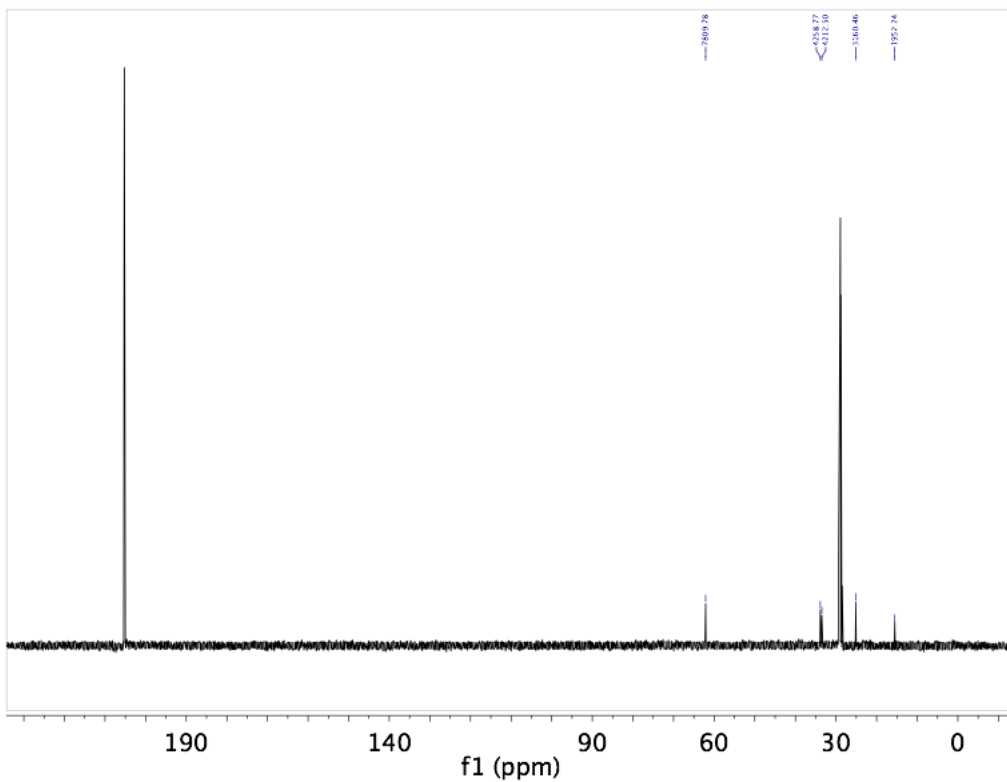
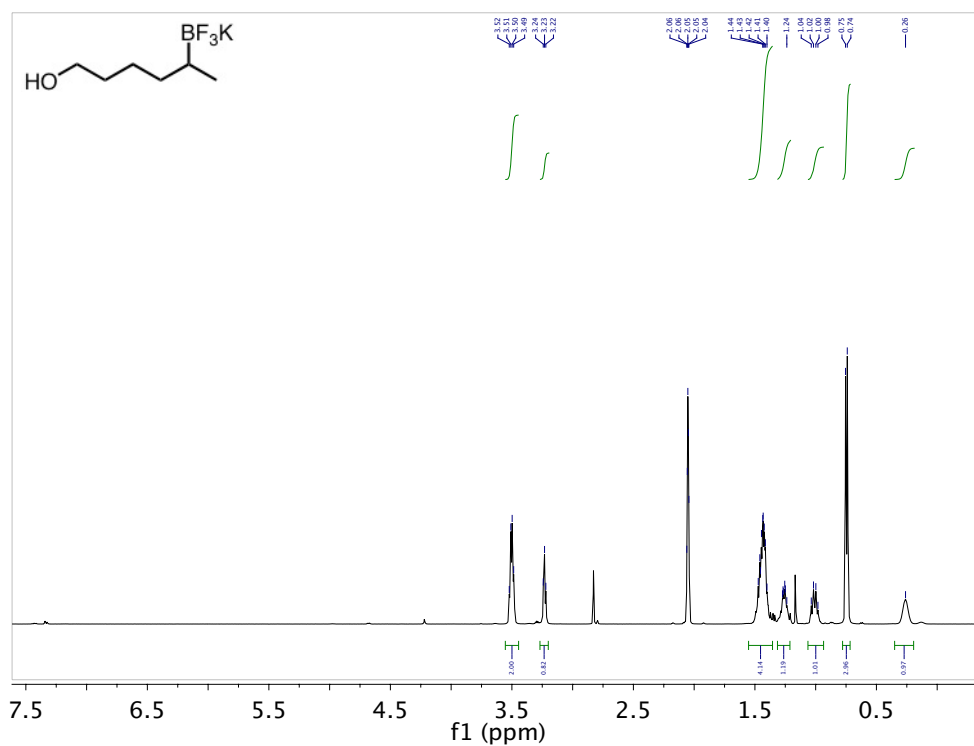


Figure 6-20: Spectra for Potassium (6-hydroxyhexan-2-yl)trifluoroborate

Potassium trifluoro(6-(pivaloyloxy)hexan-2-yl)borate

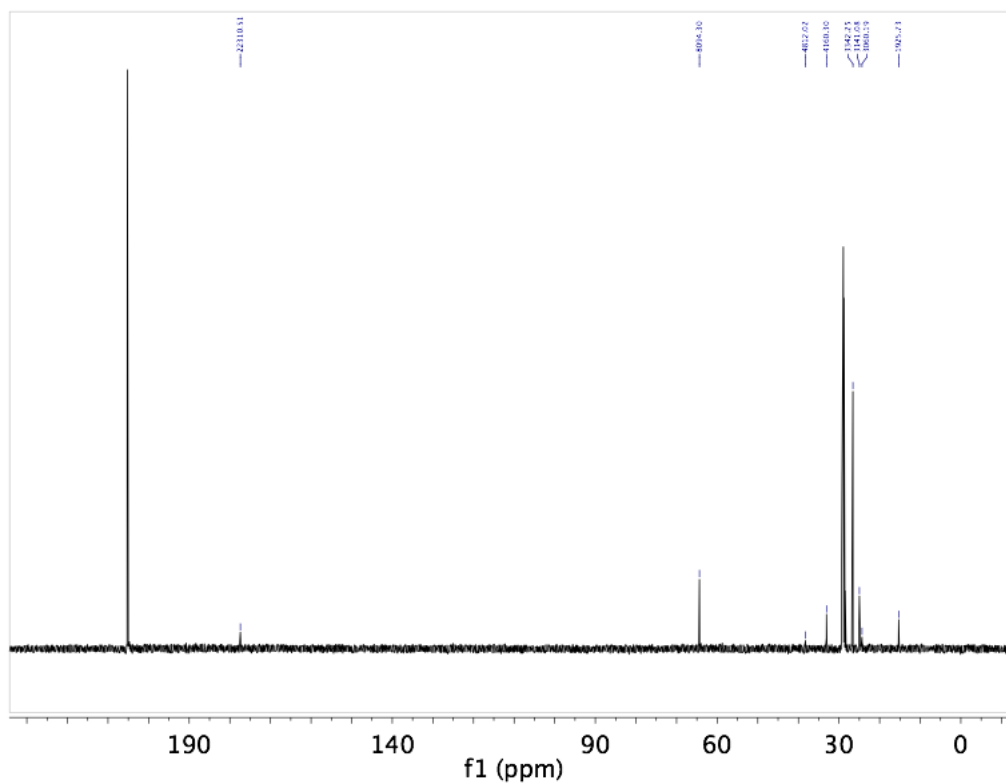
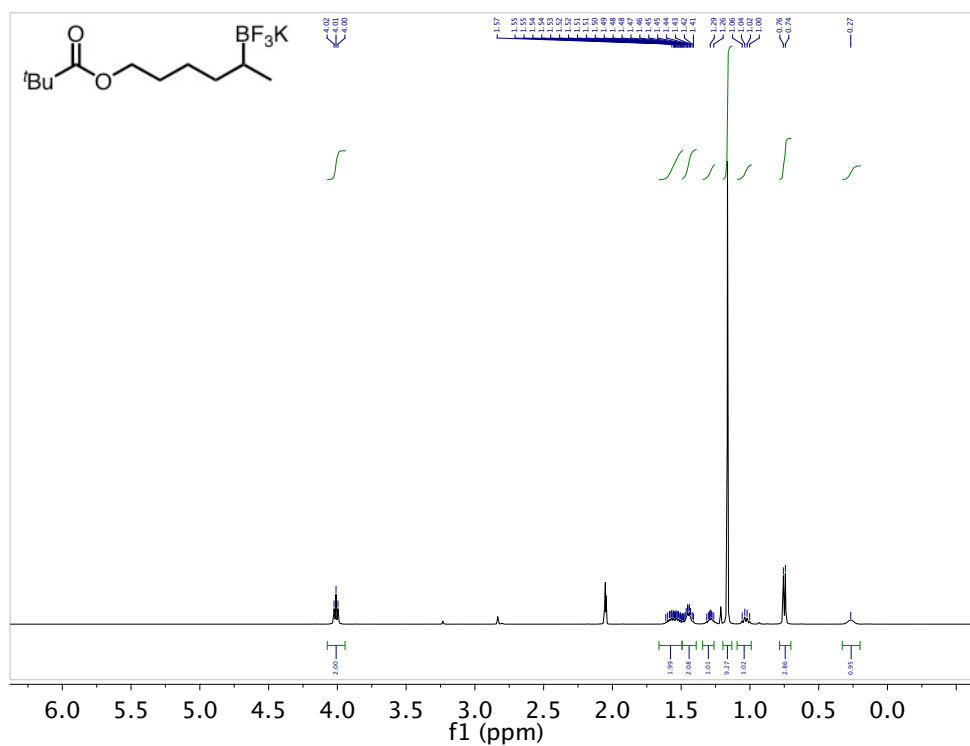


Figure 6-21: Spectra for Potassium (6-(pivaloyloxy)hexan2-yl)trifluoroborate

Potassium (4-(1*H*-indol-1-yl)butan-2-yl)trifluoroborate

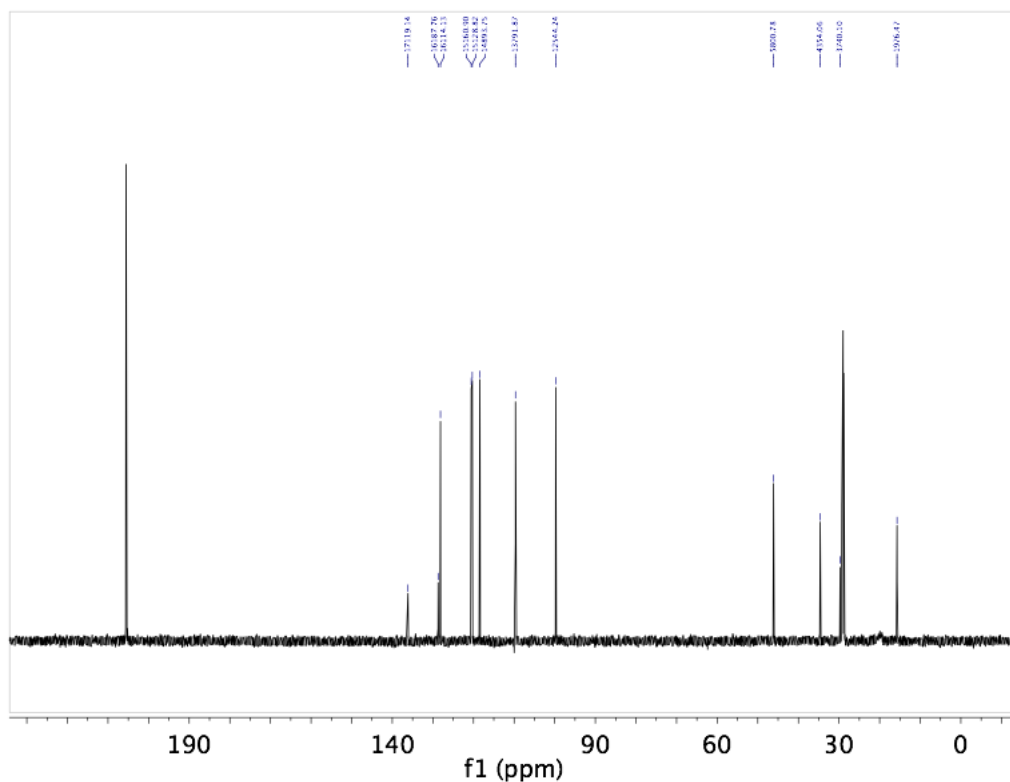
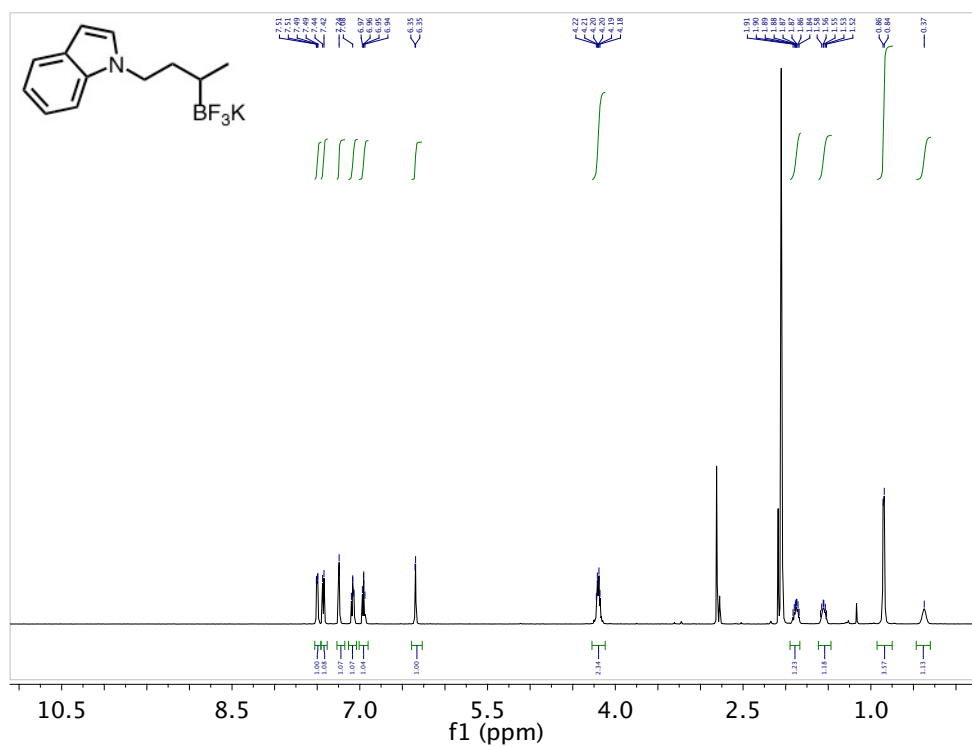


Figure 6-22: Spectra for Potassium (4-(1*H*-indol-1-yl)butan-2-yl)trifluoroborate

4-(4-phenylbutan-2-yl)biphenyl (2-52)

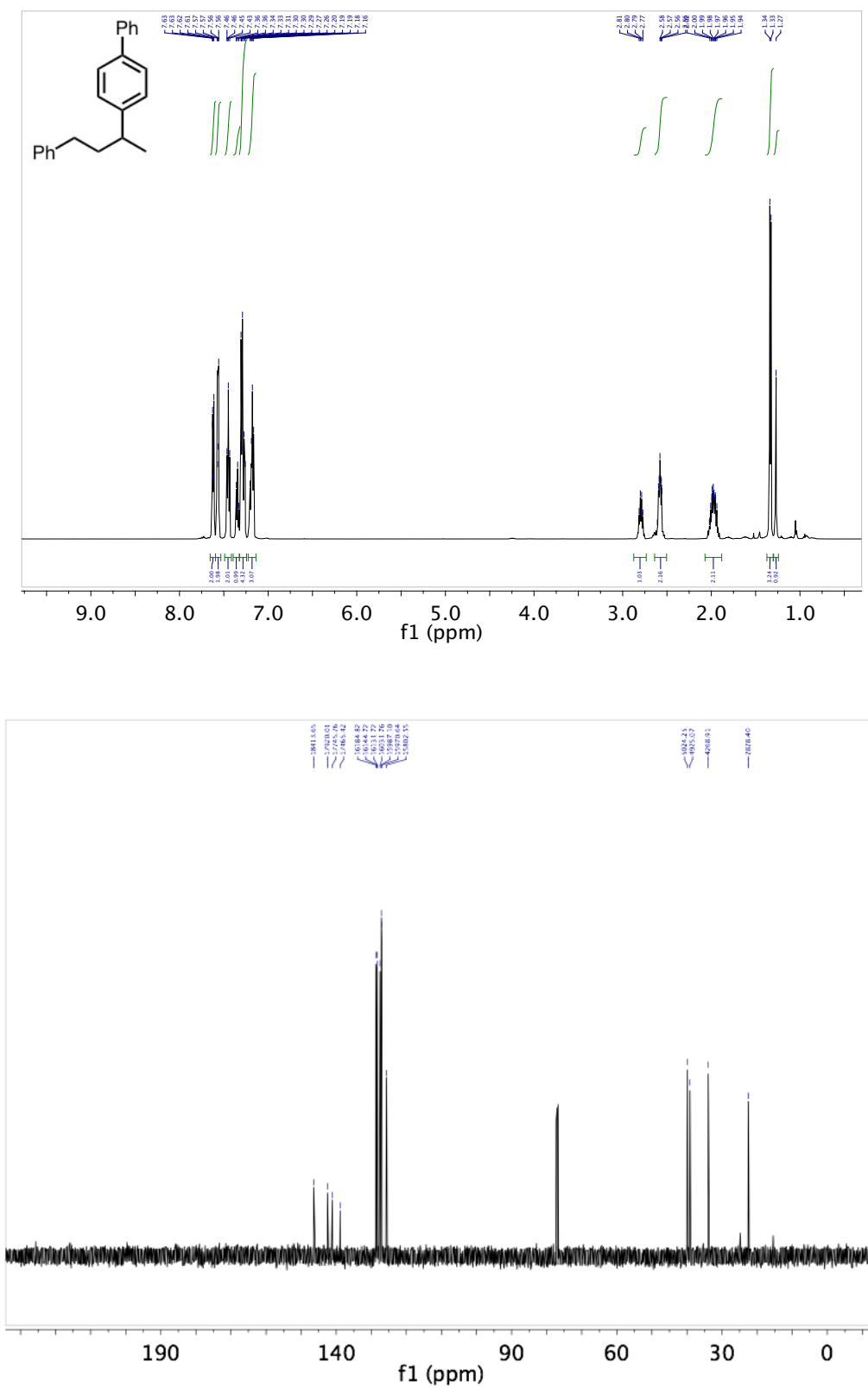


Figure 6-23: Spectra for 2-52

2-fluoro-5-(4-phenylbutan-2-yl)pyridine (2-53)

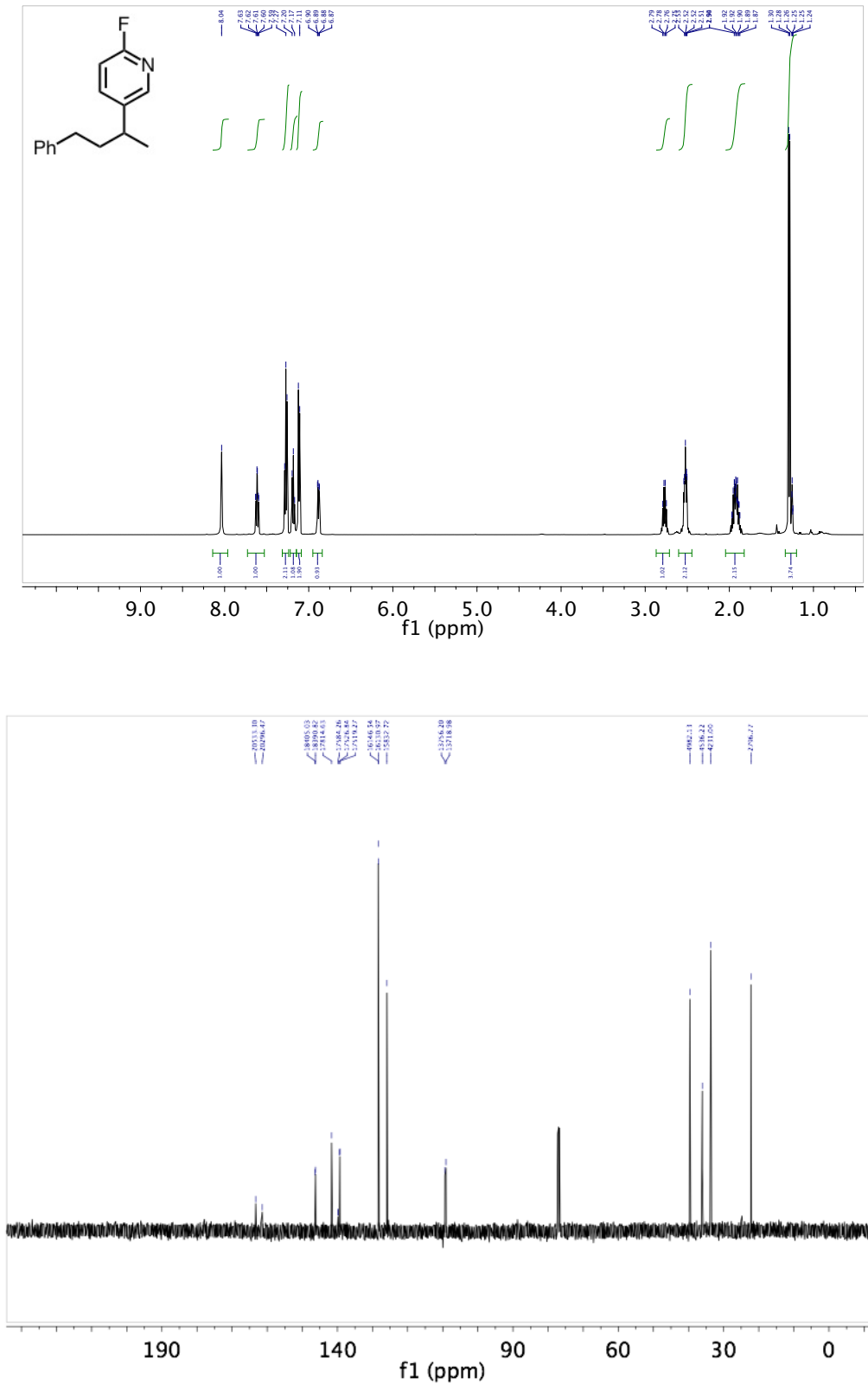


Figure 6-24: Spectra for 2-53

4-(4-Phenylbutan-2-yl)benzonitrile (2-54)

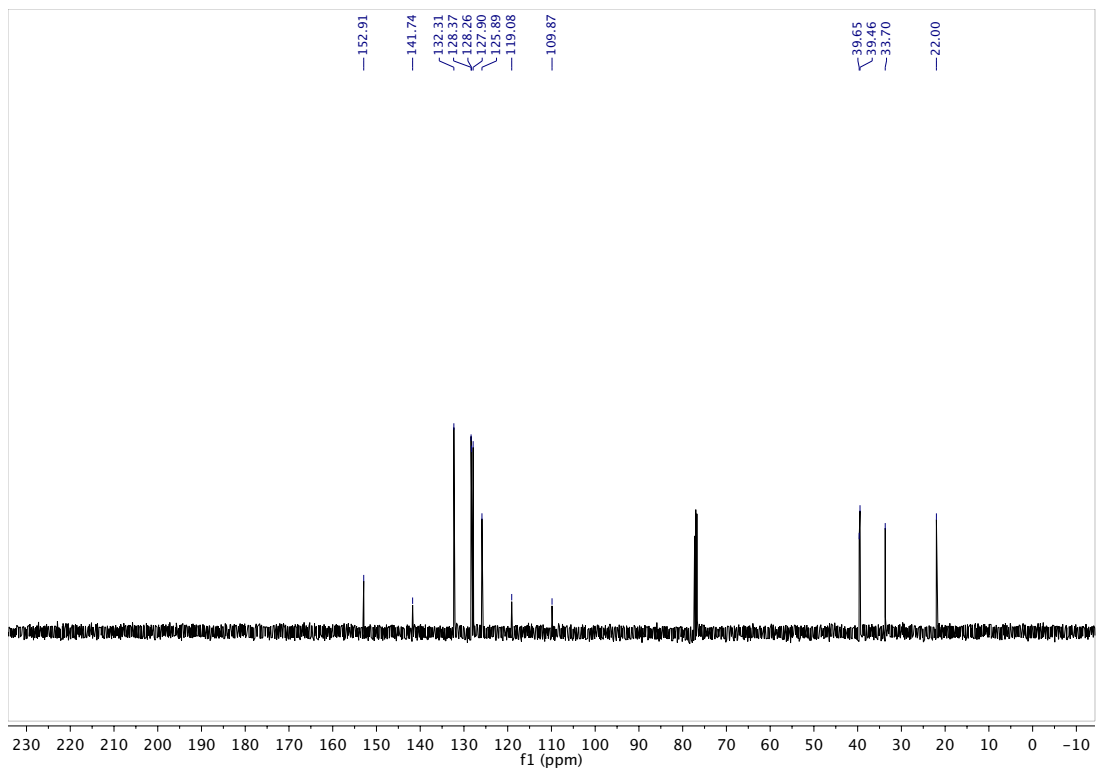
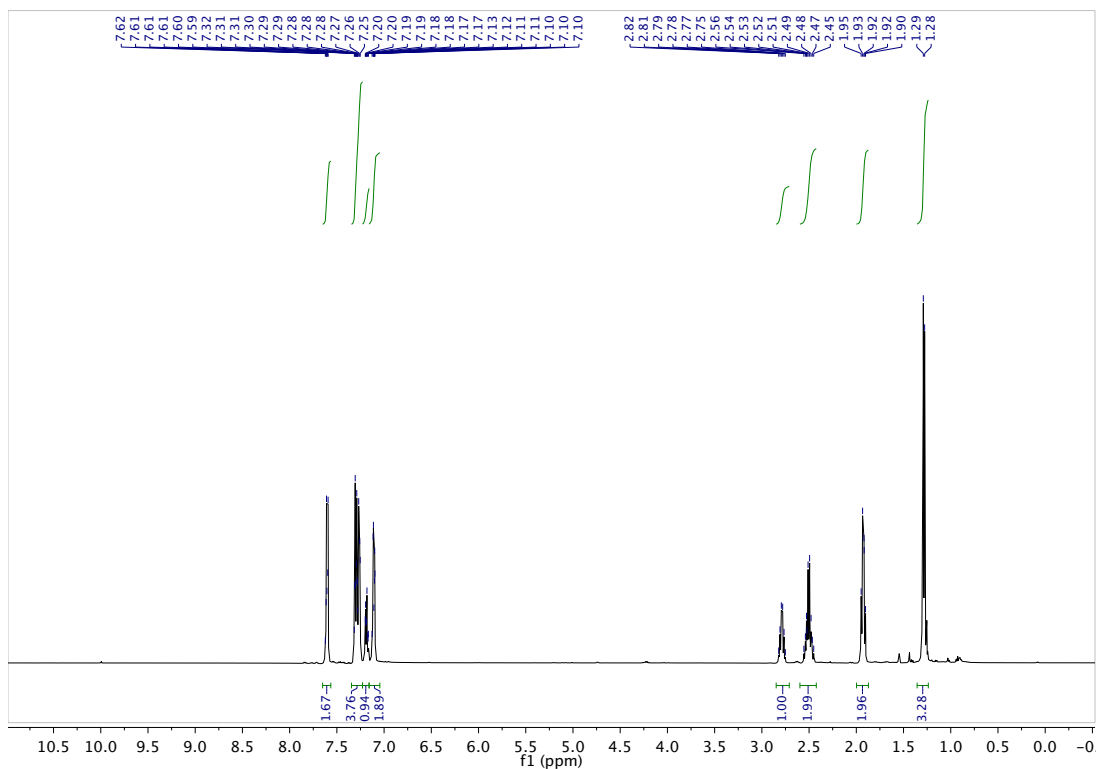


Figure 6-25: Spectra for 2-54

***N*-(4-(4-phenylbutane-2-yl)phenyl)acetamide (2-55)**

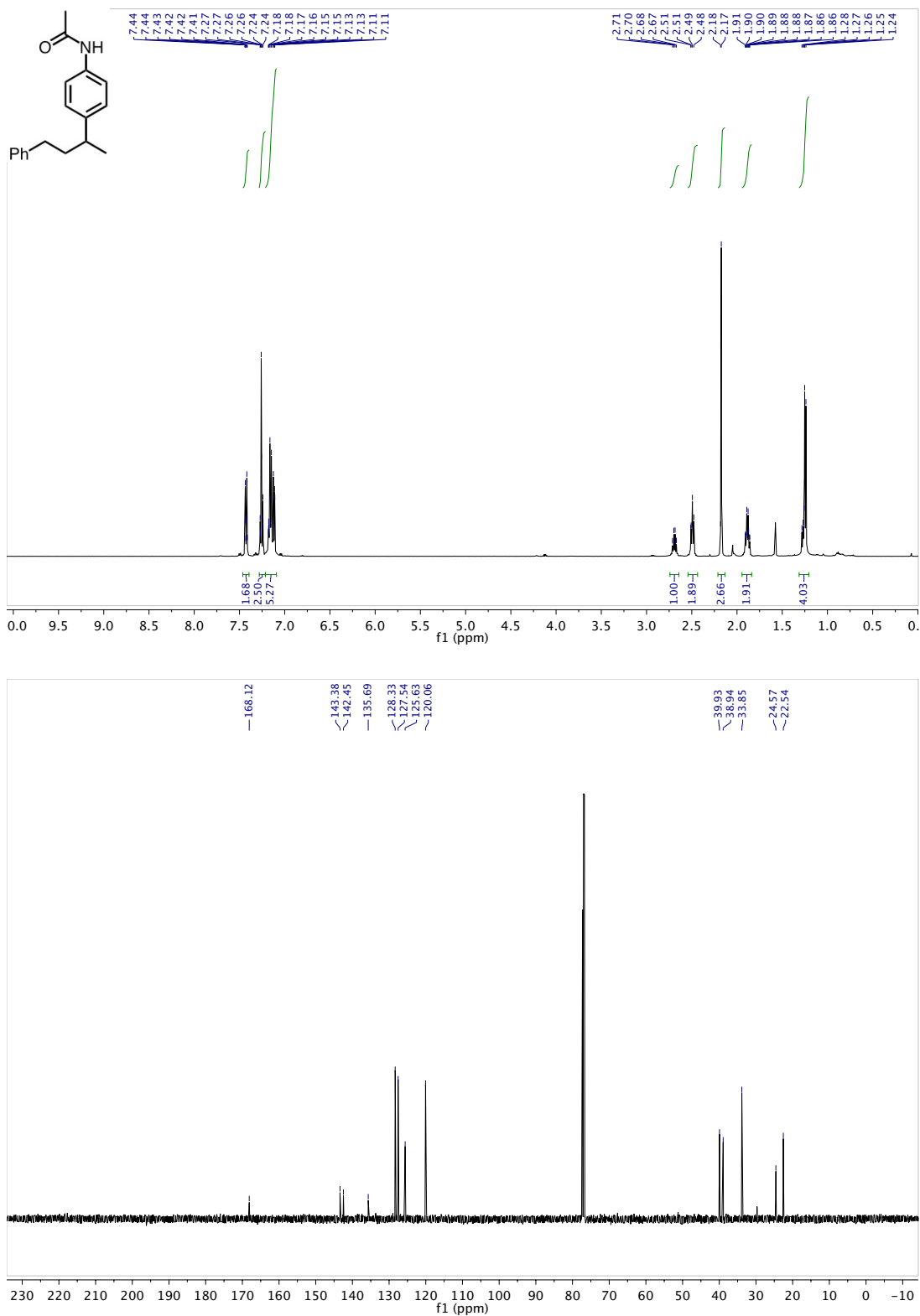


Figure 6-26: Spectra for 2-55

5-(biphenyl-4-yl)hexan-1-ol (2-56)

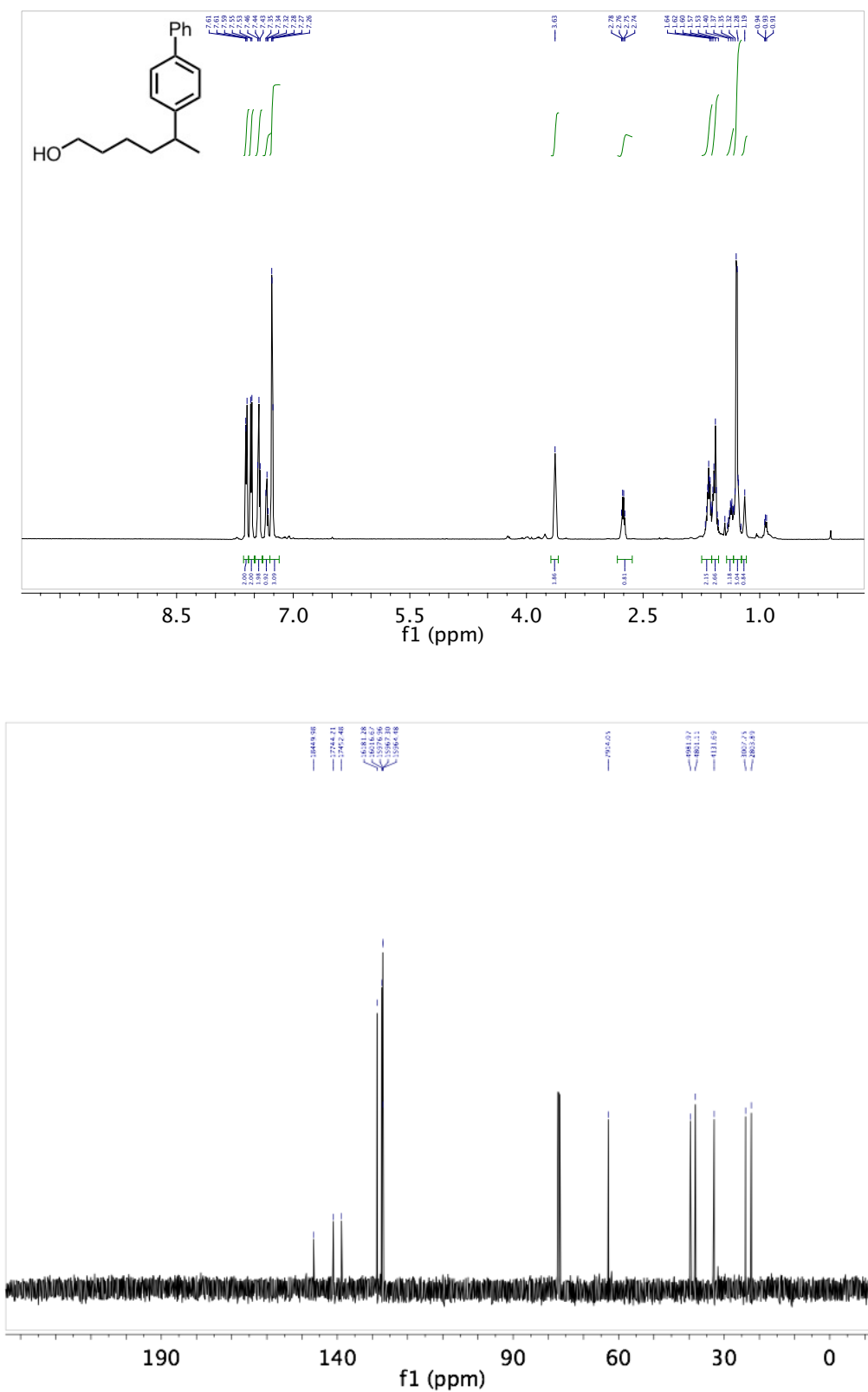


Figure 6-27: Spectra for 2-56

5-(biphenyl-4-yl)hexyl pivalate (2-57)

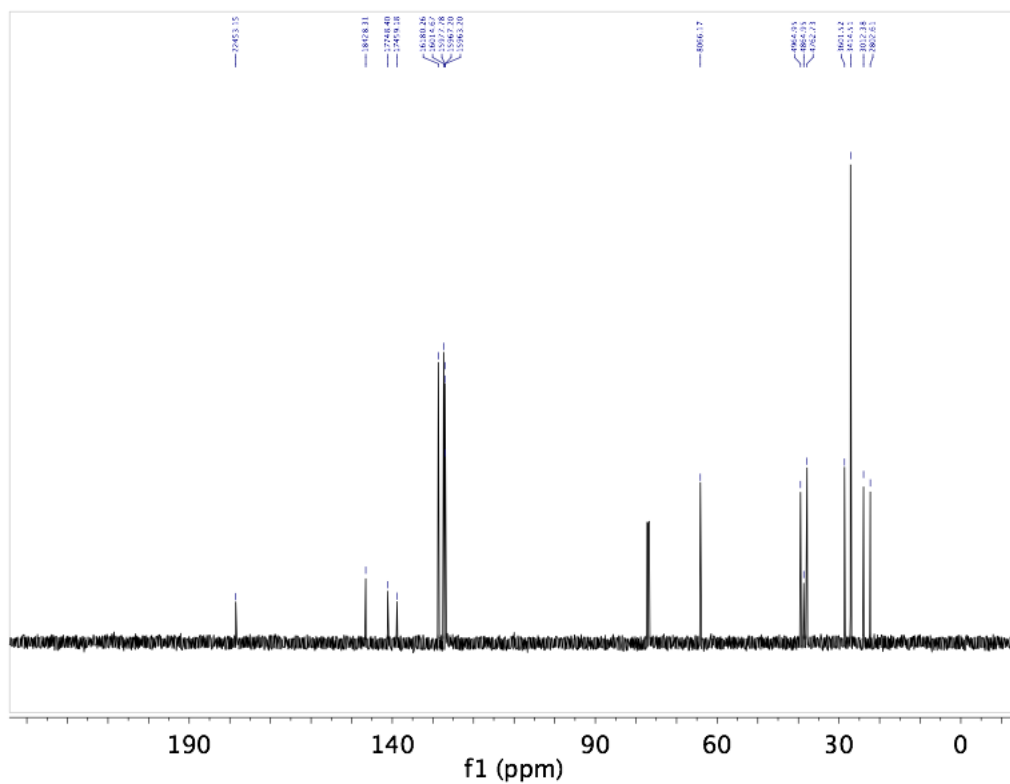
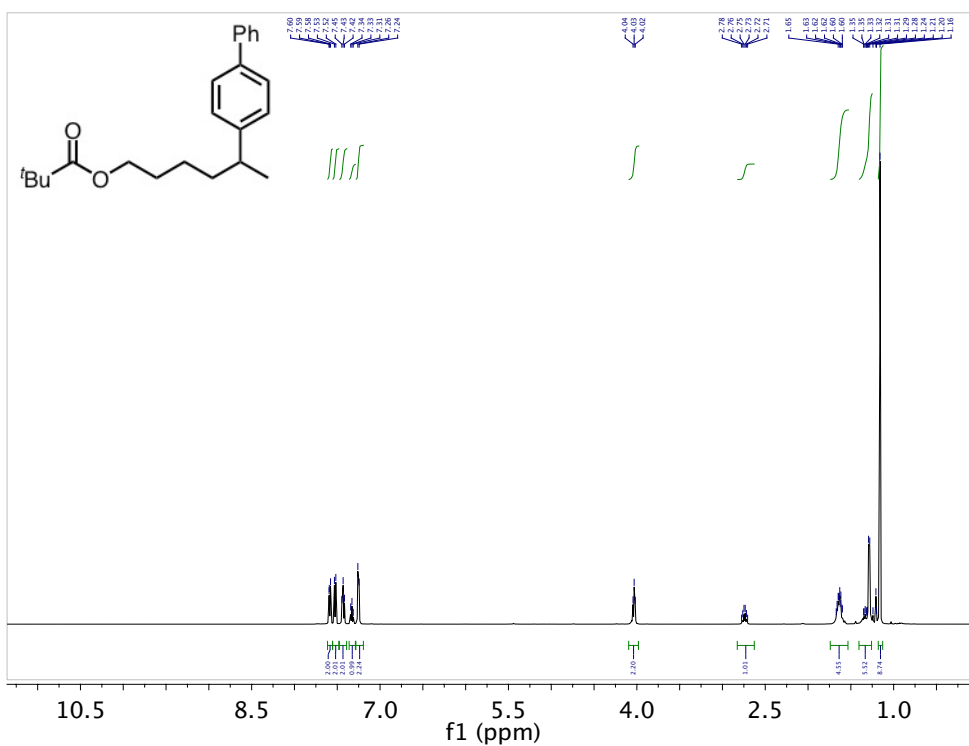
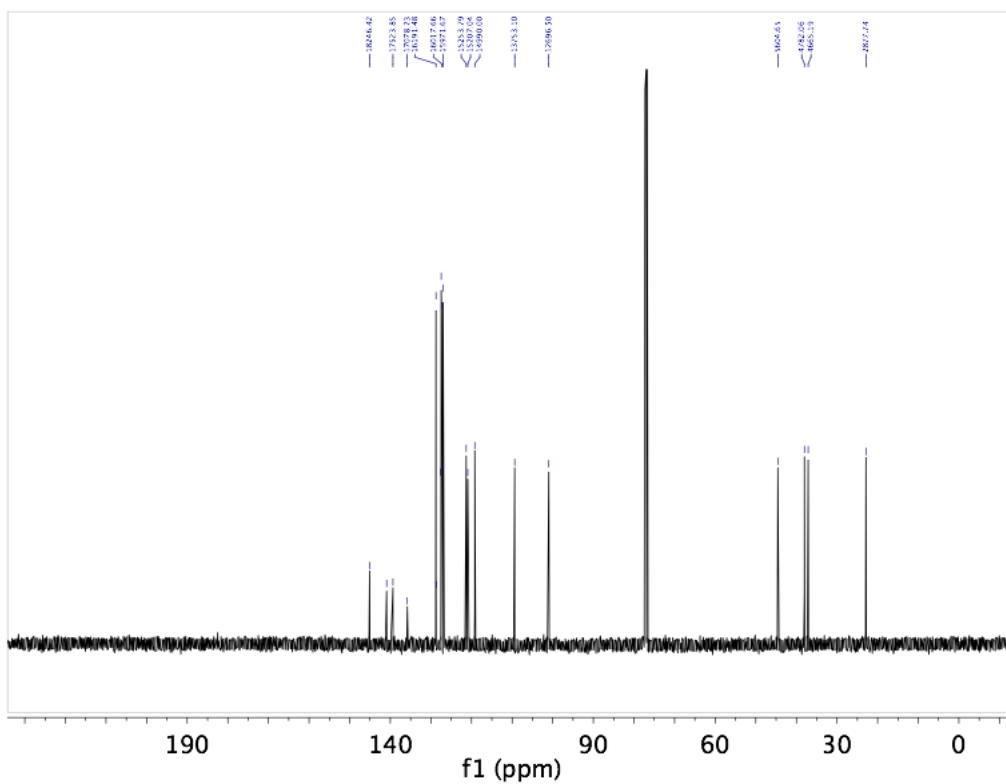
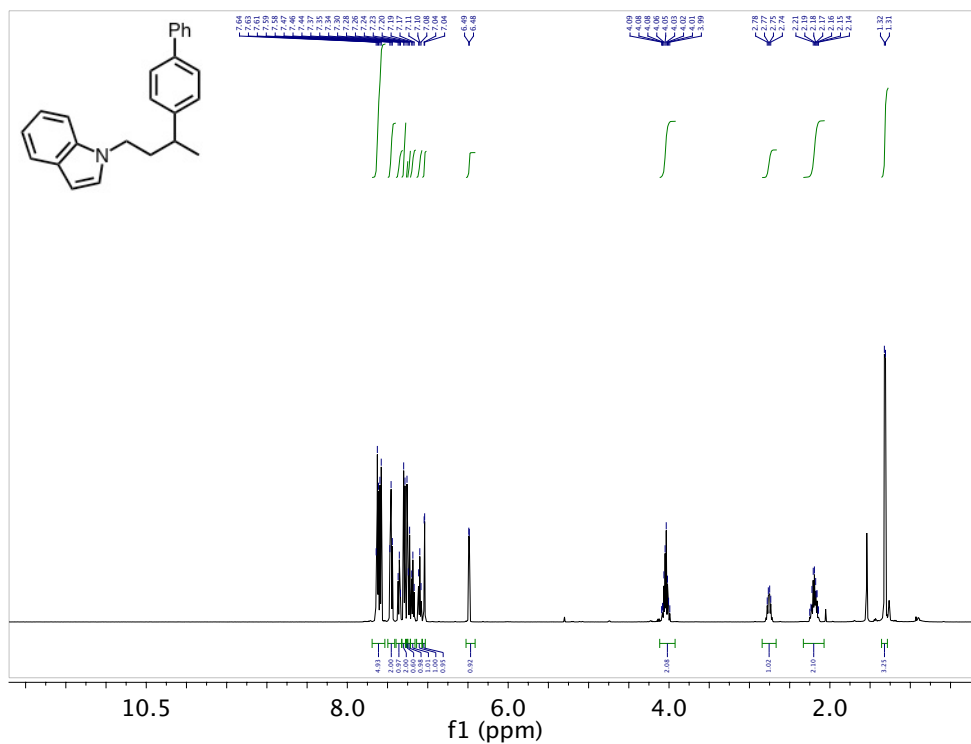


Figure 6-28: Spectra for 2-57

1-(3-(biphenyl-4-yl)butyl)-1H-indole (2-58)



4,4,5,5-tetramethyl-2-(2-methyl-4-phenylbutan-2-yl)-1,3,2-dioxaborolane (2-68)

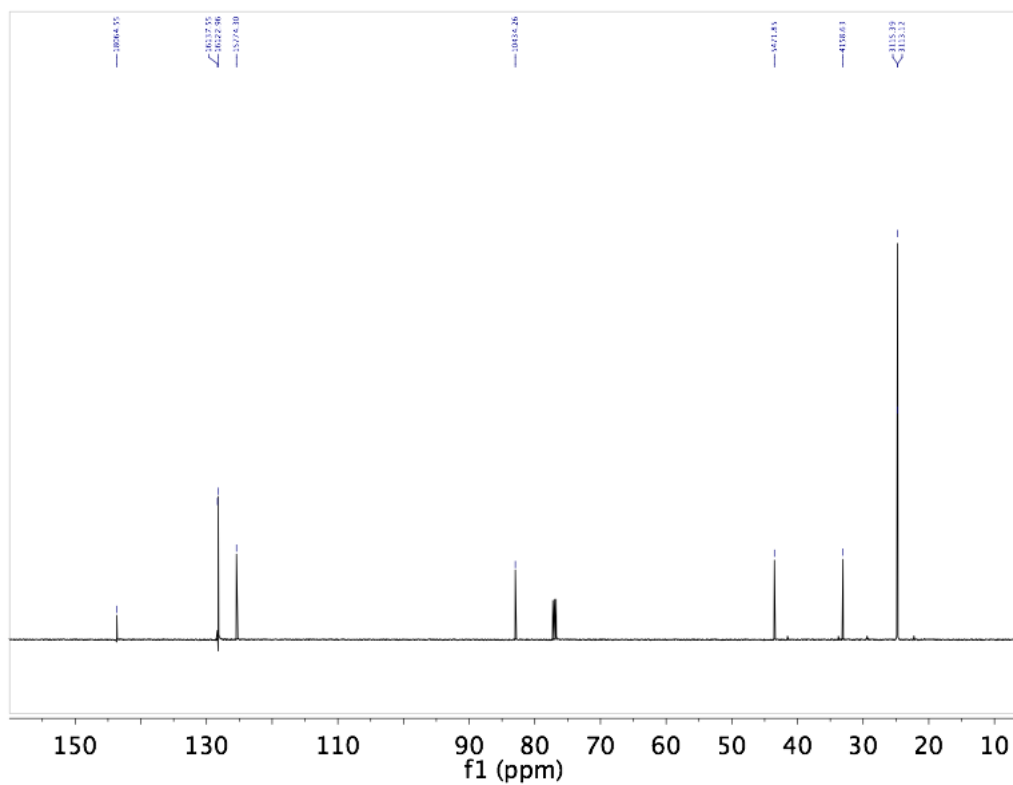
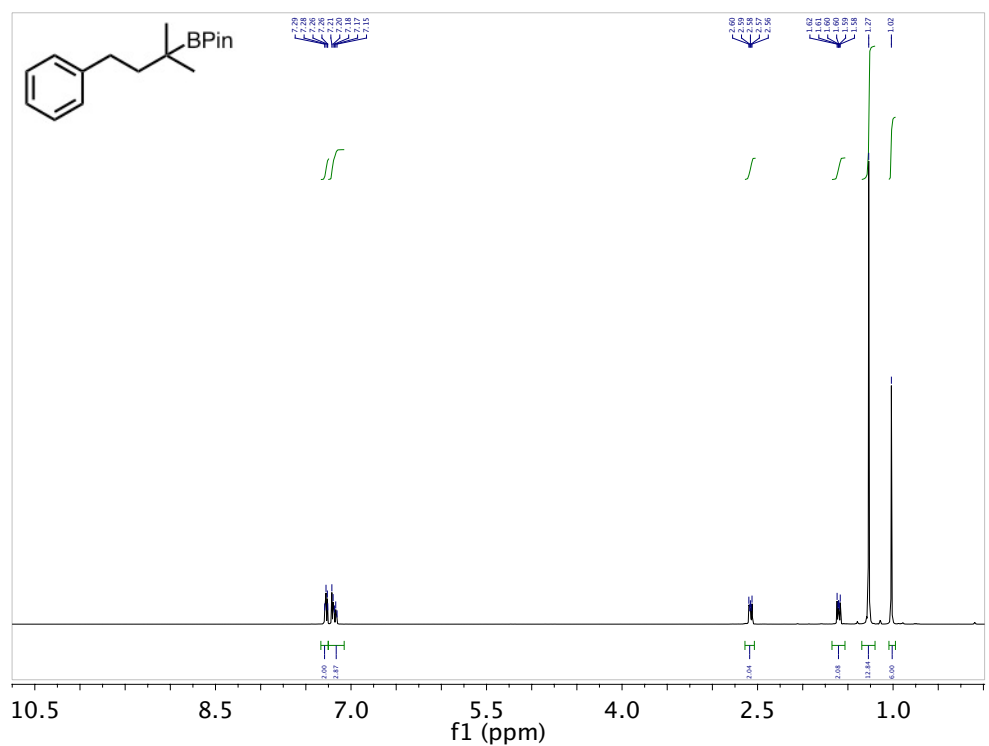


Figure 6-30: Spectra for 2-68

4,4,5,5-tetramethyl-2-(3-methyl-1-phenylpentan-3-yl)-1,3,2-dioxaborolane (2-71)

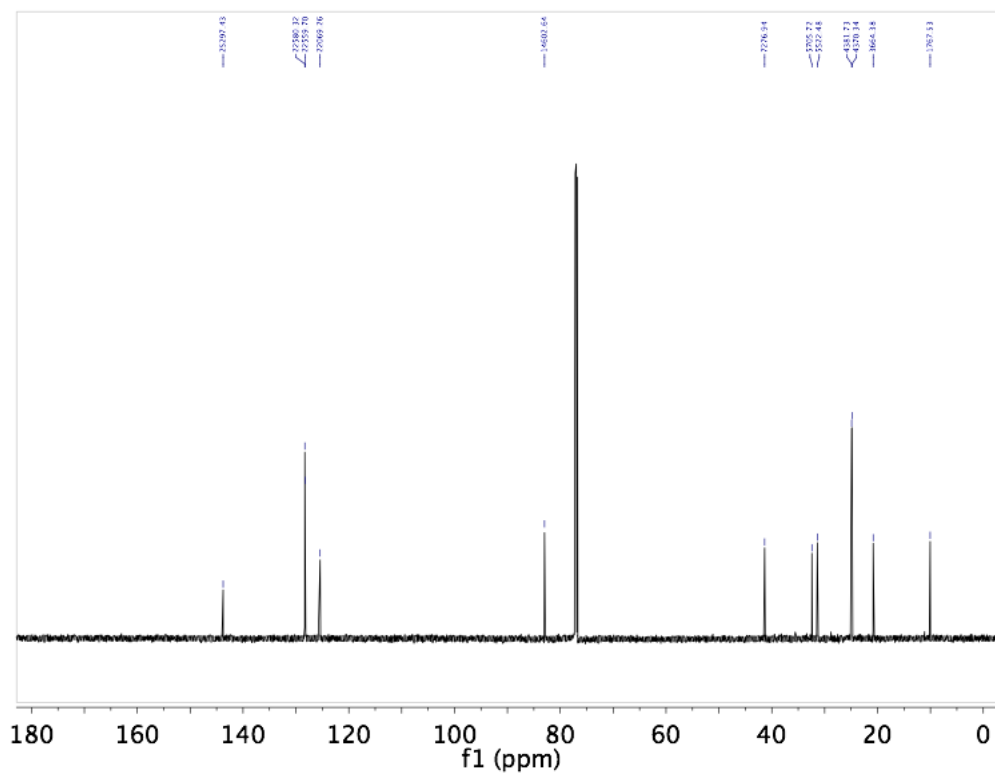
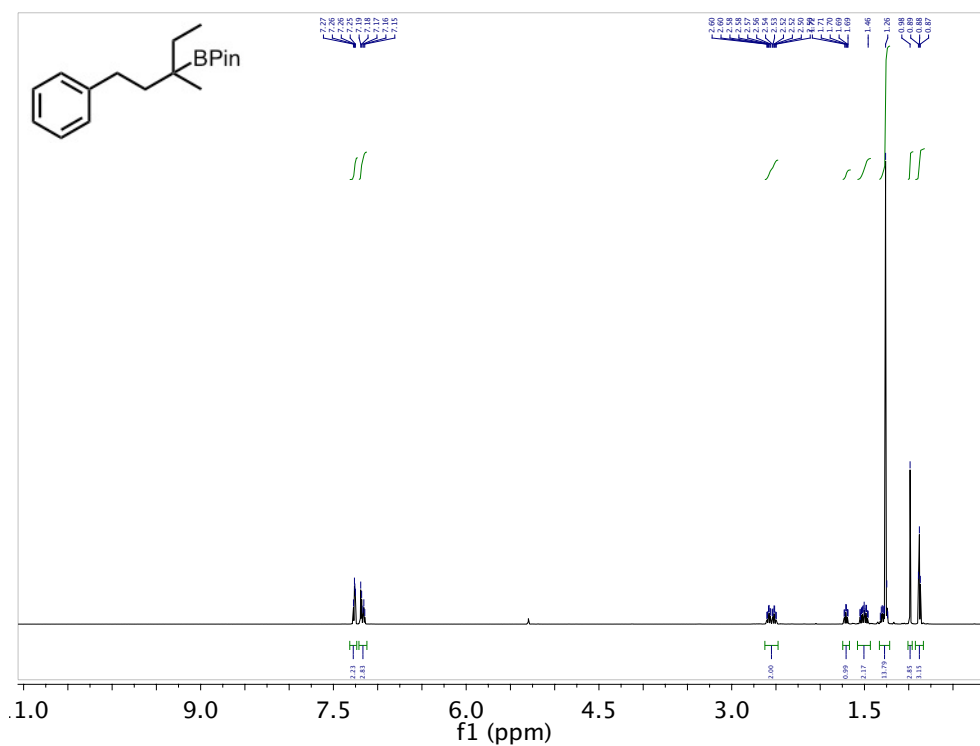


Figure 6-31: Spectra for 2-71

(3a*S*,5*R*,6*R*,7*S*,7a*S*)-5-(acetoxymethyl)-2-ethoxy-2-methyltetrahydro-3a*H*-[1,3]dioxolo[4,5-*b*]pyran-6,7-diyl diacetate (4-24)

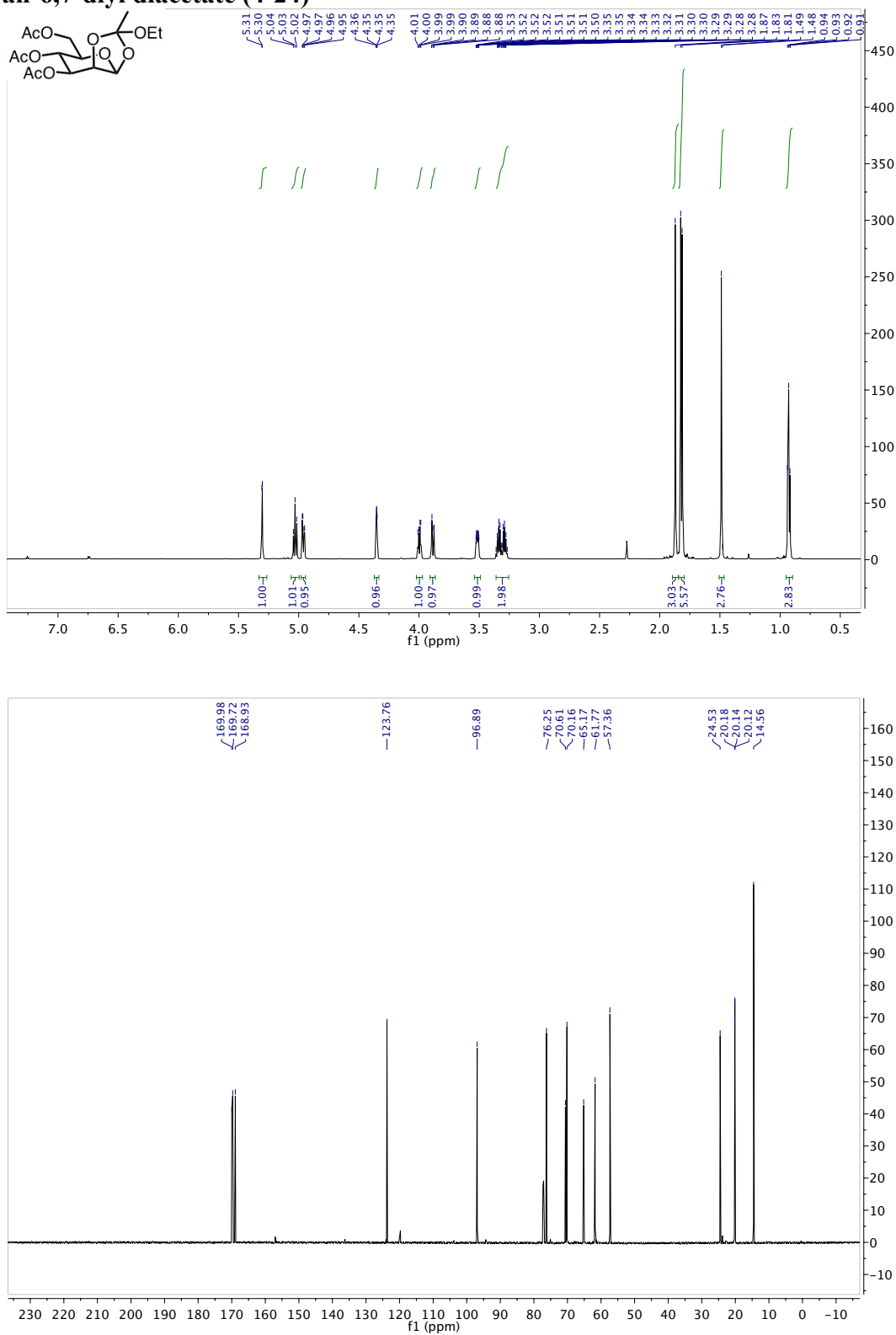


Figure 6-32: Spectra for 4-24

(3a*S*,5*R*,6*R*,7*S*,7a*S*)-6,7-bis(benzyloxy)-5-(benzyloxymethyl)-2-ethoxy-2-methyltetrahydro-3a*H*-[1,3]dioxolo[4,5-*b*]pyran (4-25)

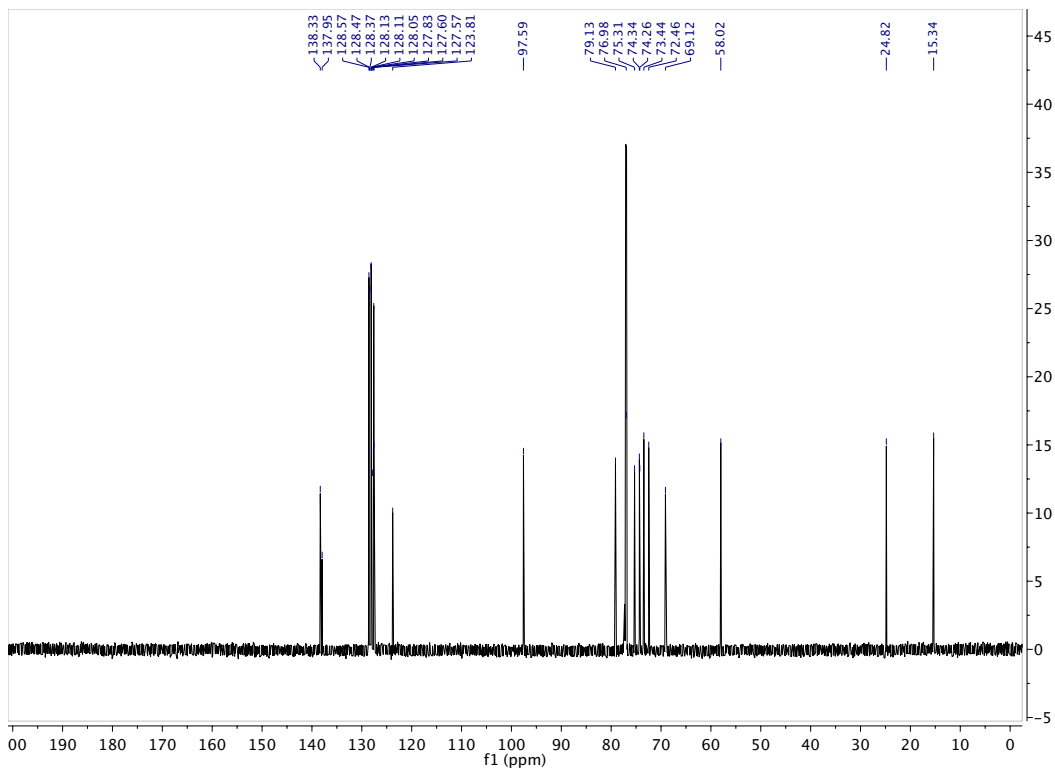
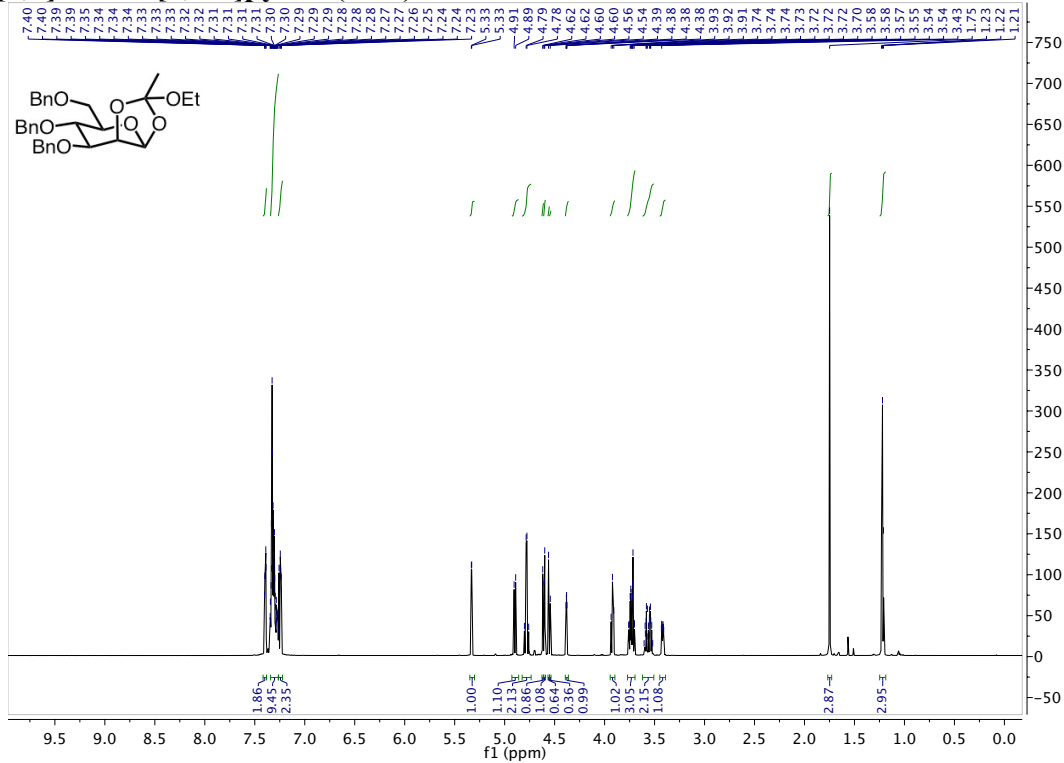


Figure 6-33: Spectra for 4-25

(2*R*,3*S*,4*S*,5*S*,6*R*)-4,5-bis(benzyloxy)-6-(benzyloxymethyl)-2-(2-iodophenoxy)tetrahydro-2*H*-pyran-3-yl acetate (4-26)

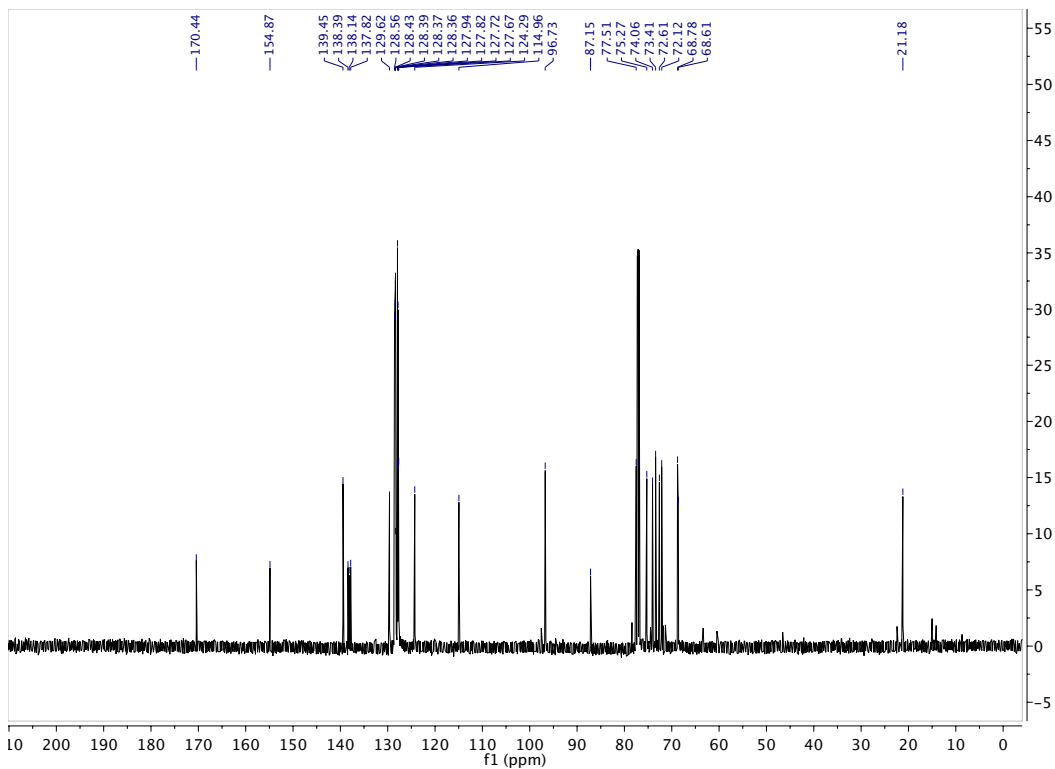
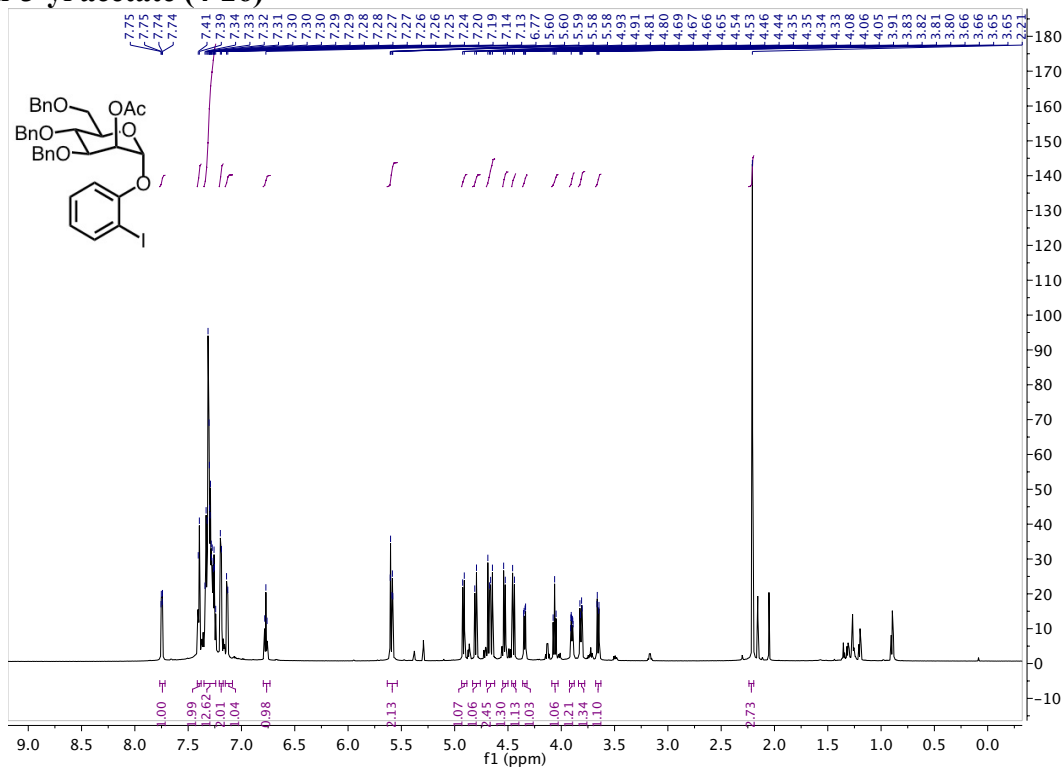


Figure 6-34: Spectra for 4-26

(2*R*,3*S*,4*R*,5*S*,6*R*)-4,5-bis(benzyloxy)-6-(benzyloxymethyl)-2-(2-iodophenoxy)tetrahydro-2H-pyran-3-ol (4-27)

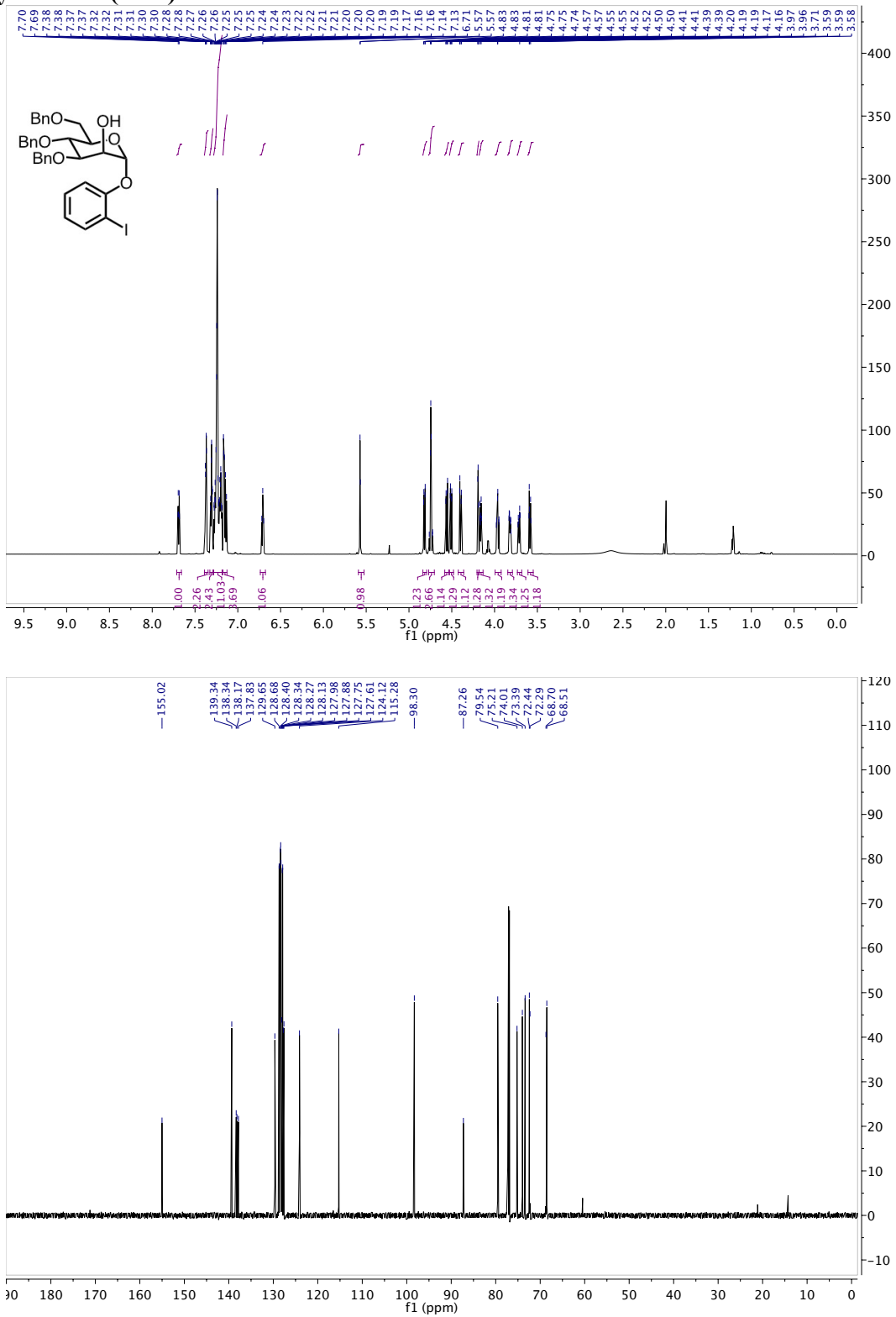


Figure 6-35: Spectra for 4-27

(2*R*,3*S*,4*R*,5*S*,6*R*)-4,5-bis(benzyloxy)-6-(benzyloxymethyl)-2-(2-((4-methoxyphenyl)ethynyl)phenoxy)tetrahydro-2*H*-pyran-3-ol (4-28)

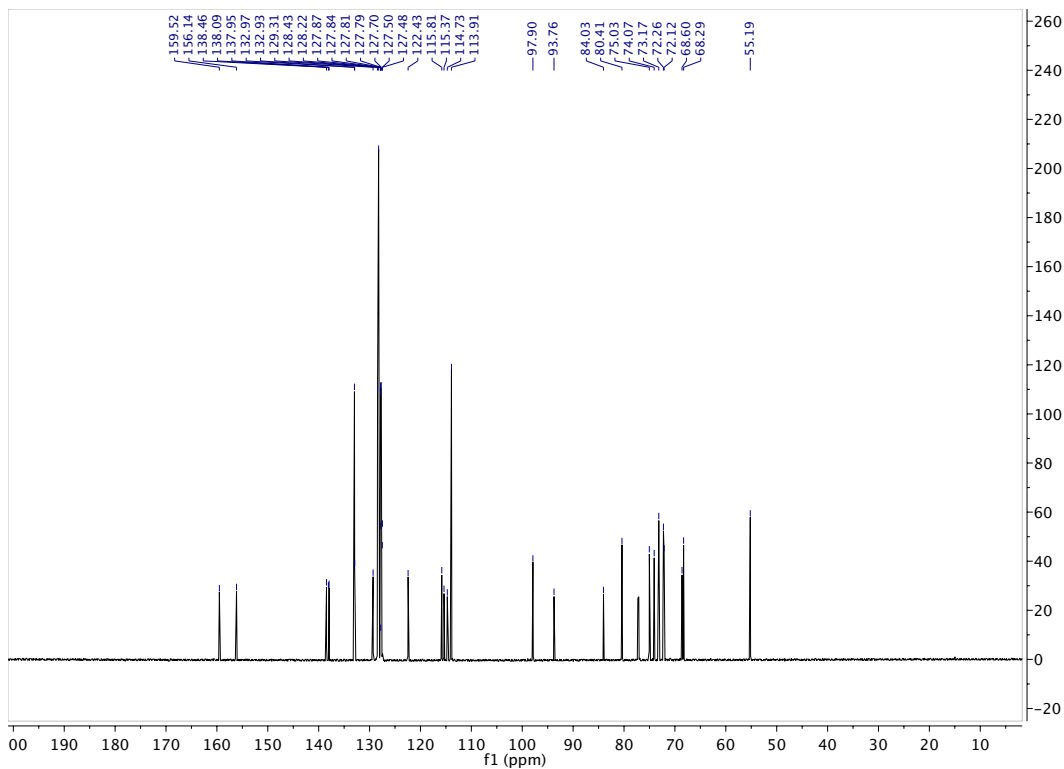
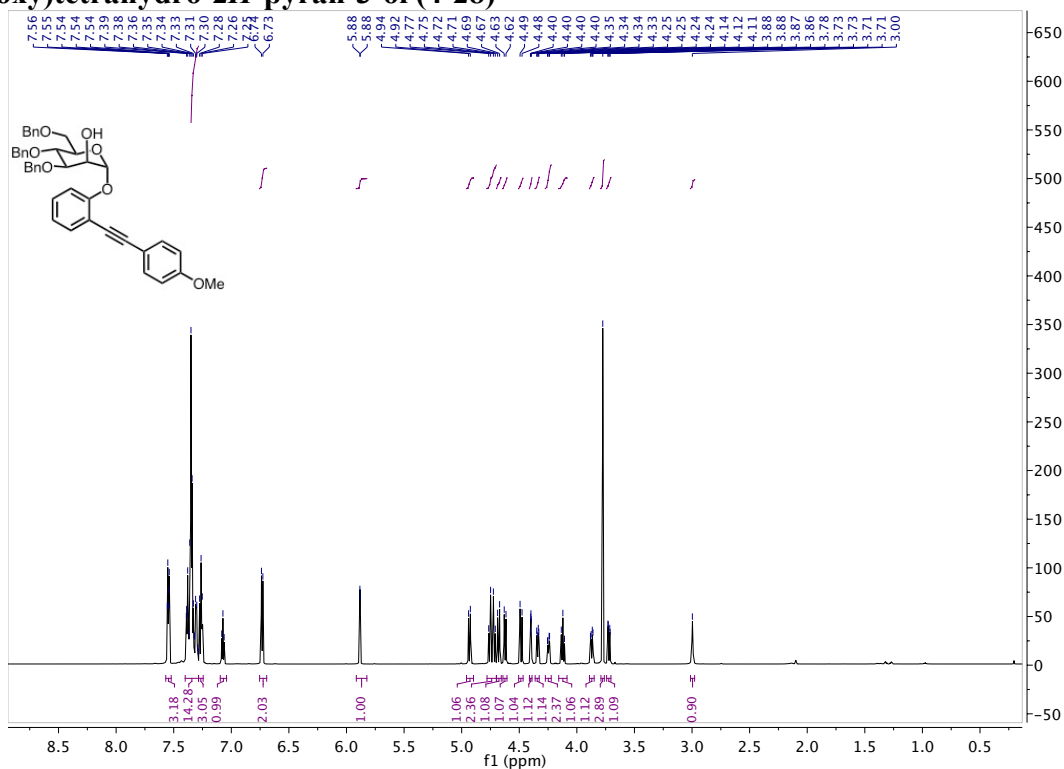


Figure 6-36: Spectra for 4-28

(3aR,5R,6R,7S,7aR)-5-(acetoxymethyl)-2-ethoxy-2-methyltetrahydro-3aH-[1,3]dioxolo[4,5-b]pyran-6,7-diyl diacetate (4-31)

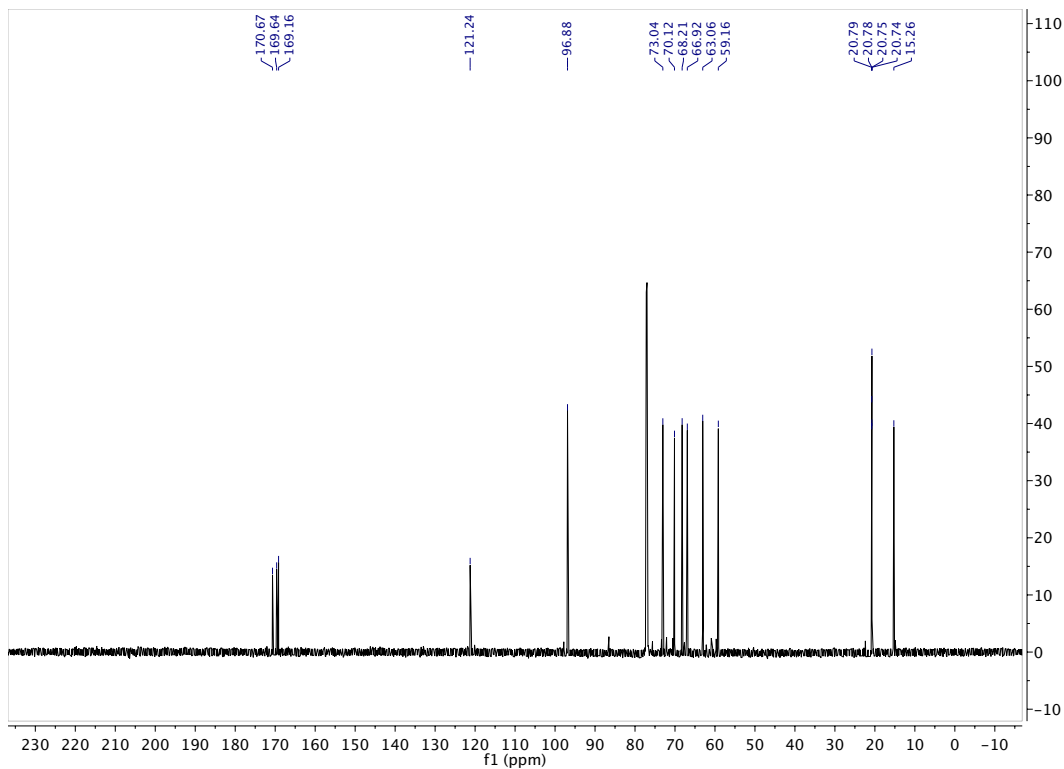
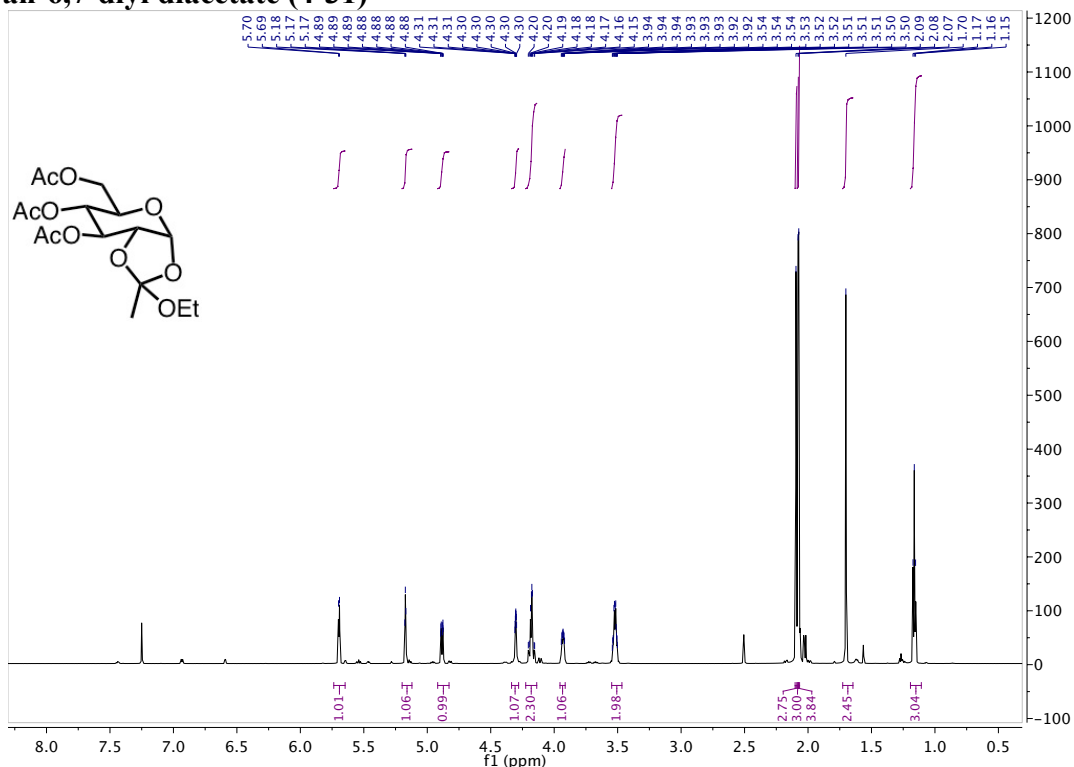


Figure 6-37: Spectra for 4-31

(3aR,5R,6R,7S,7aR)-6,7-bis(benzyloxy)-5-(benzyloxymethyl)-2-ethoxy-2-methyltetrahydro-3aH-[1,3]dioxolo[4,5-b]pyran (4-32)

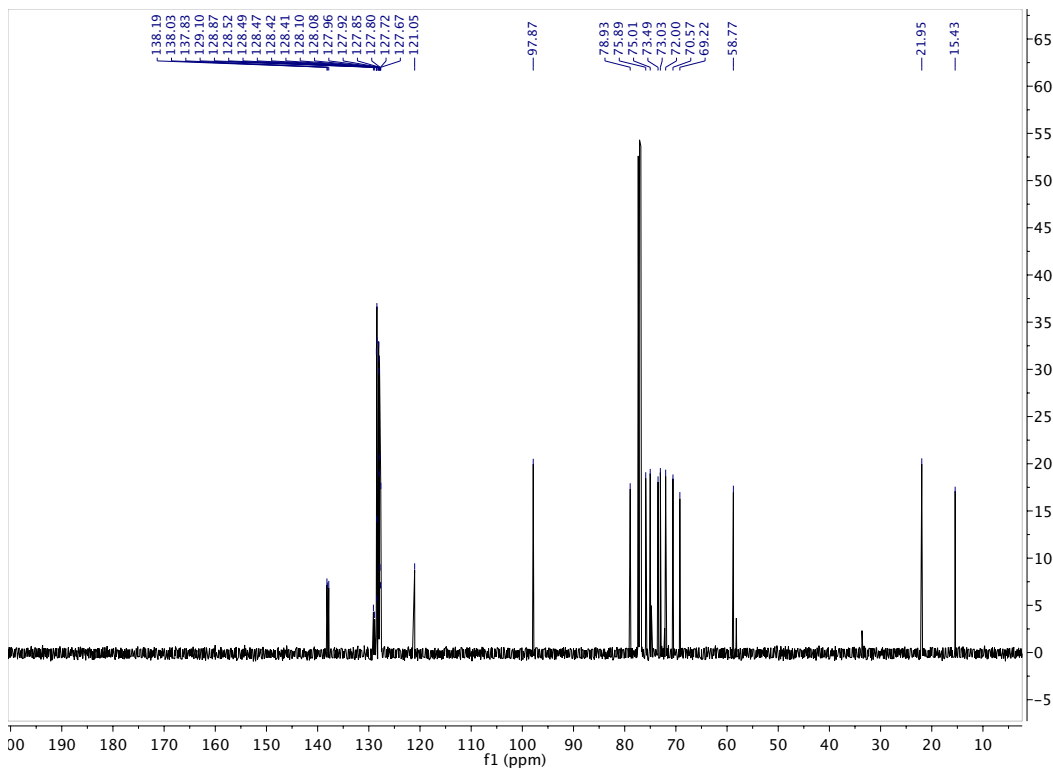
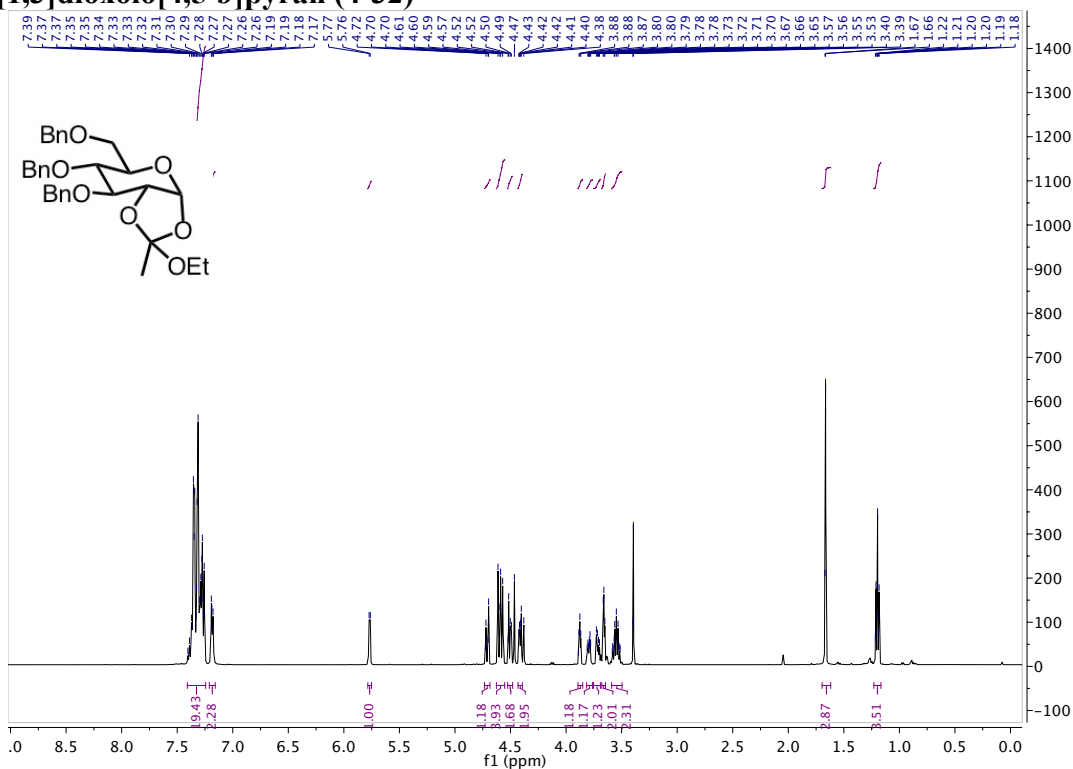


Figure 6-38: Spectra for 4-32

(2*S*,3*R*,4*S*,5*R*,6*R*)-4,5-bis(benzyloxy)-6-(benzyloxymethyl)-2-(2-iodophenoxy)tetrahydro-2*H*-pyran-3-yl acetate (4-33)

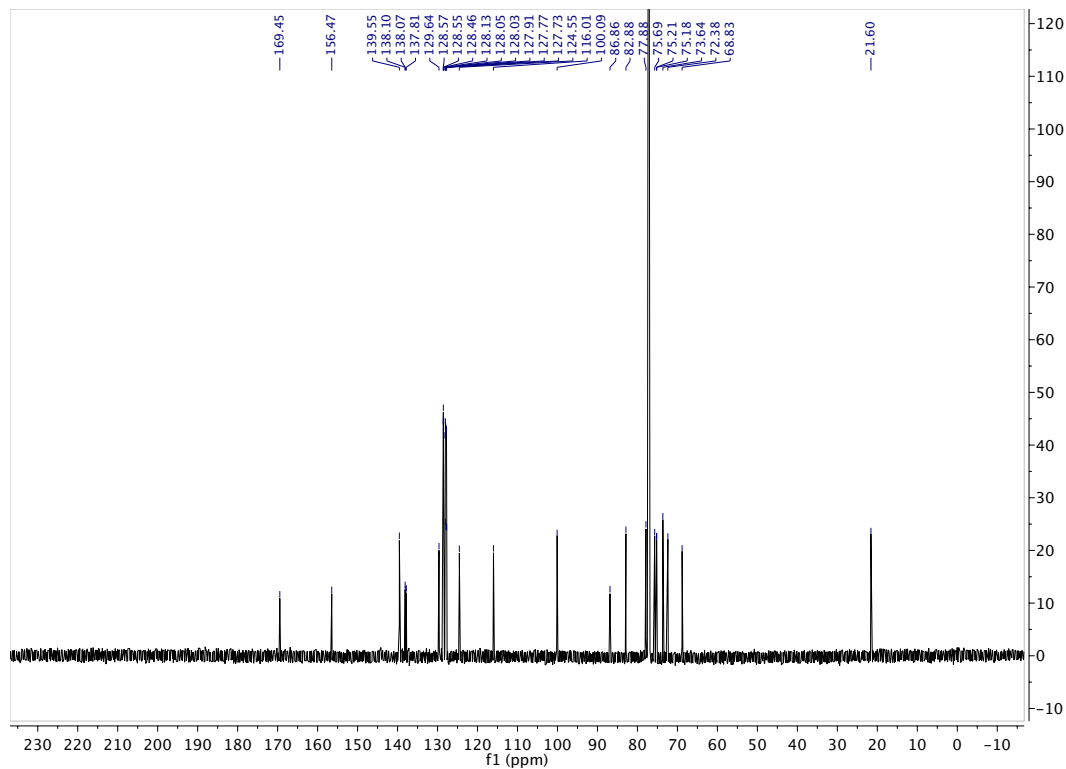
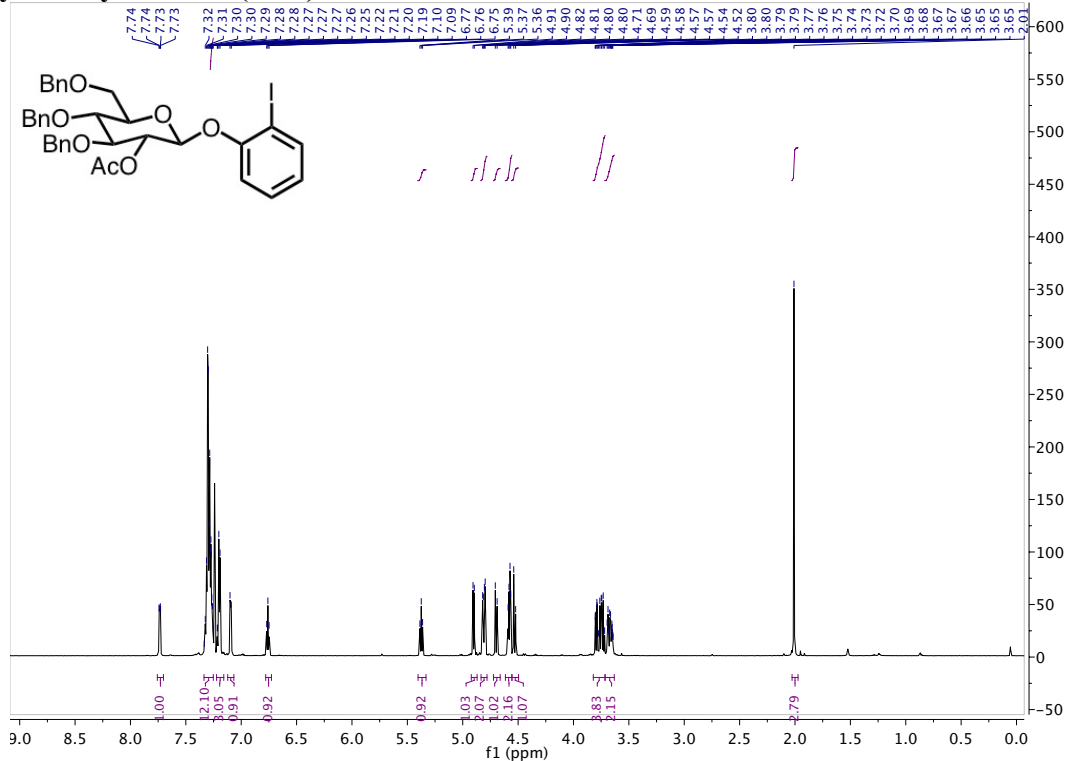


Figure 6-39: Spectra for 4-33

(2*S*,3*R*,4*S*,5*R*,6*R*)-4,5-bis(benzyloxy)-6-(benzyloxymethyl)-2-(2-iodophenoxy)tetrahydro-2*H*-pyran-3-ol (4-35)

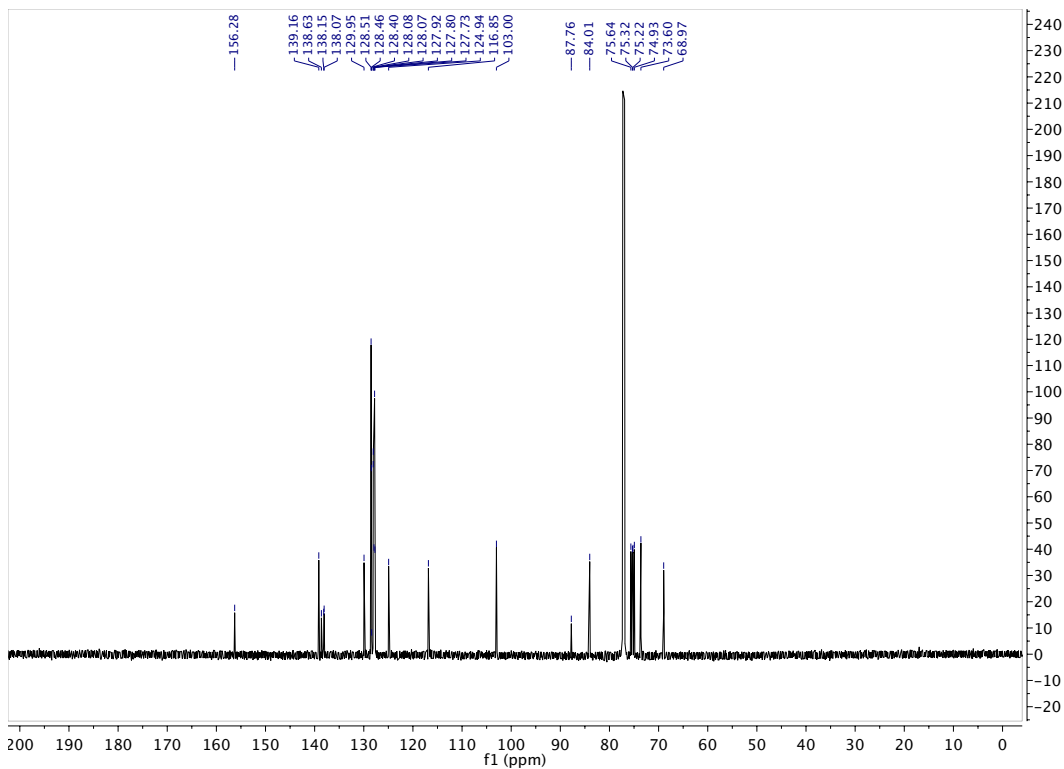
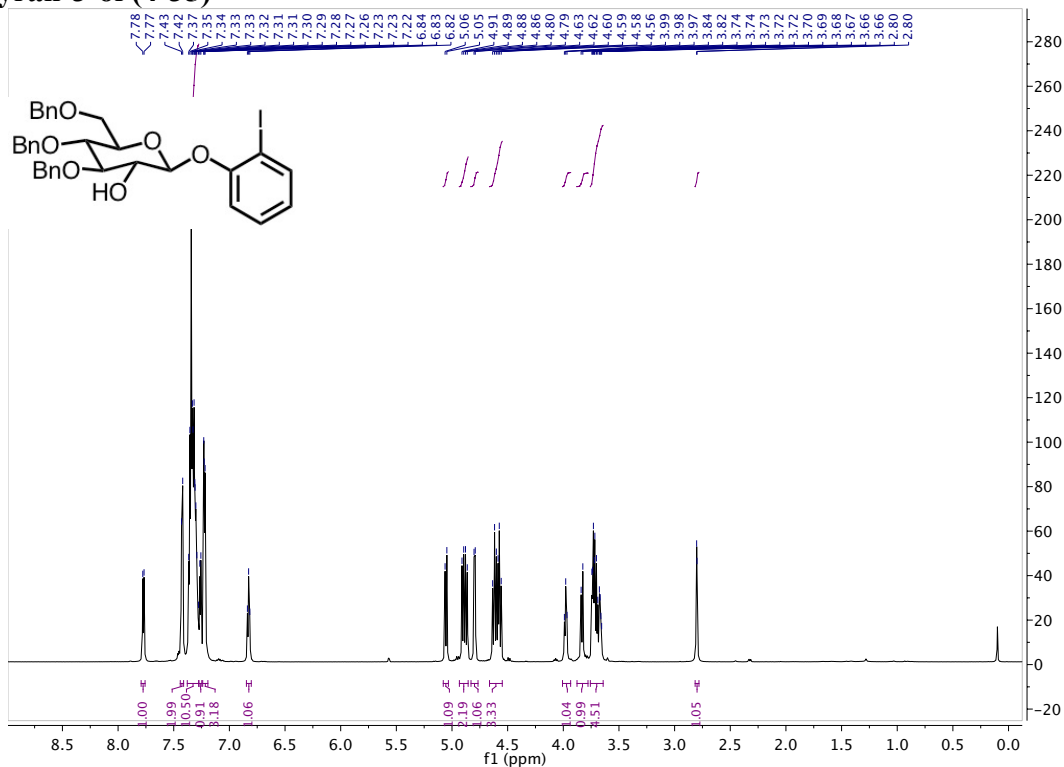


Figure 6-40: Spectra for 4-35

(2*S*,3*R*,4*S*,5*R*,6*R*)-4,5-bis(benzyloxy)-6-(benzyloxymethyl)-2-(2-((4-methoxyphenyl)ethynyl)phenoxy)tetrahydro-2*H*-pyran-3-ol (4-36)

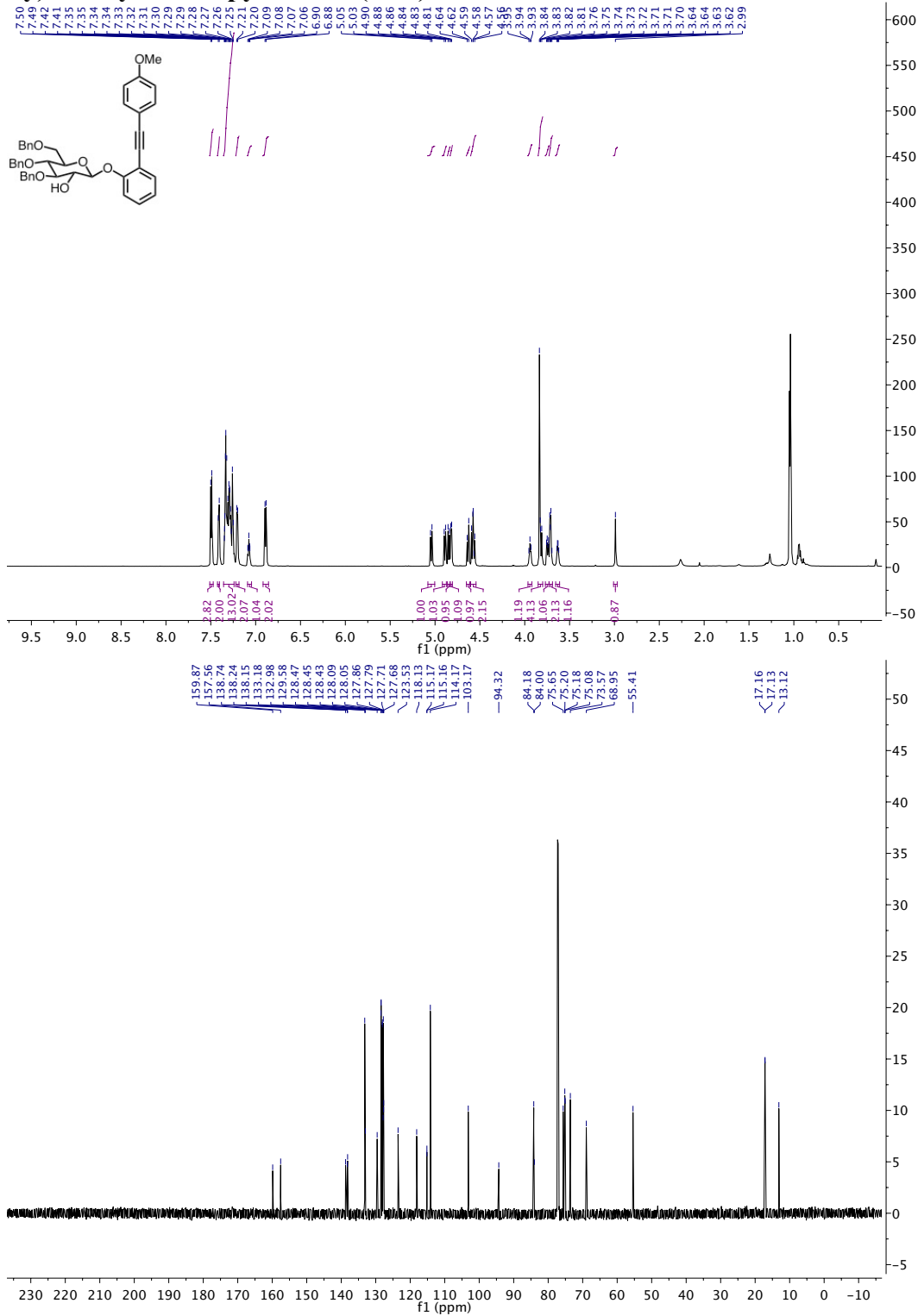


Figure 6-41: Spectra for 4-36

(2*R*,3*R*,4*R*,5*S*,6*R*)-4,5-bis(benzyloxy)-6-(benzyloxymethyl)-2-(2-iodophenoxy)tetrahydro-2*H*-pyran-3-ol (4-37)

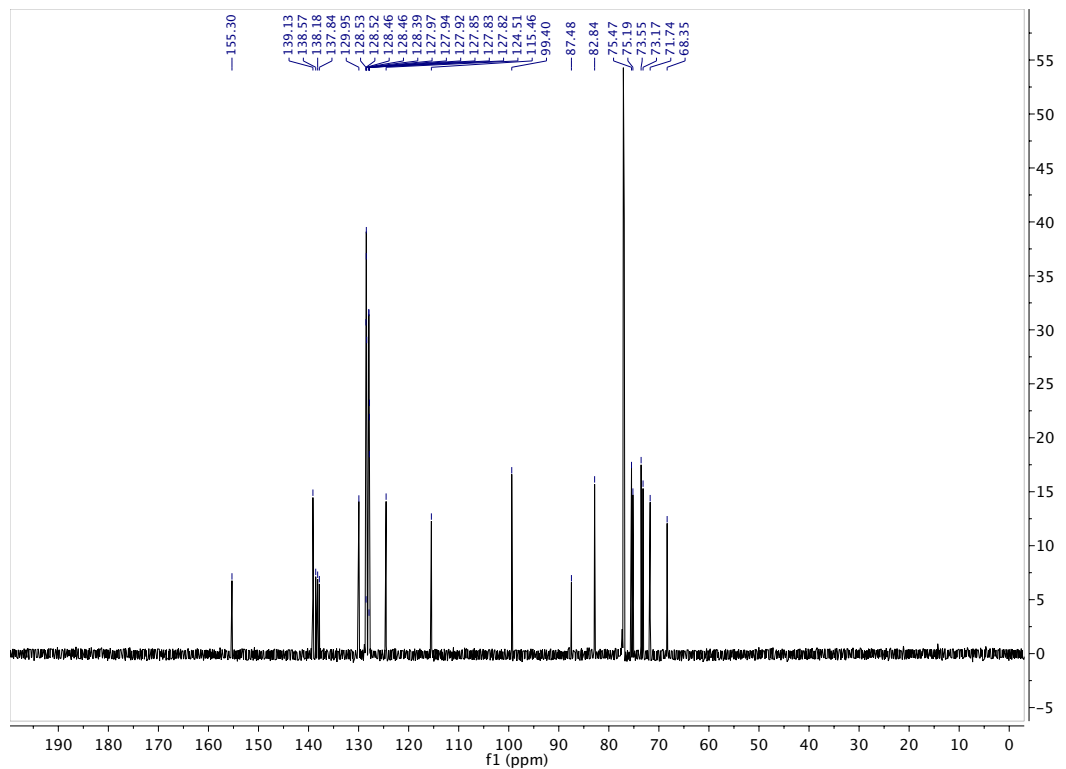
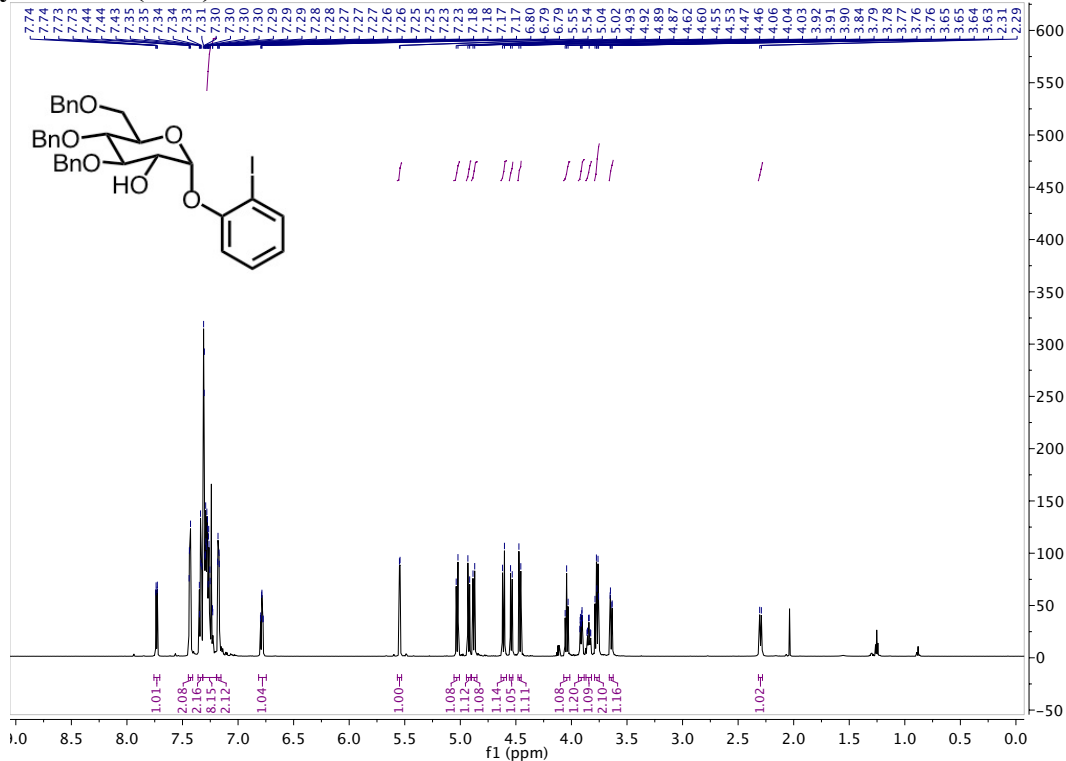


Figure 6-42: Spectra for 4-37

(2*R*,3*R*,4*R*,5*S*,6*R*)-4,5-bis(benzyloxy)-6-(benzyloxymethyl)-2-(2-((4-methoxyphenyl)ethynyl)phenoxy)tetrahydro-2*H*-pyran-3-ol (4-38)

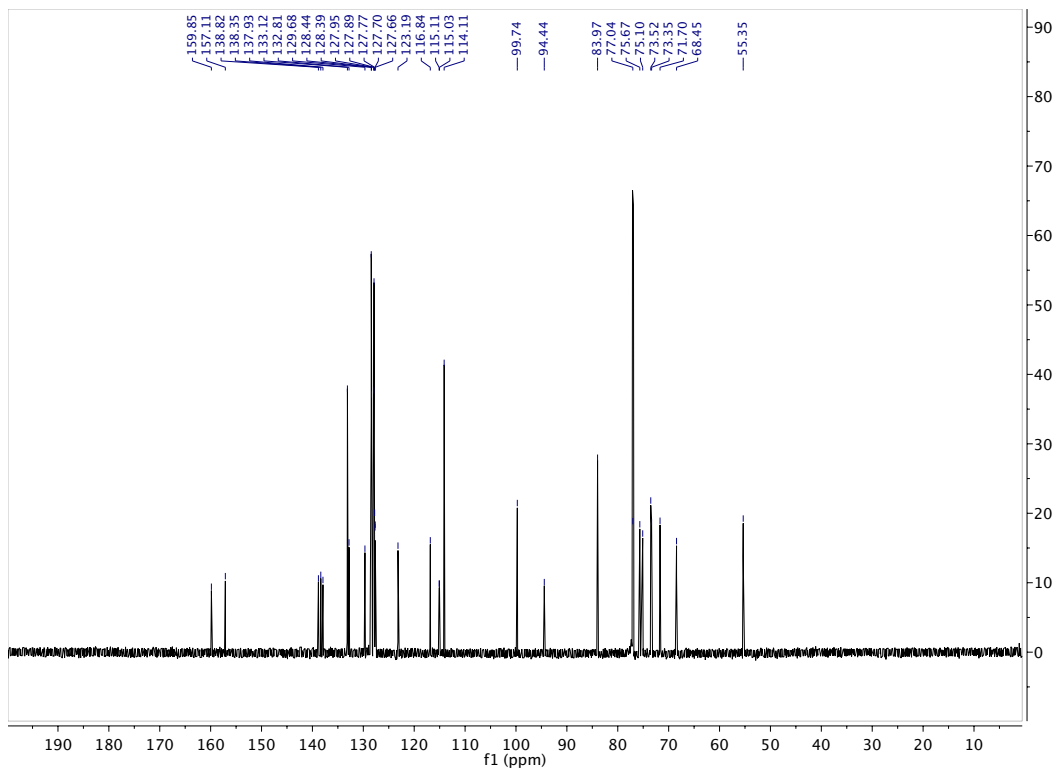
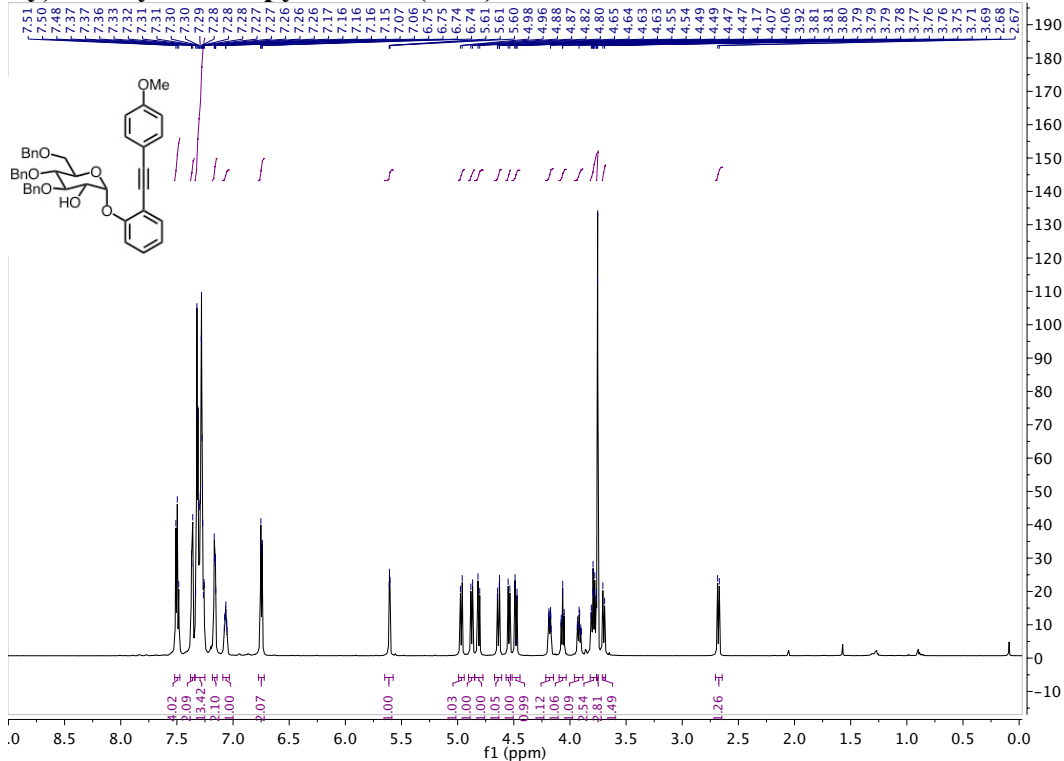


Figure 6-43: Spectra for 4-38

((2*R*,3*S*,4*S*,5*S*,6*R*)-4,5-bis(benzyloxy)-6-(benzyloxymethyl)-2-(2-((4-methoxyphenyl)ethynyl)phenoxy)tetrahydro-2*H*-pyran-3-yloxy)diisopropylsilane (4-21)

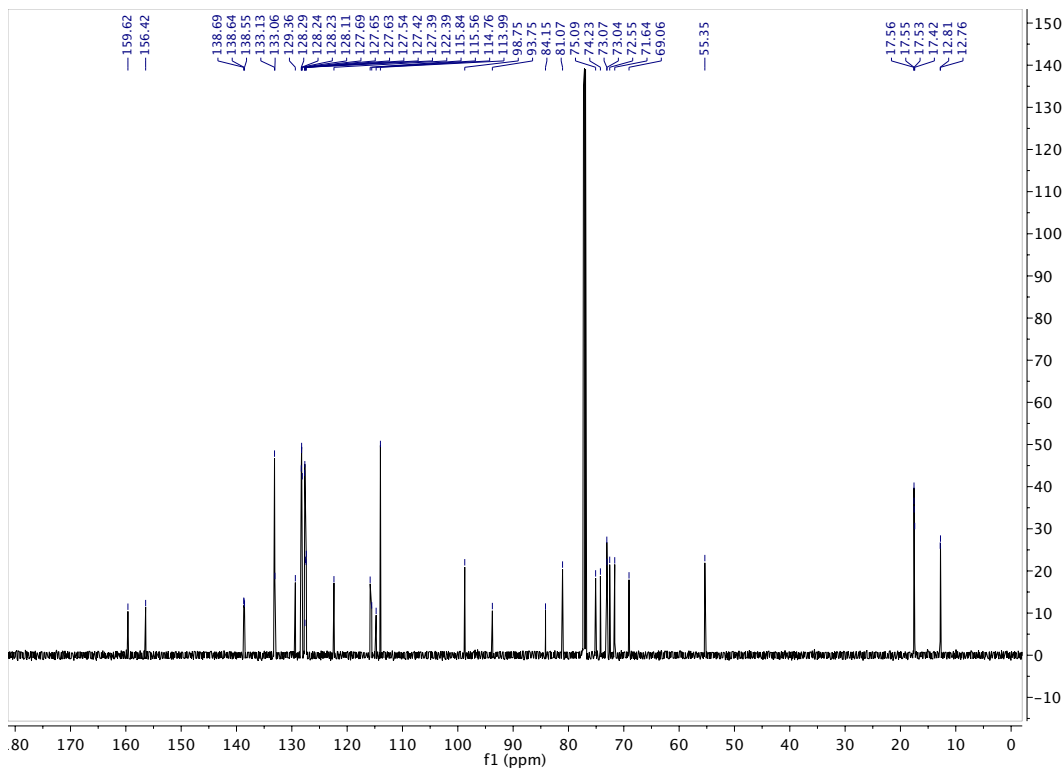
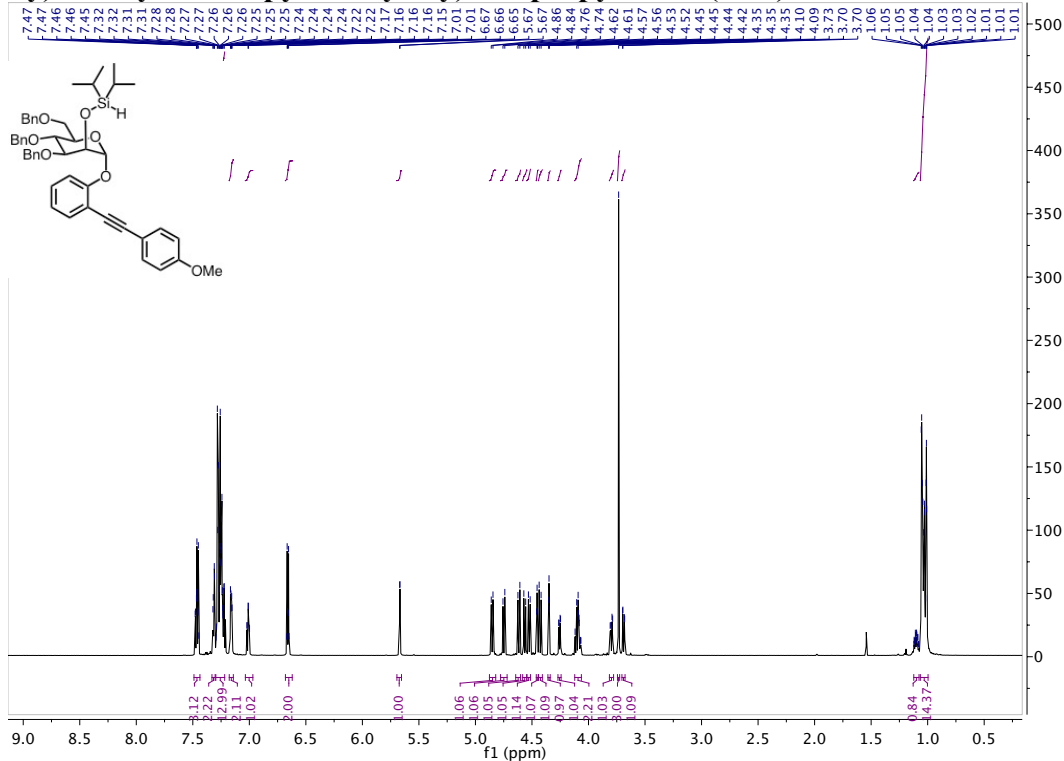


Figure 6-44: Spectra for 4-21

((2*R*,3*S*,4*S*,5*S*,6*R*)-4,5-bis(benzyloxy)-6-(benzyloxymethyl)-2-(2-((4-methoxyphenyl)ethynyl)phenoxy)tetrahydro-2*H*-pyran-3-yloxy)dimethylsilane (4-29)

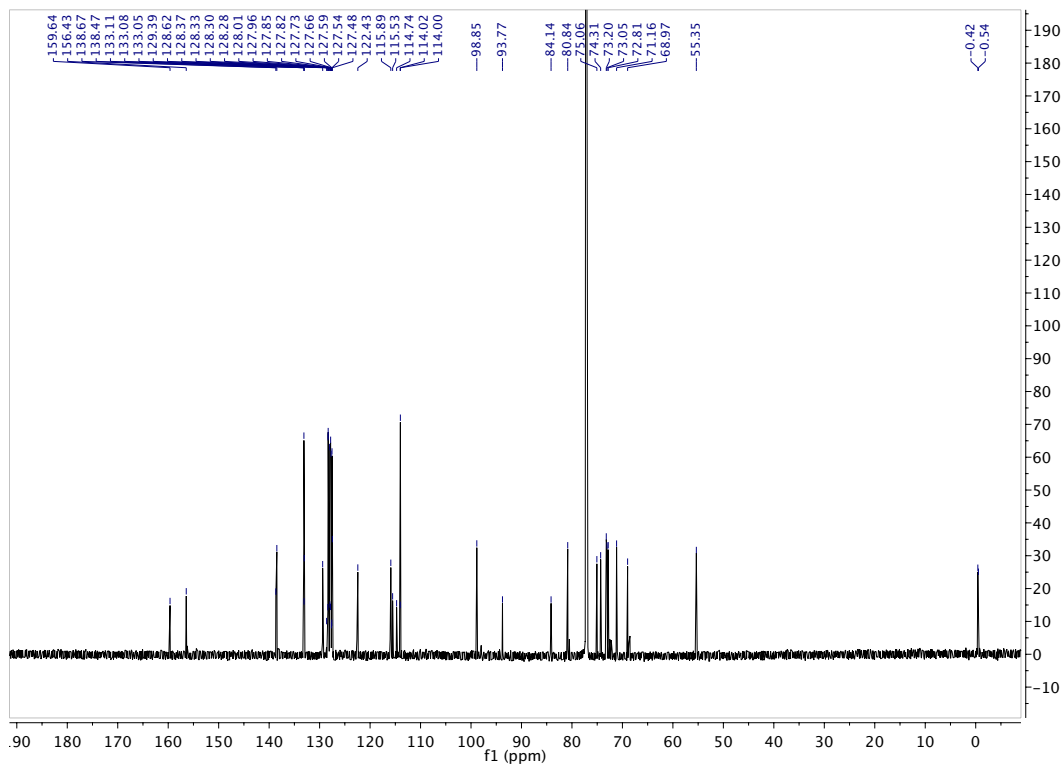
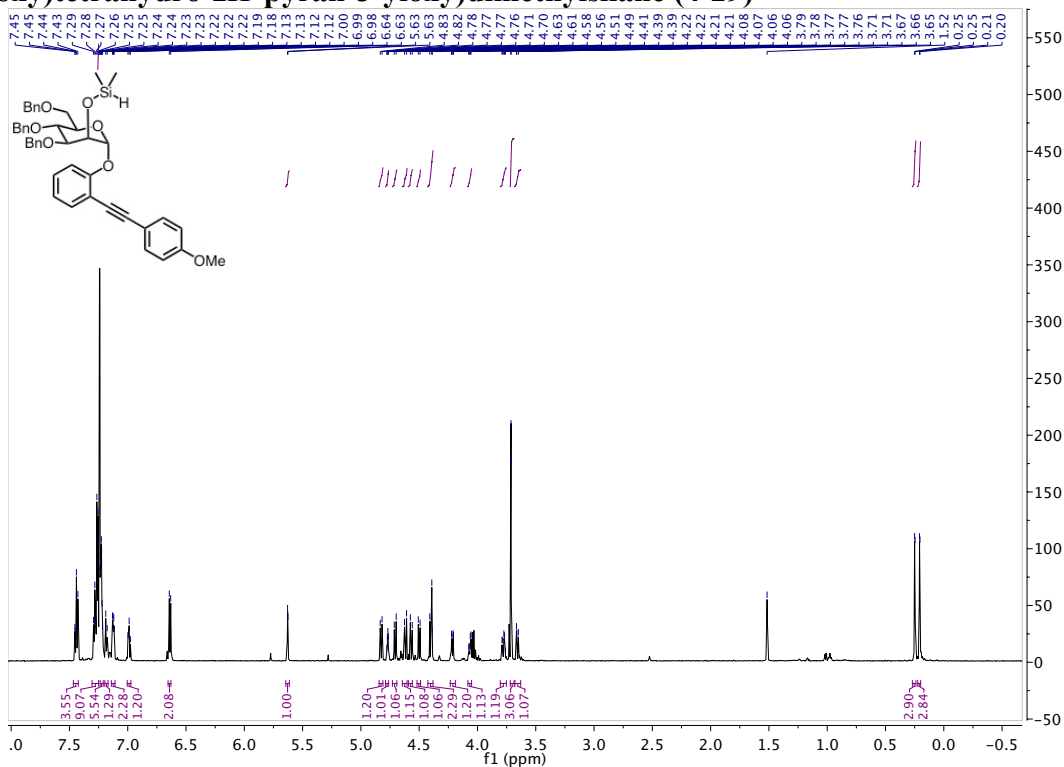


Figure 6-45: Spectra for 4-29

((2*R*,3*S*,4*S*,5*S*,6*R*)-4,5-bis(benzyloxy)-6-(benzyloxymethyl)-2-(2-((4-methoxyphenyl)ethynyl)phenoxy)tetrahydro-2*H*-pyran-3-yl)oxy)diisobutylsilane (4-30)

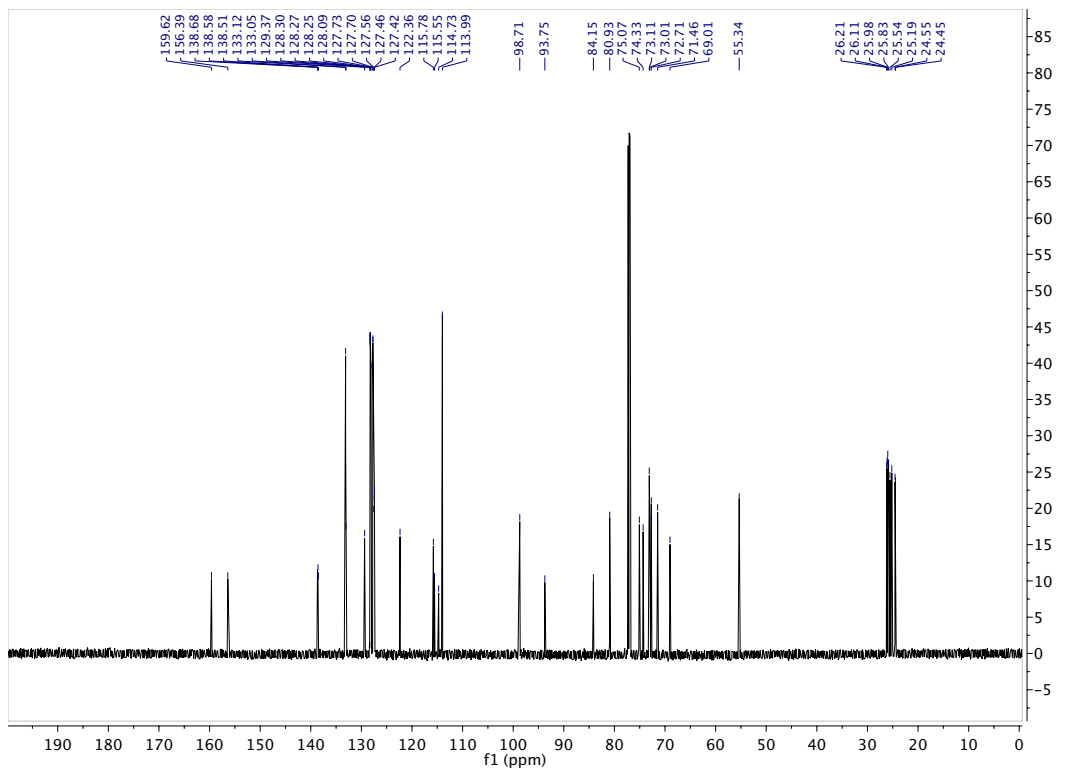
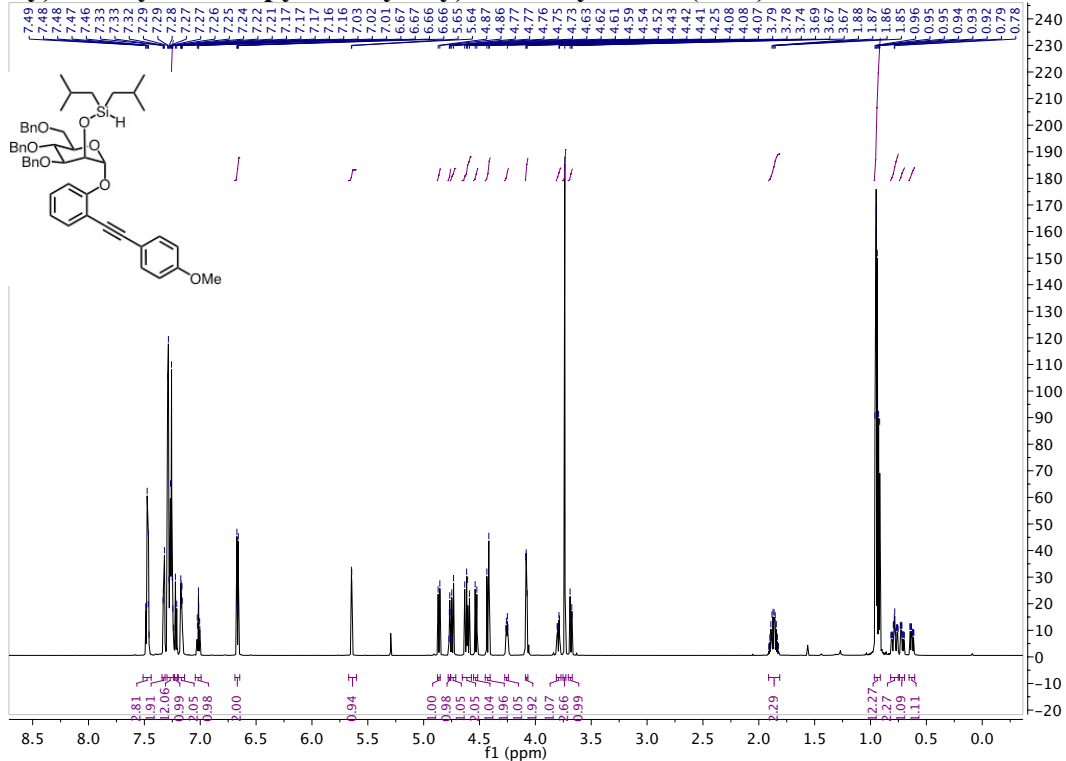


Figure 6-46: Spectra for 4-30

((2*S*,3*R*,4*R*,5*R*,6*R*)-4,5-bis(benzyloxy)-6-(benzyloxymethyl)-2-(2-((4-methoxyphenyl)ethynyl)phenoxy)tetrahydro-2*H*-pyran-3-yloxy)diisopropylsilane (4-22)

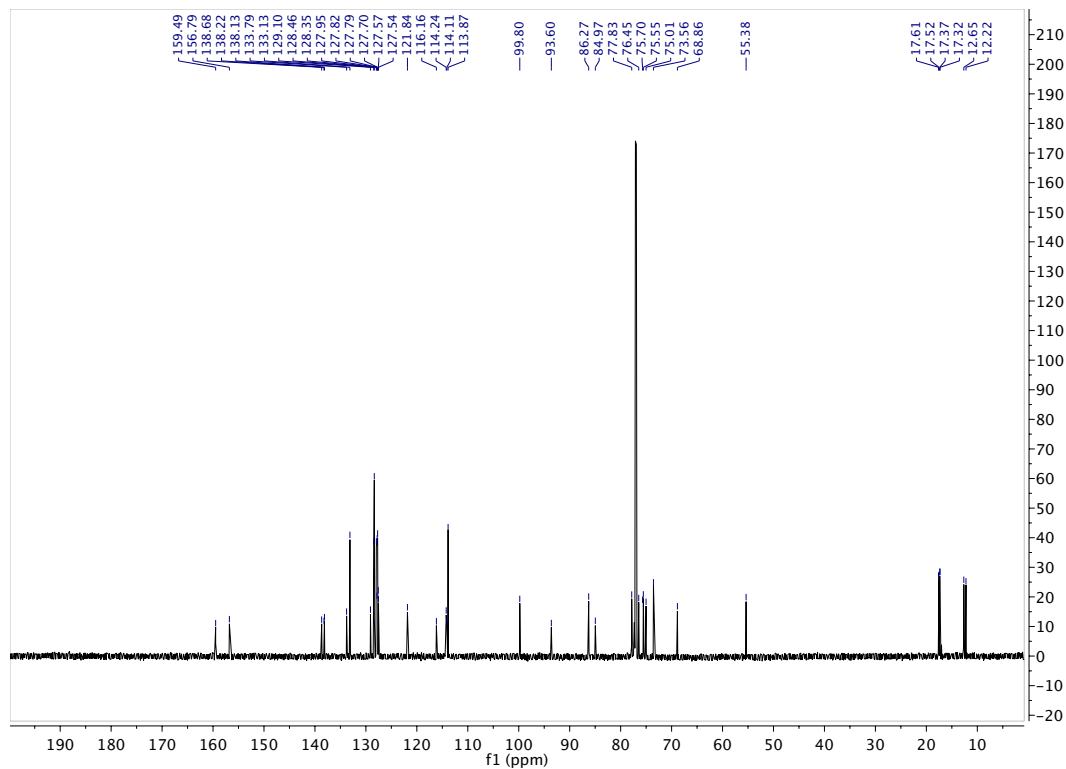
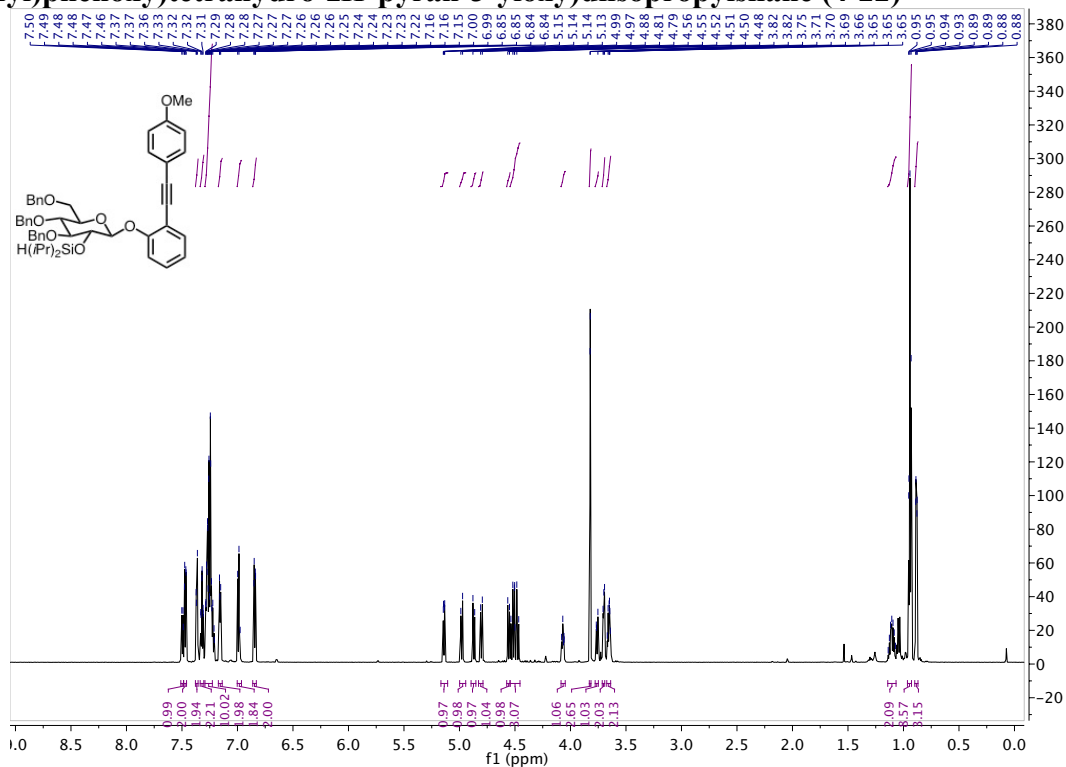


Figure 6-47: Spectra for 4-22

((2*R*,3*R*,4*S*,5*S*,6*R*)-4,5-bis(benzyloxy)-6-(benzyloxymethyl)-2-(2-((4-methoxyphenyl)ethynyl)phenoxy)tetrahydro-2*H*-pyran-3-yloxy)diisopropylsilane (4-39)

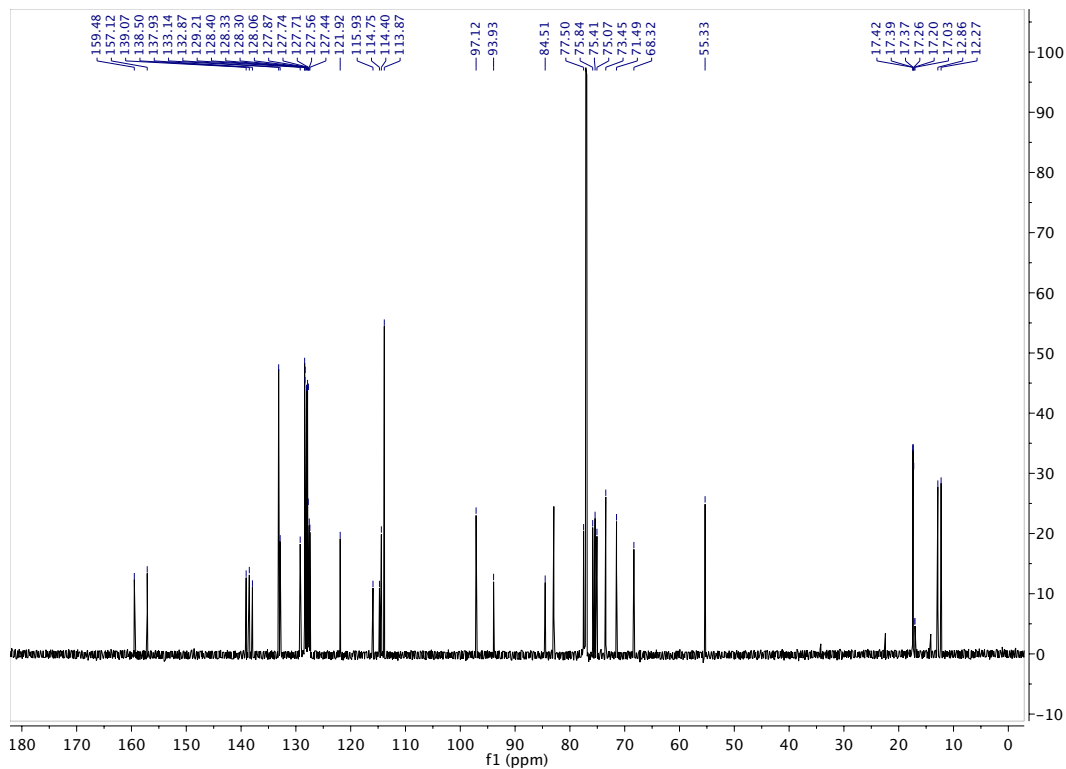
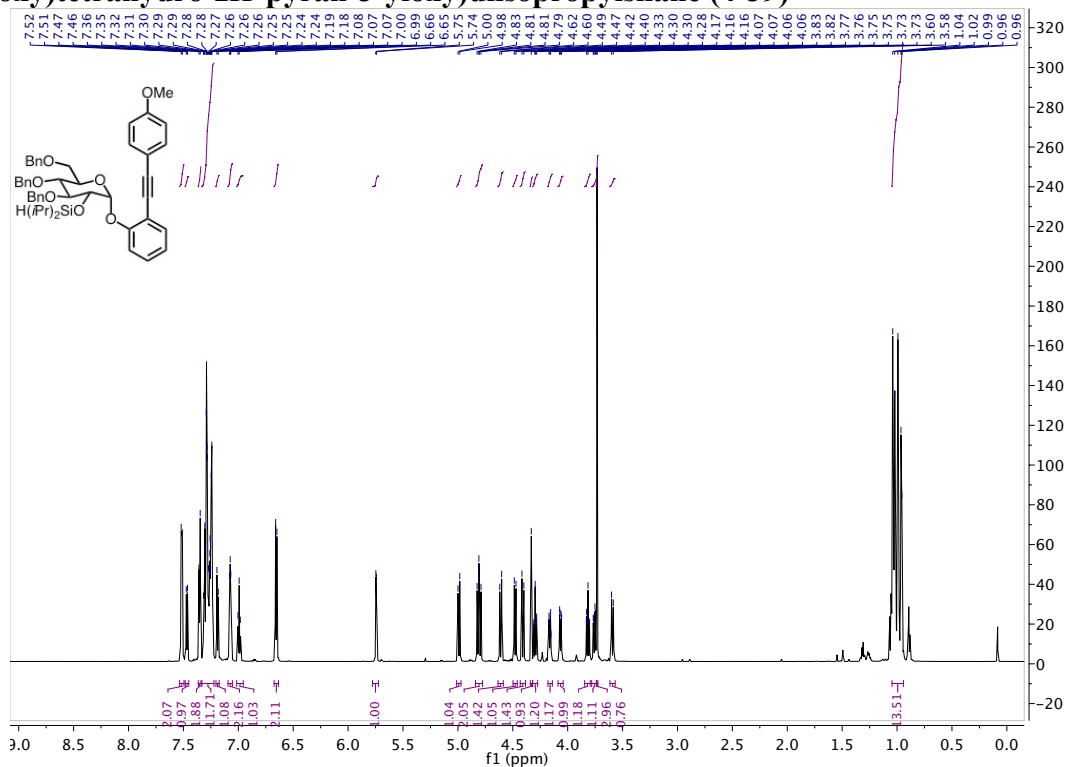


Figure 6-48: Spectra for 4-39

((2R,3S,4S,5S,6R)-4,5-bis(benzyloxy)-6-(benzyloxymethyl)-2-(2-((4-methoxyphenyl)ethynyl)phenoxy)tetrahydro-2H-pyran-3-yloxy)((1R,2S,5R)-2-isopropyl-5-methylcyclohexyloxy)dimethylsilane (4-40)

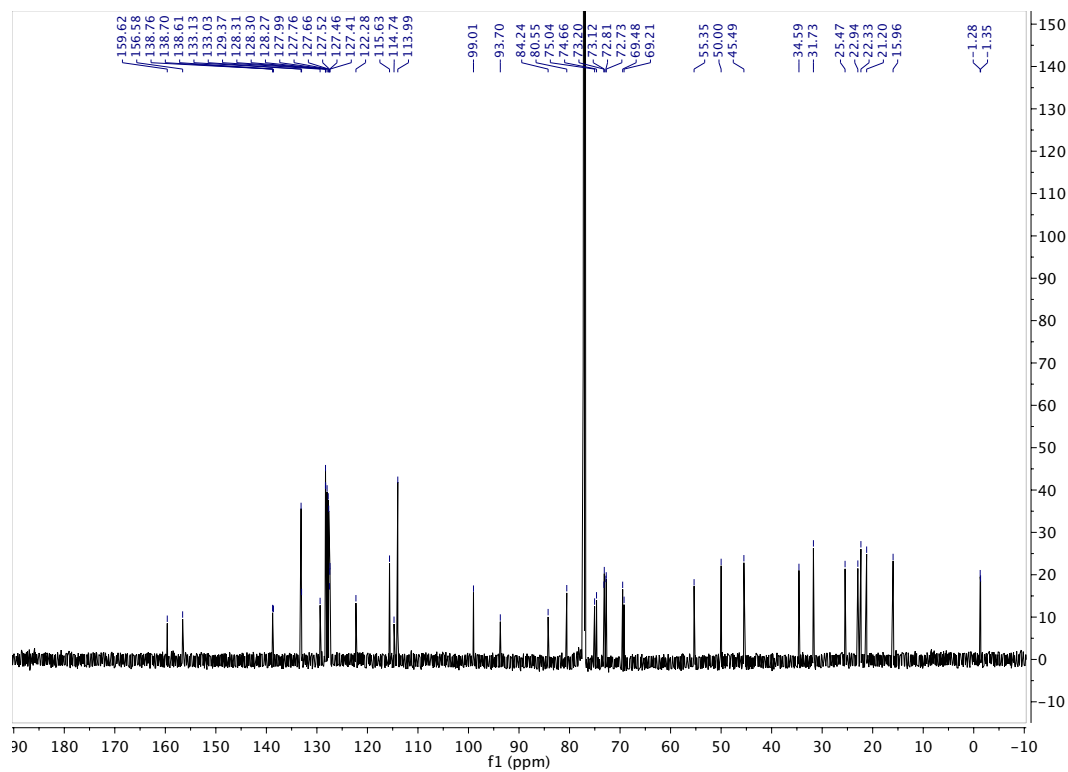
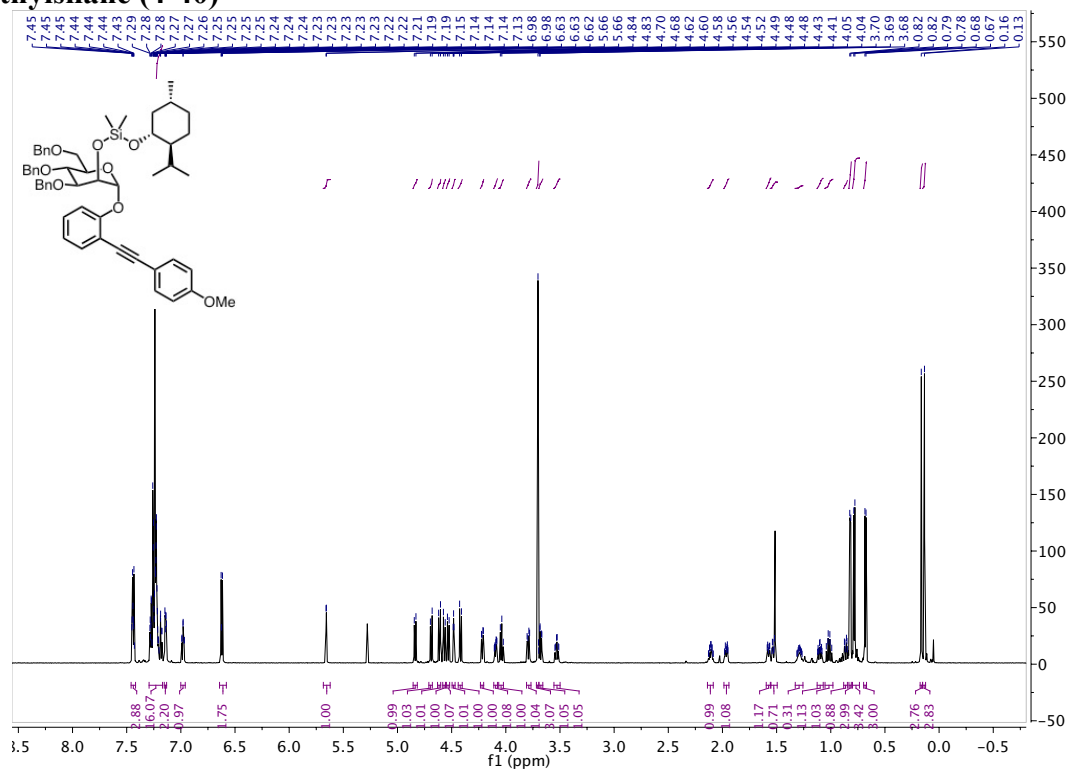


Figure 6-49: Spectra for 4-40

((2*R*,3*S*,4*S*,5*S*,6*R*)-4,5-bis(benzyloxy)-6-(benzyloxymethyl)-2-(2-((4-methoxyphenyl)ethynyl)phenoxy)tetrahydro-2*H*-pyran-3-yloxy)diisopropyl((1*R*,2*S*,5*R*)-2-isopropyl-5-methylcyclohexyloxy)silane (4-41)

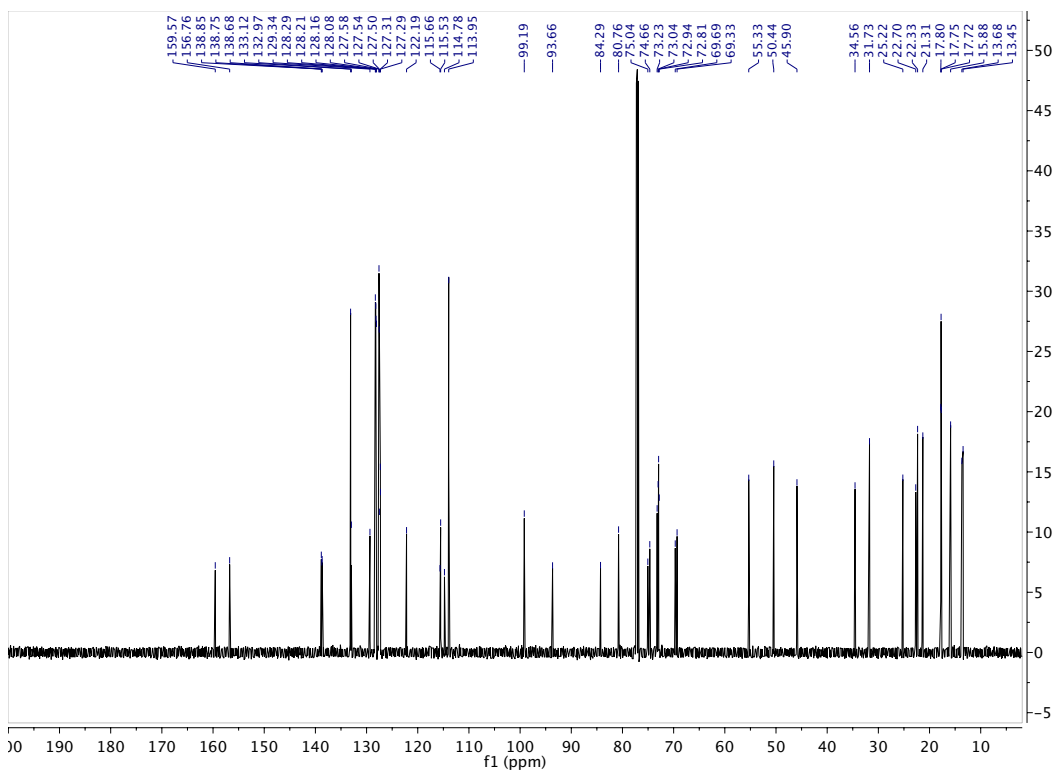
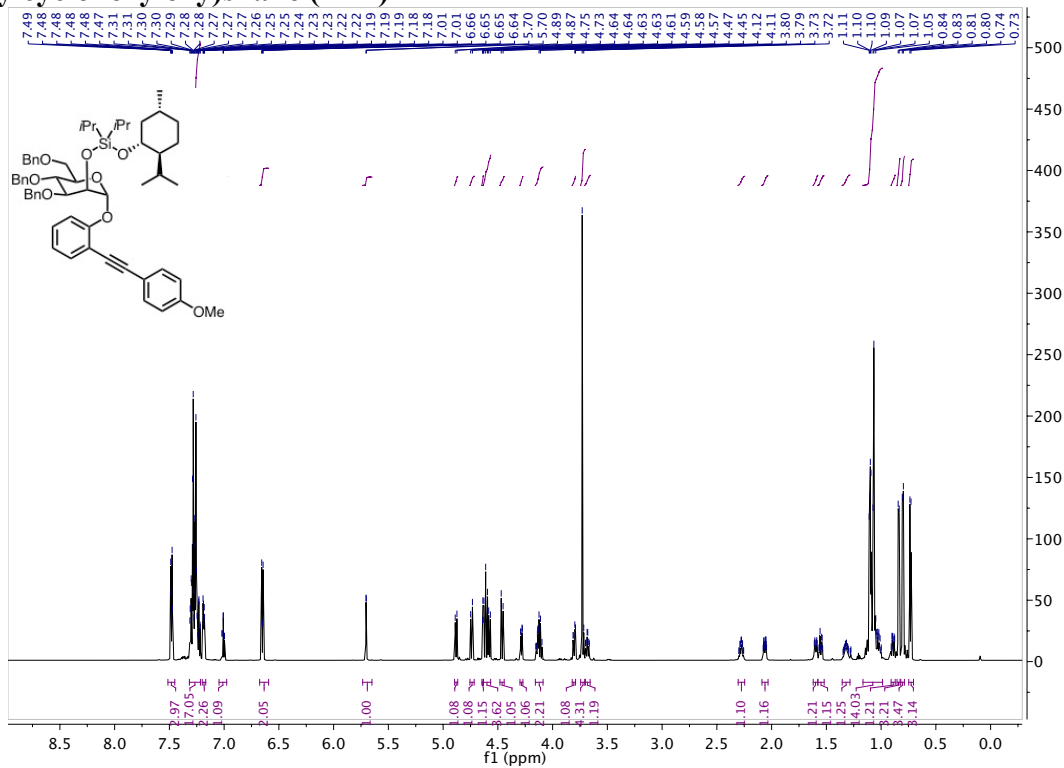


Figure 6-50: Spectra for 4-41

((2*R*,3*R*,4*R*,5*R*,6*S*)-4,5-bis(benzyloxy)-2-(benzyloxymethyl)-6-methoxytetrahydro-2*H*-pyran-3-yloxy)((2*R*,3*S*,4*S*,5*S*,6*R*)-4,5-bis(benzyloxy)-6-(benzyloxymethyl)-2-(2-((4-methoxyphenyl)ethynyl)phenoxy)tetrahydro-2*H*-pyran-3-yloxy)diisopropylsilane (4-44)

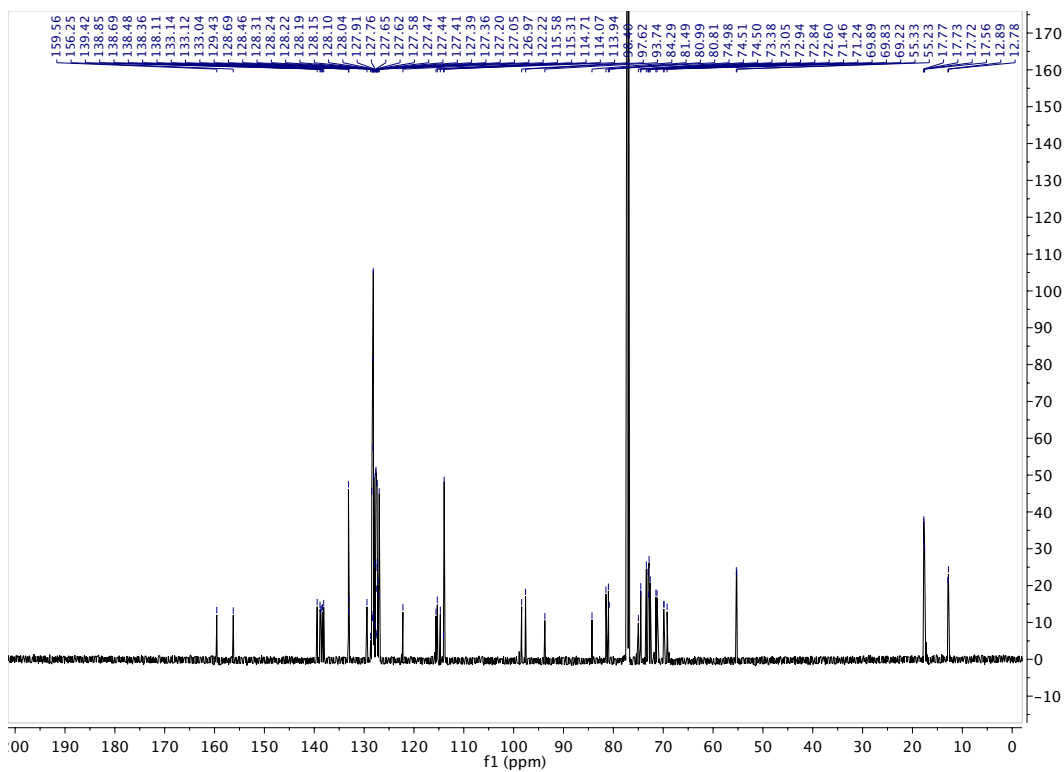
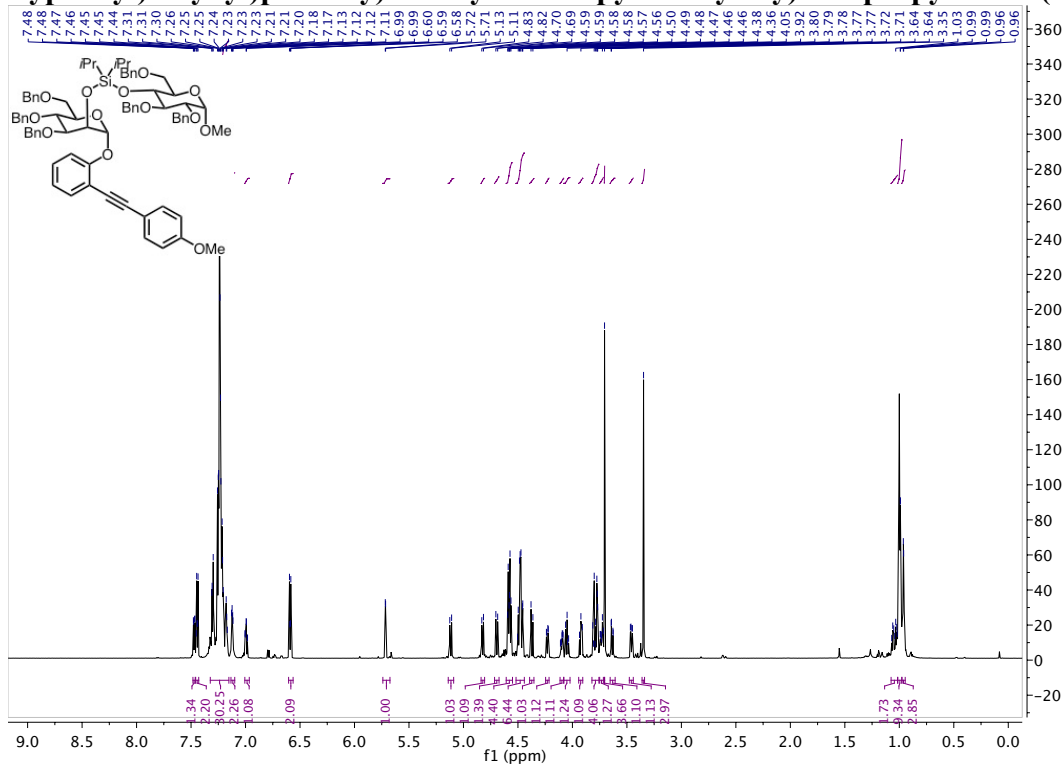


Figure 6-52: Spectra for 4-44

((2R,3S,4S,5S,6R)-4,5-bis(benzyloxy)-6-(benzyloxymethyl)-2-(2-((4-methoxyphenyl)ethynyl)phenoxy)tetrahydro-2H-pyran-3-yloxy)diisopropyl(((2R,3R,4S,5S,6R)-3,4,5-tris(benzyloxy)-6-methoxytetrahydro-2H-pyran-2-yl)methoxy)silane (4-46)

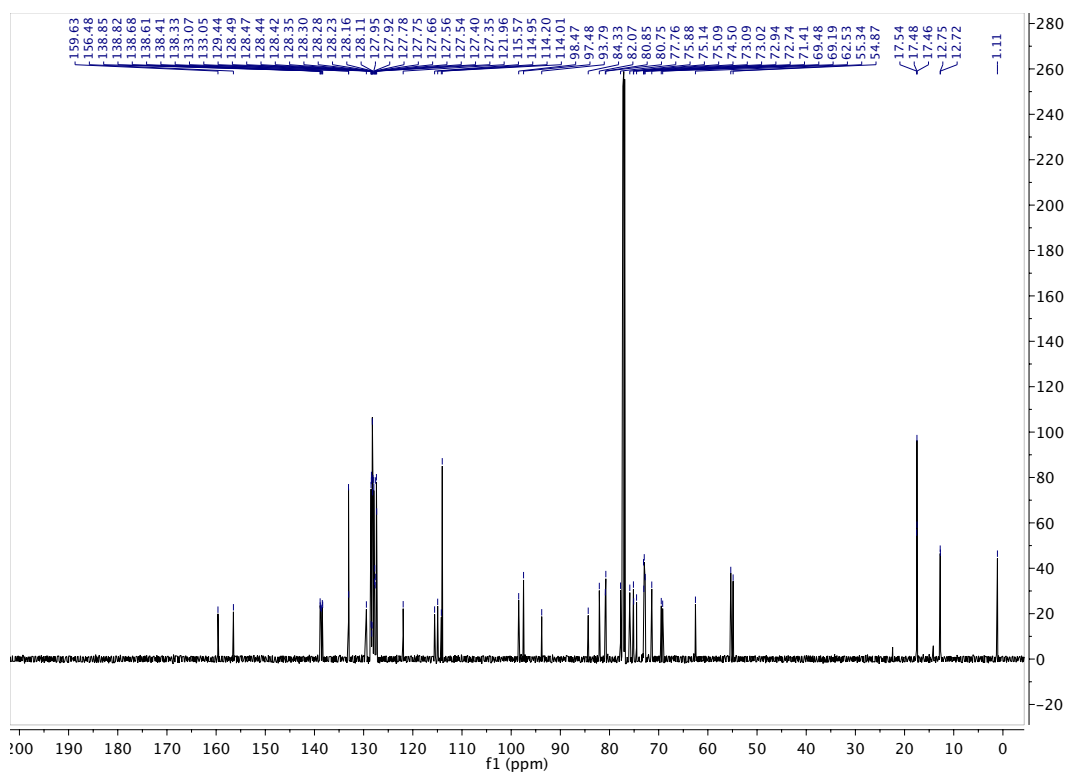
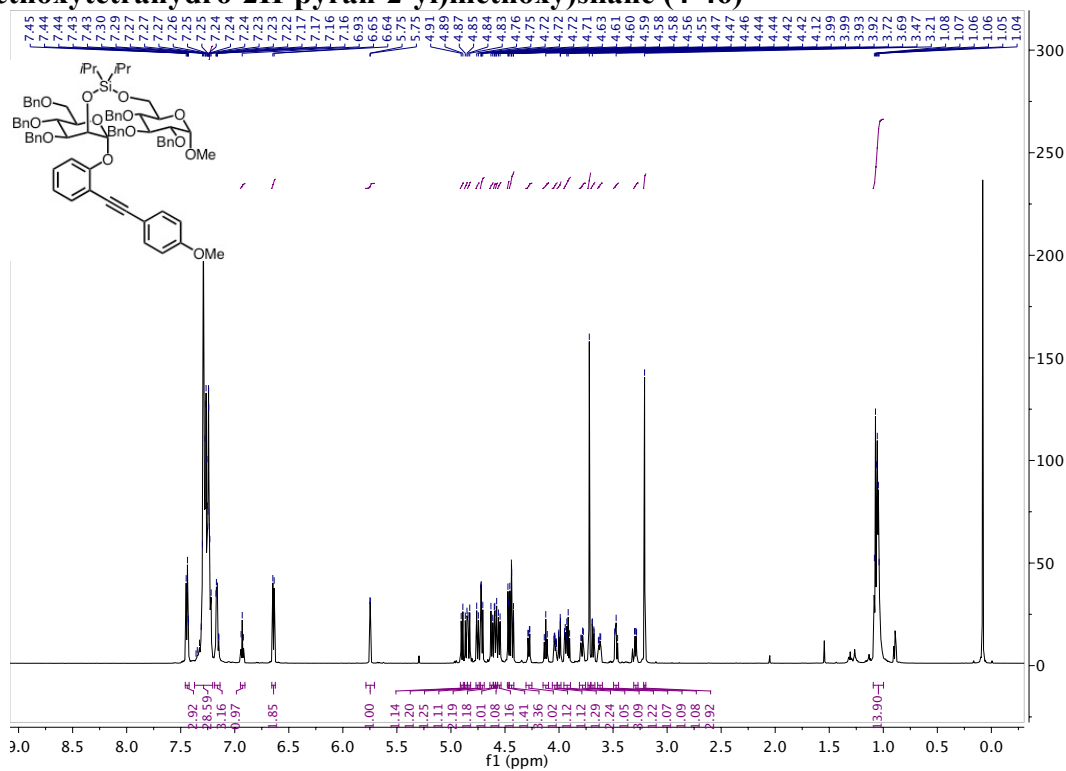
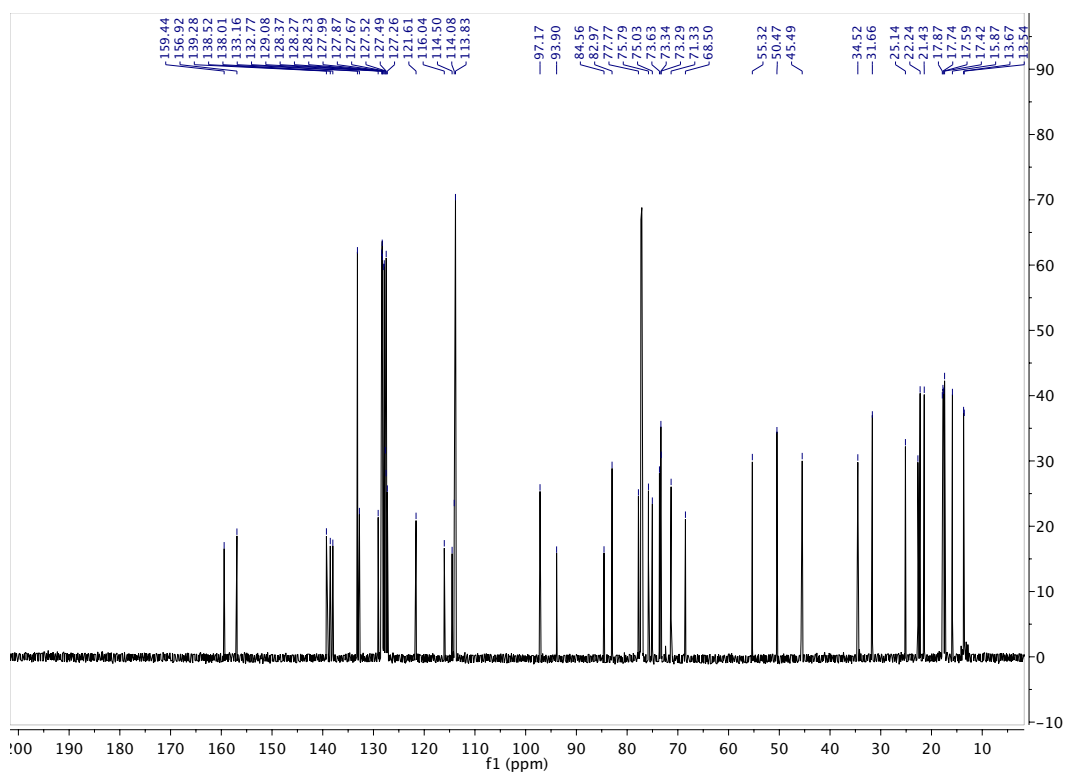
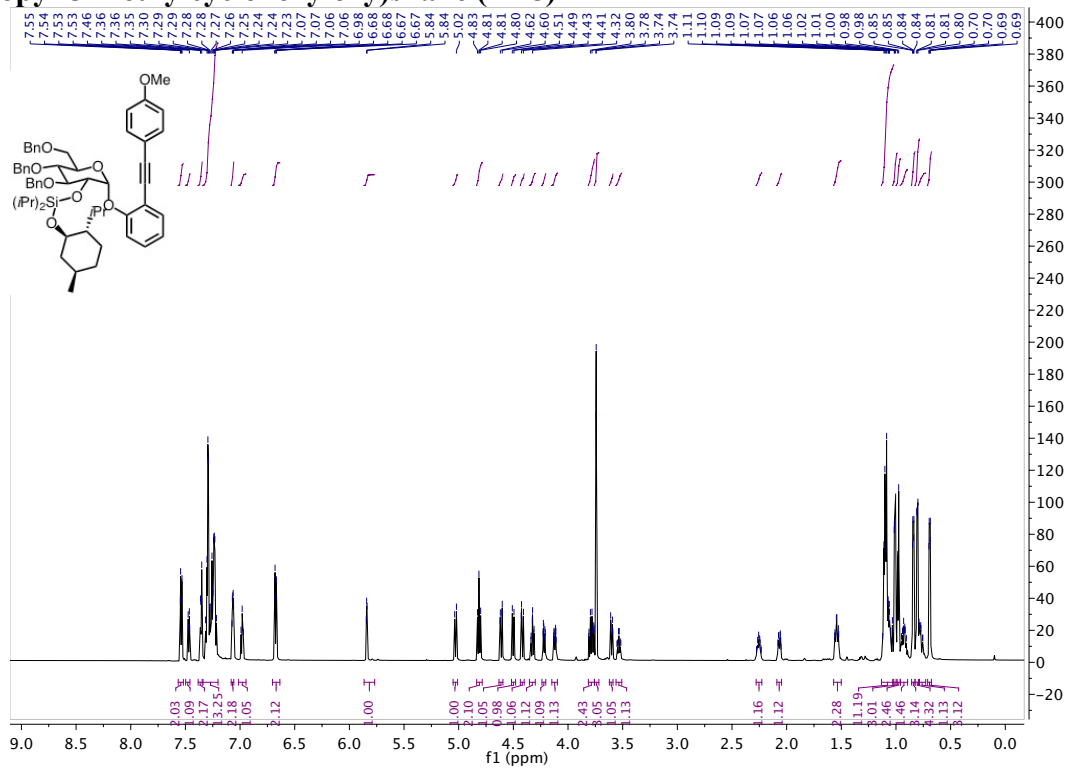


Figure 6-53: Spectra for 4-46

((2*R*,3*R*,4*S*,5*S*,6*R*)-4,5-bis(benzyloxy)-6-(benzyloxymethyl)-2-(2-((4-methoxyphenyl)ethynyl) phenoxy)tetrahydro-2*H*-pyran-3-yloxy)diisopropyl((1*R*,2*S*,5*R*)-2-isopropyl-5-methylcyclohexyloxy)silane (4-48)



Figure

6-54:

Spectra

for

4-48

References

- (1) Margrey, K. A.; Nicewicz, D. A. *Acc. Chem. Res.* **2016**, *49*, 1997–2006.
- (2) Hurd, D. T. *J. Am. Chem. Soc.* **1948**, *70*, 2053–2055.
- (3) Brown, H. C.; Rao, B. C. S. *J. Am. Chem. Soc.* **1959**, *81*, 6423–6428.
- (4) Brown, H. C.; Subba Rao, B. C. *J. Org. Chem.* **1957**, *22*, 1136–1137.
- (5) Brown, H. C.; Chandrasekharan, J. *J. Am. Chem. Soc.* **1984**, *106*, 1863–1865.
- (6) Brown, H. C.; Knights, E. F.; Scouten, C. G. *J. Am. Chem. Soc.* **1974**, *96*, 7765–7770.
- (7) Brown, H. C.; Secuten, C. G.; Liotta, R. *J. Am. Chem. Soc.* **1979**, *101*, 96–99.
- (8) Brown, H. C.; Desai, M. C.; Jadhav, P. K. *J. Org. Chem.* **1982**, *47*, 5065–5069.
- (9) Brown, H. C.; Jadhav, P. K.; Mandal, A. K. *J. Org. Chem.* **1982**, *47*, 5074–5083.
- (10) Stien, D.; Anderson, G. T.; Chase, C. E.; Koh, Y. H.; Weinreb, S. M. *J. Am. Chem. Soc.* **1999**, *121*, 9574–9579.
- (11) Corey, E. J.; Gorzynski Smith, J. *J. Am. Chem. Soc.* **1979**, *101*, 1038–1039.
- (12) Suto, T.; Yanagita, Y.; Nagashima, Y.; Takikawa, S.; Kurosu, Y.; Matsuo, N.; Sato, T.; Chida, N. *J. Am. Chem. Soc.* **2017**, *139*, 2952–2955.
- (13) Männig, D.; Nöth, H. *Angew. Chem. Int. Ed.* **1985**, *24*, 878–879.
- (14) Westcott, S. A.; Marder, T. B.; Baker, R. T.; Calabrese, J. C. *Can. J. Chem.* **1992**, *71*, 930–936.
- (15) Burgess, K.; Jaspars, M. *Organometallics* **1993**, *12*, 4197–4200.
- (16) He, X.; Hartwig, J. F. *J. Am. Chem. Soc.* **1996**, *118*, 1696–1702.
- (17) Bijpost, E. A.; Duchateau, R.; Teuben, J. H. *J. Mol. Catal. A. Chem.* **1995**, *95*, 121–128.
- (18) Satoh, M.; Nomoto, Y.; Miyaura, N.; Suzuki, A. *Tetrahedron Lett.* **1989**, *30*, 3789–3792.

- (19) Zhang, L.; Peng, D.; Leng, X.; Huang, Z. *Angew. Chem. Int. Ed.* **2013**, *52*, 3676–3680.
- (20) Obligacion, J. V.; Chirik, P. J. *J. Am. Chem. Soc.* **2013**, *135*, 19107–19110.
- (21) Zhang, G.; Zeng, H.; Wu, J.; Yin, Z.; Zheng, S.; Fettinger, J. C. *Angew. Chem. Int. Ed.* **2016**, *55*, 14369–14372.
- (22) Baruah, J. B.; Sen, K. *Proc. Indian Acad. Sci. - Chem. Sci.* **1994**, *106*, 1–3.
- (23) Shaver, M. P.; Vogels, C. M.; Wallbank, A. I.; Hennigar, T. L.; Biradha, K.; Zaworotko, M. J.; Westcott, S. A. *Can. J. Chem.* **2000**, *78*, 568–576.
- (24) Laitar, D. S.; Müller, P.; Sadighi, J. P. *J. Am. Chem. Soc.* **2005**, *127*, 17196–17197.
- (25) Laitar, D. S.; Tsui, E. Y.; Sadighi, J. P. *Organometallics* **2006**, *25*, 2405–2408.
- (26) Lee, Y.; Hoveyda, A. H. *J. Am. Chem. Soc.* **2009**, *131*, 3160–3161.
- (27) Corberán, R.; Mszar, N. W.; Hoveyda, A. H. *Angew. Chem. Int. Ed.* **2011**, *50*, 7079–7082.
- (28) Wang, Z.; He, X.; Zhang, R.; Zhang, G.; Xu, G.; Zhang, Q.; Xiong, T. *Org. Lett.* **2017**, *19*, 3067–3070.
- (29) Wen, L.; Cheng, F.; Li, H.; Zhang, S.; Hong, X.; Meng, F. *Asian J. Org. Chem.* **2018**, *7*, 103–106.
- (30) Iwamoto, H.; Kubota, K.; Ito, H. *Chem. Commun.* **2016**, *52*, 5916–5919.
- (31) Cai, Y.; Yang, X.-T.; Zhang, S.-Q.; Li, F.; Li, Y.-Q.; Ruan, L.-X.; Hong, X.; Shi, S.-L. *Angew. Chem. Int. Ed.* **2017**.
- (32) Albright, A.; Gawley, R. E. *J. Am. Chem. Soc.* **2011**, *133*, 19680–19683.
- (33) Lee, Y.; Jang, H.; Hoveyda, A. H. *J. Am. Chem. Soc.* **2009**, *131*, 18234–18235.
- (34) Meng, F.; Jang, H.; Hoveyda, A. H. *Chem. Eur. J.* **2013**, *19*, 3204–3214.
- (35) Yang, Y.; Shi, S. L.; Niu, D.; Liu, P.; Buchwald, S. L. *Science* **2015**, *349*, 62–66.
- (36) Xi, Y.; Butcher, T. W.; Zhang, J.; Hartwig, J. F. *Angew. Chem. Int. Ed.* **2016**, *55*, 776–780.
- (37) Xi, Y.; Hartwig, J. F. *J. Am. Chem. Soc.* **2016**, *138*, 6703–6706.
- (38) Ito, H.; Yamanaka, H.; Tateiwa, J.; Hosomi, A. *Tetrahedron Lett.* **2000**, *41*, 6821–6825.
- (39) Su, W.; Gong, T. J.; Zhang, Q.; Zhang, Q.; Xiao, B.; Fu, Y. *ACS Catal.* **2016**, *6*, 6417–

- 6421.
- (40) Sakae, R.; Hirano, K.; Miura, M. *J. Am. Chem. Soc.* **2015**, *137*, 6460–6463.
- (41) Yuan, W.; Ma, S. *Adv. Synth. Catal.* **2012**, *354*, 1867–1872.
- (42) Semba, K.; Shinomiya, M.; Fujihara, T.; Terao, J.; Tsuji, Y. *Chem. Eur. J.* **2013**, *19*, 7125–7132.
- (43) Miyaura, N.; Suzuki, A. *Chem. Rev.* **1995**, *95*, 2457–2483.
- (44) Schuster, C. H.; Coombs, J. R.; Kasun, Z. A.; Morken, J. P. *Org. Lett.* **2014**, *16*, 4420–4423.
- (45) Noreen, M.; Rasool, N.; El Khatib, M.; Molander, G. A. *J. Org. Chem.* **2014**, *79*, 7243–7249.
- (46) Tellis, J. C.; Primer, D. N. *Science* **2014**, *345*, 433–436.
- (47) Molander, G. A.; Wisniewski, S. R. *J. Am. Chem. Soc.* **2012**, *134*, 16856–16868.
- (48) Primer, D. N.; Karakaya, I.; Tellis, J. C.; Molander, G. A. *J. Am. Chem. Soc.* **2015**, *137*, 2195–2198.
- (49) Molander, G. A.; Ajayi, K. *Org. Lett.* **2012**, *14*, 4242–4245.
- (50) Li, L.; Zhao, S.; Joshi-Pangu, A.; Diane, M.; Biscoe, M. R. *J. Am. Chem. Soc.* **2014**, *136*, 14027–14030.
- (51) Ding, J.; Rybak, T.; Hall, D. G. *Nat. Commun.* **2014**, *5*, 1–9.
- (52) Zuo, Z.; Ahneman, D. T.; Chu, L.; Terrett, J. A.; Doyle, A. G.; MacMillan, D. W. C. *Science* **2014**, *345*, 437–440.
- (53) Noble, A.; McCarver, S. J.; MacMillan, D. W. C. *J. Am. Chem. Soc.* **2015**, *137*, 624–627.
- (54) Brown, H. C.; Zweifel, G. *J. Am. Chem. Soc.* **1961**, *83*, 2544–2551.
- (55) Liskey, C. W.; Hartwig, J. F. *J. Am. Chem. Soc.* **2013**, *135*, 3375–3378.
- (56) Nave, S.; Sonawane, R. P.; Elford, T. G.; Aggarwal, V. K. *J. Am. Chem. Soc.* **2010**, *132*, 17096–17098.
- (57) Furuya, T.; Ritter, T. *Org. Lett.* **2009**, *11*, 2860–2863.
- (58) Vedejs, E.; Chapman, R. W.; Fields, S. C.; Lin, S.; Schrimpf, M. R. *J. Org. Chem.* **1995**,

- 60, 3020–3027.
- (59) Molander, G. A.; Cavalcanti, L. N.; Canturk, B.; Pan, P. S.; Kennedy, L. E. *J. Org. Chem.* **2009**, *74*, 7364–7369.
- (60) Bagutski, V.; Ros, A.; Aggarwal, V. K. *Tetrahedron* **2009**, *65*, 9956–9960.
- (61) Matteson, D. S.; Majumdar, D. *Organometallics* **1983**, *2*, 230–236.
- (62) Sadhu, K. M.; Matteson, D. S. *Organometallics* **1985**, *4*, 1687–1689.
- (63) Leonori, D.; Aggarwal, V. K. *Acc. Chem. Res.* **2014**, *47*, 3174–3183.
- (64) Stymiest, J. L.; Dutheuil, G.; Mahmood, A.; Aggarwal, V. K. *Angew. Chem. Int. Ed.* **2007**, *46*, 7491–7494.
- (65) Blakemore, P. R.; Marsden, S. P.; Vater, H. D. *Org. Lett.* **2006**, *8*, 773–776.
- (66) Blakemore, P. R.; Burge, M. S. *J. Am. Chem. Soc.* **2007**, *129*, 3068–3069.
- (67) Dreher, S. D.; Dormer, P. G.; Sandrock, D. L.; Molander, G. A. *J. Am. Chem. Soc.* **2008**, *130*, 9257–9259.
- (68) Dudnik, A. S.; Fu, G. C. *J. Am. Chem. Soc.* **2012**, *134*, 10693–10697.
- (69) Atack, T. C.; Lecker, R. M.; Cook, S. P. *J. Am. Chem. Soc.* **2014**, *136*, 9521–9523.
- (70) Bull, J. A. *Angew. Chem. Int. Ed.* **2012**, *51*, 8930–8932.
- (71) Moran, W. J.; Morken, J. P. *Org. Lett.* **2006**, *8*, 2413–2415.
- (72) Paptchikhine, A.; Cheruku, P.; Engman, M.; Andersson, P. G. *Chem. Commun.* **2009**, 5996–5998.
- (73) Malik, H. a.; Sormunen, G. J.; Montgomery, J. *J. Am. Chem. Soc.* **2010**, *132*, 6304–6305.
- (74) Miller, Z. D.; Montgomery, J. *Org. Lett.* **2014**, *16*, 5486–5489.
- (75) Liu, P.; Montgomery, J.; Houk, K. N. *J. Am. Chem. Soc.* **2011**, *133*, 6956–6959.
- (76) Miller, Z. D.; Li, W.; Belderrain, T. R.; Montgomery, J. *J. Am. Chem. Soc.* **2013**, *135*, 15282–15285.
- (77) Jackson, E. P.; Montgomery, J. *J. Am. Chem. Soc.* **2015**, *137*, 958–963.
- (78) Jang, H.; Zhugralin, A. R.; Lee, Y.; Hoveyda, A. H. *J. Am. Chem. Soc.* **2011**, *133*, 7859–

7871.

- (79) Kageyuki, I.; Yoshida, H.; Takaki, K. *Synthesis* **2014**, *46*, 1924–1932.
- (80) Semba, K.; Nakao, Y. *J. Am. Chem. Soc.* **2014**, *136*, 7567–7570.
- (81) Moon, J. H.; Jung, H. Y.; Lee, Y. J.; Lee, S. W.; Yun, J.; Lee, J. Y. *Organometallics* **2015**, *34*, 2151–2159.
- (82) Gutierrez, O.; Tellis, J. C.; Primer, D. N.; Molander, G. A.; Kozlowski, M. C. *J. Am. Chem. Soc.* **2015**, *137*, 4896–4899.
- (83) Brown, H. C.; Ayyangar, N. R.; Zweifel, G. *J. Am. Chem. Soc.* **1964**, *86*, 397–403.
- (84) Thomas, S. P.; Aggarwal, V. K. *Angew. Chem. Int. Ed.* **2009**, *48*, 1896–1898.
- (85) Lee, K. S.; Brown, M. K.; Hird, A. W.; Hoveyda, A. H. *J. Am. Chem. Soc.* **2006**, *128*, 7182–7184.
- (86) Wang, H.; Lu, G.; Sormunen, G. J.; Malik, H. A.; Liu, P.; Montgomery, J. *J. Am. Chem. Soc.* **2017**, *139*, 9317–9324.
- (87) Smith, J. R.; Collins, B. S. L.; Hesse, M. J.; Graham, M. A.; Myers, E. L.; Aggarwal, V. K. *J. Am. Chem. Soc.* **2017**, *139*, 9148–9151.
- (88) Scheuermann, M. L.; Johnson, E. J.; Chirik, P. J. *Org. Lett.* **2015**, *17*, 2716–2719.
- (89) Jia, X.; Zhang, L.; Qin, C.; Leng, X.; Huang, Z. *Chem. Commun.* **2014**, *50*, 11056.
- (90) Weljange, N. M.; McGuinness, D. S.; Gardiner, M. G.; Patel, J. *Dalt. Trans.* **2016**, *45*, 10842.
- (91) Ogawa, T.; Ruddy, A. J.; Sydora, O. L.; Stradiotto, M.; Turculet, L. *Organometallics* **2017**, *36*, 417–423.
- (92) Tseng, K. N. T.; Kampf, J. W.; Szymczak, N. K. *ACS Catal.* **2015**, *5*, 411–415.
- (93) Kerchner, H. A.; Montgomery, J. *Org. Lett.* **2016**, *18*, 5760–5763.
- (94) Primer, D. N.; Molander, G. A. *J. Am. Chem. Soc.* **2017**, *139*, 9847–9850.
- (95) *The Organic Chemistry of Sugars*; Levy, D.; Fügedi, P., Eds.; Taylor & Francis Group: Boca Raton, FL, 2005.
- (96) Mensink, R. A.; Boltje, T. J. *Chem. Eur. J.* **2017**, *23*, 17637–17653.

- (97) Koenigs, W.; Knorr, E. *Ber.* **1901**, *34*, 957–981.
- (98) Demchenko, A. V. *Synlett* **2003**, 1225–1240.
- (99) Barresi, F.; Hindsgaul, O. *J. Am. Chem. Soc.* **1991**, *113*, 9376–9377.
- (100) Barresi, F.; Hindsgaul, O. *Can. J. Chem.* **1994**, 1447–1465.
- (101) Barresi, F.; Hindsgaul, O. *Synlett* **1992**, 759–761.
- (102) Ennis, S. C.; Fairbanks, A. J.; Tennant-Eyles, R. J.; Yeates, H. S. *Synlett* **1999**, 1387–1390.
- (103) Ennis, S. C.; Fairbanks, A. J.; Slinn, C. A.; Tennant-Eyles, R. J.; Yeates, H. S. *Tetrahedron* **2001**, *57*, 4221–4230.
- (104) Seward, C. M. P.; Cumpstey, I.; Aloui, M.; Ennis, S. C.; Fairbanks, A. J.; Redgrave, A. J. *Chem. Commun.* **2000**, 1409–1410.
- (105) Aloui, M.; Chambers, D. J.; Cumpstey, I.; Fairbanks, A. J.; Redgrave, A. J.; Seward, C. M. P. *Chem. Eur. J.* **2002**, *8*, 2608–2621.
- (106) Ito, Y.; Ogawa, T. *Angew. Chem. Int. Ed.* **1994**, *33*, 1765–1767.
- (107) Dan, A.; Ito, Y.; Ogawa, T. *Tetrahedron Lett.* **1995**, *36*, 7487–7490.
- (108) Dan, A.; Ito, Y.; Ogawa, T. *J. Org. Chem.* **1995**, *60*, 4680–4681.
- (109) Dan, A.; Lergenmüller, M.; Amano, M.; Nakahara, Y.; Ogawa, T.; Ito, Y. *Chem. Eur. J.* **1998**, *4*, 2182–2190.
- (110) Ito, Y.; Ohnishi, Y.; Ogawa, T.; Nakahara, Y. *Synlett* **1998**, *5*, 1102–1104.
- (111) Lergenmüller, M.; Nukada, T.; Kuramochi, K.; Dan, A.; Ogawa, T.; Ito, Y. *Eur. J. Org. Chem.* **1999**, 1367–1376.
- (112) Seifert, J.; Lergenmüller, M.; Ito, Y. *Angew. Chem. Int. Ed.* **2000**, *39*, 531–534.
- (113) Ohnishi, Y.; Ando, H.; Kawai, T.; Nakahara, Y.; Ito, Y. *Carbohydr. Res.* **2000**, *328*, 263–276.
- (114) Ito, Y.; Ando, H.; Wada, M.; Kawai, T.; Ohnishi, Y.; Nakahara, Y. *Tetrahedron* **2001**, *57*, 4123–4132.
- (115) Matsuo, I.; Ito, Y. *Carbohydr. Res.* **2003**, *338*, 2163–2168.

- (116) Matsuo, I.; Wada, M.; Manabe, S.; Yamaguchi, Y.; Otake, K.; Kato, K.; Ito, Y. *J. Am. Chem. Soc.* **2003**, *125*, 3402–3403.
- (117) Matsuo, I.; Totani, K.; Tatami, A.; Ito, Y. *Tetrahedron* **2006**, *62*, 8262–8277.
- (118) Ito, Y.; Ogawa, T. *J. Am. Chem. Soc.* **1997**, *119*, 5562–5566.
- (119) Leigh, C. D.; Bertozzi, C. R. *J. Org. Chem.* **2008**, *73*, 1008–1017.
- (120) Pratt, M. R.; Leigh, C. D.; Bertozzi, C. R. *Org. Lett.* **2003**, *5*, 3185–3188.
- (121) Stork, G.; Kim, G. *J. Am. Chem. Soc.* **1992**, *114*, 1087–1088.
- (122) Stork, G.; La Clair, J. J. *J. Am. Chem. Soc.* **1996**, *118*, 247–248.
- (123) Bols, M. *J. Chem. Soc., Chem. Commun.* **1992**, 913–914.
- (124) Bols, M. *Acta Chem. Scand.* **1993**, *47*, 829–834.
- (125) Bols, M.; Hansen, H. C. *Chem. Lett.* **1994**, 1049–1052.
- (126) *Handbook of Chemical Glycosylation: Advances in Stereoselectivity and Therapeutic Relevance*; Demchenko, A. V, Ed.; Wiley-VHC: Weinheim, Germany, 2008.
- (127) Michael, A. *Am. Chem.* **1879**, 305–312.
- (128) Fischer, E. *Chem. Ber.* **1893**, 2400–2412.
- (129) Ferrier, R. J.; Hay, R. W.; Vethaviasar, N. *Carbohydr. Res.* **1973**, *27*, 55–61.
- (130) Nicolaou, K. C.; Seitz, S. P.; Papahatjis, D. P. *J. Am. Chem. Soc.* **1983**, *105*, 2430–2434.
- (131) Garegg, P. J.; Henrichson, C.; Norberg, T. *Carbohydr. Res.* **1983**, *116*, 162–165.
- (132) Pougny, J. R.; Jacquinet, J. C.; Nassr, M.; Duchet, D.; Milat, M. L.; Sinay, P. *J. Am. Chem. Soc.* **1977**, *99*, 6762–6763.
- (133) Mukaiyama, T.; Nakatsuka, T.; Shoda, S.-I. *Chem. Lett.* **1979**, 487–490.
- (134) Soms, L.; Nemeth, I. *J. Carbohydr. Chem.* **1993**, *12*, 679–684.
- (135) Halcomb, R. L.; Danishefsky, S. J. *J. Am. Chem. Soc.* **1989**, *111*, 6661–6666.
- (136) Fraser-Reid, B.; Mootoo, D. R. *Carbohydr. Res.* **1988**, *174*, 99–112.
- (137) Mootoo, D. R.; Fraser-Reid, B. *Tetrahedron* **1990**, *46*, 185–200.

- (138) Mootoo, D. R.; Date, V.; Fraser-Reid, B. *J. Am. Chem. Soc.* **1988**, *110*, 2662–2663.
- (139) Fraser-Reid, B.; López, J. C. In *Topics in Current Chemistry*; Fraser-Reid, B.; Cristóbal López, J., Eds.; Springer Berlin Heidelberg: Berlin, Heidelberg, 2011; Vol. 301, pp. 1–29.
- (140) Mukai, C.; Itoh, T.; Hanaoka, M. *Tetrahedron Lett.* **1997**, *38*, 4595–4598.
- (141) Kwan Soo Kim; Jin Hwan Kim; Yong Joo Lee; Yong Jun Lee; Park, J. *J. Am. Chem. Soc.* **2001**, *123*, 8477–8481.
- (142) Hotha, S.; Kashyap, S. *J. Am. Chem. Soc.* **2006**, *128*, 9620–9621.
- (143) Vidadala, S. R.; Thadke, S. A.; Hotha, S. *J. Org. Chem.* **2009**, *74*, 9233–9236.
- (144) Chen, X.; Shen, D.; Wang, Q.; Yang, Y.; Yu, B. *Chem. Commun.* **2015**, *51*, 13957–13960.
- (145) Shu, P.; Xiao, X.; Zhao, Y.; Xu, Y.; Yao, W.; Tao, J.; Wang, H.; Yao, G.; Lu, Z.; Zeng, J.; Wan, Q. *Angew. Chem. Int. Ed.* **2015**, *54*, 14432–14436.
- (146) Xiao, X.; Zhao, Y.; Shu, P.; Zhao, X.; Liu, Y.; Sun, J.; Zhang, Q.; Zeng, J.; Wan, Q. *J. Am. Chem. Soc.* **2016**, *138*, 13402–13407.
- (147) Chen, W.; Zeng, J.; Wang, H.; Xiao, X.; Meng, L.; Wan, Q. *Carbohydr. Res.* **2017**, *452*, 1–5.
- (148) Lönn, H. *Carbohydr. Res.* **1985**, *134*, 115–121.
- (149) Lönn, H. *Carbohydr. Res.* **1985**, *139*, 105–113.
- (150) Fügedi, P.; Garegg, P. J. *Carbohydr. Res.* **1986**, *149*, 2–5.
- (151) Veeneman, G. H.; van Leeuwen, S. H.; van Boom, J. H. *Tetrahedron Lett.* **1990**, *31*, 1331–1334.
- (152) Veeneman, G. H.; van Boom, J. H. *Tetrahedron Lett.* **1990**, *31*, 275–278.
- (153) Oscarson, S. In *Carbohydrates in Chemistry and Biology*; 2000; pp. 93–116.
- (154) Yao, C. H.; Lee, J. C. *Tetrahedron* **2014**, *70*, 6757–6762.
- (155) Fukase, K.; Kinoshita, I.; Kanoh, T.; Nakai, Y.; Hasuoka, A.; Kusumoto, S. *Tetrahedron* **1996**, *52*, 3897–3904.
- (156) Kajimoto, T.; Morimoto, K.; Ogawa, R.; Dohi, T.; Kita, Y. *Chem. Pharm. Bull.* **2016**, *64*, 838–844.

- (157) Saliba, R. C.; Wooke, Z. J.; Nieves, G. A.; Chu, A.-H. A.; Bennett, C. S.; Pohl, N. L. B. *Org. Lett.* **2018**, *20*, 800–803.
- (158) Heuckendorff, M.; Jensen, H. H. *Carbohydr. Res.* **2018**, *455*, 86–91.
- (159) Xia, M.; Yao, W.; Meng, X.; Lou, Q.; Li, Z. *Tetrahedron Lett.* **2017**, *58*, 2389–2392.
- (160) Kitowski, A.; Jiménez-Moreno, E.; Salvadó, M.; Mestre, J.; Castellón, S.; Jiménez-Osés, G.; Bouteira, O.; Bernardes, G. J. L. *Org. Lett.* **2017**, *19*, 5490–5493.
- (161) Buchan, Z. A.; Bader, S. J.; Montgomery, J. *Angew. Chem. Int. Ed.* **2009**, *48*, 4840–4844.
- (162) Partridge, K. M.; Bader, S. J.; Buchan, Z. A.; Taylor, C. E.; Montgomery, J. *Angew. Chem. Int. Ed.* **2013**, *52*, 13647–13650.
- (163) Walk, J. T.; Buchan, Z. A.; Montgomery, J. *Chem. Sci.* **2015**, *6*, 3448–3453.
- (164) Knauff, A. R. Development and Application of a Regioselective Nickel-Catalyzed Macrocyclization Method; and Development of Bench Stable Sugar Silanes for Use in Copper-Catalyzed Dehydrogenative Silylations, 2013.
- (165) Buchan, Z. A. Sugar Silanes in Carbohydrate Synthesis: Applications Towards Site-Selective Glycosylation, 2011.
- (166) Hu, Y.; Yu, K.; Shi, L. L.; Liu, L.; Sui, J. J.; Liu, D. Y.; Xiong, B.; Sun, J. S. *J. Am. Chem. Soc.* **2017**, *139*, 12736–12744.
- (167) Wu, F. F.; Zhou, J. N.; Fang, Q.; Hu, Y. H.; Li, S.; Zhang, X. C.; Chan, A. S. C.; Wu, J. *Chem. Asian J.* **2012**, *7*, 2527–2530.
- (168) Kaur, H.; Zinn, F. K.; Stevens, E. D.; Nolan, S. P. *Organometallics* **2004**, *23*, 1157–1160.
- (169) Collins, B. S. L.; Suero, M. G.; Gaunt, M. J. *Angew. Chem. Int. Ed.* **2013**, *52*, 5799–5802.
- (170) Kawasaki, T.; Tanaka, H.; Tsutsumi, T.; Kasahara, T.; Sato, I.; Soai, K. *J. Am. Chem. Soc.* **2006**, *128*, 6032–6033.
- (171) Chen, C.; Dugan, T. R.; Brennessel, W. W.; Weix, D. J.; Holland, P. L. *J. Am. Chem. Soc.* **2014**, *136*, 945–955.
- (172) Rawat, V.; Chouthaiwale, P. V.; Suryavanshi, G.; Sudalai, A. *Tetrahedron Asymmetry* **2009**, *20*, 2173–2177.
- (173) Li, X.; Gu, X.; Li, Y.; Li, P. *ACS Catal.* **2014**, *4*, 1897–1900.
- (174) Choy, P. Y.; Lau, C. P.; Kwong, F. Y. *J. Org. Chem.* **2011**, *76*, 80–84.

- (175) Synthesi, C.-C.-; Hoffmann, W.; Haeberlin, E.; Rohde, T. *Synthesis* **2002**, *2*, 207–212.
- (176) Lu, D. F.; Zhu, C. L.; Sears, J. D.; Xu, H. *J. Am. Chem. Soc.* **2016**, *138*, 11360–11367.
- (177) Molander, G. A.; Shin, I. *Org. Lett.* **2012**, *14*, 4458–4461.
- (178) Kotammagari, T. K.; Gonnade, R. G.; Bhattacharya, A. K. *Org. Lett.* **2017**, *19*, 3564–3567.